Criterion III

3.3.1 Number of Research Papers published per Teacher in the Journals notified on UGC CARE List during the last five years

2018-19 to 2022-23

GLOBAL RESEARCH CANVAS

ISSN 2394-5427 multidisciplinary, peer-reviewed (refereed) journal

NATIONAL SEMINAR

17-18 April-2023

युवा पीढ़ी के समग्र विकास में शिक्षा, साहित्य और संस्कृति की भूमिका

యువత సమగ్రాభివృద్ధి లో విద్య, సాహితీ ,సంస్కృతు ల పాత్ర

Role of Education, Literature and Culture in the Holistic Development of Youth

Executive Editor
Dr. P.K. jayalakshmi

Editor
Manoj kumar

St. Joseph's College for Women (A)
Visakhapatnam - 530 004
REACCREDITED BY NAAC & ISO 9001: 2015 CERTIFIED

'उठो, जागो और तब तक रुको नहीं जब तक कि तुम अपना लक्ष्य प्राप्त नहीं कर लेते'

तेलुगु भाषा खंड

141-194

యువత సమగ్రాభివృద్ధిలో విద్య, సాహితీ, సంస్కృతుల పాత్ర

peer-reviewed (refereed) journal ISSN 2394-5427 GLOBAL RES

విద్యా విలువలు - ఆవశ్యకత

డా॥ కనపాల జోసఫ్
తెలుగు శాఖ అధ్యక్షులు
ఆంధ్ర క్రైస్తవ కళాశాల
గుంటూరు
చరవాణి : 9849025505

కలానుగుణంగా విద్యా భోధనో ఉహాకందని మార్పులు చోటు చేసుకుంటున్న సంగతినిచూస్తూనే ఉన్నాము. ఈ మార్పు విద్యార్థులకు ఎంత వరకు ఉపయోగ కరంగా ఉన్నాయో అన్న దానికి సరైన సమాధానం చెప్పడం కష్టమే దీనిని సింహా వలోకనం చేసుకోవాల్సిన అవశ్యకత ఎంతైనా ఉంది దీనిని పరిశీలించినప్పుడు సంప్రదాయ కాలపు విద్యకు ఆధునిక కాలపు విద్యకు మధ్య ఉండే ప్రధాన తేడ విలువలు కోరవడడమే. ఒకప్పుడు విద్యా భోదనలో ఉపమానాలను, కథలను జోడించి భోదన జరిగేది. అందువల్ల ఏక కాలంలో పాఠ్యాంశల మార్పులతో పాటు ఆ కథల్లోనూ, ఉపమానల్లోనూ బోలెడంత విలువలు ఉండేవి. అలాగే భోధనలో అప్పనిసరిగా సాహితీ, సాంస్కృతిక అంశాలను జోడిస్తూ భోధన ఉండేది. తద్వారా విద్యానంతరం విద్యార్థులు నైతిక విలువలను అభరణంగా కలిగి సాంఘిక, సాంస్కృతిక అంశాలను జోడిస్తూ భోదన ఉండేది. తద్వారా విద్యానంతరం విద్యార్థులు నైతిక విలువలను ఆభరణంగా కలిగి సాంఘికసాంస్కృతిక సంబంధాలను కలిగి తమకంటూ ఒక ప్రత్యేకమైనా వ్యక్తిత్వాన్ని కలిగి ఉండేవారు. దీనికి తోడు జీవిత చరిత్రలు, సజ్జనుల సాంగత్యం సంపూర్ణవిలువలుతో కూడి సంపూర్ణ వ్యక్తిత్వానికి, దీర్గకాళిక శ్రేయస్సుకు గొడుగులాగా ఉండేవి.

విలువల విద్య నిర్వచనం. విద్యార్థుల్లో అభ్యాసనా అనుభాలను కలిగించడానికి ఉపాధ్యాలు అధ్యాపకులు విభిన్న భోదనా పద్దతులను పాటిస్తూ ఉంటారు. వారి వారి మానసిక స్థితులను బట్టి రక రకాల ఉపమానాల ద్వారా జీవితపు విలువలను జతచేస్తూ భోధన జరిగేది. దీనివల్ల వారిలో సానుకూల దృక్పదం, సామర్థ్యం కలగడాన్నే విలువలతో కూడిన విద్యగా చెప్పుకోవచ్చు. నిజానికి విలుపతో కూడిన విద్య అంటే ఒకరికొకరు విలువలను వినిమయం చేసుకొనే ప్రక్రియ. ఈ ప్రక్రియ మానవ సమాజంలో కావుచ్చు తమ సొంత శ్రేయస్సు కోసం కావచ్చు. వీటిని కాపాడుకోవాలంటే విలువలను లక్ష్యం కలిగిన వారికే మాత్రమే సాధ్యం అవుతుంది.

విలువల విద్యను ప్రధానంగా మూడు అంశాలుగా విభజించవచ్చు.

సాధరణ అంశాలతో కూడిన విలువల విద్య

విద్యాలయాల ఆధారంగా విలువల విద్య విలువల

ప్రపంచ వ్యాప్తంగా విలువలతో కూడిన విద్య ఉదాహరణలు.

సాధారణ అంశాలతో కూడిన విలువల విద్య : సాధారణంగా ప్రజలు సమాజంలో కానసాగించడంలోనూ, మత పద్ధతలును పాటించడం లోను చట్ట పరమైన కొన్ని పద్ధతులతకు లోబడి వ్యవహరించి తీరాలి. అయితేఇవి ఒక్కో సారి వారిలో విచక్షణ కలిగి ఉన్నందువల్ల మంచి, చెడులను గ్రహించే గల్గుతారు. అలాగే విద్యార్థులను అప్పుడప్పుడూ నేరుగా సమాజంలోకి వారిని తీసుకొని వెళ్ళడం వల్ల అనేక సంఘటనలు వారి అనుభవంలోకి వస్తుంటె. ముఖ్యంగా సమాజంలోని అనేక రుగ్మతలు వల్ల ఏర్పడ్డ సాంఘిక అసమానతలు, ఇంకా అనేక విషయాలను ప్రత్యక్షంగా చూడడం వల్ల తార్కికమైన ఆలోచనలకు తెర తీస్తారు. ఆక్రమంలో తమకంటూ కొన్ని విలువలను ఆపాదించుకుంటారు. ఇలా సంక్రమించిన విలవలనే సాధారణ అంశాలతో కూడిన విలువల విద్యని అంటారు.

విద్యాలయాల ఆధారంగా విలువల విద్య :

నిజానికి ఈ దేశానికి క్రైస్తవం వచ్చిన తరువాత మత వ్యాప్తిలో భాగంగా అనేక విద్యాలయాలు నెలకొల్పబడ్డాయి. ఈ సంస్థల్లో చదివిన విద్యార్థులకు జీవితానికి అవసరమైన ఎన్నో విలువలతో కూడిన విద్యను అందించారు. ప్రేమ ఆదరణ, పొరుగువారి పట్ల దయా గుణం, క్షమించే గుణం, సేవాగుణం తల్లితండ్రుల పట్ల, దేశం పట్ల భాద్యత కలిగి ఉండడం, దైవభక్తి ఇలా అనేక అంశాలతో కూడిన విద్యను అందించడం వల్ల వారికి ప్రాదమిక దశనుండే ఉన్నత విలువలు కలిగి ఉండటానికి మార్గం చూపినట్లినది. అలాగే చాలా కాలం నుండి బ్రహ్మ కుమారి విద్యాలయాలు కూడా ఈ లక్ష్యం తో సమాజానికి ఉన్నత విలువలను భోధిస్తోంది. ఐక్యత, శాంతి, ఆనందం, వినయం, సరళత, నమ్మకం, స్వేచ్ఛ, సహకారం, నిజాయితీ, మొదలైన అనేక అంశాలను భోధిస్తున్నారు.

అలాగే 1995 హ్యూమన్ వాల్యూస్ ఎడ్యుకేషన్ తర్వాత పాఠ్యప్రణాళికలో " మానవ విలువలలో విద్య" ను ప్రవేశ పెట్టింది. ఈ ప్రణాళిక ద్వారా కథలు చెప్పించడం. ఉల్లేఖనాలు, గుంపులుగాఆ కలిసి పాడటం, అభ్యాస ప్రక్రియను అలవాటు చేయడం దీని లక్ష్యం ఈ క్రమంలో నేర్చుకున్న విలువలు తదనంతర కాలంలో సృజనాత్మకమైన, విధ్వంశకమైన జీవాలని పొందడానికి వీలు కలుగుతుంది. ఈ లక్ష్యంతో ఆంధ్రప్రదేశ్ ప్రభుత్వం ఉన్నత విద్యా పాఠ్య ప్రణాళికలో విలువలను విద్యనైచ్ఛిక అంశంగా ప్రవేశ పెట్టింది.

విలువల విద్యకు ఉదాహరణలు :

మన దేశంలో మానవ వనరుల అభివృద్ధి మంత్రిత్వ శాఖ పాఠశాల స్థాయి నుండి కళాశాల స్థాయి వరకు విలువలతో కూడిన విద్యను ప్రోత్సహిస్తోంది. అందుకోసం ఉపాధ్యాయులకు,అధ్యాపకులకు ప్రత్యేకమైన శిక్షణను అందిస్తోంది. ప్రపంచ దేశాలు విలువల విద్యకు ప్రత్యేక నిధులు కేటాయించడం, శిక్షణ సంస్థలను నెలకొల్పడం జరుగుతోంది.

ఇలాంటి జాతీయ సదస్సులు ఇలాంటి అంశంతో నిర్వహించడం అభినందనీయం.

ఉపయుక్త గ్రంధాలు :-

విద్య సంస్కృతి మరియు విలువలు యం. లీసేస్టర్

విద్యలో విలువలు మరియు విలువలతో విద్య లండన్ స్మార్ ప్రెస్

పాఠశాలలో నైతికవిద్య మియు తత్వ శాస్త్రం యస్. ఏ. వి.ఇ.టి పేపర్స్

నైతిక విద్యగా ఫిలసాఫికల్ టీచింగ్ జర్నల్ ఆఫ్ మోరల్ ఆఫ్ మోరల్ ఎడ్యుకేషన్

HEAT TRANSFER IMPACTS ON CASSON FLUID FLOW

Dr. B Suseelavathi [1]*, Dr. K Moses [2] , Dr Y A S J Prasanna kumari [3] and Dr Ch Vijaya Kumari [4]

[1] Department of Mathematics, S.S. & N. College, Narasaraopet- 522601, A.P. (INDIA)

[2]Department of Mathematics, Andhra Christian College, Guntur- 522001, A.P. (INDIA)

[3]Department of Chemistry, S.S. & N. College, Narasaraopet- 522601, A.P. (INDIA

[4]Department of Physics, S.S. & N. College, Narasaraopet- 522601, A.P. (INDIA)

[*]E-mail: lathabyneni@ gmail.com

Introduction

Ahmadi and Gerold[1] studied on the influence of flow rate, flow behaviour, and particle attention on the heat transfer coefficient of a CuO/water nanofluid each experimentally and theoretically and proved enormous enhancement in the heat transfer coefficient relative to the low concentrations. Buongiorno [2] proposed an alternative rationalization for the extraordinary heat transfer coefficient increases. Hady et al.[3] explored with the flow and heat transfer characteristics of a viscous nanofluid over a nonlinearly stretching sheet in the presence of thermal radiation, covered in the energy equation, and variable wall temperature.Nadeem et al. [4] introduced the modelling of a two-dimensional Williamson fluid for a stretching sheet.Hayat et al. [5] modelled and analyzed by the usage of Rheological expressions of Williamson fluid , the consequence of chemically reactive flow of nanomaterial, involves thermophoresis and Brownian motion.

The intention of the present work is to attain a numerical solution to the boundary layer flow, heat and mass transfer of nanofluid over a cylinder with first order velocity and convective conditions by means of the use of the fourth-order Runge Kutta integration scheme along with shooting process.

Mathematical Formulation

A regular two-dimensional laminar incompressible boundary layer flow of a Casson Williamson fluid flowing upon a stretching cylinder with thermal radiation is regarded in this

study. Let $U_w(x) = ax/l$ be denote the velocity of the surface, here $a > 0$ is a constant quantity and l is the characteristic length.

$$\tau_{ij} = \begin{cases} 2\left(\mu_f + P_y\sqrt{2\pi}\right)e_{ij} & \pi > \pi_C \\ 2\left(\mu_f + P_y\sqrt{2\pi_c}\right)e_{ij} & \pi < \pi_C \end{cases}$$

In the above equation $\pi = e_{ij}e_{ij}$ and e_{ij} denotes the $(i,j)^{th}$ component of the deformation rate, π be the product of the component of deformation rate itself, π_C be a critical value of this product based on the non-Newtonian model, μ_f be the plastic dynamic viscosity of the Casson fluid and P_y be the yield stress of the fluid.

The governing equations of the fluid flow can be written as

$$\frac{\partial(ru)}{\partial x} + \frac{\partial(ru)}{\partial r} = 0 \qquad (1)$$

$$u\frac{\partial u}{\partial x} + v\frac{\partial u}{\partial r} = \upsilon_f\left[\left(1+\frac{1}{\beta}\right)\frac{\partial^2 u}{\partial r^2} + \frac{1}{r}\frac{\partial u}{\partial r} + \frac{\Gamma}{\sqrt{2}r}\left(\frac{\partial u}{\partial r}\right)^2 + \sqrt{2}\Gamma\frac{\partial u}{\partial r}\frac{\partial^2 u}{\partial r^2}\right] - \frac{\sigma B_0^2}{\rho_f}u \qquad (2)$$

$$\left(u\frac{\partial T}{\partial x} + v\frac{\partial T}{\partial r}\right) = \frac{\alpha}{r}\frac{\partial}{\partial r}\left(r\frac{\partial T}{\partial r}\right) + \tau\left[D_B\frac{\partial C}{\partial r}\frac{\partial T}{\partial r} + \frac{D_T}{T_\infty}\left(\frac{\partial T}{\partial r}\right)^2\right] + \frac{1}{(\rho C_P)_f}\left(-\frac{1}{r}\frac{\partial}{\partial r}(rq_r) + \mu\left(\frac{\partial u}{\partial y}\right)^2 + \sigma B_0^2 u^2\right) \qquad (3)$$

where u and v are the components of velocity of the fluid in the $x, y-$ axes respectively, the electric charge density is σ, the magnetic induction is B_0, $\upsilon_f = \frac{\mu_f}{\rho_f}$ is the kinematic viscosity of the fluid, μ_f is the dynamic viscosity, the density of the fluid is ρ_f and T is the surface temperature parameter. The temperature on the wall is T_w and C_w is the concentration of the wall, U_w is the stretching velocity, U_∞ is the free stream velocity and the ambient is held at constant temperature T_∞ and constant concentration C_∞, q_r is the radiative heat flux. The

thermal diffusivity is $\alpha = \frac{k}{(\rho C_p)_f}$, the ratio between the effective heat capacity of the nanoparticle material and heat capacity of the base fluid is $\tau = \frac{\rho C_p}{(\rho C_p)_f}$,

$$u = U_w(x) + \left(1 + \frac{1}{\beta}\right)\frac{\partial u}{\partial r},\ v = 0,\ -k\frac{\partial T}{\partial r} = h_f(T_w - T),\ \text{at}\, r = R, \tag{5}$$

$$u \to 0,\ T \to T_\infty,\ \text{as}\, r \to \infty$$

q_r is the radiative heat flux and by using the Roseland approximation it is written as:

$$q_r = -\frac{-4\sigma_s}{3k_e}\frac{\partial T^4}{\partial r} \tag{6}$$

Where σ_s the Stephen Boltzmann constant and the mean absorption coefficient are is k_e.

The term T^4, is written as a linear combination of temperature. Taylor series may be used forexpanding T^4, about a free stream temperature T_∞ and deleting terms of higher-order, we obtain:

$$T^4 \cong 4T_\infty^3 T - 3T_\infty^4 \tag{7}$$

Then the radiation term in equation (3) converted to the following form

$$\frac{\partial q_r}{\partial r} = -\frac{16\sigma_s T_\infty^3}{3k_e}\frac{\partial^2 T}{\partial r^2} \tag{8}$$

Substituting equations (6) and (8), equation (3) gets modified as

$$u\frac{\partial T}{\partial x} + v\frac{\partial T}{\partial r} = \left(\alpha + \frac{16\sigma_s T_\infty^3}{3k_e(\rho C_p)_f}\right)\frac{\partial^2 T}{\partial r^2} + \frac{1}{r}\left(\alpha + \frac{16\sigma_s T_\infty^3}{3k_e(\rho C_p)_f}\right)\frac{\partial T}{\partial r}$$
$$+\tau\left[D_B\frac{\partial C}{\partial r}\frac{\partial T}{\partial r} + \frac{D_T}{T_\infty}\left(\frac{\partial T}{\partial r}\right)^2\right] + \frac{1}{(\rho C_P)_f}\left(\mu\left(\frac{\partial u}{\partial r}\right)^2 + \sigma B^2 u^2\right) \tag{9}$$

Let $\psi(x,r)$ be a stream function in the flow field. Here $u = \frac{1}{r}\frac{\partial \psi}{\partial r}, v = -\frac{1}{r}\frac{\partial \psi}{\partial x}$.

Theequationof continuity (1) is satisfied by the above functions.

The suitable similarity transformations are considered as:

$$\eta=\sqrt{\frac{a}{l\upsilon_f}}\left(\frac{r^2-R^2}{2R}\right),\psi=\sqrt{\frac{a\upsilon_f}{l}}\,xRf(\eta),\theta(\eta)=\frac{T-T_\infty}{T_w-T_\infty}$$

$$Nt=\tau D_T\frac{T_w-T_\infty}{T_\infty\upsilon_f},Nb=\tau D_B\frac{C_w-C_\infty}{\upsilon_f},M=\frac{\sigma B_0^2 l}{\rho_f a},\quad Rd=\frac{4\sigma_s T_\infty^3}{k_e k},\ \Pr=\frac{\upsilon_f}{\alpha},\tag{10}$$

Using these similarity transformations, the governing equations (2), (3) and (9) aretransformed into the following form:

$$\left(1+\frac{1}{\beta}\right)(1+2n\eta)f'''+n\left(2+\frac{1}{\beta}\right)f''+ff''-f'^2-Mf'$$
$$+\frac{3}{2}(1+2n\eta)^{\frac{1}{2}}n\lambda f''^2+\lambda(1+2n\eta)^{\frac{3}{2}}f''f'''=0\tag{11}$$

$$(1+\frac{4}{3}\mathrm{Rd})\left((1+2n\eta)\theta''+2n\theta'\right)$$
$$+\Pr\left(f\theta'-f'\theta+Ecf''^2+M\,Ec\,f'^2+(1+2n\eta)(Nb\theta'\phi'+\mathrm{Nt}\,\theta'^2)\right)=0\tag{12}$$

Here n is the Curvature parameter, M is the Hartmann number, the radiation parameter is Rd, $\Pr$ is the Prandtl number, Sc is the Schmidt number, the thermophoresis parameter is Nt, Nb are the Brownian motion parameter and λ Wiesenberger number. Now the boundary conditions become to the following form:

$$\left.\begin{aligned}&f(0)=0,f'(0)=1+\alpha_1\left(1+\frac{1}{\beta}\right)f''(0),\theta'(0)=-\mathrm{Bi}_1(1-\theta(0)),\\&\text{at }\eta=0,\\&f'(\eta)\to0,\theta(\eta)\to0,\text{ as }\eta\to\infty\end{aligned}\right\}\tag{14}$$

Where $\alpha_1 = \frac{r}{R}\sqrt{\frac{a}{l\upsilon_f}}$ the first-order velocity is slip parameter, $\mathrm{Bi}_1 = \frac{h_f}{k}\frac{R}{r}\sqrt{\frac{l\upsilon_f}{a}}$ is the thermalBiot number $\mathrm{Bi}_2 = \frac{k_m}{D_m}\frac{R}{r}\sqrt{\frac{l\upsilon_f}{a}}$ is the concentration Biot number. The skin frictioncoefficient C_f, the local Nusselt number Nu_x and the local Sherwood number Sh_x arestudied. These parameters denote the surface drag, wall heat transfer rate and mass transferrate respectively. The definitions of these quantities are given by:

$$C_f = \frac{2\tau_w}{\rho_f U_w^2}, Nu_x = \frac{xq_x}{k\left(T_w - T_\infty\right)}, \tag{15}$$

In which $\tau_w = \left(1+\frac{1}{\beta}\right)\mu_f\left(\frac{\partial u}{\partial r}\right)_{r=R}, q_w = -k\left(1+\frac{16\sigma_s T_\infty^3}{3k_e k}\right)\left(\frac{\partial T}{\partial r}\right)_{r=R},$

$$q_m = -D_B\left(\frac{\partial T}{\partial r}\right)_{r=R} \tag{16}$$

While the non-dimensional definitions of skin friction coefficient, Nusselt number andSherwood number are written as:

$$\mathrm{Re}_x^{\frac{1}{2}} C_f = \left(1+\frac{1}{\beta}\right) f''(0), \mathrm{Nu}_x\, \mathrm{Re}_x^{-\frac{1}{2}} = -\left(1+\frac{4}{3}Rd\right)\theta'(0), \tag{17}$$

Where $\mathrm{Re}_x = \frac{U_w(x)x}{\upsilon_f}$ is the local Reynolds number?

Results and Discussion

This study analyzes the impacts of the important physical parameters on dimensionless velocity, temperature distribution, and non-dimensional concentration profiles with the help of the graphs and tables. To obtain the desired accuracy, we have compared our results with previously published results by Gnaneswara Reddy et al. [6].Our results agreed with the previous results as illustrated in **Table 1**The following values are taken for important parameters in calculation.

$$M = Rd = 0.5,\ \alpha_1 = Bi_1 = Bi_2 = \beta = Nt = Nb = \lambda = 0.1,\ \mathrm{Pr} = 3,\ Sc = 10,\ n = 0.12$$

Table 1: Comparison of values of Skin friction coefficient $-f''(0)$ with previous results, when $\Pr = \alpha_1 = Bi_1 = Bi_2 = Nt = Sc = Rd = \beta = \lambda = 0,\ Nb = 0.000001, n = 0.12$

M	Gnaneswara Reddy et al. [22]	Present results
0	-1	-1
0.5	1.1180331	1.1180332
1.0	1.4142135	1.4140133
5.0	2.4494896	2.4414678
10.0	3166241	3166231

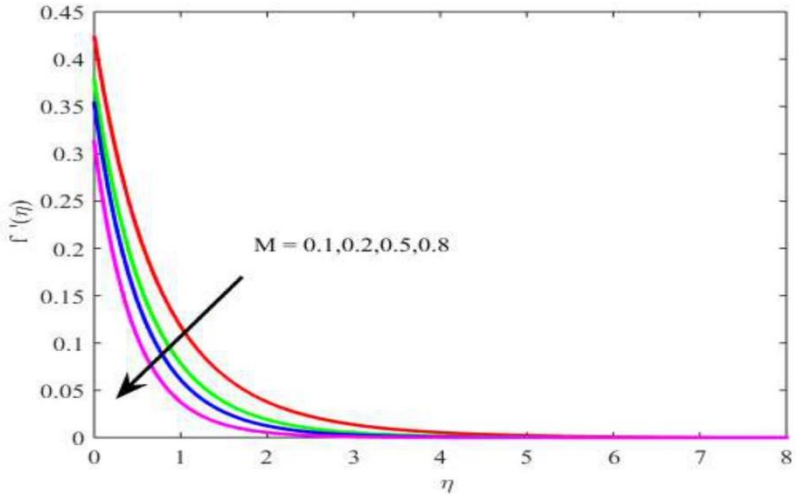

Fig.2 Influence of M on velocity profile.

Fig.2 exhibits the decreasing nature of the velocity profile $f'(\eta)$ and also the boundary layer thickness for higher values of M . This indicates that the increase in M helps to thin of the boundary layer. The velocity profiles exponentially reduce to zero at shorter distances from the sheet for growing values of M .

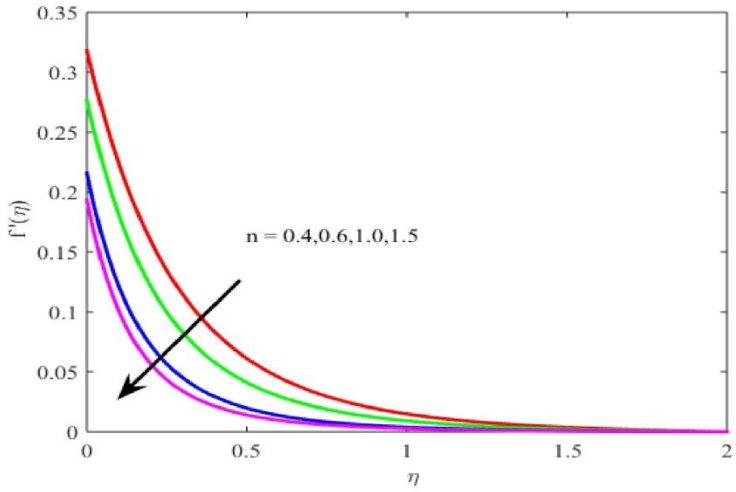

Fig.3 Influence of n on velocity profile.

Fig.3 shows the impact of the curvature parameter on non-dimensional velocity distribution $f'(\eta)$. A rise in the curvature parameter results , decrease in the nondimensional velocity. Resistance force is created by the magnetic field on the fluid in the boundary layer. This force causes restriction to the motion of the fluid. So the magnetic parameter reduces the dimensionless velocity.

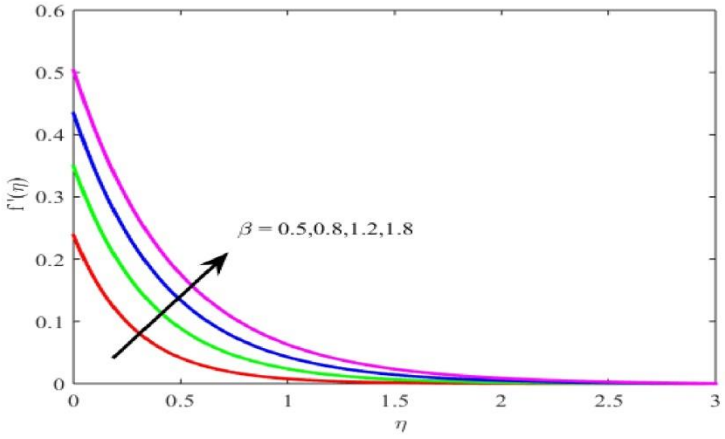

Fig.4 Influence of β on velocity profile.

Fig.4 explicates the increasing nature of velocity profile for rising values of Casson fluid parameter.

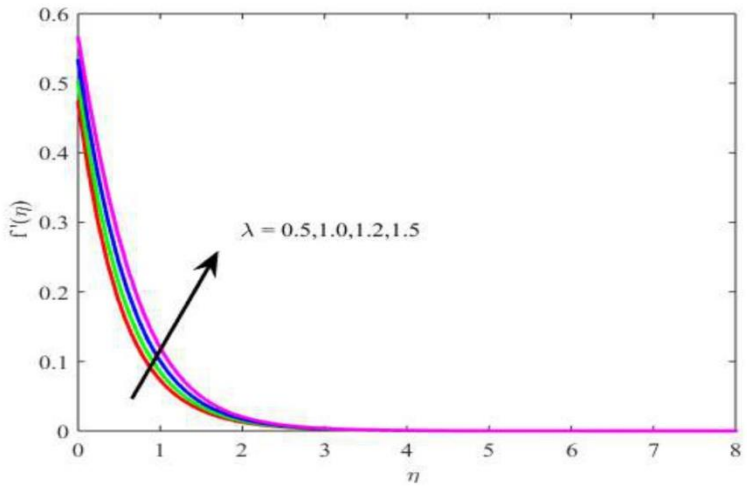

Fig.5 Influence of λ on velocity profile.

Fig.5 illuminates the effect the Wiesenberger number λ on velocity profile. It depicts the velocity profile increased with the increment of λ .

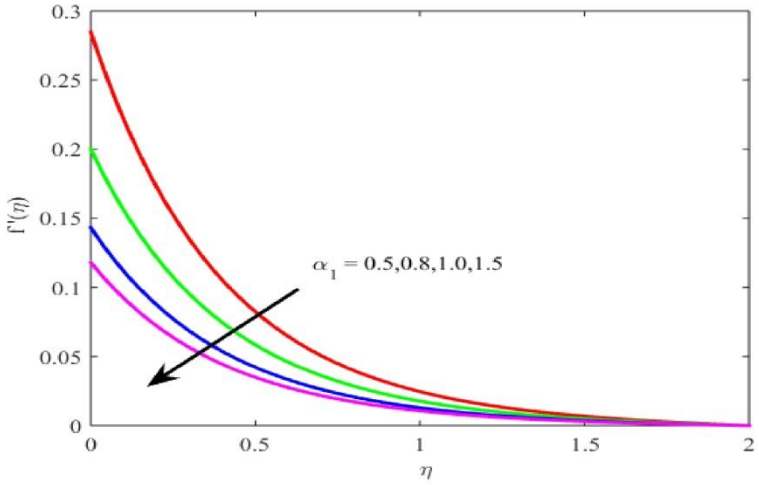

Fig.6 Influence of α_1 on velocity profile.

Fig.6 explains the influence of first-order velocity slip parameter on the dimensionless velocity profile $f'(\eta)$. The dimensionless velocity profile $f'(\eta)$ decreases with increasing values of the first-order velocity slip parameter α_1.

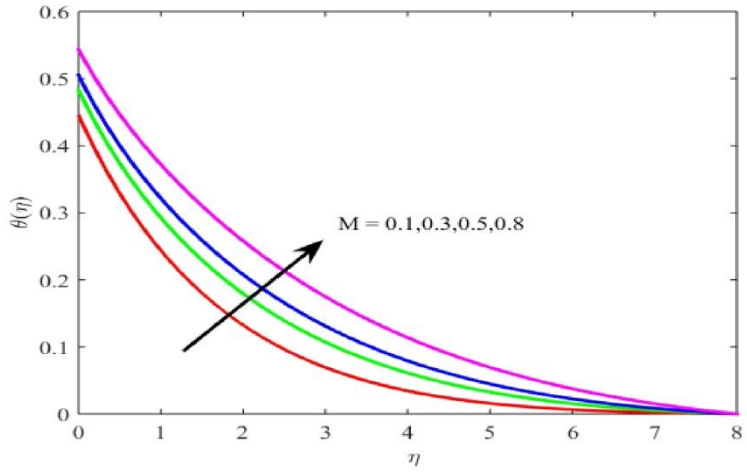

Fig.7 Influence of M on temperature profile.

Fig.7 represents the impact of the magnetic parameter on energy distribution. The effect of magnetic field reduces the fluid velocity whereas it intensifies thermal boundary layer thickness. Thermal energy is defined as an additional work done required for dragging the fluid under the influence of the magnetic field. Thermal energy heats up the conducting fluid and upgrades the temperature profile. Thus, the magnetic field in the flow regime intensifies the thermal boundary layer thickness.

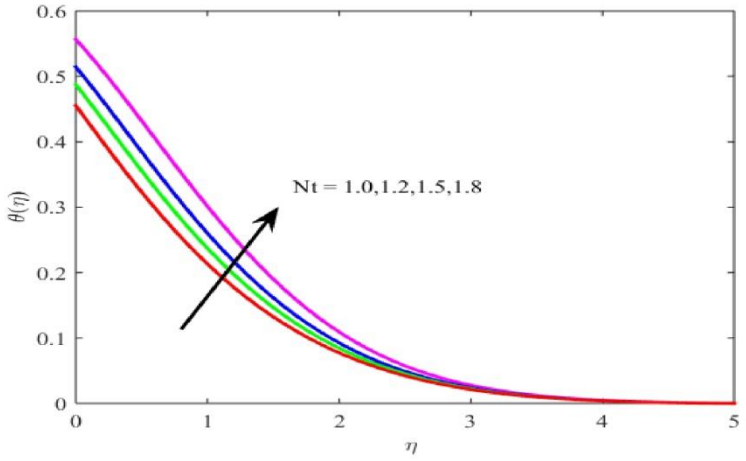

Fig.8 Influence of Nt on temperature profile.

Fig.8 exhibits the influence of the thermophoresis parameter on temperature profile. The energy distribution grows with increment in the values of the thermophoresis parameter.

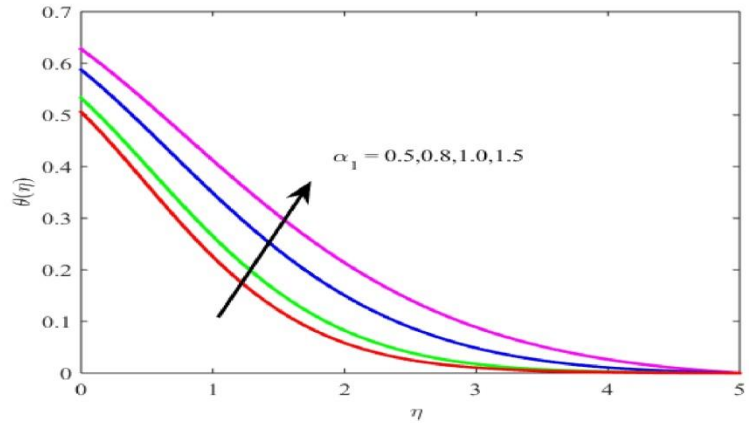

Fig.9 Influence of α_1 on temperature profile.

The impact of first-order velocity slip parameter on temperature profile is explained in Fig.9, the temperature rises with a rising in first-order velocity slip parameter.

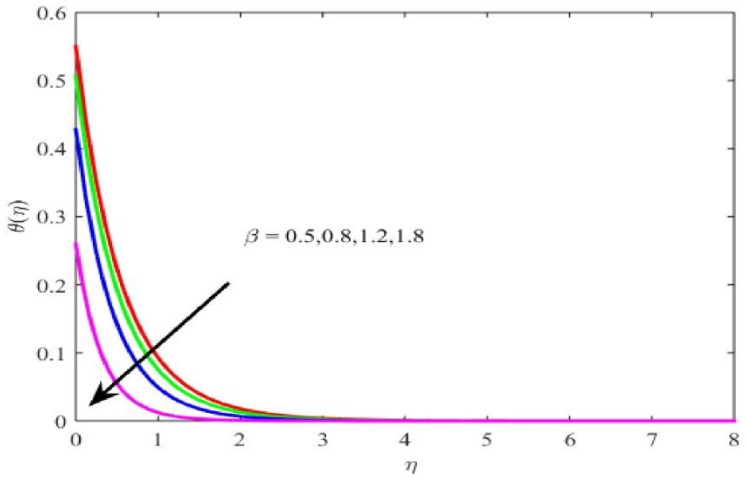

Fig.10 Influence of β on temperature profile.

Fig.10 exhibits the influence of Casson fluid parameter on temperature profile. There is a decrease in temperature profile for increasing values of Casson fluid parameter.

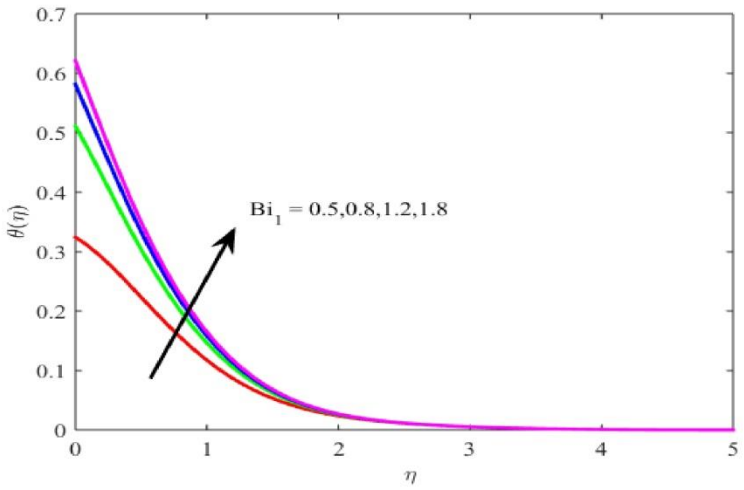

Fig.11 Influence of Bi_1 on temperature profile.

Fig.11 represents the influence of thermal Biot number on temperature profile. There is an increment in temperature profile for increasing values of thermal Biot number.

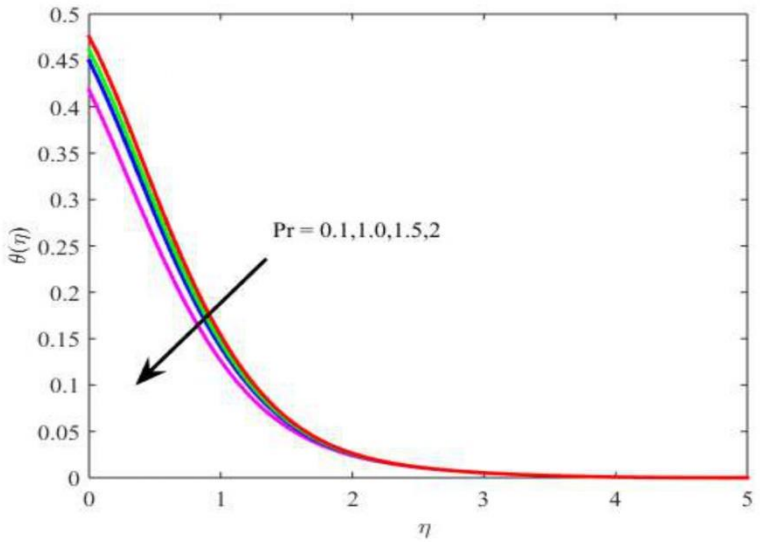

Fig.12 Influence of Pr on temperature profile.

The impact of Prandtl number on the thermal boundary layer is drawn in Fig.12 the Prandtl number is a material property. This number varies from one fluid to another fluid. It is inversely proportional to thermal conductivity and directly proportional to viscosity. Increasing values of this number reduce the thermal diffusivity. Consequently, the heat flows below the fluid. And the thermal boundary layer thickness reduces with growing values of

5 CONCLUSION

In the present chapter, the numerical investigations have been carried out the boundary layerflow, heat transfer of Williamson Casson nanofluid over a cylinder with first-order velocity slip,thermal and concentration Biot numbers. Discussion about the impacts of different emergingparameters on velocity profile $f'(\eta)$, temperature distribution $\theta(\eta)$, theskin friction coefficient, Nusselt number is done with the help of plotsand numerical results are tabulated. The key observations of this studyare shortly written as:

1.Thenvelocity intensifies with increasing values of Casson parameter, Weissenberg number and a reverse behavior is found to be true with increasing values of Magnetic parameter, curvature parameter, first order velocity slip parameter.

2. The temperature intensifies with increasing values of the magnetic parameter, thermophoresis parameter, first order velocity slip parameter, thermal Biot number, Radiation parameter. While the opposite nature is traced out with the growing values of Casson parameter, Prandtl number, Weissenberg number.

References

1. Computational Fluid Dynamics Modeling of Momentum and Heat Transfer in Nanofluids Masoudeh Ahmadi and Gerold A. Willing

2. Convective Transport in Nanofluids by J. Buongiorno

3. Radiation effect on viscous flow of a nanofluid and heat transfer over a nonlinearly stretching sheet by Hady

4. Flow of a Williamson fluid over a stretching sheet by Nadeem and Hussain

5. MHD 2D flow of Williamson nanofluid over a nonlinear variable thicked surface with melting heat transfer by T. Hayat, Gulnaz Bashir, M. Waqas, A. Alsaedi

6. Comparative analysis on non-linear radiative heat transfer on MHD Casson nanofluid past a thin needle by MG Reddy,B Souayeh, P Sreenivasulu, T Poornima, M Rahimi-Gorji, (Journal of Molecular Liquids)

Journal of Physics: Conference Series

On FNS - Compactness in Fuzzy Neutrosophic Supra Topological Spaces

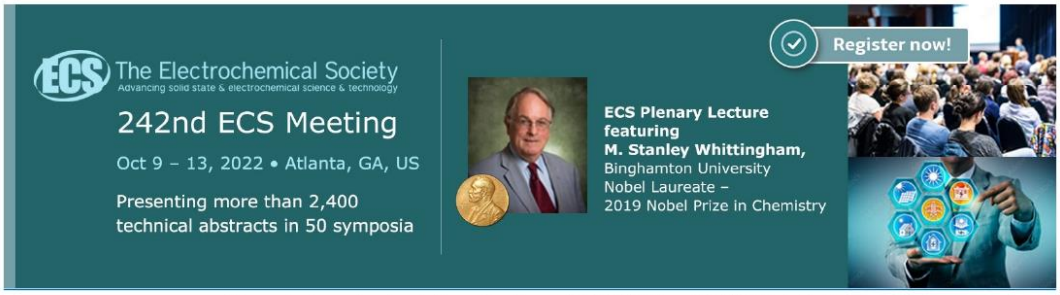

ON FNS - COMPACTNESS IN FUZZY NEUTROSOPHIC SUPRA TOPOLOGICAL SPACES

V Amarendra Babu[1,4] and J Aswini[2,5], K Moses[3,6]

[1] Department of Mathematics, Acharya Nagarjuna University, Nagarjuna Nagar, A.P- India,
[2] Department of Mathematics, Acharya Nagarjuna University, Nagarjuna Nagar, A.P- India,
[3] Department of Mathematics, Andhra Christian Degree & PG Collage Guntur, A.P- India,
[4]amarendrab4@gmail.com
[5]aswinijampana9@gmail.com
[6]kommalapati26@gmail.com

Abstract: In this paper, we introducing fuzzy neutrosophic supra first countable (FNS - FCS), fuzzy neutrosophic supra second countable (FNS- SCS) and fuzzy neutrosophic supra compactness (FNS- compactness), fuzzy neutrosophic supra Q^{μ} - compactness (FNS - Q^{μ} - compactness) in fuzzy neutrosophic supra topological space (FNSTS). we derive the union of two FNS – compact spaces is also FNS – compact space and similarly the union of two FNS -Q^{μ} - compact spaces is also FNS - Q^{μ} - compact space. Also we define some theorems using finite intersection property and productive property. Finally we observe that our notions preserve under one – one, onto and continuous mapping.

1. Introduction: In 1965, Zadeh [9] introduced the notion of fuzzy sets. The study of fuzzy topological spaces was first initiated by chang [4] in 1968. K. Atanassov [8] introduced the notion of intuitionistic fuzzy sets (Ifs) in 1986. Later Coker [5,6] introduced intuitionistic fuzzy topological space. In 1983[2], Mashhour et al. introduced the concepts of supra topological spaces, supra open sets& supra closed sets. Later on 1987, ME Abd El-Monsef et al [10] introduced the concept of fuzzy supra topological as a natural generalization of the notion of supra topological spaces.

In 2002, Florentin Smarandache [15] introduced the extend the IFsets into Nsets. Nset is classified into 3 independent functions. In 2012, Salama, Alblowi [1,13,14] introduced the NTY. NTSs are very natural generalizations of FTSs. In 2014, Salama, Smarandache and valeri [14] introduced the concept of neutrosophic closed sets and continuous functions. Dogen Coker [3,7]& Bayhan introduced Fuzzy-compactness in IFTSs. In 2018,2019,[11,12] Md.Aman Mahbub introduced some properties of compactness in IFTSs and On Q-Compactness in IFTSs.

In this paper two definitions of FNS - compactness in ‘fuzzy ‘neutrosophic supra ‘topological ‘space and some of their features are defined.

2. Preliminaries:

2.1. Definition:[15]Let X be a nonempty set and P is a fuzzy neutrosophic set (FNS) is an object having the form $P=\{\langle l,T_P(l),I_P(l),F_P(l)\rangle : l\in X\}$,where the functions

$T_P : X \to]^-0,1^+[$, $I_P : X \to]^-0,1^+[$, $F_P : X \to]^-0,1^+[$

denote the degree of membership function $(T_P(l))$, the degree of indeterminacy function ($I_P(l)$), and the degree of non membership ($F_P(l)$) respectively, each element $l\in X$ to the set P and

$^+0 \le T_P(l)\le I_P(l)\le F_P(l)\le 1^+$, for each $l\in X$.

A FNS $P=\{\langle l,T_P(l),I_P(l),F_P(l)\rangle : l\in X\}$ can be identified to an ordered triple $\langle l,T_P,I_P,F_P\rangle$ on $]^-0,1^+[$ on X.

2.2. Definition: [1,15] Let X be a nonempty set and the 'FNSs P & R be in the form $P=\{\langle l,T_P(l),I_P(l),F_P(l)\rangle : l\in X\}$ & $R=\{\langle l,T_R(l),I_R(l),F_R(l)\rangle : l\in X\}$ in X

1. $CO(P)=\{\langle 1-T_P(l),1-I_P(l),1-F_P(l)\rangle : l\in X\}$
2. $P\subseteq R \Leftrightarrow T_P(l)\le T_R(l), I_P(l)\le I_R(l), F_P(l)\ge F_R(l)$, for all $l\in X$,
3. $P-R=\{\langle l,T_P(l)\wedge F_R(l),I_P(l)\wedge(1-I_R(l)),F_P(l)\vee T_R(l)\rangle : l\in X\}$
4. $[]P=\{\langle l,T_P(l),I_P(l),1-T_P(l)\rangle : l\in X\}$
5. $\langle\ \rangle P=\{\langle l,1-F_P(l),I_P(l),F_P(l)\rangle : l\in X\}$
6. $0_{FN}=\langle l,0,0,1\rangle$ and $1_{FN}=\langle l,1,1,0\rangle$

2.3. Definition: [15] Let $\{P_j : j\in K\}$ be an arbitrary family of FNSs in X, where $P_j=\{\langle l,T_{P_j}(l),I_{P_j}(l),F_{P_j}(l)\rangle : l\in X\}$ then

1. $\cap P_j=\{\langle l,\wedge_{j\in K}T_{P_j}(l),\wedge_{j\in K}I_{P_j}(l),\vee_{j\in K}F_{P_j}(l)\rangle : l\in X\}$
2. $\cup P_j=\{\langle l,\vee_{j\in K}T_{P_j}(l),\vee_{j\in K}I_{P_j}(l),\wedge_{j\in K}F_{P_j}(l)\rangle : l\in X\}$

2.4. Definition: [13,17] A fuzzy neutrosophic supra topology (FNST), Let X be a nonempty set & τ^{μ} be a family of FNS subsets in X, satisfying the following axioms.

$0_{FN}, 1_{FN} \in \tau^{\mu}$

$\cup M_i \in \tau^{\mu}, \forall \{M_i : i \in K\} \subseteq \tau^{\mu}$

In the pair, (X, τ^{μ}) is said to be a Fuzzy neutrosophic supra topological space (FNSTS) and any FNSS in τ^{μ} is known as Fuzzy neutrosophic supra open set (FNSOS) in X. The element of τ^{μ} are called FNSOSs. The complement of FNSOS in the FNSTS (X, τ^{μ}) is called fuzzy neutrosophic supra closed set (FNSCS).

2.5. Definition: [3] Let M and N are IFSs on X and Y. Then the product of IFSs M and N denoted by $M \times N$ is defined by $M \times N = \{(r,t), T_M \times T_N, F_M \times F_N\}$ where $(T_M \times T_N)(r,t) = \min(T_M(r), T_N(t))$ and $(F_M \times F_N)(r,t) = \max(F_M(r), F_N(t))$ for all $(r,t) \in X \times Y$. Obviously $0 \le (T_M \times T_N) + (F_M \times F_N) \le 1$. This definition can be extended to an arbitrary family of IFSs.

2.6 .Definition: [3] Let $(X_i, Y_i), i = 1,2$ be two IFTSs. The product topology $\tau_1 \times \tau_2$ on $X_1 \times X_2$ is the IFT generated by $\{p_i^{-1}(V_i) : V_i \in \tau_i, i = 1,2\}$ where $p_i : X_1 \times X_2 \to X_i, i = 1,2$ are the projection maps and IFTS $\{X_1 \times X_2, \tau_1 \times \tau_2\}$ is called the product IFTS of $(X_i, Y_i), i = 1,2$. In this case $\delta = \{p_i^{-1}(V_i) : V_i \in \tau_i, i \in K\}$ is a sub base and $B = \{V_1 \times V_2 : V_i \in \tau_i, i = 1,2\}$ is base for $\tau_1 \times \tau_2$ in $X_1 \times X_2$

2.7. Definition: [14] (i) If $M = \langle T_M, I_M, F_M \rangle$ is a NS on Y, then the preimage of M under *h*, denoted by $h^{-1}(M)$, is a NS in X defined by $h^{-1}(M) = \langle h^{-1}(T_M), h^{-1}(I_M).h^{-1}(F_M) \rangle$.
(ii) If $N = \langle T_N, I_N, F_N \rangle$ is a NS in X, then the image of N under *h*, denoted by $h(N)$, is a NS in Y defined by $h(N) = \langle h(T_N), h(I_N).h(F_N) \rangle$.

2.8 .Definition: [14] Let $(X, \tau^{\mu}), (Y, \sigma^{\mu})$ be FNTSs. A function $h : X \to Y$ is called neutrosophic Continuous, if $h^{-1}(M) \in \tau^{\mu}$ for all $M \in \sigma^{\mu}$ and *h* is called Neutrosophic Open, if $h(N) \in \sigma^{\mu}$ for all $N \in \tau^{\mu}$.

2.9. Definition: [16] A collection ϑ of NS on a set X is called basis (or base) for a NTS on X, if
(i) For each $p_N^x \in X$, there exists $E \in \vartheta$ such that $p_N^x \in E$,
(ii) If $p_N^x \in E_1 \cap E_2$, where $E_1, E_2 \in \vartheta$ then $\exists E_3 \in \vartheta$ such that $p_N^x \in E_3 \subseteq E_1 \cap E_2$.

2.10. Definition: [11,12](i) Let (X, τ^{μ}) be a NTS and E be a NS on X. If a family $\{\langle l, T_{E_i}, I_{E_i}, F_{E_i} \rangle : l \in K\}$ of NOSs on X satisfies the condition, $\cup \{\langle l, T_{E_i}, I_{E_i}, F_{E_i} \rangle : l \in K\} = 1_N$, then it is said to be a neutrosophic open cover of X. A finite sub family of neutrosophic open cover

$\{\langle l, T_{E_l}, I_{E_l}, F_{E_l}\rangle : l \in K\}$ of X, which is also NOC of X is called a finite sub cover of $\{\langle l, T_{E_l}, I_{E_l}, F_{E_l}\rangle : l \in K\}$.

3. FNS – First and Second countable space in FNSTS

3.1. Definition: A FNSTS (X, τ^{μ}) is called fuzzy neutrosophic supra first countable space (FNS – FCS) if for every FNP P_{FN} there exists a countable local base.

3.2. Example: Let $X = \{l, m, n\}$ and $\tau^{\mu} = \{0_{FN}, 1_{FN}, M_1, M_2, M_3\}$, where

$$M_1 = \left\{\left\langle \frac{l}{0.25}, \frac{l}{0.45}, \frac{l}{0.75}\right\rangle \left\langle \frac{m}{0.28}, \frac{m}{0.45}, \frac{m}{0.72}\right\rangle \left\langle \frac{n}{0.35}, \frac{n}{0.55}, \frac{n}{0.65}\right\rangle\right\},$$

$$M_2 = \left\{\left\langle \frac{l}{0.45}, \frac{l}{0.45}, \frac{l}{0.55}\right\rangle \left\langle \frac{m}{0.48}, \frac{m}{0.45}, \frac{m}{0.52}\right\rangle \left\langle \frac{n}{0.55}, \frac{n}{0.55}, \frac{n}{0.45}\right\rangle\right\} \text{ and}$$

$$M_3 = \left\{\left\langle \frac{l}{0.55}, \frac{l}{0.45}, \frac{l}{0.45}\right\rangle \left\langle \frac{m}{0.65}, \frac{m}{0.45}, \frac{m}{0.35}\right\rangle \left\langle \frac{n}{0.75}, \frac{n}{0.55}, \frac{n}{0.25}\right\rangle\right\}. \text{ Then } (X, \tau^{\mu}) \text{ is a FNSTS.}$$

Let $P_{FN} = \left\{\left\langle \frac{l}{0.35}, \frac{l}{0.45}, \frac{l}{0.65}\right\rangle \left\langle \frac{m}{0.38}, \frac{m}{0.45}, \frac{m}{0.62}\right\rangle \left\langle \frac{n}{0.45}, \frac{n}{0.55}, \frac{n}{0.55}\right\rangle\right\}$ be a FNP.

$\mathrm{H}(P_{FN}) = \{V_1, V_2\}$, where $V_1 = \left\{\left\langle \frac{l}{0.45}, \frac{l}{0.45}, \frac{l}{0.55}\right\rangle \left\langle \frac{m}{0.48}, \frac{m}{0.45}, \frac{m}{0.52}\right\rangle \left\langle \frac{n}{0.55}, \frac{n}{0.55}, \frac{n}{0.45}\right\rangle\right\}$,

$$V_2 = \left\{\left\langle \frac{l}{0.55}, \frac{l}{0.45}, \frac{l}{0.45}\right\rangle \left\langle \frac{m}{0.65}, \frac{m}{0.45}, \frac{m}{0.35}\right\rangle \left\langle \frac{n}{0.75}, \frac{n}{0.55}, \frac{n}{0.25}\right\rangle\right\}.$$

Write $\mathrm{N}^{*} = \left\{\left\langle \frac{l}{0.85}, \frac{l}{0.55}, \frac{l}{0.25}\right\rangle \left\langle \frac{m}{0.88}, \frac{m}{0.55}, \frac{m}{0.22}\right\rangle \left\langle \frac{n}{0.95}, \frac{n}{0.55}, \frac{n}{0.15}\right\rangle\right\}$ is a FNSNHD of FNP P_{FN}.

Then $V_1, V_2 \subseteq \mathrm{N}^{*}$. Therefore $\mathrm{H}(P_{FN})$ is local base of FNP P_{FN}. Hence (X, τ^{μ}) is FNS – FCS.

3.3. Theorem: Let (X, τ^{μ}) & (Y, δ^{μ}) are any FNSTSs and $h : X \to Y$ is onto Open and FNS – continuous mapping. If (X, τ^{μ}) is FNS – FCS then (Y, δ^{μ}) is also FNS – FCS.

Proof: Suppose ${P_{FN}}^{y}$ is a FNP on Y. Since $h : (X, \tau^{\mu}) \to (Y, \delta^{\mu})$ is onto then $\exists$ FNP ${P_{FN}}^{y} \in Y \ni h({P_{FN}}^{x}) = {P_{FN}}^{y}$. Since (X, τ^{μ}) is FNS – FCS then $\exists$ a countable local base. Say H of ${P_{FN}}^{x}$. We have to prove that h (H) has a countable local base in Y at ${P_{FN}}^{y}$. Since H is countable, so h (H) is countable. Let N be a FNSNHD of ${P_{FN}}^{y}$.

Since h is FNS – continuous then h^{-1} (N) $\in \tau^{\mu}$ such that ${P_{FN}}^{x} \in h^{-1}$ (N) & $\exists$ $\mathrm{H}^{*} \in$ H such that ${P_{FN}}^{x} \in \mathrm{H}^{*} \subseteq$

h^{-1} (N). Since h is open, $h(P_{FN}{}^{x}) \in h$ (H) $\subseteq$ N. So $P_{FN}{}^{y} \in h(\mathrm{H}^{*}) \subseteq$ G. Hence h (H) is countable local base for Y. Therefore (Y, δ^{μ}) is also FNS – FCS.

3.4. Definition: A FNSTS (X, τ^{μ}) is called fuzzy neutrosophic supra second countable space (FNS – SCS) if it has a countable base.

3.5. Example: Let $X = \{p, q, r\}$ and $\tau^{\mu} = \{0_{FN}, K, L, M, 1_{FN}\}$, where

$$K = \left\{\left\langle \frac{l}{0.24}, \frac{l}{0.45}, \frac{l}{0.76}\right\rangle \left\langle \frac{m}{0.34}, \frac{m}{0.45}, \frac{m}{0.66}\right\rangle \left\langle \frac{n}{0.44}, \frac{n}{0.55}, \frac{n}{0.56}\right\rangle\right\},$$

$$L = \left\{\left\langle \frac{l}{0.46}, \frac{l}{0.45}, \frac{l}{0.54}\right\rangle \left\langle \frac{m}{0.48}, \frac{m}{0.45}, \frac{m}{0.52}\right\rangle \left\langle \frac{n}{0.54}, \frac{n}{0.55}, \frac{n}{0.46}\right\rangle\right\} \text{ and}$$

$$M_3 = \left\{\left\langle \frac{l}{0.58}, \frac{l}{0.45}, \frac{l}{0.42}\right\rangle \left\langle \frac{m}{0.64}, \frac{m}{0.45}, \frac{m}{0.36}\right\rangle \left\langle \frac{n}{0.74}, \frac{n}{0.55}, \frac{n}{0.26}\right\rangle\right\}. \text{ Then } (X, \tau^{\mu}) \text{ is a FNSTS.}$$

Let $P_{FN} = \left\{\left\langle \frac{l}{0.34}, \frac{l}{0.45}, \frac{l}{0.66}\right\rangle \left\langle \frac{m}{0.38}, \frac{m}{0.45}, \frac{m}{0.62}\right\rangle \left\langle \frac{n}{0.44}, \frac{n}{0.55}, \frac{n}{0.56}\right\rangle\right\}$ be a FNP.

Here $P_{FN} \in L \subseteq \mathrm{N}^{*}$ and $P_{FN} \in M \subseteq \mathrm{N}^{*}$, where $\mathrm{N}^{*} = \{\mathrm{N} / \mathrm{N} \supseteq \mathrm{L} \,\&\, \mathrm{M}\}$. Then H = {L & M} is countable base for τ^{μ}. Hence (X, τ^{μ}) is FNS – SCS.

3.6. Theorem: Let (X, τ^{μ}) & (Y, δ^{μ}) are any FNSTSs and $h : X \to Y$ is onto Open and FNS – continuous mapping. If (X, τ^{μ}) is FNS – SCS then (Y, δ^{μ}) is also FNS – SCS.

Proof: Suppose (X, τ^{μ}) is a FNS – SCS. Then H is countable base for τ^{μ}, h (H) is countable collection in Y. Now show that h (H) is countable base for τ^{μ}. Let V be a FNSNHD of FNP $P_{FN}{}^{y} \in Y$. So $P_{FN}{}^{y} \in V$ and since h is onto $\exists P_{FN}{}^{x} \in X \ni h\left(P_{FN}{}^{x}\right) = P_{FN}{}^{y} \in V$. So $P_{FN}{}^{x} \in h^{-1}(V)$ is FNSNHD of (X, τ^{μ}) and it is FNS – SCS then $\exists\, \mathrm{H}^{*} \in \mathrm{H}$ & $\mathrm{H} \subseteq \tau^{\mu}$ such that $P_{FN}{}^{x} \in \mathrm{H} \subseteq h^{-1}$ (V). So $h\left(P_{FN}{}^{x}\right) \in h\,(\mathrm{H}^{*}) \subseteq$ V. So $P_{FN}{}^{y} \in h\,(\mathrm{H}) \subseteq$ V. Hence h (H) is countable base for τ^{μ}. Therefore (Y, δ^{μ}) is also FNS – SCS.

4. FNS - Compactness in FNSTS

In this section we define two definitions of fuzzy neutrosophic supra compactness (FNS – Compact) in fuzzy neutrosophic supra topological space (FNSTS) and established several 'properties of such notions'.

4.1. Definition: Let (X, τ^{μ}) be a FNSTS. A family $\{G_k : k \in K\}$ of 'fuzzy neutrosophic supra open sets in X satisfies the condition, $\bigcup \{G_k : k \in K\} = 1_{FN}$. Then it is called fuzzy neutrosophic supra open cover (FNS – O – C) of X.

4.2. Example: Let $X=\{l,m\}$ and $\tau^{\mu}=\{0_{FN},1_{FN},\gamma_1,\gamma_2,\gamma_3,\gamma_4\}$, where

$\gamma_1=\left\{\left\langle\frac{l}{1},\frac{l}{1},\frac{l}{0.15}\right\rangle\left\langle\frac{m}{1},\frac{m}{1},\frac{m}{0.10}\right\rangle\right\}$, $\gamma_2=\left\{\left\langle\frac{l}{0.66},\frac{l}{0.45},\frac{l}{0.34}\right\rangle\left\langle\frac{m}{0.74},\frac{m}{0.45},\frac{m}{0.26}\right\rangle\right\}$,

$\gamma_3=\left\{\left\langle\frac{l}{0.77},\frac{l}{0.54},\frac{l}{0.23}\right\rangle\left\langle\frac{m}{0.82},\frac{m}{0.54},\frac{m}{0.25}\right\rangle\right\}$ and $\gamma_4=\left\{\left\langle\frac{l}{0.85},\frac{l}{0.55},\frac{l}{0}\right\rangle\left\langle\frac{m}{0.95},\frac{m}{0.55},\frac{m}{0}\right\rangle\right\}$.

Then (X,τ^{μ}) is a FNSTS and $\cup\{\gamma_k:k=1,2,3,4\}=1_{FN}$. Hence $\{\gamma_1,\gamma_2,\gamma_3,\gamma_4\}$ is FNS – open cover in X.

4.3. Definition: Let (X,τ^{μ}) be a FNSTS. A finite sub family of fuzzy neutrosophic supra open cover $\{G_k:k\in K\}$ on X, which is also a fuzzy neutrosophic supra open cover of X, is called fuzzy neutrosophic supra finite sub cover (FNS – F – SC) of X.

4.4. Definition: A FNSTS (X,τ^{μ}) is called FNS – Compact if each FNSO – cover of X has a FNS finite sub cover.

4.5. Example: Let $X=\{l,m\}$ and $\tau^{\mu}=\{0_{FN},1_{FN},\gamma_1,\gamma_2,\gamma_3,\gamma_4\}$, where

$\gamma_1=\left\{\left\langle\frac{l}{1},\frac{l}{1},\frac{l}{0.15}\right\rangle\left\langle\frac{m}{1},\frac{m}{1},\frac{m}{0.10}\right\rangle\right\}$, $\gamma_2=\left\{\left\langle\frac{l}{0.66},\frac{l}{0.45},\frac{l}{0.34}\right\rangle\left\langle\frac{m}{0.74},\frac{m}{0.45},\frac{m}{0.26}\right\rangle\right\}$,

$\gamma_3=\left\{\left\langle\frac{l}{0.77},\frac{l}{0.54},\frac{l}{0.23}\right\rangle\left\langle\frac{m}{0.82},\frac{m}{0.54},\frac{m}{0.25}\right\rangle\right\}$ and $\gamma_4=\left\{\left\langle\frac{l}{0.85},\frac{l}{0.55},\frac{l}{0}\right\rangle\left\langle\frac{m}{0.95},\frac{m}{0.55},\frac{m}{0}\right\rangle\right\}$.

Then (X,τ^{μ}) is a FNSTS and $\cup\{\gamma_k:k=1,2,3,4\}=1_{FN}$. Hence $\{\gamma_1,\gamma_2,\gamma_3,\gamma_4\}$ is FNS – open cover in X. And also $\{\gamma_1,\gamma_2,\gamma_4\}$ is FNS – F – SC of X. Therefore (X,τ^{μ}) is a FNS – compact.

4.6. Remark: Every fuzzy neutrosophic supra topological space need not be a FNS – compact following the example 4.7.

4.7. Example: Let $X=\{l,m\}$ and $\tau^{\mu}=\{0_{FN},1_{FN},\gamma_1,\gamma_2,\gamma_3\}$, where

$\gamma_1=\left\{\left\langle\frac{l}{0.45},\frac{l}{0.25},\frac{l}{0.65}\right\rangle\left\langle\frac{m}{0.35},\frac{m}{0.55},\frac{m}{0.75}\right\rangle\right\}$, $\gamma_2=\left\{\left\langle\frac{l}{0.65},\frac{l}{0.35},\frac{l}{0.45}\right\rangle\left\langle\frac{m}{0.75},\frac{m}{0.65},\frac{m}{0.55}\right\rangle\right\}$ and

$\gamma_3=\left\{\left\langle\frac{l}{0.55},\frac{l}{0.25},\frac{l}{0.45}\right\rangle\left\langle\frac{m}{0.45},\frac{m}{0.55},\frac{m}{0.65}\right\rangle\right\}$. Then (X,τ^{μ}) is a FNSTS but

$\cup\{\gamma_k:k=1,2,3\}=\gamma_2\neq 1_{FN}$. Hence (X,τ^{μ}) is not a FNS – compact of X.

4.8. Theorem: A FNSTS (X,τ^{μ}) is FNS – compact. Let $\eta^{\mu}\subseteq\tau^{\mu}$, then (X,η^{μ}) is also FNS – compact.

Proof: Let $\{G_k:k\in K\}$ be FNS – O – C of X. Since $\eta^{\mu}\subseteq\tau^{\mu}$, $\{G_k:k\in K\}$ be FNS – O – C of X.

Since X is FNS – compact, $\exists$ FNS – F – SC $\{G_k : k \in K\}$ of X.
This turn to show that (X, η^{μ}) is also FNS – compact.

4.9. Theorem: Let (X, τ^{μ}) be a FNSTS and M, N are FNS – compact subsets of X. Then $M \cup N$ is also FNS – compact.
Proof: Let (X, τ^{μ}) be a FNSTS and M, N are FNS – compact subsets of X. To show that $M \cup N$ is also FNS – compact. Let $\{G_k : k \in K\}$ be a FNS – O – C of both M, N and $M \cup N$. Since M, N are FNS – compact subsets of X. Then M and N have FNS – F – SC. Let $\{G_k : k = 1 \text{to} K\}$ be FNS – F – SC of M and $\{G_l : l = 1 \text{to} L\}$ be FNS – F – SC of N. Then $\cup \{G_k : k = 1 \text{to} K\} = 1_{FN}, \cup \{G_l : l = 1 \text{to} L\} = 1_{FN}$.
$\cup \{G_k : k = 1 \text{to} K + L\} = 1_{FN}$. Hence this FNS – O – C $\{G_k : k \in K\}$ contains FNS – F – SC of $M \cup N$.
Therefore $M \cup N$ is FNS – compact.

4.10. Theorem: Let (X, τ^{μ}), (Y, δ^{μ}) be FNSTSs and let $h : X \to Y$ be a FNS – continuous surjection. If (X, τ^{μ}) is FNS – compact, then (Y, δ^{μ}) is also FNS – compact.
Proof: Given that h is FNS – continuous and onto and (X, τ^{μ}) is FNS – compact.
Let us consider $\gamma_k = \{G_k : k \in K\}$ be a FNS – O – C for Y, then $\cup \gamma_k = 1_{FN}$.
Since h is FNS – continuous, $h^{-1}(\cup \gamma_k) = h^{-1}(1_{FN}) \Rightarrow \cup h^{-1}(\gamma_k) = 1_{FN}$.
Since γ_k is FNSO in Y, for every $k \in K$ as the map h is FNS – continuous.
Thus the family $\{h^{-1}(\gamma_k) : k \in K\}$ is a FNS – O – C for X and since X is FNS – compact.
Then $\exists$ a FNS – F – SC $\{h^{-1}(\gamma_j) : j = 1 \text{to} n\} \ni \cup \{h^{-1}(\gamma_j) : j = 1 \text{ to} n\} = 1_{FN}$.
Now, $h(\cup_{j=1}^{n} h^{-1}(\gamma_k)) = h(1_{FN}) \Rightarrow \cup_{j=1}^{n} h(h^{-1}(\gamma_k)) = h(1_{FN}) \Rightarrow \cup_{j=1}^{n} (\gamma_k) = 1_{FN}$, (as the map h is surjective). Therefore Y is FNS – compact space.

4.11. Theorem: Let (X, τ^{μ}), (Y, δ^{μ}) be FNSTSs and let $h : X \to Y$ be a FNS – open function and (Y, δ^{μ}) be a FNS – compact. Then (X, τ^{μ}) is FNS – compact.
Proof: Let $h : X \to Y$ be a FNS – open function and (Y, δ^{μ}) be a FNS – compact.
Let $\gamma_k = \{G_k : k \in K\}$ be a FNS – O – C for X. Since h is FNS – open function, $h(\gamma_k)$ is a FNS – O – C of Y. Since Y is FNS – compact, $h(\gamma_k)$ contains a FNS – F – SC, $\{h(\gamma_{k1}, \gamma_{k2}, \gamma_{k3}, ... \gamma_{kn})\}$. Then $\{\gamma_{k1}, \gamma_{k2}, \gamma_{k3}, ... \gamma_{kn}\}$ is a FNS – F – SC for X. Thus X is FNS – compact.

4.12. Theorem: The image of FNS – compact space under a FNS – continuous map is FNS – compact space.
Proof: Let $h : X \to Y$ be a FNS – continuous map from a FNS – compact space (X, τ^{μ}) onto a FNSTS (Y, δ^{μ}). Let $\gamma_k = \{G_k : k \in K\}$ be a FNS – O – C for (Y, δ^{μ}). Since h is FNS – continuous, $\{h^{-1}(\gamma_k) : k \in K\}$ is a FNS – O – C of (X, τ^{μ}). We know that (X, τ^{μ}) is FNS – compact, the FNS – O –

C $\{h^{-1}(\gamma_k) : k \in K\}$ of (X, τ^{μ}) has a FNS – F – SC $\{h^{-1}(\gamma_k) : k = 1,2,....n\}$.Therefore $P = \cup_{k\in K}^{n} h^{-1}(\gamma_k)$. Then $h(p) = \cup_{k\in K}^{n}(\gamma_k)$, that is $Q = \cup_{k\in K}^{n}(\gamma_k)$. Thus $\{\gamma_{k1}, \gamma_{k2}, \gamma_{k3},.....\gamma_{kn}\}$ is a FNS – F – SC of $\{(\gamma_k) : k \in K\}$ for (Y, δ^{μ}). Hence (Y, δ^{μ}) is a FNS – compact.

4.13. Definition: (*a*) Let (X, τ^{μ}) be a FNSTSs and *H* is FNSS on X. If a family $\{G_k : k \in K\}$ of FNSOSs on X satisfies the condition, $H \subseteq \cup\{G_k : k \in K\}$, then it is said to be a FNS – O – C of *H*. A finite subfamily of the FNS – O – C $\{G_k : k \in K\}$ of *H*, which is also a FNS – O – C of *H*, is said to be a FNS – F – SC of $\{G_k : k \in K\}$.
(*b*) A FNS *H* in FNSTS (X, τ^{μ}) is said to be FNS – compact iff every FNS – O – C of *H* has a FNS – F – SC.

4.14. Theorem: Let (X, τ^{μ}), (Y, δ^{μ}) be FNSTSs and let $h : X \to Y$ be a FNS – continuous function. If *H* is FNS – compact in (X, τ^{μ}) and then *h (H)* is also FNS – compact in (Y, δ^{μ}).
Proof: Let $Q = \{\gamma_k : k \in K\}$, where $\{\gamma_k = \langle \gamma_{k1}, \gamma_{k2}, \gamma_{k3}\rangle : k \in K\}$ be a FNS – O – C of *h (H)*.
Then, by the definition of FNS – continuity $P = \{h^{-1}(\gamma_k) : k \in K\}$ is a FNS – O – C of *H*. Since *H* is FNS – compact, $\exists$ a FNS – F – SC of P, i.e., there exists $\{\gamma_{k1}, \gamma_{k2}, \gamma_{k3},.....\gamma_{kn}\}$ such that $H \subseteq \cup_{k=1}^{n} h^{-1}(\gamma_k)$. Hence *h (H)* $\subseteq h(\cup_{k=1}^{n} h^{-1}(\gamma_k)) \subseteq \cup_{k=1}^{n} h(h^{-1}(\gamma_k)) \subseteq \cup_{k=1}^{n}(\gamma_k)$. Therefore, *h (H)* is also FNS – compact.

4.15. Definition: Let (X, τ^{μ}) be a FNSTS then the family $\{G_k : k \in K\}$ of fuzzy neutrosophic supra closed sets in X satisfies finite intersection property (FIP) if every finite sub family $\{G_k : k = 1,2,..., m\}$ of the family satisfies the condition, $\cap\{G_k : k \in K\} \neq 0_{FN}$.

4.16. Theorem: A FNSTS (X, τ^{μ}) is a FNS – compact iff the collection of FNSCSs in X having the FIP has a non empty intersection.
Proof: Suppose that X is fuzzy neutrosophic supra compact.Let $\{\gamma_k : k \in K\}$ be a family of FNSCSs in X. Also assume $\{\gamma_k : k \in K\}$ has finite intersection property. Now we have to show that $\cap\{\gamma_k : k \in K\} \neq 0_{FN}$. On the contrary way suppose that $\cap\{\gamma_k : k \in K\} = 0_{FN} \Rightarrow \overline{\cap_{k\in K}\ \gamma_k} = \overline{0_{FN}}$ $\Rightarrow \cup_{k\in K} \overline{\gamma_k} = 1_{FN}$. Clearly $\cup_{k\in K}\ \overline{\gamma_k} = \cup\{\gamma_k : k \in K\} = 1_{FN}$. For every $k \in K$, γ_k is FNSCS of X. Therefore $\overline{\gamma_k}$ is FNSOS of X. Thus $\{\overline{\gamma_k} : k \in K\}$ is FNS – O – C of X. Since X is FNS – compact, therefore this FNS – O – C has FNS – F – SC, say, $\cup\{\overline{\gamma_k} : k = 1,2,...., m\} = 1_{FN}$.
Then $\cap\{\gamma_k : k = 1,2,...., m\} = 0_{FN}$. Thus the above considered family does not satisfy FIP, which is a contradiction. Therefore, $\cap\{\gamma_k : k \in K\} \neq 0_{FN}$. Conversely, assume that the family of FNSCS of X having FIP has nonempty intersection. To show that X is fuzzy neutrosophic supra compact.
Let $\{G_k : k \in K\}$ be a FNS – O – C of X. Suppose that this FNS – O – C has no FNS – F – Sc. That is for

every finite sub collection of this cover, say $\bigcup\{G_k : k \in K\} \neq 1_{FN} \Rightarrow \bigcap\{\overline{G_k} : k \in K\} \neq 0_{FN}$. As each G_k is FNSOS of X and each $\overline{G_k}$ is FNSCS of X. Thus, $\{\overline{G_k} : k \in K\}$ is a family of FNSCS of X having FIP. So by the hypothesis it has nonempty intersection, that is $\bigcap\{\overline{G_k} : k \in K\} \neq 0_{FN} \Rightarrow \bigcup\{G_k : k \in K\} \neq 1_{FN}$. This shows that $\{G_k : k \in K\}$ is not FNS – O – C for X. which is a contradiction. Therefore the given family should have a FNS – F – SC. This shows that X is fuzzy neutrosophic supra compact.

4.17. Theorem: Show that the following statements are equivalent
(I) X is FNS – compact
(II) For every $\{F_i\}$, where $F_i = \langle T_{F_i}, I_{F_i}, F_{F_i} \rangle$ of FNSC subsets of X, with $\bigcap F_i = 0_{FN}$ implies $\{F_i\}$ contains FNS – finite subclass $\{F_{i1}, F_{i2}, \ldots\ldots, F_{in}\}$ with $F_{i1} \cap F_{i2} \cap, \ldots\ldots \cap F_{in} = 0_{FN}$.

Proof: $(I) \Rightarrow (II)$. Suppose $\bigcap F_i = 0_{FN}$. Then by De Morgan's Law, $(\bigcap F_i)^C = (0_{FN})^C \Rightarrow \bigcup F_i^C = 1_{FN}$. So $\{F_i^C\}$ is a FNS – O – cover of X. Since X is FNS – compact then $\exists F_{i1}^C, F_{i2}^C, \ldots\ldots, F_{in}^C \in \{F_i^C\}$ such that $F_{i1}^C \cup F_{i2}^C \cup \ldots\ldots \cup F_{in}^C = 1_{FN}$. Then

$0_{FN} = (1_{FN})^C = \left(F_{i1}^C \cup F_{i2}^C \cup \ldots\ldots \cup F_{in}^C\right)^C = \left(F_{i1}^C\right)^C \cap \left(F_{i2}^C\right)^C \cap \ldots\ldots \cap \left(F_{in}^C\right)^C$ by De Morgan's Law

$F_{i1} \cap F_{i2} \cap, \ldots\ldots \cap F_{in}$. Therefore $F_{i1} \cap F_{i2} \cap, \ldots\ldots \cap F_{in} = 0_{FN}$. So we have to prove that $(I) \Rightarrow (II)$.

$(II) \Rightarrow (I)$. Let $\{G_i\}$ be a FNS – O – C of X, where $G_i = \langle T_{G_i}, I_{G_i}, F_{G_i} \rangle$. i.e. $\bigcup G_i = 1_{FN}$.

By De Morgan's Law, $0_{FN} = (1_{FN})^C = \left(\bigcup G_i\right)^C = \bigcap G_i^C$.

Since, each G_i is FNSO, so $\{G_i^C\}$ is a class of FNSCSs & by (II). $\exists G_{i1}^C, G_{i2}^C, \ldots\ldots, G_{in}^C \in \{G_i^C\}$ Such that $G_{i1}^C \cap G_{i2}^C \cap \ldots\ldots \cap G_{in}^C = 0_{FN}$. So by De Morgan's Law,

$1_{FN} = (0_{FN})^C = \left(G_{i1}^C \cap G_{i2}^C \cap \ldots\ldots \cap G_{in}^C\right)^C = G_{i1} \cup G_{i2} \cup \ldots\ldots \cup G_{in}$. Therefore X is FNS – compact. So we have to prove that $(II) \Rightarrow (I)$.

4.18. Theorem: Let FNSTSs (X_1, τ_1^μ) and (X_2, τ_2^μ) be a FNS – compact. Then the product FNST $\tau_1^\mu \times \tau_2^\mu$ on $X_1 \times X_2$ is FNS – compact.

Proof: Consider (X_1, τ_1^μ) and (X_2, τ_2^μ) be a FNS – compact. Let $M_i = (T_{M_i}, I_{M_i}, F_{M_i}) \in \tau_1^\mu$ with $\bigcup M_i = 1_{FN}$ and $N_i = (T_{N_i}, I_{N_i}, F_{N_i}) \in \tau_2^\mu$ with $\bigcup N_i = 1_{FN}$.

Now $M_i \times N_i = (T_{M_i}, I_{M_i}, F_{M_i}) \times (T_{N_i}, I_{N_i}, F_{N_i}) = (T_{M_i} \times T_{N_i}, I_{M_i} \times I_{N_i}, F_{M_i} \times F_{N_i})$, where

$(T_{M_i} \times T_{N_i})(r,t) = \min(T_{M_i}(r), T_{N_i}(t)), (I_{M_i} \times I_{N_i})(r,t) = \min(I_{M_i}(r), I_{N_i}(t)), (F_{M_i} \times F_{N_i})(r,t) = \max(F_{M_i}(r), F_{N_i}(t))$

where $r \in X_1, t \in X_2$. So, $M_i \times N_i = 1_{FN}$. But by definition of product topology, $M_i \times N_i \in \tau_1^\mu \times \tau_2^\mu$. i.e $\{M_i \times N_i\}$ is family of FNSOSs in $X_1 \times X_2$. Choose $\bigcup (M_i \times N_i) = 1_{FN}$. Since (X_1, τ_1^μ) is FNS – compact then $\{M_i\}$ has FNS – finite subclass $\{M_{ij}\}$ such that $\bigcup M_{ij} = 1_{FN}$ and also (X_2, τ_2^μ) is FNS –

compact then $\{N_i\}$ has FNS – finite subclass $\{N_{ij}\}$ such that $\cup N_{ij} = 1_{FN}$, where $j = 1,2,...,n$.
Hence $\cup M_{ij} \times \cup N_{ij} = 1_{FN}$. Therefore the product FNST $\left(X_1 \times X_2, \tau_1^{\mu} \times \tau_2^{\mu}\right)$ is also FNS – compact.

5. FNS – Q^{μ} – compactness in FNSTS

In this section two definitions of FNS – Q^{μ} – compactness in fuzzy neutrosophic supra topological space and established several properties of such notions are established.

5.1. Definition: Let $\left(X, \tau^{\mu}\right)$ be a FNSTS and E be a FNSS in X. A family M $= \{P_i : i \in I\}$ of FNS sets in X, where $P_i = \left\langle T_{P_i}, I_{P_i}, F_{P_i} \right\rangle$. Then M is said to be FNS $-Q^{\mu}$ – cover of E, if $E \subseteq \cup P_i$, $T_E(l) + T_{P_i}(l) \geq 1_{FN}$, for each T_{P_i} and some $l \in X$. If each P_i is FNSO then M is said to be FNS $-Q^{\mu}$ – Open cover of E.
A sub family of FNS – Q^{μ} – cover of FNSS E in X which is also FNS – Q^{μ} – cover of E is said to be FNS – Q^{μ} – sub cover of E.

5.2. Definition: A FNSS E in X is called a FNS – Q^{μ} – compact if every FNS – Q^{μ} – open cover of E has a FNS – Q^{μ} – finite sub cover. i.e. $\exists P_{i1}, P_{i2}, ..., P_{in} \in$ M such that $E \subseteq \cup P_{ij}$, $T_E(l) + T_{P_{ij}}(l) \geq 1_{FN}$, for each $T_{P_{ij}}$ and some $l \in X$, j = 1,2,…..,m.

5.3. Example: Let $X = (r,s,t)$ & $\tau^{\mu} = \{0_{FN}, 1_{FN}, P_1, P_2\}$, where

$$P_1 = \left\{\left\langle \frac{r}{0.55,0.55,0.45} \right\rangle \left\langle \frac{s}{0.65,0.55,0.35} \right\rangle \left\langle \frac{t}{0.75,0.55,0.25} \right\rangle\right\},$$

$$P_2 = \left\{\left\langle \frac{r}{0.58,0.55,0.42} \right\rangle \left\langle \frac{s}{0.68,0.55,0.32} \right\rangle \left\langle \frac{t}{0.78,0.55,0.22} \right\rangle\right\}, \text{ Then } \left(X, \tau^{\mu}\right) \text{ is FNSTS.}$$

Write $E = \left\{\left\langle \frac{r}{0.48,0.55,0.52} \right\rangle \left\langle \frac{s}{0.52,0.55,0.48} \right\rangle \left\langle \frac{t}{0.63,0.55,0.37} \right\rangle\right\}$ be a FNSS in X.
Here $E(r) \subseteq \cup P_i(r)$, $T_E(r) + T_{P_i}(r) \geq 1$, $E(s) \subseteq \cup P_i(s)$, $T_E(s) + T_{P_i}(s) \geq 1$ and $E(t) \subseteq \cup P_i(t)$, $T_E(t) + T_{P_i}(t) \geq 1_{FN}$. Therefore $\{P_1, P_2\}$ is a FNS – Q^{μ} – open cover of E and P_1 or P_2 is a FNS – Q^{μ} – finite sub cover of E.

5.4. Theorem: Let $\left(X, \tau^{\mu}\right)$ be a FNSTS and P, R are FNS – Q^{μ} – compact subsets of $\left(X, \tau^{\mu}\right)$. Then $P \cup R$ is FNS – Q^{μ} – compact in $\left(X, \tau^{\mu}\right)$.
Proof: Let $\left(X, \tau^{\mu}\right)$ be a FNSTS and P, R are FNS – Q^{μ} – compact subsets of $\left(X, \tau^{\mu}\right)$. To show that

$P \cup R$ is FNS – Q^{μ} – compact in (X, τ^{μ}). Let M = $\{E_i : i \in I\}$ be a FNS – Q^{μ} – open cover of P and N = $\{F_i : i \in I\}$ be a FNS – Q^{μ} – open cover of R in (X, τ^{μ}). Now $P \subseteq \cup E_i$ and $R \subseteq \cup F_i$.
$\Rightarrow P \cup R \subseteq \cup E_{ij} \cup \cup F_{ij} \Rightarrow P \cup R \subseteq \cup(E_{ij} \cup F_{ij})$, j = 1,2,…,m. By definition of FNS – Q^{μ} – compactness, $T_P(r) + T_{E_i}(r) \geq 1_{FN}$ and $T_R(r) + T_{F_i}(r) \geq 1_{FN}$, for some $r \in X$.
$\Rightarrow T_{P \cup R}(r) + T_{E_i \cup F_i}(r) \geq 1_{FN}$. i.e. M ∪ N = $\{E_i \cup F_i\}$ is FNS – Q^{μ} – cover of $P \cup R$. Since P is FNS – Q^{μ} – compact in (X, τ^{μ}). Then P has FNS – Q^{μ} – finite sub cover, $\exists P_{i1}, P_{i2}, ..., P_{in} \in E_i$ such that $P \subseteq \cup E_{ij}$, $T_P(r) + T_{E_{ij}}(r) \geq 1_{FN}$ for some $r \in X, j = 1,2,..., m$ and also R is FNS – Q^{μ} – compact in (X, τ^{μ}). Then R has FNS – Q^{μ} – finite sub cover, $\exists R_{i1}, R_{i2}, ..., R_{in} \in F_i$ such that $R \subseteq \cup F_{ij}$, $T_R(r) + T_{F_{ij}}(r) \geq 1_{FN}$ for some $r \in X, j = 1,2,..., m$. Now $P \subseteq \cup E_{ij}$ and $R \subseteq \cup F_{ij}$,
$\Rightarrow P \cup R \subseteq \cup(E_{ij} \cup F_{ij})$, Also $T_P(r) + T_{E_{ij}}(r) \geq 1_{FN}$ and $T_R(r) + T_{F_{ij}}(r) \geq 1_{FN}$, for some $r \in X$.
$\Rightarrow T_{P \cup R}(r) + T_{E_{ij} \cup F_{ij}}(r) \geq 1_{FN}$. Hence $\{E_{ij} \cup F_{ij}\}$ is a FNS – Q^{μ} – finite sub cover of $P \cup R$. Therefore $P \cup R$ is FNS – Q^{μ} – compact in (X, τ^{μ}).

5.5. Theorem: Let (X, τ^{μ}) & (Y, δ^{μ}) be FNSTSs and $h : X \to Y$ is bijective, FNSO and FNS – continuous. If FNSS E is FNS – Q^{μ} – compact in (X, τ^{μ}) and then $h(E)$ is FNS – Q^{μ} – compact in (Y, δ^{μ}).

Proof: Let N = $\{P_i \in \delta^{\mu}\}$ be a FNS – Q^{μ} – open cover of $h(E)$ with $h(E) \subseteq \cup P_i$ and $T_{h(E)}(r) + T_{P_{ij}}(r) \geq 1_{FN}$, for some $r \in X$. Since $P_i \in \delta^{\mu}$ then $h^{-1}(P_i) \in \tau^{\mu}$ and $h(E) \subseteq \cup P_i$
$\Rightarrow E \subseteq h^{-1}(\cup P_i)$, for some $r \in X \Rightarrow T_E(r) + T_{h^{-1}(P_{ij})}(r) \geq 1_{FN}$. Since E is FNS – Q^{μ} – compact then a family H = $\{h^{-1}(P_i) : i \in I\}$ is FNS – Q^{μ} – open cover of E. Further since E is FNS – Q^{μ} – compact in (X, τ^{μ}) then $\exists h^{-1}(P_{i1}), h^{-1}(P_{i2}), ..., h^{-1}(P_{in}) \in \tau^{\mu}$ such that $E \subseteq \cup h^{-1}(P_{ij})$ and $T_E(r) + T_{h^{-1}(P_{ij})}(r) \geq 1_{FN}$, for some $r \in X$, j = 1,2,.....,m.
$\Rightarrow h(T_E(r)) + h(T_{h^{-1}(P_{ij})}(r) \geq h(1_{FN}) \Rightarrow T_{h(E)}(r) + T_{P_{ij}}(r) \geq 1_{FN}$, as h is FNS – continuous. But $E \subseteq \cup h^{-1}(P_{ij}) \Rightarrow h(E) \subseteq h(\cup h^{-1}(P_{ij})) \Rightarrow h(E) \subseteq \cup P_{ij}$. Hence $P_{ij} \in \delta^{\mu}$ such that $h(E) \subseteq \cup P_{ij}$ & $T_{h(E)}(r) + T_{P_{ij}}(r) \geq 1_{FN}$. Therefore $h(E)$ is FNS – Q^{μ} – compact in (Y, δ^{μ}).

5.6. Theorem: Let (X, τ^{μ}) be a FNSTS and E be a FNSS on X. if a family $\{F_i : i \in I\}$ of FNSC sub sets of X with $\cap F_i = 0_{FN}$ implies $\{F_i\}$ contains finite subclass $\{F_{i1}, F_{i2}, ..., F_{in}\}$ with

$F_{i1} \cap F_{i2} \cap ..... \cap F_{in} = 0_{FN}$. Then E is FNS – Q^{μ} – compact in $\left(X, \tau^{\mu}\right)$.

Proof: Given that $\bigcap F_i = 0_{FN}$. Then by De Morgan's Law, $(\bigcap F_i)^C = (0_{FN})^C$.

$\Rightarrow \bigcup F_i^C = 1_{FN}$. Let M= $\{H_i : i \in I\}$ be a FNS – Q^{μ} – open cover of E in $\left(X, \tau^{\mu}\right)$.

So $E \subseteq \bigcup H_i, T_E(r) + T_{H_i}(r) \geq 1_{FN}$ for some $r \in X$. Since each H_i is FNSO then $\{H_i^C\}$ is a class of FNSCSs and by given condition, $\exists H_{i1}^C, H_{i2}^C, ..., H_{in}^C \in \{H_i^C\}$ such that $H_{i1}^C \cap H_{i2}^C \cap ..... \cap H_{in}^C = 0_{FN}$.

So by De Morgan's Law, $1_{FN} = (1_{FN}^C) = \left(H_{i1}^C \cap H_{i2}^C \cap ..... \cap H_{in}^C\right)^C = H_{i1} \cup H_{i2} \cup ..... \cup H_{in}$.

Hence $E \subseteq \bigcup H_{ij}, T_E(r) + T_{H_{ij}}(r) \geq 1_{FN}, j = 1,2,...., n$, for some $r \in X$. Therefore E is FNS – Q^{μ} – compact in $\left(X, \tau^{\mu}\right)$.

5.7. Theorem: Let $\left(X, \tau^{\mu}\right)$ be a FNSTS and M, N are FNS – Q^{μ} – compact on $\left(X, \tau^{\mu}\right)$. Then $(M \times N)$ is FNS – Q^{μ} – compact in $\left(X \times X, \tau^{\mu} \times \tau^{\mu}\right)$.

Proof: Let K = $\{H_i : i \in I\}$, where $H_i \in \tau^{\mu} \times \tau^{\mu}$ be a FNS – Q^{μ} – cover of $M \times N$ in $\left(X \times X, \tau^{\mu} \times \tau^{\mu}\right)$. Then $M \times N \subseteq \bigcup H_i$ and $T_{M \times N}(r,t) + T_{H_i}(r,t) \geq 1_{FN}$, for some $(r,t) \in X \times X$. Now write $H_i = P_i \times R_i$, where $P_i \times R_i \in \tau^{\mu}$. Thus $M \times N \subseteq \bigcup H_i$

$\Rightarrow M \times N \subseteq \bigcup (P_i \times R_i) \Rightarrow M \subseteq \bigcup P_i, N \subseteq \bigcup R_i$. Also $T_{M \times N}(r,t) + T_{P_i \times R_i}(r,t) \geq 1_{FN}$, for some $(r,t) \in X \times X$. Hence it is clear that $T_M(r) + T_{P_i}(r) \geq 1_{FN}$, for some $r \in X$ and $T_N(t) + T_{R_i}(t) \geq 1_{FN}$, for some $t \in X$. Therefore $\{P_i : i \in I\}$ and $\{R_i : i \in I\}$ are FNS – Q^{μ} – open cover of M and N. Since M & N are compacts then $\{P_i : i \in I\}$ and $\{R_i : i \in I\}$ have FNS – Q^{μ} – finite sub covers of M and N. Say, $\{P_{ij} : j \in I_n\}$ and $\{R_{ij} : j \in I_n\}$ such that $M \subseteq \bigcup P_{ij}, T_M(r) + T_{P_{ij}}(r) \geq 1_{FN}$, for some $r \in X$ and $N \subseteq \bigcup R_{ij}, T_N(t) + T_{R_{ij}}(t) \geq 1_{FN}$, for some $t \in X$. Thus $M \times N \subseteq \bigcup (P_{ij} \times R_{ij})$. $\Rightarrow M \times N \subseteq \bigcup H_{ij}$ and $T_{M \times N}(r,t) + T_{H_{ij}}(r,t) \geq 1_{FN}$, for some $(r,t) \in X \times X$. Therefore $(M \times N)$ is also FNS – Q^{μ} – compact on $\left(X \times X, \tau^{\mu} \times \tau^{\mu}\right)$.

6. Acknowledgments

The authors are highly grateful to the refers for their valuable comments and suggestions for improving the paper. The second author gratefully acknowledges the support provided by UGC, New Delhi under NFST research grant during this research work.

7. References

[1] Alblowi, S.A. Salama. A, and Mohamed Eisa, 2013, new concepts of neutrosophic sets, *inter. Jour. Math. & comp. Appli. Research,* **vol 3 (3),** pp. 95 – 102.

[2] A.S. Mashhour, A.A. Allan, F.S. Mahmoud & F.H. Khedr, on supra topological space, *Indian J. Pure*

Appl. Math. **14 (4),** 1983, 502 – 510.
[3] Bayhan, s., and D. Coker, 1996. On fuzzy separation axioms in IFTS, *BUSEFAL,* **67,** 77 – 87.
[4] C.L. Chang, fuzzy topological spaces, *J. Math. Anal. Appli.* **24** (1968), 182 – 190.
[5] D. Coker, an introduction to intuitionistic fuzzy topological spaces, *fuzzy sets & systems,* 88 (1997), **no.1,** 81 – 89.
[6] D. Coker, M. Demirci, on intuitionistic fuzzy points, *NIFS,* **1 (2),** 1995, pp. 79 – 84.
[7] D. Coker, and S. Bayhan, 2001, on separation axioms in ITS, *int. J. of math. Sci.,* **27(10),** 621-630.
[8] K.T. Atanassov, intuitionistic fuzzy sets, *fuzzy sets & systems,* 20 (1986), **no.1,** 87 – 96.
[9] L.A. Zadeh, fuzzy sets, *Inform. And control* **8**(1965), 338 – 353.
[10] M.E. Abd, EI – Monsef & A.E. Ramadan, on fuzzy supra topological spaces, *Indian J. Pure Appl. Math.* **18(4),** 1987, 322 – 329.
[11] Md. Aman Mahbub, Md. Sahadat Hossain and M. Altab Hossain, some properties of compactness in IFTS, *Intern. J. Fuzzy mathematical Archive,* **vol.16, no. 2,** 2018, 39 – 48.
[12] Md. Aman Mahbub, Md. Sahadat Hossain and M. Altab Hossain, on Q – compactness in IFTS, *J. Bangladesh Acad. Sci.,* **vol. 43, No. 2,** 197 – 203, 2019.
[13] Salama, A.A. Alblowi, A.A, 2012, neutrosophic set & neutrosophic topological spaces, *ISOR jour. Of Mathematics,* **vol 3, issue 4,** pp. 31 – 35.
[14] Salama. A.A, Smarandache, Florentin & Valeri. K, 2014, neutrosophic closed set and neutrosophic continuous functions, *neutrosophic sets & systems,* **4,**pp. 4 – 8.
[15] Smarandache. F (2002), neutrosophy & neutrosophic logic. *First international conference on neutrosophic set, probability & statistics, university of New Mexico, gallup.NM, 87301, USA.*
[16] S.Das, IFTS, department of mathematics, *national institute of technology,* may, 2013.
[17] V. Amarendra Babu & J. Aswini, fuzzy neutrosophic supra topological spaces, *advances & appli. In math. Scie.* **Vol 20, issue 8,** 2021, pp. 1339 – 1347.

Journal of Non-Crystalline Solids 575 (2022) 121210

Contents lists available at ScienceDirect

Journal of Non-Crystalline Solids

journal homepage: www.elsevier.com/locate/jnoncrysol

The influence of Cu^{2+} ions on the ionic, electronic conductivity and optical characteristics of Li_2O-SrO-B_2O_3 system

A. Ramesh Babu [a], S. Yusub [b,*], V. Aruna [a], N. Sree Ram [a], P.M. Vinaya Teja [c], Y. Chaitanya [a]

[a] Department of Physics, Bapatla Engineering College, Bapatla-522102, A.P., India
[b] Freshman Engineering Department, Lakireddy Bali Reddy College of Engineering (Autonomous), Mylavaram-521230, A.P., India
[c] Department of Physics, A.C. College, Guntur 522001, A.P., India

ARTICLE INFO

Keywords:
Glasses
X-ray diffraction
ESR
Infrared spectroscopy
Optical properties
Dielectric properties

ABSTRACT

Melt quenching technique was used for preparing the glass network $10Li_2O$-30SrO-(60-x)B_2O_3: xCuO ($0 < x < 1$, where x = 0, 0.2, 0.4, 0.6, 0.8, and 1 mol%). The samples were investigated by analysing spectroscopic and dielectric properties. X-ray diffraction (XRD) asserted the glassy nature of the samples. Optical absorption spectra of the specimens displayed a prime band centred nearly at 750 nm due to Cu^{2+} ions. A continuous increase in the intensity of this band is noticed with a rise in the concentration of CuO. Electron spin resonance (ESR) spectra of the glasses confirmed the existence of Cu^{2+} ions. Spin-Hamiltonian parameters of the specimens were estimated. An analysis on the Fourier transform infrared (FTIR) curves confirmed the bands due to conventional borate units. The dielectric investigations supported the depolymerization of the specimens with an increase in the content of CuO.

1. Introduction

Among the different types of glass formers, B_2O_3 is identified as the best glass former. Borate glasses possess high thermal stability and teeny melting point. These glasses are used as the basic host materials in preparing solid state lasers, electro-optic switches, optical converters, electro-optic modulators, and luminescent materials [1–7]. Li_2O is one of the notable glass modifiers. It infiltrates the specimen by bursting B-O-B links and establishes bonding defects. Lithium ions generate non-bridging oxygen's (NBOs) in the system. Optical characteristics of the samples are modified by NBOs [1–5]. Borate glasses combined with alkaline earth oxides find technical applications in solar energy converters, phosphors, radiation dosimetry, vacuum ultraviolet optics, semiconductor lithography, and numerous electronic equipments [3,5]. The quality of borate glasses can be upgraded by adding SrO in a suitable proportion. The Sr^{2+} ions create hollow spaces and trouble-free paths to facilitate the motion of ions by breaking the B-O-B bonds [3,5].

The ionic and electronic conductivities of lithium borate glasses are very much improved when they are amalgamated with multivalent transition metal ions [1–5]. The ionic conductivity is expected owing to the migration of lithium ions. Electronic conductivity is predicted because of the electron hopping among polyvalent transition metal ions [1–5]. Borate glasses alloyed with CuO are used as memory elements [1, 6,7]. Cu^0, Cu^+, Cu^{2+}, and Cu^{3+} are the specific valance states of copper in borate glasses [1,8,9]. As the glass formers, Cu^+ ions strengthen the glass network. Cu^{2+} ions perform in the same way as those of glass modifiers. These ions engage octahedral positions and modify the network [10–12]. Cu^{3+} ions generate Li-O-Cu layers in the glass. Such glass can be used as the cathode material in new generation's lithium ion batteries [6–11]. The collection of Cu^0 particles augments the mechanical stability of the glasses. This phenomenon is used in designing optical memory and optoelectronic devices [6–11]. There is a chance for Cu^+ ions to transform into Cu^0 and Cu^{2+} ions by electrochemical reduction and oxidation methods continuously. The existence of such copper particles and ions simultaneously enhances the electrical characteristics (both polaronic and ionic conductivities) of the glasses [1,10].

Literature survey reveals that B. Ashok et al. prepared the Na_2O-Al_2O_3-B_2O_3-CuO glasses. They carried out electron paramagnetic resonance (EPR) and Optical absorption studies on the Na_2O-Al_2O_3-B_2O_3 glasses using Cu^{2+} as a spin probe [6]. B. Sumalatha et al. investigated the spectroscopic properties of 10RO + 30ZnO + 60B_2O_3 (R = Mg, Ca and Sr) and 10SrO + (30 -x)ZnO + 60B_2O_3 + xCuO (x = 0, 0.1, 0.3, 0.5, and 0.7 wt.%) glasses [7]. B.J.R.S. Swamy et al. studied the thermoluminescence (TL) characteristics of γ-ray irradiated calcium fluoro

* Corresponding author.
E-mail address: syedyusuf1985@gmail.com (S. Yusub).

https://doi.org/10.1016/j.jnoncrysol.2021.121210
Received 24 June 2021; Received in revised form 1 October 2021; Accepted 4 October 2021
Available online 14 October 2021

borophosphate glasses doped with different concentrations of CuO [8]. A.M. Abdelghany and Amal Behairy investigated the antibacterial characteristics and structural correlation of copper ions in cadmium borate glasses [9]. Although, a significant number of recent research articles are available on borate glasses doped with copper ions, but most of them are concentrated on structural studies by means of optical absorption, ESR, FTIR, and Raman investigations. Virtually, no articles are found on the dielectric characteristics of Li_2O-SrO-B_2O_3 glasses alloyed with copper ions. In the present study, we have carried out the spectroscopic and dielectric properties of the glasses.

The focus of this research article is to examine electronic, ionic conductivity of the specimens, to estimate the dielectric parameters σ_{ac}, ε' and tanδ (a.c. conductivity, dielectric constant and dielectric loss) over an extensive range of frequencies and temperature, to detect the valance state of dopant ions in the samples by taking investigations on optical absorption, ESR spectra and to explore the structural modifications in the samples by analyzing FTIR curves.

2. Materials and methods

We selected the composition $10Li_2O$-30SrO-(60-x)B_2O_3-xCuO (x = 0, 0.2, 0.4, 0.6, 0.8, and 1 mol%) for the present discussion. The basic chemicals Li_2CO_3, $SrCO_3$, H_3BO_3, and CuO were analytical grade reagents, 99.99% pure and from Loba industry, Mumbai, India. These basic materials were used for preparing the glasses. The chemicals were blended in proper quantities in an agate mortar. This amalgam was relocated into a porcelain crucible and melted at 950 °C for 20 minutes. The resultant flux was poured on a brass plate. This brass plate with flux was kept in another furnace and maintained at a temperature of 400 °C for annealing. The prepared samples were free from defects. The color of the specimens was detected to change from light to dark blue. These specimens are labelled as follows.

$$C0: 10Li_2O - 30SrO - 60B_2O_3$$

$$C2: 10Li_2O - 30SrO - 59.8B_2O_3 - 0.2CuO$$

$$C4: 10Li_2O - 30SrO - 59.6B_2O_3 - 0.4CuO$$

$$C6: 10Li_2O - 30SrO - 59.4B_2O_3 - 0.6CuO$$

$$C8: 10Li_2O - 30SrO - 59.2B_2O_3 - 0.8CuO$$

$$C10: 10Li_2O - 30SrO - 59.0B_2O_3 - 1.0CuO$$

X-ray diffractometer, SO-DEBYE FLUX 202 model was used in recording the XRD spectra of the specimens. VIBRA HT device was used for measuring density of the samples with an exactness of ±0.0001 g/cm^3. Density of the glasses was estimated by applying the Archimedes' principle using O-Xylene (99.99% pure) as the buoyant.

The sizes of the glasses were decreased to 1.0 cm x 1.0 cm x 0.1 cm and it was ground and polished to the highest optical quality for optical absorption investigations. These studies were carried out in the wavelength range 200-1200 nm. Optical absorption studies were investigated using UV-Vis-NIR spectrophotometer, JASCO V-670 model with a correctness of ±0.1 nm. Powder of 100 mg of glass was taken in a quartz tube for studying ESR spectra by operating JOEL-FE-1X spectrometer with a resolution of 2.35 μT at ambient temperature. The X-band frequency of the apparatus was set at 9.154 GHz and the field modulation frequency at 100 kHz. The strength of the magnetic field was varied up to 500 mT. FTIR of the specimens were analyzed in the wavenumber range 400-1600 cm^{-1} with an exactness of ±0.1 cm^{-1} by operating the JASCO-FTIR-5300 spectrometer.

For estimating the dielectric parameters, sizes of the specimens were modified to 1.0 cm x 1.0 cm x 0.2 cm. The samples were coated with a thin silver layer on both sides to act as electrodes. LF-impedance analyzer, Hewlett-Packard model 4192A was used to measure the dielectric variables in the temperature range 30-300 °C and the frequency was varied from 1 to 1000 kHz. The exactness in measuring the values of ε' and tanδ was ±0.001 and ±0.0001. A.c. voltage breakdown tester, ITL Model BOV-7 with a correctness of ±0.01 kV/cm was used for measuring the dielectric breakdown strength (DBS) of glasses.

3. Results

3.1. X-Ray diffraction

All synthesized specimens are exhibited in Fig. 1. The glasses C0 and C2 are clear, transparent, and colourless. The color of the samples was noticed to change from light to dark blue. General examination reveals that the samples are free from gaps, bubbles, and defects. XRD spectra of work models C0, C4, and C8 are displayed in Fig. 2. An inspection of these curves validates the amorphous character of the specimens.

Physical parameters

The measured values of molecular weight (M) and density (ρ) are used in estimating the physical parameters of the specimens such as molar volume (V_m), copper ion concentration (N_i), polaron radius (R_p), interionic distance (R_i), and boron-boron separation ($d_{B\text{-}B}$). The magnitudes of d, M, and N_i of the samples were escalated with a rise in the content of CuO, where as quantities such as V_m, $d_{B\text{-}B}$, R_i, and R_p indicated the decreasing trend. These physical parameters shed some light on the structural variations in the glasses. All these physical parameters are presented in Table 1.

3.2. Optical properties

Optical absorption spectra of Li_2O-SrO-B_2O_3: CuO samples are probed in a wavelength range 200-1200 nm. Fig. 3 exhibits the optical absorption spectra of specimens. No absorption peak is identified for the undoped glass (C0). From the optical absorption curves, the cut-off wavelength (λ_c) is noticed for the glass C0 at 284 nm. A gradual increase in the magnitude of λ_c is observed with an increase in the concentration of copper ions. A broad absorption band is observed for the doped glasses. The indirect and direct optical band gaps (E_o) of the specimens are estimated from the Tauc plots as shown in Fig. 4 and Fig. 5, respectively. The values of E_o of the samples are computed by using the following relation given by Eq. (1) [1,13–16].

$$\alpha(\upsilon) = B(h\upsilon - E_o)^m / h\upsilon \quad (1)$$

All terms in the above equation have usual meanings [1,13]. The curves are drawn between $(\alpha h\nu)^{1/2}$ as a variable of hυ and $(\alpha h\nu)^2$ as a function of hυ. These plots are shown in Fig. 4 and Fig. 5. The values of E_o are deduced by extending the linear parts of these curves to the X-axis. A regular decrease in the value of E_o is discovered for the samples from C0 to C10. Urbach energy (ΔE) of the specimens is related to α(υ) as given below [1–5].

$$Ln\alpha(\upsilon) = (h\upsilon/\Delta E) + \text{constant} \quad (2)$$

.The curves drawn between Lnα(υ) and hυ are termed as Urbach plots. These Urbach plots are demonstrated in Fig. 6. The reciprocals of the slopes of these curves in the linear parts are described as Urbach energies of the samples. The estimated values of ΔE of the glasses increase with a rise in the content of impurity atoms. The synopsis of the data on optical absorption is furnished in Table 2. Using indirect band gaps, the refractive indices (n) of the specimens are determined by the formula given below. The refractive indices of the samples are noticed to increase with a rise in the concentration of dopant [1,17,18].

$$\frac{n^2-1}{n^2+2} = 1 - \sqrt{\frac{E_o}{20}} \quad (3)$$

The reflection loss (R_L) of the samples was estimated by taking their refractive indices. The following equation was used for finding the

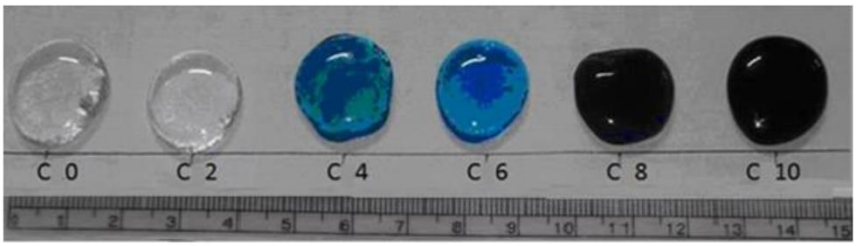

Fig. 1. Physical appearance of the glasses in the present investigation.

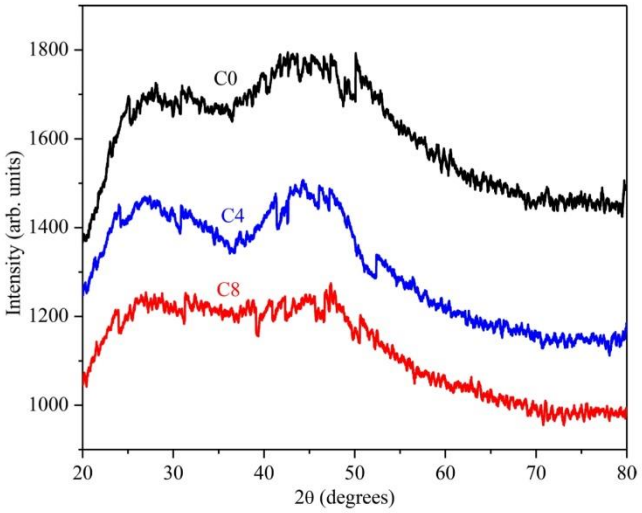

Fig. 2. XRD curves of the $10Li_2O$-30SrO-(60-x)B_2O_3: xCuO glass system for x = 0, 0.4, 0.8 mol% (glasses C0, C4, C8).

Table 1
Physical properties of Li_2O-SrO-B_2O_3 glasses doped with CuO.

Glass	Density ρ (g/cm^3) (±0.0001)	Average molecular weight M (g/mol) (±0.0001)	Molar Volume V_m (cm^3/mol) (±0.001)	Copper ion conc. N_i (x10^{21} ions/cm^3) (±0.0001)	Boron-Boron separation d_{B-B} (Å) (±0.001)	Interionic distance R_i (Å) (±0.0001)	Polaron radius R_p (Å) (±0.0001)
C0	2.5499	61.0980	23.960	-	3.677	-	-
C2	2.5588	61.1177	23.885	5.0432	3.667	5.8312	2.3499
C4	2.5677	61.1377	23.810	10.1183	3.657	4.6234	1.8632
C6	2.5766	61.1574	23.735	15.2251	3.647	4.0347	1.6259
C8	2.5855	61.1773	23.661	20.3637	3.637	3.6619	1.4757
C10	2.5944	61.1972	23.588	25.5339	3.628	3.3959	1.3685

values of R_L of specimens [1,17,18].

$$R_L = \frac{n^2 - 1}{n^2 + 2} \tag{4}$$

An increase in the magnitude of R_L is identified with a rise in the content of CuO. The molar refraction (R_m) of all models is computed by taking the relation given below [1,17,18].

$$R_m = \frac{(n^2 - 1)}{(n^2 + 2)} V_m \tag{5}$$

The values of R_m of the specimens are observed to escalate with a rise in the content of impurity atoms. The magnitude of R_m is maximum for the glass C10. The molar electronic polarizabilities (α_m) of the specimens are estimated using the following equation given below [1,17,18].

$$\alpha_m = \left(\frac{3}{4\pi N}\right) R_m \tag{6}$$

Here N is Avagadro's number. The evaluated value of α_m is the least for the glass C0. A continuous rise in the values of α_m of samples is noticed with a rise in the content of CuO. The values of metallization

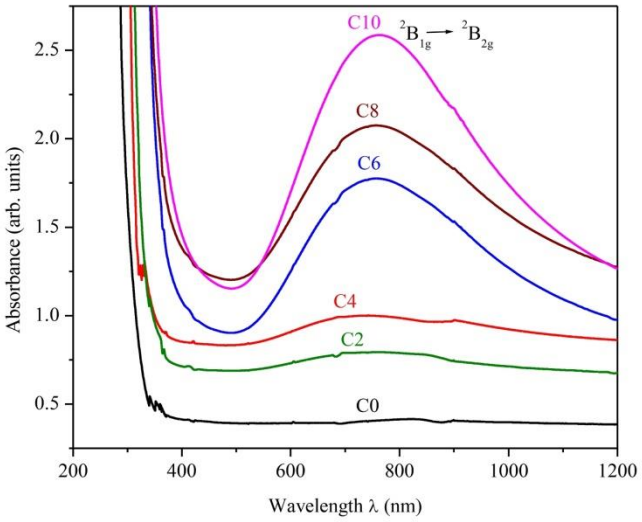

Fig. 3. Optical absorption spectra of Li_2O-SrO-B_2O_3: CuO glasses at ambient temperature.

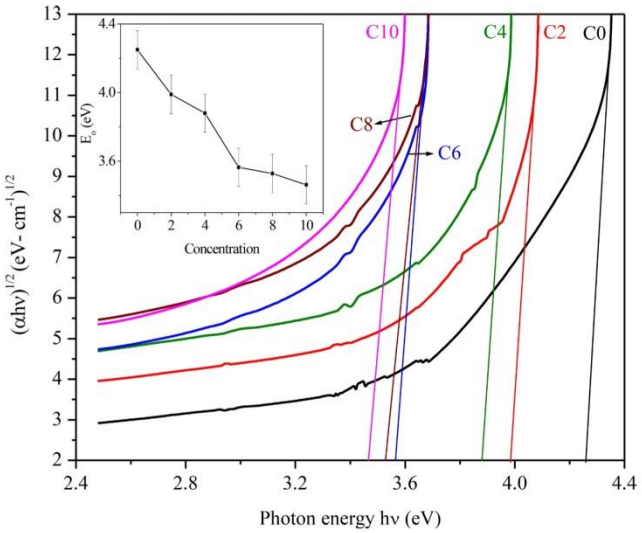

Fig. 4. Tauc plots to evaluate the indirect optical band gaps of Li_2O-SrO-B_2O_3: CuO glasses. Inset shows the error bars in calculating the optical band gap (E_o) of the specimens. The sources of all the lines drawn are the observations evaluated using the values of α (α = A/t where "A" is the absorbance and "t" is the thickness of the sample) and hυ (hυ = hc/λ). An arrow head (→) is used to show the specimens C6 and C8.

criterion (M_c) of the samples are determined by applying equation (7). A decrease in the magnitude of M_c is found for the samples from C0 to C10 [1,17,18].

$$M_c = 1 - R_L = 1 - \frac{n^2 - 1}{n^2 + 2} = \sqrt{\frac{E_o}{20}} \tag{7}$$

Optical electronegativities (χ) of the specimens are calculated using the values of indirect band gap (E_o) of the specimens. The given relation is used for calculating the values of χ [1,17,18].

$$\chi = 0.2688\, E_o \tag{8}$$

It is detected that the value of χ decreases gradually with an increase in the concentration of CuO. The electronic polarizability (α_e) of glasses is calculated by using the equation given below [1,17,18].

$$\alpha_e = -0.9\chi + 3.5 \tag{9}$$

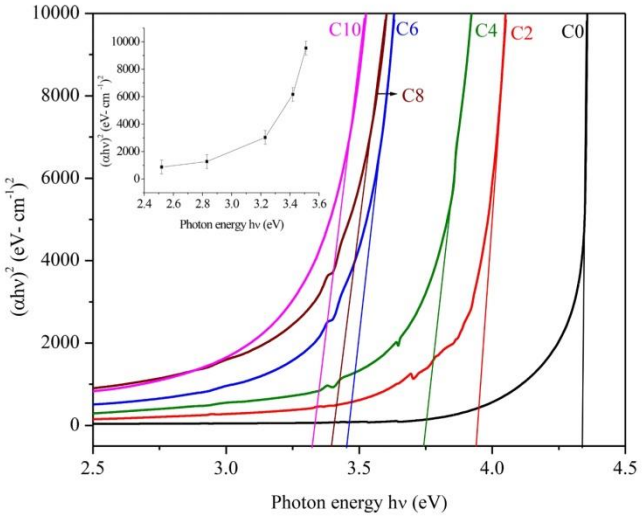

Fig. 5. Tauc plots to estimate the direct optical band gaps of Li_2O-SrO-B_2O_3: CuO glasses. Inset displays the error bars obtained for the sample C10. The sources of all the lines drawn are the observations evaluated using the values of α (α = A/t where "A" is the absorbance and "t" is the thickness of the sample) and hυ (hυ = hc/λ). An arrow head (→) is used to show the sample C8.

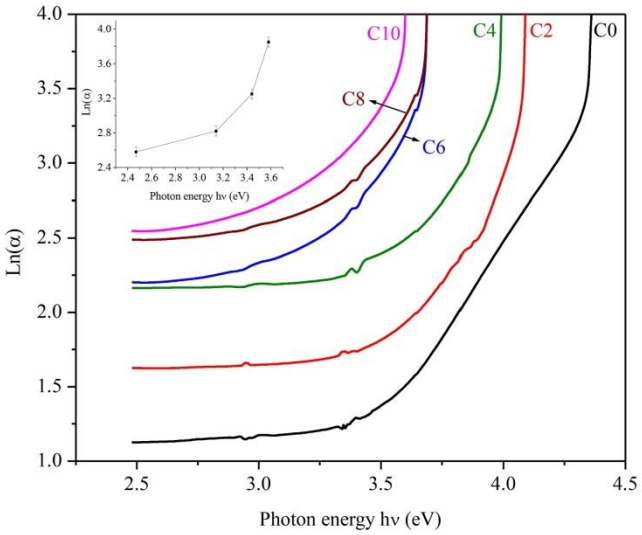

Fig. 6. Urbach (ΔE) plots of Li_2O-SrO-B_2O_3: CuO glasses. Inset manifests the error bars obtained for the specimen C10. The sources of all the lines drawn are the observations calculated using the values of α (α = A/t where "A" is the absorbance and "t" is the thickness of the sample) and photon energy hυ (hυ = hc/λ). An arrow head (→) is used to show the specimens C6 and C8.

An increase in the values of α_e is recognized for the specimens from C0 to C10.

The optical basicity (Λ_{th}) of the samples was evaluated by using the equation given below [1].

$$\wedge_{th} = x(Li_2O) \wedge (Li_2O) + x(SrO) \wedge (SrO) + x(B_2O_3) \wedge (B_2O_3) + x(CuO) \wedge (CuO) \quad (10)$$

Where x(Li_2O), x(SrO), x(B_2O_3), and x(CuO) are the mole fractions of the basic materials in this network. The values of Optical basicity of

Table 2
Summary of the data on optical absorption spectra of Li_2O-SrO-B_2O_3 glasses doped with CuO.

Glass	Cut off wavelength λ_c (nm) (±0.1)	Band position nm $^2B_{1g} \rightarrow {}^2B_{2g}$ (±0.1)	Indirect Optical band gap E_o (eV) (±0.001)	Direct Optical band gap E_o (eV) (±0.001)	Urbach energy ΔE (eV) (±0.001)
C0	284	—	4.258	4.337	0.259
C2	303	726	3.989	3.943	0.315
C4	311	736	3.880	3.742	0.374
C6	333	749	3.564	3.456	0.432
C8	336	752	3.528	3.400	0.441
C10	344	754	3.462	3.328	0.513

components $\Lambda(Li_2O) = 0.81$, $\Lambda(SrO) = 1.08$, $\Lambda(B_2O_3) = 0.425$, and $\Lambda(CuO) = 1.11$. The oxide ion polarizability (α_0^{2-}) and optical basicity (Λ_{th}) of the specimens are connected by the relation as given below [1,17,18].

$$\wedge_{th} = 1.67\left(1 - \frac{1}{\alpha_0^{2-}}\right) \tag{11}$$

The computed values of α_0^{2-} are detected to increase steadily for the glasses from C0 to C10. The oxygen packing density (OPD) of the specimen is evaluated by making use of the following equation [1,17,19].

$$OPD = \frac{\rho \times r \times 1000}{M} \tag{12}$$

Where ρ is the density of the sample, 'r' is the number of oxygen atoms per formula unit.

M is the molecular weight of a sample. The magnitude of OPD of the samples exhibited an increasing trend with an increase in the dosage of CuO. The evaluated quantities of the above variables are furnished in Table 3.

3.4. ESR

ESR spectra of Li_2O-SrO-B_2O_3: CuO glasses are displayed in Fig. 7. As the sample (C0) is free from the transition metal ions, no ESR signal is recognized. When C0 is doped with different concentrations of copper ions, four parallel signals and four perpendicular signals are anticipated due to ^{63}Cu and ^{65}Cu nuclei. In the present discussion, three parallel and three perpendicular components are recognized in the weak and strong magnetic field zones for all doped samples. Intensity of these components increases with an increase in the concentration of copper ions in the specimens. Spin-Hamiltonian parameters (SHP) $g_{||}$, $g_{\perp}$ and $A_{||}$ are estimated and recorded in Table 4. These values suggested the availability of Cu^{2+} ions in the glasses by settling in tetragonally distorted octahedral sites. The equation for estimating the SHP is given in the published articles [20–23].

3.5. FTIR

FTIR studies reveal the structural variations in the glasses. An analysis of these studies gives information about the vibrating groups in the specimens. The vibrating bands and their allotments are mentioned in Table 5. Fig. 8 displays the FTIR curves of the glasses in a wavenumber scale 400-1600 cm^{-1}. We detected vibrational bands at 587, 704, 945, 1044, 1247, and 1387 cm^{-1} [1–5,16,24]. A poor band at 587 cm^{-1} is expected due to extending oscillations of Cu-O bonds [9,12,16,24]. The intensity of this band is recognized to rise with a gain in the concentration of CuO in the doped samples. A band at 704 cm^{-1} is detected as a result of B-O-B bending vibrations [1–5,9,12,16,24]. The intensity of this band rises in accordance with the content of dopant. A broad band at 945 cm^{-1} and a weak shoulder at 1044 cm^{-1} are expected due to the waving of B-O bonds in BO_4 units [1–5]. Intensity of such bands is observed to fall with an increase in the number of impurity ions. A weak band at 1247 and a strong band at 1387 cm^{-1} are expected as a result of waving of B-O linkages in BO_3 species [1–5]. Intensity of such bands is escalated with a raise in the quantum of CuO.

3.6. Dielectrics studies

The insulating nature of the specimens was investigated by analysing the dielectric properties. The values of ε′ and tanδ were evaluated in a temperature range 30-300 °C and in a frequency limit 10^3-10^6 Hz. The computed values of ε′ and tanδ for the basic sample C0 at 30 °C and at a frequency of 1 kHz are 6.85 and 0.025 continuously. A regular decrease in the value of ε′ and tanδ is detected with a rise in frequency for the samples at any temperature. The values of ε′ and tanδ are identified to amplify with an increase in temperature and concentration of CuO. Fig. 9 displays the response of ε′ with temperature at 10 kHz for the samples. From this figure, it is observed that there is a minute increase in the value of ε′ at lower temperatures up to 100 °C but increases sharply at higher temperatures after 250 °C. Fig. 9 confirmed that the values of ε′ are the least for glass C0 and the highest for glass C10 at any temperature and at a frequency of 10 kHz. Inset discloses the modification of ε′ at distinct frequencies for the model C6. The alteration of tanδ with temperature is exhibited in Fig. 10 for all glasses at 100 kHz.

The values of $tan\delta_{max}$ are shifted towards lower temperature with a gain in the content of dopant. This phenomenon indicates the relaxation character of the glasses. The values of tanδ increased rapidly at higher temperatures. Inset displays the magnification of tanδ with temperature for various frequencies for the test-piece C8. The values of $tan\delta_{max}$ and the temperature region of relaxation are furnished in Table 6. The activation energy for dipoles (W_d) is estimated for all specimens by using the formula given in Eq. (13) and noted in Table 6 [1–5].

$$f = f_0 exp(-W_d / KT) \tag{13}$$

The values of W_d are recognized to reduce systematically for the specimens. Magnitude of W_d is minimum for the glass C10 and maximum for the specimen C0. The following expression is used for evaluating a.c. conductivity of (σ_{ac}) of all glasses [1–5].

Table 3
Different physical variables of Li_2O-SrO-B_2O_3 glasses doped with CuO.

Physical variable	C0	C2	C4	C6	C8	C10
Refractive index n (±0.0001)	2.1036	2.1834	2.2255	2.2628	2.2684	2.2842
Reflection losss R_L (±0.0001)	0.5456	0.5534	0.5604	0.5766	0.5802	0.5830
Molar Refraction R_m (cm^3/mol) (±0.0001)	13.0734	13.2256	13.3574	13.7069	13.7562	13.7847
Molar electronic polarizability α_m (Å^3) (±0.0001)	5.1845	5.2448	5.2971	5.4357	5.4553	5.4665
Metallization criterion M_c (±0.0001)	0.4543	0.4466	0.4395	0.4234	0.4197	0.4170
Electronegativity χ (±0.0001)	1.1098	1.0722	1.0386	0.9636	0.9472	0.9348
Electron polarizability α_e (Å^3) (±0.0001)	0.2163	0.2194	0.2222	0.2286	0.2301	0.2312
Optical basicity Λ_{th} (±0.0001)	0.6678	0.6691	0.6706	0.6719	0.6733	0.6747
Oxide ion polarizability $\alpha_{O^{2-}}$ (Å^3) (±0.0001)	1.6663	1.6685	1.6709	1.6731	1.6755	1.6779
Oxygen Packing Density OPD (mol/L) (±0.001)	91.813	92.054	92.301	92.548	92.795	93.042

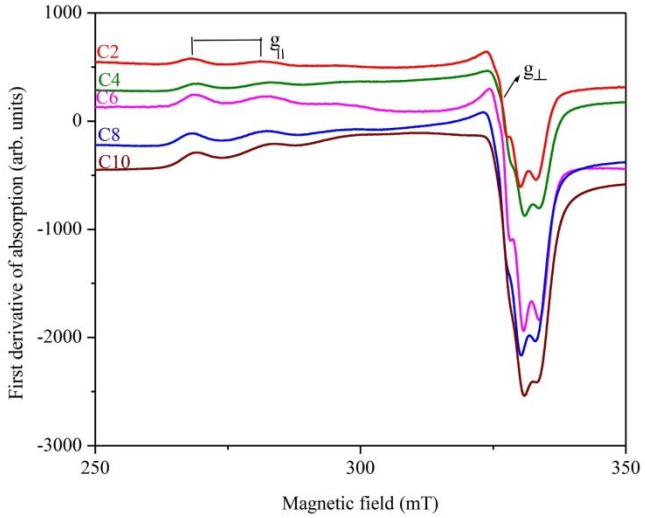

Fig. 7. ESR spectra of Li_2O-SrO-B_2O_3: CuO glasses. In the figure, arrow head is used to indicate $g_\perp$.

Table 4
Spin-Hamiltonian parameters of Li_2O-SrO-B_2O_3 glasses doped with CuO.

Sample	$g_\parallel$ 0.0001±))	$g_\perp$ (±0.0001)	$A_{\parallel}$ (x10^{-4} cm^{-1}) (±0.001)	$g_\parallel/A_\parallel$ 0.001±))
C2	2.3913	2.0627	136.983	174.569
C4	2.3821	2.0545	139.683	170.536
C6	2.3871	2.0539	133.956	178.200
C8	2.3933	2.0663	152.386	157.055
C10	2.3817	2.0602	148.285	160.613

Table 5
Various band positions in the FTIR spectra of Li_2O-SrO-B_2O_3 glasses doped with CuO.

Wavenumber (cm^{-1}) (±0.1)	IR band assignment
1387	B-O extensions in BO_3 species from various categories of the borate family.
1247	B-O oscillations in BO_3 species from pyro and ortho borate family.
1044	Vibrations of BO_4 tetrahedra, which are present as tetraborate and diborate groups.
945	B-O vibrations in BO_4 groups from various categories of borate family.
704	Bending vibrations of B-O-B in BO_3 triangles.
587	Vibrations of Cu-O bonds.

$$\sigma_{ac} = \omega\varepsilon'\varepsilon_o \tan\delta \quad (14)$$

All terms have usual meanings [1–5]. Fig. 11 manifests the alteration of σ_{ac} as a variable of 1000/T at 500 kHz for the specimens.

From this figure it is understood that at high temperature the value of σ_{ac} is maximum. The estimated values of σ_{ac} at 100 kHz are listed in Table 7. The values of activation energy for conduction (AEC) for the samples are computed from the linear part of the plots and recorded in Table 7. Inset demonstrates the deviation of σ_{ac} with AEC for all specimens at a frequency of 100 kHz and at a temperature of 100 °C. This plot is a straight line showing the linearity between σ_{ac} and AEC.

The determined least and the highest values of AEC are 0.177 and 0.799 for the glasses C10 and C0 continuously. Fig. 12 displays the variation of σ_{ac} with 1000/T for the sample C4 at various frequencies. This figure recommends an improvement in σ_{ac} of model C4 with a rise in frequency. The measured dielectric breakdown strength (DBS) of all models is recorded in Table 7. A steady decrease in the measured values of DBS of the specimens is recognized with a gain in the content of CuO. The maximum and minimum quantities of DBS are 8.72 and 7.46 kV/cm for the glasses C0 and C10 continuously.

4. Discussion

4.1. X-Ray Diffraction

The sample C0 is colorless and transparent. This observation supports that the basic glass C0 has no traces of transition metal ions. Light to dark blue color of the glasses from C2 to C10 indicates the amplification of copper ions in the divalent state (Fig. 1). Cu^{2+} ions have an unfilled d-orbital, so these ions are responsible for the color of glasses [1,7–12]. The sharp Bragg's peaks are absent in XRD of the specimens (Fig. 2). This outcome suggests the aperiodic nature of glasses. However, the two humps noticed in the spectra indicate the short periodicity of the specimens.

4.2. Physical Parameters

The variations in the values of density (ρ) reflect the structural changes in the models (Table 1). A regular rise in the value of ρ is expected owing to a gain in the cross-link density, coordination number, size of internal cavities, and structural compactness of the network [1–5]. A modification in the values of ρ is anticipated owing to the replacement of boron cation by the copper ion. A gradual decrease in the values of molar volume (V_m) suggests a continuous increase of B^{3+} ions in BO_3 units. The radius of B^{3+} ions in the BO_3 units is less than the radius of B^{3+} ions in BO_4 units [1–5]. A systematic rise in the values of N_i indicates the amplification of copper ions. A decrease in the values of interionic distance R_i improves the polaron hopping between Cu^+ and Cu^{2+} ions. The decreasing quantities of $d_{B\text{-}B}$ validate the compact character of the specimens. The microscopic quantities of R_p specify the localization of electrons (Table 1) [1–5].

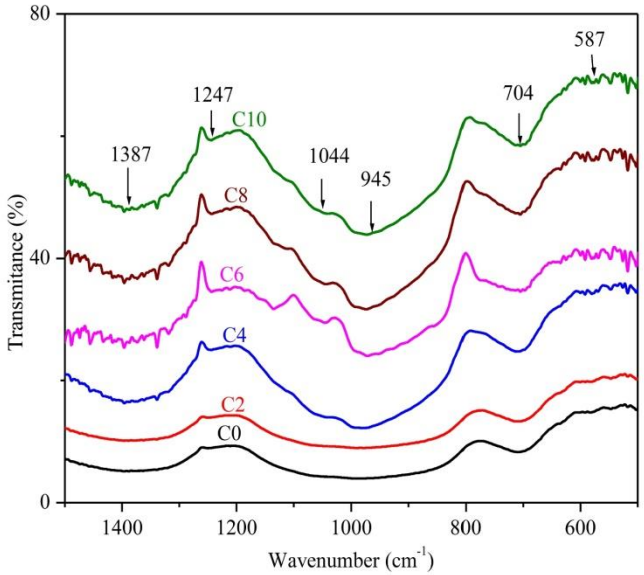

Fig. 8. FTIR spectra of CuO doped Li_2O-SrO-B_2O_3 glasses. In the figure, arrow heads (↓) are used to show the specific bands.

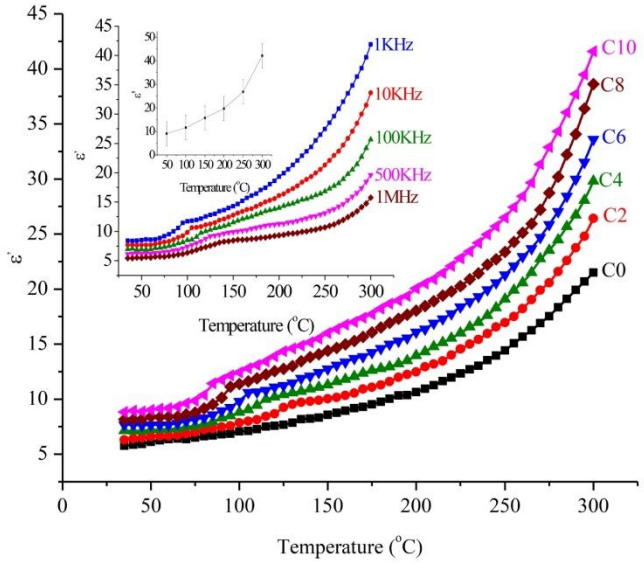

Fig. 9. Modification of ε{\prime} with temperature at 10 KHz for different concentrations of CuO in Li_2O-SrO-B_2O_3 glasses. Inset exhibits the alteration of ε{\prime} with temperature for various frequencies of glass C6. Inset displays the error bars obtained for the sample C6 at 1 kHz. The sources of all lines drawn are the observations measured using Hewlett-Packard (model 4192A), LF-impedance analyzer.

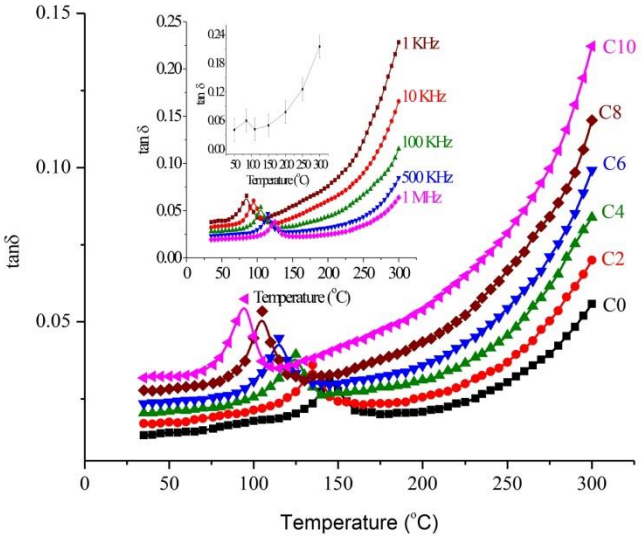

Fig. 10. Variation of tanδ with temperature at 100 KHz for different contents of CuO in Li_2O-SrO-B_2O_3 glasses. Inset displays the modification of tanδ with temperature at different frequencies of the glass C8. Inset manifests the error bars for the glass C8 at 1 kHz. The sources of all lines drawn are the observations measured using Hewlett-Packard (model 4192A), LF-impedance analyzer.

Table 6
Synopsis of the data on dielectric loss of Li_2O-SrO-B_2O_3 glasses doped with CuO at 10 kHz.

Glass	$(\tan\delta)_{max}$ (±0.0001)	Temp. region of relaxation (±1) °C	AE for dipoles (W_d) (±0.001) eV
C0	0.0234	124-142	6.210
C2	0.0277	101-119	6.054
C4	0.0303	108-132	5.900
C6	0.0332	99-129	5.748
C8	0.0354	91-126	5.598
C10	0.0408	83-124	5.449

4.3. Optical absorption

A continuous amplification in the intensity of the absorption band nearly at 750 nm is noticed for the Li_2O-SrO-B_2O_3 glasses (Fig. 3). This observation supported the magnification of Cu^{2+} ions in the tetragonally distorted octahedral locations. This absorption band is allocated to $^2B_{1g} \rightarrow {}^2B_{2g}$ transition of Cu^{2+} ions [12–16]. Widening of this band is credited to overlapping of $^2B_{1g} \rightarrow {}^2E_g$, $^2B_{1g} \rightarrow {}^2A_{1g}$, and $^2B_{1g} \rightarrow {}^2B_{2g}$ electron transitions [1,7–12]. An investigation of absorption plots indicated an increase of λ_c (absorption edge) with the magnification of Cu^{2+} ions (Table 2). A decrease in the values of optical band gap (E_o) (Fig. 4 and Fig. 5) specifies an increase in the semiconducting character of the samples (Table 2). This outcome supported the amplification of Cu^{2+} ions [1,7–12]. A gain in Cu^{2+} ions causes the magnification of non-bridging oxygens (NBOs). These NBOs act as donor centres and lead to a decrease in the value of E_o. The amplification of NBOs causes the generation of deformations analogous to bond angle distortion and dangling bonds. These defects are the sources for a continuous increase in the Urbach energy (ΔE) (Fig. 6 and Table 2) of the models [1,7–12].

A gradual rise in the evaluated values of refractive index (n) (Table 3) proves the amplification of non-bridging oxygens (NBOs) in the specimens [1,17,18]. A gain in reflection loss (R_L) confirms the rise in the metallic temper of the models [1,15]. The molar polarizability (α_m) is associated with the molar refractivity (R_m). A rise in the values of α_m stipulates the strengthening of NBOs [1,17,18]. A decrease in the values of M_c (metallization criterion) hints a rise in the conducting nature of the glasses. The electronegativity (χ) of a sample indicates its covalent nature. A gradual decrease in the amount of χ with an increase in the content of CuO supports a decrease in the covalent nature of the specimens [1,17,18]. The ionic nature of glasses can be decided by the magnitude of its electron polarizability (α_e) [1,17,18]. A continuous gain in the values of α_e validates the gradual increase in the ionic temper of the specimens. Ionic nature of the glass can be assessed by its optical basicity (Λ_{th}) (Table 3). A systematic rise in the values of Λ_{th} with a gain in the content of CuO promoted a gradual rise in the ionic essence of the specimens [1,18]. A gradual increase in the concentration of NBOs is supported by an improvement in the oxide ion polarizability($\alpha_O{}^{2-}$) of the specimens [1,17,18]. Oxygen packing density (OPD) (Table 3) suggests the agglomeration of NBOs in the sample. An increase in the values of OPD authenticates an amplification of NBOs in the glasses [1,17,18]. These results endorse an increase in the ionic temper of the glasses.

4.4. ESR

ESR spectra confirmed the existence of paramagnetic ions in the glasses (Fig. 7 and Table 4). Among Cu^+ and Cu^{2+} ions, Cu^{2+} ion has the paramagnetic nature [20–23]. These Cu^{2+} ions occupy tetragonally distorted octahedral sites in the specimens [20–23]. The electron spin of Cu^{2+} ion is S = 1/2 and the nuclear spin I = 3/2 for ^{63}Cu and ^{65}Cu nuclei [20–23]. Due to these parameters, four parallel and four perpendicular components are predicted, but in this discussion three parallel and three perpendicular components are detected. Intensity of these components increases in proportionate to the content of CuO. These observations support the magnification of Cu^{2+} ions in the models. These ions create NBOs in the glasses resulting in decrease in rigidity of the specimens. An analysis on g values suggests that $g_{||} > g_\perp > g_e$. It is clear evidence that copper ions in the specimens are coordinated by six ligands [20–23]. Variations in the values of $g_{||}$, $g_\perp$ and $A_{||}$ are anticipated due to the internal transitions and distortion of ligand field near Cu^{2+} ions. The ratio

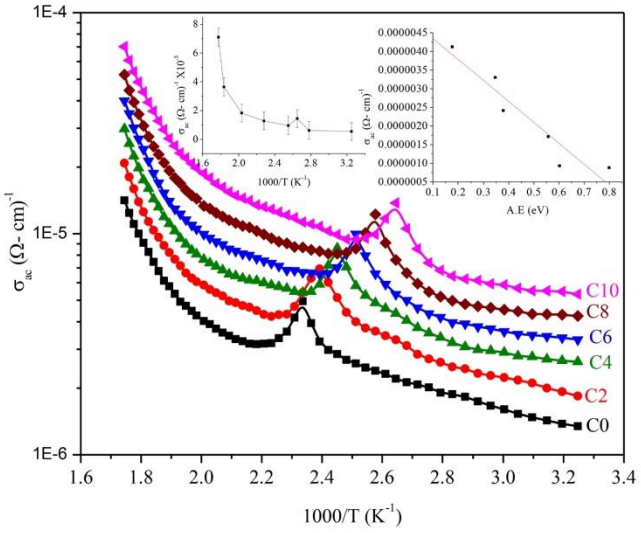

Fig. 11. Variation of σ_{ac} with 1000/T at 500 kHz for different concentrations of dopant of Li_2O-SrO-B_2O_3 glasses. Inset gives the response of σ_{ac} with activation energy (A.E.) at 100 °C of Li_2O-SrO-B_2O_3 samples at 100 kHz. Inset shows the error bars obtained for the specimen C10 at 500 kHz. The values of σ_{ac} are estimated using the relation $\sigma_{ac} = \omega\varepsilon\{\backslash prime\}\varepsilon_o \tan\delta$. Activation energy for conduction is estimated using the relation A.E. = 2.303 * K * slope * 10^3 eV.

Table 7
Dossier of the data on ac. conductivity of Li_2O-SrO-B_2O_3 glasses doped with CuO at 100 kHz.

Glass	σ_{ac} at 100 °C (10^{-6}) (Ω·cm)$^{-1}$ (±0.001)	N(E_F) (10^{20} eV^{-1}/cm^3) (±0.001)			Activation energy for conduction (eV) (±0.001)	Dielectric break down strength kV/cm (±0.01)
		Austin	Butcher	Pollak		
C0	0.881	8.234	3.435	8.172	0.799	8.72
C2	0.930	8.016	3.344	8.550	0.602	8.55
C4	1.714	11.177	4.662	11.364	0.557	8.18
C6	2.403	13.235	5.521	13.456	0.378	7.98
C8	3.303	15.516	6.473	15.775	0.346	7.75
C10	4.123	17.334	7.231	17.623	0.177	7.46

of g_{II}/A_{II} confirms the presence of copper (Cu^{2+}) ions in models in the octahedral states [1,20–23]. The gain in Cu^{2+} ions in the glasses is also supported by the studies on optical absorption spectra.

4.5. FTIR

FTIR of glasses reveals the structural modifications in them (Fig. 8 and Table 5). The glass network Li_2O-SrO-B_2O_3: CuO combines glass modifiers and formers. Addition of modifier oxides like Li_2O causes the breaking of B-O-B bonds [1,2,4]. This leads to depolymerization of the glass. Addition of SrO to a glass network leads to the conversion of BO_4 species into BO_3 groups by creating SrO polyhedron when it is surrounded by BO_4 units [3,5,24]. Such an arrangement is treated as a defect. When CuO is added to the specimen C0, copper ions crumple and distort the BO_4 units. Intensity of vibrational bands owing to BO_3 units, B-O-B bending oscillations, and Cu-O vibration increases at the cost of intensity of bands owing to BO_4 groups with a rise in the quantum of copper ions. This is a clear indication that impurity ions exist in the samples in the divalent state and act as modifiers. Such Cu^{2+} ions enhance NBOs in the specimens which act as donor centres [1,9,16]. Due to these donor centres, the conductivity of the samples increases. This outcome is also assisted by the decrease in the value of E_o and a rise in the magnitude of ΔE of the specimens. Amplification of Cu^{2+} ions is also confirmed by an increase in the intensity of ESR signals of the samples. All these results validated a gradual deterioration in the hardness of the sample with a rise in the dose of dopant.

4.6. Dielectrics studies

Dielectric studies (Fig. 9 to Fig. 12) are useful in estimating the insulating properties of glasses. At lower temperatures and for smaller concentrations of CuO, the dielectric variables such as ε′ (dielectric constant), tanδ (dielectric loss), and σ_{ac} (a.c. conductivity) are small (Table 6 and Table 7). It is expected that at lower temperatures Cu^+ ions are dominating the Cu^{2+} ions. Cu^+ ions behave like network formers and strengthen the glass. As the concentration of CuO is increased, the Cu^+ ions are converted into Cu^{2+} ions while preparing the specimens. A continuous amplification of Cu^{2+} ions in the doped samples is perceived. The outcome is supported by the studies on optical absorption and ESR spectra. These Cu^{2+} ions modify the glass like that of Li^+ ions [1,8]. Such modifiers create bonding defects and generate non-bridging oxygens (NBOs). These defects produce free paths for the transport of charge carriers and enhance the dielectric parameters.

An increase in defects is detected gradually in the glasses from C0 to C10 [1,8]. Because of these defects, the dipoles are aligned in the direction of field. This phenomenon leads to a rise in the magnitude of $\tan\delta_{max}$ and a decrease in the values of activation energy for dipoles in the glasses from C0 to C10. The dielectric relaxation peaks are detected when copper ions are in the divalent state in the glasses. A contraction of the relaxation peaks indicates the degree of freedom of the dipoles to rotate in the direction of field. These results confirmed a systematic decay in the strength of a sample with a gain in the content of dopant.

Defect model proposed by Ingram is applied for explaining the electrical conduction in the high temperature zone [25–28]. A plot sketched against σ_{ac} and activation energy for conduction exhibited near linearity. This event indicates that an increase in conductivity is

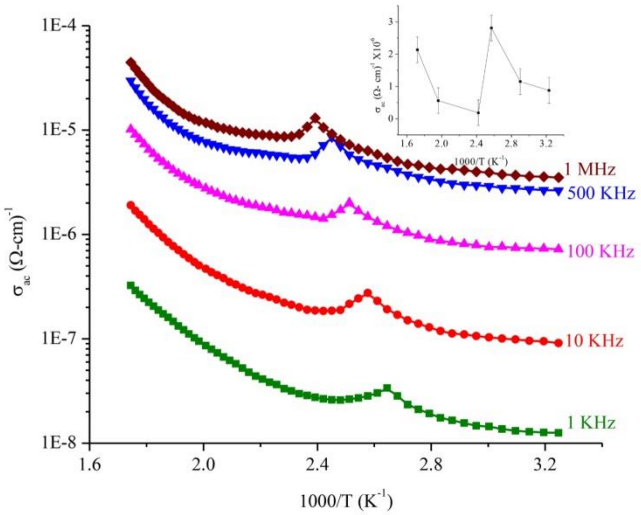

Fig. 12. Response of σ_{ac} with 1000/T for specimen C4 at various frequencies. Inset shows the error bars obtained for specimen C4 at 10 kHz. The values of σ_{ac} are estimated using the relation $\sigma_{ac} = \omega\varepsilon\{\prime\}\varepsilon_o\tan\delta$.

proportional to the movement of charge carriers in the high temperature region. The massive Sr^{2+} ions are almost motionless within the time interval of the hopping phenomenon of Li^+ ions [3,5]. Finally, it is concluded that in a high temperature region the conductivity is due to the movement of monovalent Li^+ ions [1–5]. The concentration of Cu^{2+} ions increases with a rise in the quantum of CuO. Such Cu^{2+} ions enhance the defects by creating easy paths for the movement of Li^+ ions, leading to an increase in the ionic conductivity of the glasses [1,8]. The electronic conduction is credited to the hopping of electrons between Cu^+ and Cu^{2+} ions. At lower concentrations of dopant, the Cu^+ ions are dominating in the specimens [1,8]. The Cu^+ ions play the role of glass formers and hamper the movement of Li^+ ions. Thus, the conductivity is low at lower concentrations of CuO (Table 7) [1,8].

Amidst various types of conduction techniques in the glasses, conduction in a localized state near the Fermi level occurs when σ_{ac} is independent of temperature and fluctuates in accordance with the frequency. Conductivity of current specimens in the lower temperature region (roughly up to 360 K) can be assigned to this process [1–5]. By using the quantum mechanical tunnelling model, the values of the density of energy states $N(E_F)$ are estimated at a temperature of 373 K and at a frequency of 100 kHz by using the following relation [1].

$$\sigma(\omega) = \eta e^2 KT\left\{N(E_F)^2\alpha^{-5}\omega\left[Ln\left(\nu_{ph}/\omega\right)\right]\right\}^4 \quad (15)$$

Where $\eta = \pi/3$ [1] $= 3.66\pi^2/6$ [1] $= \pi^4/96$ [1], with the usual meanings of notations [1]. A continuous rise in the value of $N(E_F)$ with a raise in the dose of CuO indicates the amplification of deformation in the specimens. This outcome suggests a gradual increase in Cu^{2+} ions which increase the defects in the glasses. The same result is also supported by an increase in Urbach energy, decrease in the optical band gap, and studies on the ESR spectra.

By applying an alternating electric field (E) to a dielectric, the heat of the dielectric loss is extricated. Heat loss per unit volume (L) of a specimen is denoted by [1]

$$L\left(W/m^3\right) = E^2\omega\varepsilon'\varepsilon_o\tan\delta \quad (16)$$

From the above equation, it is learnt that greater the value of $\varepsilon'\tan\delta$ larger is the value of L. The large amount of heat released causes an increase in temperature of the model. This event leads to the breakdown of the dielectric. Therefore, the dielectric breakdown strength (DBS) of a glass is inversely proportional to the applied voltage. In the present investigation, the rise in magnitude of $\varepsilon'\tan\delta$ is detected with a gain in the concentration of CuO. This is a cause for the continuous decrease in the values of DBS of the glasses from C0 to C10. This phenomenon supports a gradual decrease in the rigidity of the samples with a gain in the quantum of copper ions. The magnitude of DBS is the least for the glass C10. This result hints the maximum defects in the sample C10.

Optical absorption and ESR studies of the specimens suggested an increase in Cu^{2+} ions with an increase in the content of CuO. A decrease in the optical band gap of glasses hints an increase in the semiconducting nature of glasses. This result is also supported by an increase in the dielectric properties of glasses. FTIR spectra reveal an increase in the intensity of BO_3 units with an increase in the concentration of dopant. This outcome suggests a gradual decrease in the rigidity of the glass. All results are in support of an increase in conductivity of the glasses with a rise in the content of dopant.

5. Conclusions

The glass network $10Li_2O$-30SrO-(60-x)B_2O_3-xCuO ($0 \leq x \leq 1$) was synthesized by the melt quench and heat treatment process. XRD validated the aperiodic nature of the glasses. Optical absorption spectra supported the magnification of Cu^{2+} ions in the models in proportionate to the quantum of CuO. A gradual decrease in the values of optical band gap hints a continuous betterment in the semiconducting essence of the samples. An increase in the value of optical basicity supported the advancement in the ionic temper of the glasses. ESR spectra approved the existence and augmentation of Cu^{2+} ions in the glasses with a rise in the content of CuO. FTIR exhibited an increase in intensity of the bands owing to BO_3 units for the models from C0 to C10. Dielectric studies suggested the gain in the conductivity of the samples with an increase in the concentration of CuO.

Credit Author Statement

All persons who meet authorship criteria are listed as authors, and all authors certify that they have participated sufficiently in the work to take public responsibility for the content, including participation in the concept, design, analysis, writing, or revision of the manuscript. Furthermore, each author certifies that this material or similar material has not been and will not be submitted to or published in any other publication before its appearance in the Materials Research Bulletin.

Authorship contributions

The specific contributions made by each author are as follows:

Category 1

Conception and design of study: A. Ramesh Babu, S. Yusub, V. Aruna, N. Sree Ram, P.M. Vinaya Teja, Y. Chaitanya;

Acquisition of data: A. Ramesh Babu, S. Yusub, V. Aruna, P.M. Vinaya Teja;

Analysis and/or interpretation of data: S. Yusub, A. Ramesh Babu, V. Aruna, N. Sree Ram.

Category 2

Drafting the manuscript: S. Yusub, A. Ramesh Babu, V. Aruna, P.M. Vinaya Teja;

Revising the manuscript critically for important intellectual content: S. Yusub, A. Ramesh Babu, V. Aruna, N. Sree Ram, Y. Chaitanya.

Category 3

Approval of the version of the manuscript to be published (the names of all authors must be listed):

A. Ramesh Babu, S. Yusub, V. Aruna, N. Sree Ram, P.M. Vinaya Teja, Y. Chaitanya.

Declaration of Interest Statement

We wish to draw the attention of the Editor to the following facts which may be considered as potential conflicts of interest and to significant financial contributions to this work. [OR] We wish to confirm that there are no known conflicts of interest associated with this publication and there has been no significant financial support for this work that could have influenced its outcome. We confirm that the manuscript has been read and approved by all named authors and that there are no other persons who satisfied the criteria for authorship but are not listed. We further confirm that the order of authors listed in the manuscript has been approved by all of us. We confirm that we have given due consideration to the protection of intellectual property associated with this work and that there are no impediments to publication, including the timing of publication, with respect to intellectual property. In so doing we confirm that we have followed the regulations of our institutions concerning intellectual property. We further confirm that any aspect of the work covered in this manuscript that has involved either experimental animals or human patients has been conducted with the ethical approval of all relevant bodies and that such approvals are acknowledged within the manuscript. We understand that the Corresponding Author is the sole contact for the Editorial process (including Editorial Manager and direct communications with the office). He is responsible for communicating with the other authors about progress, submissions of revisions and final approval of proofs. We confirm that we have provided a current, correct email address which is accessible by the Corresponding Author and which has been configured to accept email from syedyusuf1985@gmail.com. I, Dr. S. Yusub, on behalf of all authors, am affixing my signature.

With best regards

24-06-2021

Dr. S. Yusub

Corresponding author

Dr. A. Ramesh Babu

Co-author

Dr. V. Aruna

Co-author

N. Sree Ram

Co-author

Dr. P.M. Vinaya Teja

Co-author

Y. Chaitanya

Co-author

Declaration of Competing Interest

We wish to draw the attention of the Editor to the following facts which may be considered as potential conflicts of interest and to significant financial contributions to this work. [OR] We wish to confirm that there are no known conflicts of interest associated with this publication and there has been no significant financial support for this work that could have influenced its outcome. We confirm that the manuscript has been read and approved by all named authors and that there are no other persons who satisfied the criteria for authorship but are not listed. We further confirm that the order of authors listed in the manuscript has been approved by all of us. We confirm that we have given due consideration to the protection of intellectual property associated with this work and that there are no impediments to publication, including the timing of publication, with respect to intellectual property. In so doing we confirm that we have followed the regulations of our institutions concerning intellectual property. We further confirm that any aspect of the work covered in this manuscript that has involved either experimental animals or human patients has been conducted with the ethical approval of all relevant bodies and that such approvals are acknowledged within the manuscript. We understand that the Corresponding Author is the sole contact for the Editorial process (including Editorial Manager and direct communications with the office). He is responsible for communicating with the other authors about progress, submissions of revisions and final approval of proofs. We confirm that we have provided a current, correct email address which is accessible by the Corresponding Author and which has been configured to accept email from syedyusuf1985@gmail.com. I, Dr. S. Yusub, on behalf of all authors, am affixing my signature.

Acknowledgements

All persons who have made substantial contributions to the work reported in the manuscript (e.g., technical help, writing and editing assistance, general support), but who do not meet the criteria for authorship, are named in the Acknowledgements and have given us their written permission to be named. If we have not included an Acknowledgements, then that indicates that we have not received substantial contributions from non-authors.

References

[1] V. Aruna, S. Yusub, M. Venkateswarlu, A. Ramesh Babu, K. Anitha, Efficacy of copper ions on lithium ion conductivity, electron hopping, optical band gap, metallization criterion and morphology of Li_2O-B_2O_3-P_2O_5 glasses, J. Non-Cryst. Solids 15 (2020), 120015, https://doi.org/10.1016/j.jnoncrysol.2020.120015.

[2] S. Yusub, D. Krishna Rao, The role of chromium ions on dielectric and spectroscopic properties of Li_2O-PbO-B_2O_3-P_2O_5 glasses, J. Non-Cryst. Solids 398-399 (2014) 1–9, https://doi.org/10.1016/j.jnoncrysol.2014.04.022.

[3] A. Ramesh Babu, S. Yusub, P.M. Vinaya Teja, P. Srinivasa Rao, V. Aruna, D. Krishna Rao, Effect of Cr_2O_3 on the structural, optical and dielectric studies of LiF-SrO-B_2O_3 glasses, J. Non-Cryst. Solids 520 (2019), 119428, https://doi.org/10.1016/j.jnoncrysol.2019.05.004.

[4] S. Yusub, T. Narendrudu, S. Suresh, D.Krishna Rao, Structural investigation of vanadium ions doped Li_2O-PbO-B_2O_3-P_2O_5 glasses by means of spectroscopic and dielectric studies, J. Mol. Struct. 1076 (2014) 136–146, https://doi.org/10.1016/j.molstruc.2014.07.055.

[5] A.Ramesh Babu, S. Yusub, Ascendancy of iron ions on lithium ion conductivity, optical band gap, Urbach energy and topology of LiF-SrO-B_2O_3 glasses, J. Non-Cryst. Solids 533 (2020), 119906, https://doi.org/10.1016/j.jnoncrysol.2020.119906.

[6] B. Ashok, G. Ramadevudu, M. Narasimha Chary, Md. Shareefuddin, EPR and Optical absorption studies of Na_2O-Al_2O_3-B_2O_3-CuO glasses, Mater. Today 5 (2018) 26883–26888, https://doi.org/10.1016/j.matpr.2018.08.172.
[7] B. Sumalatha, I. Omkaram, T. Rajavardhana Rao, Ch.Linga Raju, Alkaline earth zinc borate glasses doped with Cu^{2+} ions studied by EPR, optical and IR techniques, J. Non-Cryst. Solids 357 (2011) 3143–3152, https://doi.org/10.1016/j.jnoncrysol.2011.05.005.
[8] B.J.R.S. Swamy, R. Bhaskar Sanyal, P.Ramesh Vijay, D.Krishna Babu, N. Rao, Veeraiah, Influence of copper ions on thermoluminescence characteristics of CaF_2-B_2O_3- P_2O_5 glass system, Ceram. Int. 40 (2014) 3707–3713, https://doi.org/10.1016/j.ceramint.2013.09.053.
[9] A.M. Abdelghany, Amal Behairy, Optical parameters, antibacterial characteristics and structure correlation of copper ions in cadmium borate glasses, J. Mat. Res. Tech. 9 (2020) 10491–10497, https://doi.org/10.1016/j.jmrt.2020.07.057.
[10] Shaik Meera Saheb, P.Venkateswara Rao, R. Vijay, P. Ramesh Babu, Ch. Chandrakala, P. Syam Prasad, G. Naga Raju, Spectroscopic and, electrical investigations of copper ions in PbO-GeO_2 glasses, Res. Physics 11 (2018) 780–786, https://doi.org/10.1016/j.rinp.2018.10.012.
[11] Ch. Rajyasree, P. Michael Vinaya Teja, K.V.R. Murthy, D. Krishna Rao, Optical and other spectroscopic studies of lead zinc bismuth borate glasses doped with CuO, Physica B 406 (2011) 4366–4372, https://doi.org/10.1016/j.physb.2011.08.082.
[12] Shiv Prakash Singh, R.P.S. Chakradhar, J.L. Rao, Basudeb Karmakar, Electron paramagnetic resonance, optical absorption and photoluminescence properties of Cu^{2+} ions in ZnO-Bi_2O_3-B_2O_3 glasses, J. Mag. Mag. Mat. 346 (2013) 21–25, https://doi.org/10.1016/j.jmmm.2013.07.007.
[13] K. Srinivasulu, I. Omkaram, H. Obeid, A. Suresh Kumar, J.L. Rao, Spectral studies on Cu^{2+} ions in sodium-lead borophosphate glasses, Physica B 407 (2012) 4741–4748, https://doi.org/10.1016/j.physb.2012.09.010.
[14] O.I. Sallam, A.M. Madbouly, N.A. Elalaily, F.M. Ezz-Eldin, Physical properties and radiation shielding parameters of bismuth borate glasses doped transition metals, J. Alloys Compds. 843 (2020), 156056, https://doi.org/10.1016/j.jallcom.2020.156056.
[15] Ahmed H. Hammad, Essam B. Moustafa, Study some of the structural, optical, and damping properties of phosphate glasses containing borate, J. Non-Cryst. Solids 544 (2020), 120209, https://doi.org/10.1016/j.jnoncrysol.2020.120209.
[16] Aly Okasha, S.Y. Marzouk, A.M. Abdelghany, Design a tunable glasses optical filters using CuO doped fluoroborate glasses, Opt. Laser Tech. 137 (2021) 10682, https://doi.org/10.1016/j.optlastec.2020.106829.
[17] Seema Thakur, Vanita Thakur, Anumeet Kaur, Lakhwant Singh, Structural, optical and thermal properties of nickel doped bismuth borate glasses, J. Non-Cryst. Solids 512 (2019) 60–71, https://doi.org/10.1016/j.jnoncrysol.2019.02.012.
[18] O.A. Zamyatin, V.G. Plotnichenko, M.F. Churbanov, E.V. Zamyatina, V. V. Karzanov, Optical properties of Zinc tellurite glasses doped with Cu^{2+} ions, J. Non-Cryst. Solids 480 (2018) 81–89, https://doi.org/10.1016/j.jnoncrysol.2017.08.025.
[19] Pavan Kumar Pothuganti, Ashok Bhogi, Muralidhara Reddy Kalimi, Padma suvarna Reniguntla, Optical and A.C conductivity characterization of alkaline earth borobismuthate glasses doped with nickel oxide, Optik 220 (2020), 165152, https://doi.org/10.1016/j.ijleo.2020.165152.
[20] Douglas F. Franco, Eduar E. Carvajal, José Pedro Donoso, Maurício A.P. Silva, Antonio C. Sant'Ana, Hssen Fares, Claudio J. Magon, Marcelo Nalin, Structural and EPR Studies of Cu^{2+} ions in $NaPO_3$-Sb_2O_3-CuO glasses, J. Non-Cryst. Solids 503-504 (2019) 169–175, https://doi.org/10.1016/j.jnoncrysol.2018.09.042.
[21] B. Srinivas, Abdul Hameed, G. Ramadevudu, M. Narasimha Chary, Md. Shareefuddin, Evaluation of EPR parameters for compressed and elongated local structures of VO^{2+} and Cu^{2+} spin probes in BaO-TeO_2-B_2O_3 glasses, J. Phys. Chem. Solids 129 (2019) 22–30, https://doi.org/10.1016/j.jpcs.2018.12.042.
[22] Min-QuanKuang Xiao-HuiXu, Study on the local structure and EPR spectroscopy of copper ions in lead borate glass, Optik 152 (2018) 16–20, https://doi.org/10.1016/j.ijleo.2017.09.092.
[23] Shao-YiWu Yong-QiangXu, Chang-ChunDing Li-JuanZhang, Investigations on the EPR parameters and defect structures for Cu^{2+} in alkaline earth zinc borate glasses, Optik 127 (2016) 9167–9171, https://doi.org/10.1016/j.ijleo.2016.06.122.
[24] M.A. Ouis, M.A. Marzouk, Comparative optical, FTIR and photoluminescence spectral analysis of copper ions in BaO-B_2O_3, SrO-B_2O_3 or Bi_2O_3-B_2O_3 glasses and impact of gamma irradiation, J. Lum. 223 (2020), 117242, https://doi.org/10.1016/j.jlumin.2020.117242.
[25] Ali M. Ibrahim, Impact of MoO_3 concentration, frequency and temperature on the dielectric properties of zinc phosphate glasses, Chin. J. Phys. 68 (2020) 919–929, https://doi.org/10.1016/j.cjph.2020.07.013.
[26] S.N. Mohamed, M.K. Halimah, R.H.Y. Subban, A.K. Yahya, AC conductivity and dielectric properties in mixed ionic-electronic 20Na_2O-20CaO-(60-x)B_2O_3- xV_2O_5 glasses, Physica B 602 (2021), 412480, https://doi.org/10.1016/j.physb.2020.412480.
[27] Meena Malik, Sunita Dagar, Ashima Hooda, Ashish Agarwal, Satish Khasa, Effect of magnetic ion, Fe^{3+} on the structural and dielectric properties of Oxychloro Bismuth Borate Glasses, Sol. Sta. Sci. 110 (2020) 10649, https://doi.org/10.1016/j.solidstatesciences.2020.106491.
[28] A.M. Abdelghany, G. El-Damrawi, A.H. Oraby, M.A. Madshal, A.C conductivity and dielectric properties of CoO doped SrO-P_2O_5 glasses, Physica B 573 (2019) 22–27, https://doi.org/10.1016/j.physb.2019.08.026.

ISSN : 2277 - 7881 : Peer Reviewed & Refereed International Journal
IJMER,Volume11, Issue12 (3),December -2022
Impact Factor :8.017,IC Value : 5.16, ISI Value : 2.286

International Journal of Multidisciplinary Educational Research

(Social Sciences, Humanities, Commerce & Management, Engineering & Technology, Medicine, Sciences, Art & Development Studies, Law)

జాతీయ సదస్సు

అంశం

కాళీపట్నం రామారావు కథలు - సామాజిక నేపథ్యం

తేది : 6,7 డిశంబర్ 2022

Editor-in-Chief

Prof. Dr. Victor Babu Koppula

M.A.,M.A., M.Phil.,PDF.,D.Litt

విషయ సూచిక

INTERNATIONAL JOURNAL OF MULTIDISCIPLINARY EDUCATIONAL RESEARCH
ISSN:2277-7881; IMPACT FACTOR :8.017(2022); IC VALUE:5.16; ISI VALUE:2.286
Peer Reviewed and Refereed Journal: VOLUME 11, ISSUE 12(3): December 2022
Scopus Review ID: A2B96D3ACE3EEA2A
Article Received: 2nd December 2022
Publication Date:10th January 2023
Publisher: Sucharitha Publication, India
Digital Certificate of Publication: www.ijmer.in pdf e-CertificateofPublication-IJMER.pdf
DOI: http://ijmer.in.doi./2022/11.12.42
www.ijmer.in

వీరుడు - మహావీరుడు - కారా

డా॥ కనపాల జోసఫ్
తెలుగుశాఖ అధ్యక్షులు,
ఆంధ్రక్రైస్తవ కళాశాల,
గుంటూరు, ఆంధ్రప్రదేశ్.
చరవాణి : 9849025505

అగ్రశ్రేణి కథారచయితలు కథలు రాస్తున్న కాలంలో కాళీపట్నం రామారావు కథకుడిగా తనదైన కథా లోకాన్ని సృష్టించుకున్నాడు. గణితశాస్త్ర ఉపాధ్యాయుడిగా కొనసాగుతూనే కథానికా ప్రపంచంలో తనదైన వరవడితో కథలు రాసేవారు. 1943లో 'ప్లాటుపారమో' అనే రచనతో వీరి రచనా ప్రస్థానం ఆరంబమైంది. ఆరంభంలో దాదాపు 1964 కి ముందు మధ్యతరగతి జీవితాలను ఇతివృత్తంగా కథలు రాస్తుండేవారు. అనంతరం రావిశాస్త్రిగారి సాన్నిహిత్యం. మార్క్సిస్ట్ తాత్వక దృక్పథంతో తన ఆలోచనా పరిధిలో మార్పు చోటు చేసుకుంది. అప్పటి నుంచి నిజజీవితంలో అనుభవించిన, పరిశీలించిన కష్టాలను. సంఘర్షణలను. తన కథల్లో చోటు చేసుకున్నాయి. అలాగే సమాజంలో అట్టడగు వర్గాల జీవన సమరాన్ని సునిశితంగా పరిశీలించి తన పాత్రలలో చూపారు. ఆవిధంగా తొలుత 18 గొప్ప కథలు రాశారు.

ఈకథలు వస్తు పరంగా, శైలిపరంగా అంతకు ముందు రాసిన కథలకు భిన్నంగా, సామాజిక స్పృహతో కూడుకుని ఉండేవి. కథల్లో కనిపించే ప్రాంతాలు, అందులోని పాత్రలు, వారి మాట తీరు, చేతల తీరు బాగా పరిచయం. అందువల్ల కథల్లో ఎంతటి నాటకీయమైన సంఘటన ఉన్న వాటిని చాలా సహజంగా ఆవిష్కరిస్తాడు. అది 'కారా' కు మాత్రమే తెలిసిన కిటుకు. అందువల్ల నేమో ఇన్ని సంవత్సరాలుగదుస్తున్నా ఇప్పటికి వీరి కథలపై జాతీయ సదస్సులు, పరిశోధనలు, చర్చలు జరుగుతున్నాయంటే ప్రముఖ రచయిత, పరిశోధకులు వేల్చేరు నారాయణరావు అన్నట్లు "ఈ కథలు ఒక్కసారి చదవగానే అర్థమైపోవు ఒక్కోసారని లొతిచిన కొద్ది కొత్త విషయాలు బయట పడుతూనే ఉంటాయి అంటారు. అందుకు ఉదాహరణగా 'యజ్ఞం' కథను చేప్పుకోవచ్చు. కాళీపట్నం రామారావు రాసిన మొత్తం '54' కథలు ఇక్కడ ప్రస్తావంచటం సాధ్యం కాని పని. కనుక నాకు నచ్చిన రెండు కథల్ని గురించి ఇక్కడ ప్రస్తావిస్తాను.

గ్రామాలు 'నాగరికత' కోటు తొడుక్కోని రోజుల్లో మల్లెపూలంత తెల్లంగా ఉండేవి. అనాదిగా, వారసత్వంగా వస్తున్న సంస్కృతీ సంప్రదాయాలకు ఆచరిస్తూ ఒదుదుడుకులు లేకుండా జీవించేవారు.

Cover Page

INTERNATIONAL JOURNAL OF MULTIDISCIPLINARY EDUCATIONAL RESEARCH
ISSN:2277-7881; IMPACT FACTOR :8.017(2022); IC VALUE:5.16; ISI VALUE:2.4
Peer Reviewed and Refereed Journal: VOLUME 11, ISSUE 12(3): December
Online Copy of Article Publication Available
Scopus Review ID: A2B96D3ACF
Article Received: 2nd December
Publication Date:10th January
Publisher: Sucharitha Publication
Digital Certificate of Publication: www.ijmer.in/pdf/e-CertificateofPublication-IJMH

DOI: http://ijmer.in.doi./2022/11.12.42
www.ijmer.in

వారి మాటల్లో క్రియల్లో స్పష్టత ఉండేది. విందులు,వినోదాలు అలాగే ఉండేవి. ప్రపంచీకరణ తాకిడి గ్రామాలకు తాకనందువల్ల వినోదాలు తమకు తాముగా ఏర్పాటు చేసుకుని నేదతిరే వారు ప్రత్యేక సందర్భాలల్లో నిర్వహించే వినోద కార్యక్రమాలల్లో ఆసక్తి కలిగిన వారు స్వచ్ఛందగా పాల్గొని ప్రజల్ని ఆనంద పరుస్తూ ఉండేవారు. సాంస్కృతిక మైన వినోదంతో పాటు ఆవేశాలు, పోటీతత్వం కూడా ఉండేది. వీటిని చూపేందుకు గ్రామ ప్రజలు గుంపుల గుంపులుగా వచ్చి చూపేవారు.ఆరోజుల్లో ఇప్పటి లాగా ఆధునిక సౌకర్యాలు లేనందువల్ల ఎక్కడ ఎలాంటి వినోదాలున్నా కాలినడకన వెళ్ళేవారు.

అలాంటి సందర్భంలో గ్రామ ప్రజలందరు ఒకే చోట గుమికూడి ఉన్నందువల్ల వారి మనస్తత్వాలు, వారి మాటతీరు, వారి వ్యక్తిత్వాలు, స్వరూప స్వభావాలను సగ్నంగా, సరళంగా, సహజంగా, శాస్త్రియంగా చిత్రికరించారు. ఆ విధంగా కాళీపట్నం రామారావు తను రాసే కథలకు శాశ్వతత్వాన్ని చేకూర్చేదిశగా విశేష కృషి చేశారు అలా రాసిన కథ "వీరుడు-మహావీరుడు"

కథా సారాంశం

ఈ కథ ఇద్దరు వస్తాదులకు చెందింది. 'శ్రీరామనవమి' పండుగ రోజున వీరిద్దరిలో కుస్తీ పోటీని ఏర్పాటు చేస్తారు. అల్లి పురం వస్తాదు, గంజి పేట రౌడికి మధ్య జరిగే పోటీ ఇది. అల్లిపురం వస్తాదు ఆరడుగుల బలపంతుడు. గంజిపేట రౌడి నాలుగైదు బూతద్దాలు పెట్టుకుంటే గాని కనిపించడు పైగా సల్లిక నరంలాగా ఉంటాడు. వీరిద్దరి మధ్య జరిగే పోటీని చూపేందుకు పనీపాట లేని, కనీసం టీ కి దికాణం లేని, రోజంతా బలాదూరుగా తిరిగి ఆలస్యంగా ఇంటికెళ్ళిగా చీవాట్లు తిని, చేసేది లేక రోడ్డు మీదకు వచ్చేవాళ్ళు. ఇంకా రిక్షావాళ్లు, కంబైన్డ్ స్టడీకి బయలు దేరి స్నేహితుల ఇంట్లో పుస్తకాలు పదిలి వచ్చేవాళ్లు టీ దుకాణాలలో కప్పులు కడిగేవాళ్లు వీరందరికి ఉచితంగా దొరికే వినోదం ఇది.

సినిమాకని రెండు మైళ్ల దూరం నడిచి తీరా అక్కడికి వెళ్ళాక టిక్కెట్లు అయిపోతాయి చేసేది లేక అక్కడిక్కడ తిరుక్కుంటూ వస్తాడు పోటీల గుంపు దగ్గరకు చేరుకుంటాడు ఆ గుంపులో తను మాత్రమే కాస్త తెలివి కలిగిన వాడిగా చెప్పుకుంటాడు. ఇద్దరి మధ్య 'టగ్ ఆఫ్ వార్‌లా' కనిపించే పోటీ ఎందుకు జరుగుతుందో గుంపులోని ఏ ఒక్కడు సరై సమాధానం చెప్పడు ఈ లోగా మూడో వస్తాదు వస్తాడు చూస్తున్న గుంపుకి ఏంజరగబోతుందోనని ఒకింత ఆశ్చర్యంగా చూస్తుండగానే గంజిపేట రౌడీని రెండు దెబ్బలతో నేల కరిపించి అక్కడ నుంచి వెళతాడు.

INTERNATIONAL JOURNAL OF MULTIDISCIPLINARY EDUCATIONAL RESEARCH
ISSN:2277-7881; IMPACT FACTOR :8.017(2022); IC VALUE:5.16; ISI VALUE:2.286
Peer Reviewed and Refereed Journal. VOLUME 11, ISSUE 12(3). December 2022
Online Copy of Article Publication Available (2022 Issues)
Scopus Review ID: A2B96D3ACF3FEA2A
Article Received: 2nd December 2022
Publication Date:10th January 2023
Publisher: Sucharitha Publication, India
Digital Certificate of Publication: www.ijmer.in/pdf/e-CertificateofPublication-IJMER.pdf
DOI: http://ijmer.in.doi./2022/11.12.42
www.ijmer.in

ఈ కథ చిన్నదే కానీ ఇందులో రెండు రకాల సామాజిక వ్యవస్థలుంటాయి. ప్రజలు ఎపరివైపుంటారు. ఎవరివైపు ఉంటే మనుగడ సాగించుకోవచ్చునో చెపుతాడు. బలహీనులు బలపంతులపై ఎన్ని కేక లేసిన ప్రజలు బలహీనులకు అండగా ఉండాల్సింది పోయి బలపంతుల పంచనే చేరడంలో ఉండే ఆంతర్యాన్ని, అంతు చిక్కని జవాబుని ఈ కథలో రచయిత పాఠకులనే తేల్చుకోమని సవాలు విసురుతాడు.

నిజానికి గంజిపేట రౌడికి అల్లిపురం పస్తాదుకి మధ్య జరిగే పోటీని పేద, ధనిక వర్గాల మధ్య జరిగే పోటీగాను, అధికారానికి, ప్రతిపక్షానికి మధ్య జరిగే పోటీగా చిత్రించాడు రచయిత చూస్తున్న గుంపు ఎటూ తేల్చుకోలేక తనుబలహీనుడైనా, బలపంతుల పక్షాన నిలబడాల్సింది పోయి చివరికి బలపంతుల పక్షాన చేరి తమ కేమీ తెలియదని అమాయకంగా మొఖాలు పెట్టుకొనే ప్రజల నైజాన్ని చిత్రిస్తాడు మొత్తంగా అనాదిగా సదుస్తుంది. వర్గసమాజం సమసమాజ స్థాపనకి లెఫ్టిస్టులు సోషలిస్టు దేశాలలో, మనలాంటి అభివృద్ధి చెందుతున్న దేశాలల్లోను అనేక రూపాల్లో చేయని ప్రభుత్వం లేదు. ఇది సాధ్యపడాలంటే పీడత వర్గంలో చైతన్యం రాకపోతే ఇంక సాధ్యపడాలంటే పీడత వర్గంలో చైతన్యం రాకపోతే ఇంక వంద పళ్ళు గడిచినా పరిస్థితిలో ఏ మాత్రం మార్పు రాదు. రచయిత మాటల్లో బిగ్ పవర్ లో వున్న ఆకర్షణనే అది. మనం అనుకుంటాం కాని ఏ కాలంలోనైనా, ఏ లెవల్లోనైనా బిగ్గూ, స్మాలూ తేడాఉ వుండనే వుంటాయి. –అలాగే "జనం జూస్తు అన్నేయాలు జరగనిస్తారో? అనుకుని –న్యాయం, ధర్మం అని పెద్ద పెద్ద కబుర్లుతో చిక్కుల్లో పడతారు. పడి ఒకళ్ళకి తెద్దునా' అందరికీ తెద్దునా అని క్రైసీసులు సృష్టిస్తారు" అంటారు. ఇది ఎప్పటికి అర్థం కాని సంగతి. అందువల్ల నిమ్మళంగా ఎక్కడ పవరు ఉంటుందో ఆ పంచన ఉంటే మిగిలిన బ్రతుక్కు బరోసా ఉంటుంది.

ఉత్తమ పురుష కోణంలో సాగిన ఈ కథ ఆయా వ్యక్తుల మనస్తత్వాలను, వారి జీవన శైలిని అద్భుతంగా ఆవిష్కరించాడు. వర్తమానంలో ఏ వ్యవస్థలో పనిచేసేవారికైన ఈ కథని పోల్చవచ్చు సాధారణంగా ఈ కథని ఒక్కసారి చదివితే ఏ మాత్రం అర్థం కాదు. ఒకటికి రెండుసార్లు ఓపిగ్గా చదవగలిగితే లక్ష ఆలోచనలకు తెరతీసినట్లవుతుంది. వ్యక్తుల్లో వ్యక్తిగత స్వార్థమే తప్ప సామాజిక స్పృహ ఏ మాత్రం లేకపోవడాన్ని ఇలాంటి కథను చదవగలిగితే అర్థం అవుతుంది. ఇలాంటి సదస్సుల ద్వారా కాళీపట్నం రామారావు గారిని వారి కథల్ని గుర్తుచేసినందుకు

Biomedical
Communication

BBRC
Bioscience Biotechnology
Research Communications

Biosc.Biotech.Res.Comm. Vol 13 No (4) Oct-Nov-Dec 2020 Pp-

Indole 3-Acetic Acid Production by *Aspergillus* Species Isolated From Chilli Rhizospheres

Darsi Phebe Sarah Koti Ratnam*
Department of Botany and Microbiology, Andhra Christian College, Guntur, Andhra Pradesh, India.

ABSTRACT

In the present study soil samples were collected from different chilli rhizospheres in the vicinity of Guntur, Andhra Pradesh, India and the filed trails were conducted in the year of 2018-2019. A total of 57 microbial strains were isolated from chilli rhizosphere. All the strains were isolated from potato dextrose agar media by using 10-4 serial dilutions. Fine and clear colonies were picked and transformed into a culture tubes for further studies. For the preliminary screening there are 10 isolates were considered as fungal strains based on spore morphology. The spores are round and irregular in shape with green to light brown in colour. Preliminary identification of these fungal isolates was based on morphological and cultural characters on potato dextrose agar medium. All ten strains showed the maximum indole acetic acid production on Czepakdox agar medium. Various optimization studies like incubation period, pH, temperature and carbon and nitrogen sources were studied by affecting the indole acetic acid productions i.e., 10 days incubation period, pH 7.0 and 30°C. Carbon and nitrogen sources are also affected the indole acetic acid production in this optimization. A carbon and nitrogen source in the optimal medium plays a major role for the production indole acetic acid. Among them, the strain *Aspergillus* PB-7 in presence of Glucose and peptone showed the maximum IAA production of 110µg/ml and 75µg/ml. Successful inoculation of agricultural crops with biocontrol plant growth promoters includes the delivery of sufficient inoculum to the target, economical production of large quantities of microorganisms. Rhizospheric microbes especially plant growth promoting microorganism were promising to be developed as multifunctional biofertilizer.

KEY WORDS: PLANT GROWTH PROMOTERS (PGP), INDOLE ACETIC ACID (IAA), POTATO DEXTROSE AGAR (PDA)..

INTRODUCTION

Chilli can be grown in a wide range of Black, Brown, Red and Clay soils, but black soils which retain moisture for long periods are suitable for rain fed crop whereas well drained soils, deltaic soils and sandy loams are good under irrigated condition. Whereas Sandy and loamy soils poorly supported to chilli production when compare to black soils. Various climatic conditions like humid and hot weather supports to the chilli plants. Sometimes environmental conditions are also adversely affected the chilli growth and fruit production. India is the largest producer and consumer of chilli among other major producers in the world. India contributes about 47 per cent to the total world production, and assumes first position in terms of international trade, exporting 38 per cent of its total production.

Chilli production in India is moving northwards on increasing demand from diversified sectors and changing consumption patterns. Dry chilli production rose by nearly 52 per by nearly 52 per cent from 9.7 lakh tones in 1997-98 to about 18 lakh tonnes. More than 80% of the

ARTICLE INFORMATION

*Corresponding Author: phebesarah63@gmail.com
Received 25th Sep 2020 Accepted after revision 5th Nov 2020
Print ISSN: 0974-6455 Online ISSN: 2321-4007 CODEN: BBRCBA

Thomson Reuters ISI Web of Science Clarivate Analytics USA and Crossref Indexed Journal

Clarivate Analytics
crossref

NAAS Journal Score 2020 (4.31) SJIF: 2020 (7.728)

*Online Contents Available at: http//www.bbrc.in/
DOI: http://dx.doi.org/10.21786/bbrc/*

bacteria isolated from the rhizosphere can produce (IAA) Indole Acetic Acid (Khalid et al., 2004) in the presence of precursor, tryptophan either through root exudates or from the proteins released by the dead bacteria cells (Patten and Glick, 1996). Indole-3-acetic acid (IAA), a plant growth hormone compound, is a natural auxin produced by plants, bacteria, fungi and a diverse group of organisms. It is a metabolite derived from tryptophan by many tryptophan dependant and tryptophan independent pathways in plants as well as bacteria and fungi. These growth improvers act as biocontrol agents. (Pattern and Glick, 2002; Wesam et al., 2017).

Various soil microorganisms including bacteria, fungi (Finnie and Van Staden, 1985) and algae (Stein et al., 1990; Rifat Hayat et al., 2010) are capable of producing physiologically active growth hormones like auxins and gibberellins which may exert prominent effects on plant growth and development. Many PGPR (Plant growth promoting) microorganisms associated in chilli rhizosphere. Chilli is one of the important agriculture produce Andhra Pradesh also. Chillies from Andhra Pradesh are well known for their pungency and good red colour. Several districts like Guntur, Krishna, Prakasam, Nellore, Chittor and Anantapuram are the main chilli growing districts in Andhra Pradesh. The present study was mainly focussed on indole acetic acid production and optimization studies by fungal strains isolated from chilli rhizosphere. These strains were used as bio inoculants in application to the farmer's fields and it is useful for sustainable agriculture (Wesam et al., 2017).

MATERIAL AND METHODS

Isolation of fungi done using the rhizosphere soil samples from the chilli fields of 10 different areas of Guntur, district of Andhra Pradesh, India were collected for the study. Fungal strains were isolated on Potato Dextrose Agar (PDA) medium by soil dilution plate technique (Rapilly, 1968) using 10^{-3} to 10^{-5} dilutions. The plates were incubated at 28 ± 2°C for 5 days. Fungal colonies appeared in the plates were noted and sub cultured. After purified by single spore isolation method and they were maintained on potato dextrose agar (PDA) slants. Identification of Fungal solates was based on culture characters as well as microscopic parameters (conidiophores branching, phialides shape and position, spore size and shape) (Nagamani et al., 2006). The pure cultures were stored in the refrigerator at 4°C for further studies.

Screening of isolates for IAA production was determined based on the method described by Patten and Glick (2002) with slight modifications. One milli liter of supernatant was mixed with 2 ml of Salkowski reagent (1ml of 0.5M $FeCl_3$ in 50mL of 35% $HClO_4$) and incubated for 1hr. Development of pink colour indicated the production of IAA. The quantification of IAA was read at 540 nm in a UV- Vis spectrophotometer. A standard curve was plotted for quantification of IAA solution and uninoculated medium with a reagent as a control. The amount of IAA in the culture was expressed as µg/ml (Gordon and Weber, 1951).

Figure1: IAA production (µg/ml) by *Aspergillus* species

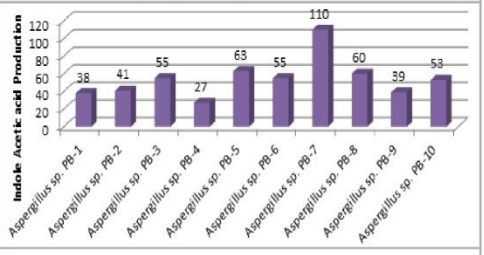

*The overall model is significant with p<0.05

Figure 2: Effect of incubation period on IAA production (µg/ml) by *Aspergillus* species PB 7

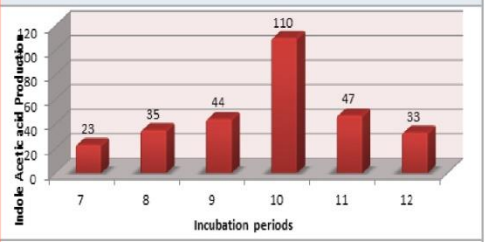

*The overall model is significant with p<0.05

The optimization studies for IAA production to determine the IAA production, different incubation periods (7, 8, 9, 10, 11 and 12 days), pH levels (4, 5, 6,7, 8 and 9) and temperature (4,20, 25, 30, 35 and 40°C) were studied. Various carbon (1%) and nitrogen (0.1%) sources were studied by using the above method.

For the statistical analysis, all measurements were carried out in triplicate. Statistical analyses were performed using one-way analysis of variance (ANOVA), and the significance of the difference between means was determined by Duncan's multiple range tests. Differences at $P < 0.05$ were considered statistically significant.

RESULTS AND DISCUSSION

A total of 57 strains were isolated from chilli fields in the vicinity of Guntur district, Andhra Pradesh, India. All the strains were tested for IAA production; among them 10 strains were positive results on Potato dextrose

agar medium (Figure-1). The present study mainly reveals the IAA production of the selected 10 fungal strains. Maximum IAA production was observed on Aspergillus sp. PB 7 strain which showed 110 µg/ml of IAA, followed by *Aspergillus* sp. PB 5 strain (63 µg/ml). Minimum IAA production was recorded in *Aspergillus* sp. PB 4 with 27 µg/ml. IAA productions by ten fungal strains between the range of 27-110 µg/ml. *Aspergillus flavus* Promoted the Growth of Soybean and Sunflower Seedlings which was reported by Humayun et al., (2019).

Optimization studies for IAA production (µg/ml) by *Aspergillus* species PB 7: For the optimization studies we selected PB 7 *Aspergillus* strain which showed maximum IAA production and was tested with the effect of incubation period, pH and temperatures, carbon and nitrogen sources.

Effect of incubation period on IAA production by *Aspergillus* species PB 7: The IAA production was started between 7 to 12 days of incubation periods (Figure-2). The maximum IAA production was observed on 10th day of incubation (110 µg/ml). Similarly Unyayar et al., (2000) and Hansan (2002) reported that the maxumum amount of IAA was synthesized during the stationnary phase of growth. May be these reason was that during stationnary phase the bacterium might be able to get maximum tryptophan from dead bacterial mass, which could result in more IAA production. Reduction of IAA production at the later might be due to release of IAA degrading enzymes by the bacteria (Hunter, 1989).

Effect of pH on IAA production (µg/ml) by *Aspergillus* species PB-7: The pH of the medium showed a significant influence on the production of IAA by fungal strains. The maximum IAA production (110 µg/ml) was observed at pH 7 (Figure-3). For many authors, the optimum pH for IAA production is between 6 to 9. However, the below and above pH 8 the production of IAA was less, because Streptomyces sp population level is more in alkaline soil than the acidic soil (Shirokikh et al., 2007; Mohite, 2013; Bharucha et al., 2013; Dasri et al., 2014).

Figure 3: Effect of pH on IAA production (µg/ml) by *Aspergillus* species PB-7

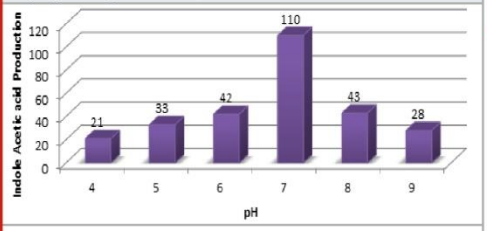

*The overall model is significant with p<0.05

Effect of different temperature on IAA production (µg/ml) by *Aspergillus* species PB-7: The effect of different temperature on IAA production by fungal strains showed that, the maximum IAA production was obtained at 30°C (65 µg/ml) followed by 35°C (44 µg/ml) and 40°C (29 µg/ml) respectively (Figure-4).

Figure 4: Effect of temperature on IAA production (µg/ml) by *Aspergillus* species PB-7

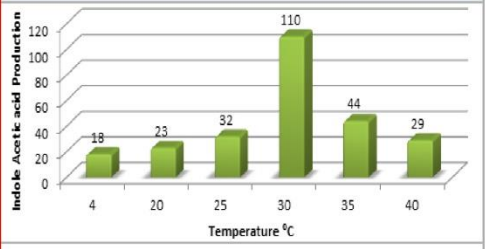

*The overall model is significant with p<0.05

Effect of different carbon source on IAA production (µg/ml) by *Aspergillus* species PB-7: Different carbon sources (mannitol, Starch, glucose, sucrose, fructose, lactose and Arabinose) were studied for their effect on IAA production by *Aspergillus* species PB-7 (Figure-5). Glucose in the medium gave maximum IAA production (110 µg/ml) followed by arabinose (51µg/ml) and lactose (48 µg/ml).

Figure 5: Effect of carbon sources on IAA production (µg/ml) by *Aspergillus* species PB-7

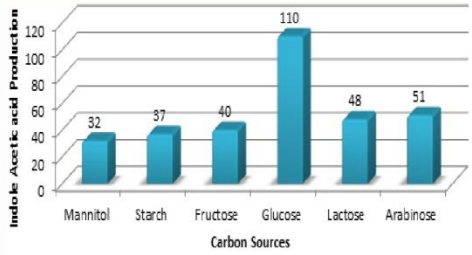

*The overall model is significant with p<0.05

Effect of different nitrogen sources on IAA production (µg/ml) by *Aspergillus* species PB-7: Various nitrogenous compounds (Ammonium sulphate, potassium chloride, Yeast extract, peptone and beef extract). These nitrogen source have a significant effect on IAA production (Figure-6). Among all the nitrogen sources used, peptone was found to be the best nitrogen source for IAA production. Organic and inorganic nitrogen sources can be utilized by *Pseudomonas* sp. prefers yeast extract (Balaji, 2012), *Pantoea agglomerans* PVM prefer beef

(Apine and Jadhav, 2011), and Ammonium sulphate was found to be for IAA production of *Acetobacter diazotrophicus* L1, the most suitable nitrogen source (Nita et al., 2011).

Figure 6: Effect of nitrogen sources on IAA production (µg/ml) by *Aspergillus* species PB-7

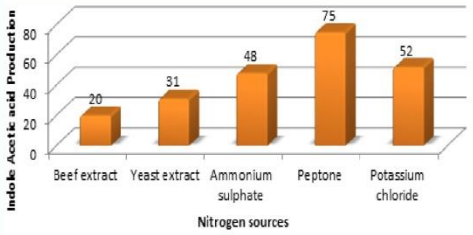

*The overall model is significant with $p<0.05$

CONCLUSION

From the results, it is clear that *Aspergillus* species PB 7 isolated form chilli rhizospheres preferred glucose and peptone as carbon and nitrogen sources respectively. The optimum conditions for this culture are incubation 12 days, pH 7.0 and 30°C temperature. There were several plant growth promoting rhizobacterial (PGPR) inoculants that seems to promote plant growth through different mechanism such as plant growth hormone production, nutrient acquisition and plant disease suppression. Thus the optimized microbial inoculants may be useful for the production of multifunctional biofertilizers.

ACKNOWLEDGEMENTS

Author would like to thank the Department of Botany and Andhra Christian College, Guntur for providing necessary facilities to complete this research work.

REFERENCES

Apine, O. A. and Jadhav, J. P. (2011). Optimization of medium for indole-3-acetic acid production using *Pantoea agglomerans* strain PVM. Journal of Applied Microbiology, 110(5), 1235-44.

Balaji, N., S. S. Lavanya, S. Muthamizhselvi and K. Tamilarasan (2012). Optimization of fermentation condition for indole acetic acid production by *Pseudomonas* species. International Journal of Advanced Biotechnology and Research, 3, 797-803.

Bharucha U., Patel K., and Trivedi U. B. (2013). Optimization of Indole Acetic Acid Production by *Pseudomonas putida* UB1 and its Effect as Plant Growth-Promoting Rhizobacteria on Mustard (*Brassica nigra*). Agric Res.

Dasri, K., Kaewharn, J., Kanso, S. and Sangchanjiradet, S., (2014). Optimization of indole-3-acetic acid (IAA) production by rhizobacteria isolated from epiphytic orchids. Asia-Pacific Journal of Science and Technology, 19: 268-275.

Finnie, J. F. and Van Staden, J. (1985). Effect of seed weed concentrate and applied hormones on *in vitro* cultured tomato roots. J Plant Physiol. 120: 215- 222.

Gordon, S.A. and Weber, R.P. (1951). Colorimetric estimation of indole acetic acid. Plant physiology, 26(1):192-195.

Hamayun, M., Hussain, A., Afzal Khan, S., Iqbal, A. and Lee, I.J., (2019). *Aspergillus flavus* promoted the growth of soybean and sunflower seedlings at elevated temperature. BioMed research international, 2019:1-13.

Hansan H.A.H. (2002). Gibberellin and auxin production by plant root fungi and their biosynthesis under salinity-calcium interaction. Rostlinna Vyroba, 48 : 101-106.

Hunter, W.J. (1989). Indole-3-acetic acid production by bacteroids from soybean root nodules. Physiol. Plant. 76 : 31-36.

Khalid A., Tahir, S., Arshad, M. and Zahir, Z.A. (2004). Relative efficiency of rhizobacteria for auxin biosynthesis in rhizosphere and non-rhizosphere soils. Aus. J. Soil Res. 42:921-926.

Mohite B. (2013). Isolation and characterization of indole acetic acid (IAA) producing bacteria from rhizospheric soil and its effect on plant growth. Journal of soil science and plant nutrition, 13(3): 638-649.

Nagamani A, Kunwar IK, and Manoharachary C. (2006). Handbook of soil fungi, IK Int Pvt Ltd. New Delhi: pp.425.

Nita B. Patil, Milind Gajbhiye, Sangita S. Ahiwale, Aparna B. Gunjal and Balasaheb P. Kapadnis. (2011). Optimization of Indole 3-acetic acid (IAA) production by *Acetobacter diazotrophicus* L1 isolated from Sugarcane. International Journal of Environmental Sciences, 2(1), 307-314.

Patten C. L. and Glick B. R. (2002). Regulation of indole acetic acid production in *Pseudomonas putida* GR12-2 by tryptophan and the stationary-phase sigma factor RpoS. Canadian journal of microbiology, 48(7):635-642.

Patten, C. L., and B.R. Glick. (1996). Bacterial biosynthesis of indole-3-acetic acid. Canadian journal of microbiology 42: 207-220.

Rapilly F. (1968). Les Techniques de mycologie en pathologie végétale. Ann. Epiphyt. 101p. Bruxelles.

Rifat Hayat, Safdar Ali, Ummay Amara, Rabia Khalid, and Iftikhar Ahmed. (2010). Soil beneficial bacteria and their role in plant growth promotion: a review. Ann

Microbiol. 60: 579- 598.
Shirokikh, I. G., Zenova, G. M., Merzaeva, O.V., Lapygina, E.V., Batalova, G.A. and Lysak, L. V. (2007). Actinomycetes in the prokaryotic complex of the rhizosphere of oats in a soddy podzolic soil. Eurasian Soil Sci. 40: 158-162.
Stein, A., Fortin, J. A. and Vallee, G. (1990). Enhanced rooting of *Picea mariana* cuttings by ecto mycorrhizal fungi. Can J Bot. 68: 492-498.
Unyayar, S., Unal, E. and Unyayar, A., (2000). Production of auxin and abscisic acid by Phanerochaete chrysosporiumme446 immobilized on polyurethane foam. Turkish Journal of Biology, 24(4):769-774.
Wesam I. A. Saber, Khalid M. Ghoneem, Younes M. Rashad and Abdulaziz A. Al-Askar. (2017). *Trichoderma Harzianum* WKY1 : an indole acetic acid producer for growth improvement and anthracnose disease control in sorghum. Biocontrol Science and Technology, 27 (5), 654–676.

International Journal of Science Academic Research
Vol. 02, Issue 03, pp.1179-1181, March, 2021
Available online at http://www.scienceijsar.com

ISSN: 2582-6425

Research Article

CHARACTERIZATION OF L- ASPARGINASE AND LIPASE PRODUCING ASPERGILLUS SP. DPB-365 ISOLATED FROM CHILLI RHIZOSPHERES

***Darsi Phebe Sarah Koti Ratnam**

Department of Botany & Microbiology, Andhra Christian College, Guntur, Andhra Pradesh, India

Received 20th January 2021; **Accepted** 16th February 2021; **Published online** 18th March 2021

Abstract

This paper describes production and characterization of L-Asparginase and Lipases from *Aspergillus* species isolated from chilli rhizosphere in the vicinity of Guntur, Andhra Pradesh. The isolated fungi were screened for L-asparaginase production using Czapek's agar media. On the basis of pink colour zone formed, ten fungal strains was selected and identified as *Aspergillus* species and names as *Apergillus* sp. DPB-365. This study investigates the optimization and production of L- Asparagine and Lipase. Days of incubation, temperature, pH, supplementary carbon and nitrogen sources on the production of L- Asparagine and Lipase was studied and accordingly optimum conditions were determined. The isolated soil fungi *Aspergillus species* is a strain that produces high levels of L- Asparagine, under optimized culture conditions, *viz.,* on the third day of incubation at an optimum pH of 7.5 and temperature of 37ºC. The isolate *Aspergillus* sp. DPB-365 showed highest enzyme L- Asparginase production 71.2 IU/mg and Lipase production 65.5 IU/mg respectively. L-asparaginase has been used as anti-tumor agent for the effective treatment of acute lymphoblastic leukemia and as food processing aid to reduce the acrylamide formation during frying of starchy foods at high temperature.

Keywords: L- Asparginase, Lipase, Aspergillus.

INTRODUCTION

Enzymes are one of the essential products acquired for the needs of human through microorganisms. Enzymes like Amylases, Lipases, L- Asparginase, Glutaminase, Proteases and Cellulases has great industrial value in the present-day market. Among these Amylases plays a crucial role in enzyme market. Most of the prominent enzymes like protease, cellulases and amylase were used in many industries. L-asparaginase belongs to an amidase group that produces aspartic acid and ammonia by asparagine hydrolysis (Wriston and Yellin, 1973, Capizzi *et al.,* 1984). The search for other asparaginase sources, like eucaryotic microorganisms, can lead to an enzyme with less adverse effects. The importance of microorganisms as L-asparaginase sources has been focused since the time it was obtained from *Escherichiacoli* and its antineoplastic activity demonstrated in guinea pig serum (Broome, 1961; Mashburn and Wriston 1964; Roberts *et al.,* 1966; Schawartz *et al.,* 1966, Boyse *et al.,* 1967). This enzyme is widely distributed, being found in L-asparaginase is widely distributed, being found in animal, microbial and plant sources. Large number of microorganisms that include *Erwiniacarotovora, Pseudomonas stutzeri*, *Pseudomonasaeruginosa* and *E. coli*. It has been observed that eukaryotic microorganisms like yeast and fungi have a potential for asparaginase production. For example, the mitosporic fungi genera such as *Aspergillus, Penicillium*, and *Fusarium*, are commonly reported in scientific literature to produce asparaginase (Abdel Fatteh *et al*., 2002; Qin and Zhao, 2003; Wade *et al*., 1971). The literature reports suggested that the enzyme produced by different microbial strains differed in some physiological, biochemical, catalytic and immunological properties. So the continuous screening program is necessary for the isolation of novel microbial strains that could produce an effective enzyme.

Corresponding Author:** ***Darsi Phebe Sarah Koti Ratnam,
Department of Botany & Microbiology, Andhra Christian College, Guntur, Andhra Pradesh, India.

To our knowledge, reports on the production of L-Asparginase from *bacillus and Aspergillus species* is very limited. In the present investigation, the one-factor-at-a-time approach was used to select the best combination of incubation period, pH, temperature, carbon, nitrogen sources studied.

MATERIALS AND METHODS

Isolation of fungi: The rhizosphere soil samples from the chilli fields of 10 different areas of Guntur, district of Andhra Pradesh, India were collected for the study. Fungal strains were isolated on Potato Dextrose Agar (PDA) medium by soil dilution plate technique (Rapilly, 1968) using 10^{-3} to 10^{-5} dilutions. The plates were incubated at 28 ± 2°C for 5 days. Fungal colonies appeared in the plates were noted and sub cultured. After purified by single spore isolation method and they were maintained on potato dextrose agar (PDA) slants. Identification of Fungal isolates was based on culture characters as well as microscopic parameters (conidiophores branching, phial ides shape and position, spore size and shape) (Nagamani *et al.,* 2006). The pure cultures were stored in the refrigerator at 4°C for further studies.

L- Asparginase production: The production of L-asparaginase was carried out by using 20 g of carob pod as a substrate under solid state fermentation. The moisture content of the flask is 65% were maintained and inoculated 1 ml of inoculum (1x107spores/ml). The content of the flask were mixed thoroughly gently beating the flasks on the palm of hand and incubated in slanting position at 35 0C for 7 days. The pH 4.5 was maintained throughout the fermentation process.

Enzyme Assay: Assay of enzyme was carried out as per Imada*et al*. 0.5 ml of 0.04 M asparagine was taken in a test tube, to which 0.5 ml of 0.5 M buffer (acetate buffer pH 5.4), 0.5 ml of enzyme and 0.5 ml of distilled water was added to make up the volume up to 2.0 ml and incubate the reaction

mixture for 30 min. After the incubation period the reaction was stopped by adding 0.5 ml of 1.5 M TCA (Trichloroacetic acid). 0.1 ml was taken from the above reaction mixture and added to 3.7 ml distilled water and to that 0.2 ml Nessler's reagent was added and incubated for 15 to 20 min. The OD was measured at 450 nm. The blank was run by adding enzyme preparation after the addition of TCA. The enzyme activity was expressed in International unit.

Lipase production: One ml of olive oil along with 100 ml basal salt solution (Peptone: 0.5 g; MgSO4.7H2O: 0.05 g; KCl: 0.05 g; KH2PO4: 0.2 g; NaNO3: 0.05 g) in 250 ml of Erlenmeyer flask were autoclaved at 15 psi for 15 minutes. These flasks were inoculated with *Aspergillus* sp. DPB-365and incubated at28±1 °C in shaking incubator (80 rpm) for 5 days.

Enzyme assay: Crude enzyme extract was prepared from the culture supernatant which was centrifuged at 10,000 rpm for 15 min at 4°C. Lipase activity was measured spectrophotometrically using pnitrophenyl acetate (pNPA) as a substrate at 45°C in 100 mM phosphate buffer of pH 7.0 (Licia *et al*., 2006). The substrate for this reaction was composed of solution A and B. Solution A contained 40 mg of p-nitro phenyl actetate dissolved in 12 ml of isopropanol, solution B contained 0.1 g of gum arabic and 0.4 ml of triton X-100 dissolved in 90 ml of distilled water. The substrate solution was prepared by adding 1 ml of solution A and 19 ml of solution B. The assay mixture contained 1 ml of the substrate, 0.5 ml of buffer, 0.1 ml of enzyme and final volume was made up to 3 ml with distilled water. The enzyme activity was stopped by adding 0.2 ml isopropanol and liberation of *p*-nitrophenol at 28 °C was detected in spectrophotometer at 400 nm. One enzyme unit was defined as 1 µmol of p-nitrophenol enzymatically released from the substrate per minute Syed *et al*., (2010).

Optimization of medium and cultural conditions: Optimization of different cultural conditions such as incubation period, pH, temperature, carbon, and nitrogen sources on the production of L-Asparginase was determined.

Effect of incubation period on L- Asparginaseand lipase production: To study the effect of incubation period on L-Aspargine production, the enzyme production by *Aspergillus* sp. DPB-365 was studied for every 24 hours up to 96 hours. For this study, the RN-7 culture was inoculated into 500 ml conical flask, containing sterile M9 broth and was incubated from 24 hours up to 96 hours at 37°C and triplicates were maintained. The optimum time, showing maximum production was taken for further experiments.

Effect of pH on L- Asparginaseand lipase Production: To study the effect of different pH on L- Aspargine production, the isolate *Aspergillus* sp. DPB-365 was grown in sterile M9 broth with various pH levels ranging from 5.0 to 9.0. and was maintained by using phosphate buffer. 0.5 ml of the 24-hour old inoculum was transferred into the sterile M9 broth at different pH and incubated at 30°C for 48 hrs and assayed for enzyme activity. The most favourable pH achieved at this step was used for further study.

Effect of temperature on L- Asparginase and lipase production: To study the effect of temperature on L-Aspargine production, the isolate *Aspergillus* sp. DPB-365 was grown in sterile M9 broth at different temperatures, ranging from 30 to 55^{O}C for 48 hrs of incubation and temperature was maintained by using respective incubators. 0.5 ml of the 24-hour old inoculum was transferred into a sterile M9 broth and was incubated and further assayed for enzyme activity.

Optimization of L- Asparginaseand lipase Production by *Aspergillus* sp. DPB-365

Effect of Different Carbon Sources on L- Asparginaseand lipaseproduction: To study the effect of carbon sources on L-Aspargine production by growing the bacterial strain *Aspergillus* sp. DPB-365 on M9 broth, the broth was supplemented with different carbon sources such as Galactose, Maltose, Fructose, Starch, Sucrose, and Cellulose, each at a concentration of 1% (w/v). 0.5 ml of the inoculum was added to a sterile M9 broth with different carbon sources, incubated at 30°C for 72 hrs and assayed.

Effect of Different Nitrogen sources on L- Asparginaseand lipase production: Different nitrogen sources like Yeast extract, Tryptone, Ammonium sulphate, Urea, Peptone and Malt extract were added to the M9 broth separately at a rate of 1% (w/v), and 0.5 ml of the inoculum from the bacterial isolate *Aspergillus* sp. DPB-365 was added to sterile M9 broth, incubated at 30°C for 72 hrs and was assayed for enzymatic activity.

Statistical Analysis: All measurements were carried out in triplicate. Statistical analyses were performed using one-way analysis of variance (ANOVA), and the significance of the difference between means was determined by Duncan's multiple range tests. Differences at $P< 0.05$ were considered statistically significant.

RESULTS

A total of 10 isolates were obtained from chilli rhizosphere in the vicinity of Guntur, Andhra Pradesh. The preliminary characterization like cultural and biochemical characteristics was done by Bergey's manual of systemic bacteriology. All the isolates belong to *Aspergillus* species according to their preliminary and biochemical studies. Different incubation (7, 8, 9, 10, 11, 12, 13 and 14 days) periods were studied for the L- Asparginase and Lipase production. Maximum enzyme production was observed by 12 days of incubation period (Table-1). In this study enzyme production of each strain is based on the specific growth rate of the strain. Growth rate and enzyme synthesis of the culture are the two main characteristics which are mainly influenced by incubation time (Ellaiah *et al*., 2002).

Table 1. Effect of incubation period on L- Aspargine and Lipase production by *Aspergillus* sp. DPB365

Sl.no	Incubation period	L- Aspargine production (IU/mg) by Aspergillus sp. DPB365	Lipase production (IU/mg) by Aspergillus sp. DPB365
1	7	18	11
2	8	27	17
3	9	36	28
4	10	42	33
5	11	59	45
6	12	71.2	65.5
7	13	60	44.7
8	14	55	21.3

*The overall model is significant with p<0.05

Different pH levels were maintained for the L- Asperginase and Lipase production by Aspergillus sp. DPB365. Maximum enzyme production was obtained from neutral pH. Acidic

phase to a neutral phase enzyme activity increased up to a pH of 4.0 and upon further increase in pH, enzymatic activity decreased (Table-2).

Table 2. Effect of pH on L- Aspargine and Lipase production by *Aspergillus* sp. DPB365

Sl.no	pH	L- Aspargine production (U/L) sp. DPB365	Lipase production (IU/mg) by Aspergillus sp. DPB365
1	4	2	18
2	5	16	24
3	6	57	32
4	7	71.2	65.5
5	8	61	41
6	9	44	32
7	10	25	21

*The overall model is significant with p<0.05

Various temperate levels were maintained for the L-Asperginase and Lipase production by Aspergillus sp. DPB365. Maximum enzyme production was obtained from 35°C nearly room temperature. Further increase in temperature enzymatic production was decreased (Table-3).

Table -3. Effect of temperature on L- Aspargine and Lipase production by *Aspergillus* sp. DPB365

Sl.no	Temperature (□C)	L- Aspargine production(U/L) by *Aspergillus*sp. DPB365	Lipase production (IU/mg) by *Aspergillus*sp. DPB365
1	4	5	2
2	15	22	14
3	20	35	21
4	25	51	30
5	30	65	42
6	35	71.2	65.5
7	40	60	41
8	45	48	22

*The overall model is significant with p<0.05

Different carbon sources were tested for L- Asparginase and Lipase production by *Aspergillus* sp. DPB365. Maximum enzyme production was obtained from Glucose was used as carbon source followed by rhamnose (Table-4). Majority of the carbon sources greatly influenced the enzyme production by *Aspergillus* sp. DPB365.

Table 4. Effect of carbon sources on L- Asparginaseand Lipase production by *Aspergillus* sp. DPB365

Sl.no	Carbon sources	L- Asparginase production (IU/mg)Aspergillussp. DPB365	Lipase production (IU/mg) by Aspergillus sp. DPB365
1	Glucose	71.2	36.4
2	Maltose	65	42.4
3	Rhamnose	70	55.1
4	Fructose	68	52.6
5	Xylose	55	58.7
6	Arabinose	52	62.7
7	Starch	63	48.4

*The overall model is significant with p<0.05

Different nitrogen sources were tested for L- Asparginase and Lipase production by *Aspergillus*sp. DPB365. Maximum enzyme production was obtained from glutamine followed by proline (Table-5).

Table -5. Effect of nitrogen sources on L- Aspargineand Lipase production by *Aspergillus* sp. DPB365

Sl.no	Nitrogen sources	L- Aspargine production (IU/mg)sp. DPB365	Lipase production (IU/mg) by Aspergillus sp. DPB365
1	Proline	73.5	42.5
2	Urea	70	51.6
3	Glutamine	88	43.8
4	Sodium nitrate	65	31.4
5	Ammonium sulphate	60	28.2
6	Peptone	68	60.5
7	Beef extract	62	51.2

*The overall model is significant with p<0.05

Acknowledgements: Author would like to greatly thankful the department of Botany and Andhra Christian College, Guntur for providing necessary facilities to complete this research work.

REFERENCES

Abdel-Fatteh Y., and Olama Z.A. 2002. L-asparaginase produced by *Pseudomonas aeruginosa* in solid state culture: evaluation and optimization of culture conditions using factorial designs. *Process Biochem,* 38, 115-122.

Boyse AE, Old LJ, Campbell HA, Mashburn LT. 1967. Suppression of murine leukaemia of various types: comparative inhibition activities of guinea pig serum L-asparaginaseand *E. coli*. *J Expl Med 125*: 17-31.

Broome JD. 1961. Evidence that the L-asparaginase activity of guinea pig serum is responsible for its antilymphoma effects. *Nature 191*: 1114-1115.

Capizzi RL, Poole M, Cooper MR, Richards F, Stuart JJ, Jakson DV, White DR, Spurr CL, Hopkins JO, Muss HB. 1984. Treatment of poor risk acute leukaemia with sequential higdone ARA-C and asparaginase. *Blood, 63*: 649-700.

Ellaiah P., Adinarayana K., Bhavani Y., Padmaja P. and Srinivasulu B. 2002. Optimization of process parameters for glucoamylase production under solid-state fermentation by a newly isolated *Aspergillus sp.Process Biochemistry.* 38 (4): 615-620.

Imada, A., Igarasi, S., Nakahama, K. and Isono, M., 1973. Asparaginase and glutaminase activities of micro-organisms. *Microbiology*, *76*(1), pp.85-99.

Licia M. P., Cintia M. R., Mario D. B and. Guillermo, R. C 2006. *Food Technol. Biotechnol*., 44(2), 247-252.

Mashburn LT, Wriston JC. 1964. Tumor inhibitory effect of Lasparaginase from *Escherichia coli*. *Arch Biochem Biophys105*: 450-452.

Nagamani A, Kunwar IK, Manoharachary C. 2006. Handbook of soil fungi, IK Int Pvt Ltd. New Delhi: pp.425.

Qin, M., and Zhao F. 2003. L-asparaginase release from *Escherichi acoli* cell's with aqueons two-phase micelles, systems. *Appl. Biochem. Biotahnol,* 110 (1), 11-21.

Rapilly F. 1968. Les Techniques de mycologie en pathologie végétale. *Ann. Epiphyt*. 101p. Bruxelles.

Roberts J, Prager MD, Bachynsky N. 1966. The antitumor activity of *E. coli* L-asparaginase. *Cancer Res 26*: 2213-2217.

Schwartz JH, Reeves JY, Broome JD. 1966. Two L-asparaginases from *E. coli* and their action against tumors. *Proc Natl AcadSci USA 56*: 1516-1519.

Syed M. N., Iqbal S., Bano S.,. Khan A. B, Ali-ul-Qader S. and Azhar, A. 2010. *African Journal of Biotechnology*, 9 (45), 7724-7732.

Wade H.E., Robinson H.K., and Philips B.W. 1971. Asparaginase and Glutaminase a ctivities of bacteria. *J. Gen. Microbiol,* 69, 299-312.

Wriston JC, Yellin T 1973. L-asparaginase: A review. *Adv Enzimol., 39*: 185.

****

IJCRT.ORG ISSN : 2320-2882

INTERNATIONAL JOURNAL OF CREATIVE RESEARCH THOUGHTS (IJCRT)

An International Open Access, Peer-reviewed, Refereed Journal

OPTIMIZATION STUDIES ON PLANT GROWTH PROMOTING BACTERIAL ISOLATES FROM CHILLI RHIZOSPHERE

Darsi Phebe Sarah Koti Ratnam*

Associate Professor, Department of Botany & Microbiology, Andhra Christian College, Guntur, Andhra Pradesh, India.

Abstract:

Plant growth promoting bacteria are known to influence the plant growth by various direct or indirect mechanisms. In search of efficient PGPR strains with multiple activities, a total of 10 bacterial isolates belonging to *Bacillus* species isolated from chilli rhizosphere, Guntur district of Andhra Pradesh, India. Out of ten only one isolate *Bacillus* sp. PB-3 showed potential activity of producing IAA, Gibberellic acid production, Siderophore production. *Bacillus* sp. PB-3 showed the maximum IAA (85 µg/ml) and Gibberellic acid productions 52 µg/ml were observed. An orange halo appears around the *Bacillus* species on CAS agar media indicates the siderophore production. The optimum conditions for siderophore production in *Bacillus* sp. PB-3 was selected for this study. CAS medium was supplemented with mannitol (18.6 µg/ml) and Urea (18.4 µg/ml) was used as carbon and nitrogen sources showed maximum amount of siderophores. These plant growth promoting abilities can make this isolate a potential PGPR candidate for its application in sustainable agriculture.

Keywords: Gibberellic acid, Indole Acetic Acid, Siderophore

Introduction:

In agriculture plant growth promoters play a major role for sustainable production. Bacteria and fungi also play a key role in agriculture. The genus *Bacillus* sp. stand out as one of the main genus of PGP used to promote of plant growth. Rhizospheric microorganisms produce vitamins, antibiotics, plant hormones, synthesis of vitamins, amino acids, auxins, cytokinins and gibberellins which stimulate plant growth and antagonism with potential plant pathogens and communication molecules that all encourage plant growth. Plant growth hormones (IAA and

Gibberellic acid) were produced in chemically defined medium using the bacterial strains Bacillus cereus, *Bacillus Licheniformis, B. pumilus and B. subtilis.* Bacterial species like *Bacillus pumilus* and *Bacillus licheniformis,* isolated from the rhizosphere of *Alnus glutinosa* L. Gaertn., both have strong growth promoting activity (Probanza *et al*., 1996). Although it was soon found that both were auxin producers (Gutierrez and Manero *et al*., 1996), the characteristics of the induced growth are also suggestive of GA-like promotion.

More than 80% of the bacteria isolated from the rhizosphere can produce (IAA) Indole Acetic Acid (Khalid *et al*., 2004) as secondary metabolite by obtaining tryptophan either through root exudates or from the proteins released by the dead bacteria cells (Patten and Glick, 1996). The metabolites obtained from microorganisms. Indole-3-acetic acid (IAA), a plant hormone compound, is a natural auxin produced by plants, bacteria, fungi and a diverse group of organisms. Indole Acetic acid is a metabolite derived from tryptophan by many tryptophan dependant and tryptophan independent mechanism in plants and bacteria. There is more than one mechanism could be present in a bacteria (Pattern and Glick, 2002). Siderophores are broadly grouped into two main categories, viz. phenolates and hydroxamates. Bradyrhizobia and rhizobia infecting Cicer, Cajanus, Vigna, Leucrena, Medicago, cluster bean, peanut and Acacia are known to produce species-specifics siderophores of hydroxamate, catechols and organic acid type as well as some unknown types of siderophores (Dudeja *et al*. 1997).

Materials and methods

Isolation

One gram representative soil sample was suspended in 10 ml of sterile distilled water and shaken thoroughly for 10 minutes. Microorganisms were isolated from collected samples by the serial dilution plate technique using Nutrient Agar Medium (NAM). Serial dilutions up to 10^{-5} of each sample were prepared by using sterilized water (Sneath, 1986). Sample dilutions were plated (in triplicates) on NAM and incubated at 35^{o} C for 24 to 48 h. Pure Colonies were picked and maintained on NAM slants at 4^{o} C and further assessed for enzyme production in liquid medium.

Indole Acetic acid production

To determine the production of IAA, culture suspension of the strain was inoculated in starch tryptone broth supplemented with 0.5% L-Tryptophan, adjusted to initial pH 7.0 and incubated for 48 h, at 30°C. After incubation, culture broth was centrifuged at 10,000 rpm for 20 min. The supernatant (5 ml) was mixed with 1ml of IN HC1 and 4 ml of Salkowski reagent and observed for the development of pink colour. Optical density was read at 530 nm in a spectrophotometer (Sinha and Basu, 1991). Standard Graph was prepared by using increasing concentration of authentic IAA (Gordon and Weber 1951).

Gibberellic acid production:

To determine the production gibberellic acid, the culture suspension was inoculated into starch broth supplemented with 60 mM concentration of mevalonic acid, adjusted with initial ph 7.0 and incubated at 30° C for 48 h. After incubation culture broth was centrifused 10000 rpm for 20 min. The supernatant was acidified to pH 2.5 with HCl and extracted using liquid-liquid (Ethyl acetate/NaHCO3) extraction (Cho *et al.*, 1979). Gibberellic acid in the ethyl acetate phase was measured by UV spectrophotometer at 254 nm (Bruckner Blechschmidt, 1991).

Siderophore production:

Siderophore production by the plant growth promoting bacteria was estimated by the method described by Schwyn and Neilands (1987). Siderophore production was indicated by orange halos around the colonies after the incubation.

Siderophore assays

For the detection of siderophore production in Bacillus sp. PB-3 was grown on the medium containing 0.5 µM of iron, and incubated for 24 h on rotary shaker at 200 rpm at room temperature. A clear orange hallo zone around the colonies appears on Chrome Azurol S (CAS) agar medium which indicate the siderophore positive.

Chrome Azurol S (CAS) Agar medium

For the detection of siderophore, Bacillus sp. PB-3 isolate was grown in synthetic medium, containing 0.5 µM of iron and incubated for 24 h on a rotary shaker at 200 at 30° C. Culture supernatant was added to the wells made on the CAS agar plates and incubated at room temperature for 24 h. Formation of yellow to orange coloured zone around the well indicates siderophore production (Schwyn and Neiland's, 1987). All glassware used to store stock solution of the medium were treated with concentrated HNO_3 and left to overnight. After 24 h, the acid was removed and the glassware was rinsed thoroughly with double distilled water.

Optimization for Siderophore production

Various factors like effect of iron concentration, effect of carbon and nitrogen sources influence the siderophore production. Quantitative estimation of siderophore production was done by using spectrophotometer (480 nm).

Effect of incubation period

For the production of siderophore different incubation periods (24, 48, 72, 96, 120, 144 and 168 h) were carried out in this study.

Effect of iron concentration on Siderophore production

In this experiment Different concentrations (10, 20, 30, 40 and 50 µM) of iron (Fecl3) was determined by growing the rhizobacteria in the basal medium upto 168 h of incubation for siderophore production.

Effect of carbon sources on Siderophore production

To study the siderophore production by using different carbon sources (Mannitol, glucose, sucrose, Succinate and citrate) were studied. The rhizobacteria were inoculated in the basal medium for 168 h of incubation and estimated the siderophore production.

Effect of nitrogen sources on Siderophore production

To study the siderophore production by using different nitrogen sources (ammonium sulphate, sodium nitrate, urea, glutamine and glycine) were replaced with 0.1% yeast extract. The rhizobacteria were inoculated in the basal medium for 144 h of incubation and estimated the siderophore production.

Results and discussion

Total of 10 isolates were obtained from chilli rhizosphere in the vicinity of Guntur, Andhra Pradesh. The preliminary characterization like cultural and biochemical characteristics of rhizobia was done by Bergey's manual of systemic bacteriology. All the isolates belong to Bacillus species according to their preliminary and biochemical studies. . All the isolates were designated as Bacillus sp. PB-1 to Bacillus sp. PB-10 and tested for plant growth promoting study (Table-1). All the isolated showed that the IAA, gibberellic acid and Siderophore productions. Isolate Bacillus sp. PB-3 showed maximum IAA and gibberellic acid productions. Tryptophan is the main precursor of IAA biosynthesis (Patten and Glick, 1996). Lee *et al.*, (2004) have reported that L- tryptophan was more active for IAA production, though bacteria were able to produce IAA in absence of tryptophan (Jayaprakashvel *et al*., 2014).

Table-1 Plant growth promoting characteristics of Bacillus species isolated from chilli rhizosphere

Isolates	Indole Acetic Acid production (µg/ml)	Gibberellic acid production (µg/ml)	Siderophore production
Bacillus sp. PB-1	-	**22.4**	-
Bacillus sp. PB-2	-	**13.8**	-
Bacillus sp. PB-3	**85.0**	**52**	+
Bacillus sp. PB-4	**38.2**	-	-
Bacillus sp. PB-5	**45.0**	-	-
Bacillus sp. PB-6	**33.8**	-	-
Bacillus sp. PB-7	-	-	+
Bacillus sp. PB-8	-	**16.7**	+
Bacillus sp. PB-9	-	-	+
Bacillus sp. PB-10	**35.1**	**22.8**	-

Effect of incubation period on siderophore production

Siderophore production started after 24 h of incubation time showed by Bacillus sp. PB-1. Maximum zone was observed after 168 h of incubation (Table-2). Maximum production was obtained at 144 h of incubation. Further increase in incubation period there is no change in the production.

Table 2: Effect of incubation period on siderophore production by Bacillus sp. PB-3

Incubation periods	Siderophore production µg/ml
24	**2.40**
48	**5.20**
72	**11.8**
96	**14.4**
120	**19.6**
144	**23.0**
168	**23.0**

* The overall model is significant with $p<0.05$

Effect of iron concentration

Iron concentration influences the siderophore production by bacillus species. Siderophore production was increase with increasing iron concentrations 10 µM to 50 µM (Table-3). Generally the siderophore production was observed in the iron restricted medium. Iron stressed conditions lead to production of strong iron-chelating agents such as siderophores (Diaz *et al*., 2002).

Table - 3.Effect of iron concentration hydroxamate type on Siderophore production

Iron concentrations (µM)	Siderophore production µg/ml
10	**2.40**
20	**5.20**
30	**11.8**
40	**19.6**
50	**13.0**

* The overall model is significant with $p<0.05$

Effect of carbon sources

Among the 5 carbon sources tested, maximum siderophore concentration was observed in Glucose containing medium, Bacillus sp. PB-3 showed the maximum siderophore production with mannitol containing the medium (18.6 µg/ml) (Table-4). The amount and the type of the siderophore produced by an organism depend on the availability of organic and inorganic nutrients (Neilands 1982; Abd-Alla, 1998). Glucose and Mannitol proved the most suitable carbon source for hydroxamate type of siderophores in *Pseudomonas aeruginosa*, *Aspergillus nidulans*, *Pseudomonas chrysogenum* and *Bradyrhizobium japonicum* (Mahmoud and Abd- Alla, 2001).

Table 4: Effect of carbon sources on siderophore production by Bacillus sp. PB-3

Carbon sources	Siderophore production µg/ml
Control	**1.20**
Mannitol	**18.6**
Glucose	**14.0**
Sucrose	**16.8**
Succinate	**11.4**
Citrate	**8.20**

* The overall model is significant with $p<0.05$

Effect of Nitrogen sources

Siderophore production by the tested microorganisms was affected by different nitrogen sources (Table -5). According to this Urea proved to be the most suitable nitrogen source for Bacillus sp. PB-3.

Table 5: Effect of nitrogen sources on siderophore production by Bacillus sp. PB-3

Nitrogen sources	Siderophore production µg/ml
Control	**3.0**
Ammonium sulphate	**14.2**
Sodium nitrate	**14.6**
Urea	**18.4**
Glutamine	**12.0**
Glycine	**13.2**

* The overall model is significant with $p<0.05$

CONCLUSION

The present strains *Bacillus* sp. PB-3 isolated from chilli rhizospheres showed that indole acetic acid, Gibberellic acid and siderophore production. For Optimization studies CAS medium was supplemented with mannitol and urea as carbon and nitrogen sources showed maximum siderophore production. This isolate may useful for biocontrol, and is evaluated to improve of siderophore production in agriculture fields.

References:

1. Abd-Alla, M.H. (1998). Growth and siderophore production in vitro of Bradyrhizobium (Lupin) strains under iron limitation. *European journal of soil biology*, 34(2):99-104.

2. Bruckner B, Blechschmidt D. (1991). The Gibberellin fermentation. *Crit Rev Biotechnol* 11: 163-192.

3. Cho KY, Sakurai A, Kamiya Y, Takahashi N, Tamura S. (1979). Effects of the new plant growth retardants of quaternary ammonium iodides on gibberellin biosynthesis in Gibberella fujikuroi. *Plant and Cell Physiology*. 20(1):75-81.

4. Dudeja S.S., Suneja S., Khurana A.L.: (1997). Iron acquisition system and its role in legume-Rhizobium symbiosis. *Indian I.Microbiol.* 37,1-11.

5. Gutierrez-Manero FJ, Ramos-Solano B, Probanza A, Mehouachi J, Tadeo FR, Talon M (2001). The plant growth-promoting rhizobacteria Bacillus licheniformis produce high amounts of physiologically active gibberillins. *Physiologia Plantarum.* 111: 206-211.

6. Gordon, S.A. and Weber, R.P. (1951). Colorimetric estimation of indole acetic acid. *Plant physiology*, 26(1):192-195.

7. Jayaprakashvel M., Abishamala, K., Periasamy, C.M., Satheesh, J., Hussain, A.J. and Vanitha, M.C., 2014. Isolation and Characterization of Indole Acetic Acid (IAA) Produced by a Halo Tolerant Marine Bacterium Isolated from Coastal Sand Dune Plants. *Biosciences Biotechnology Research Asia*, 11:263-269.

8. Khalid A., Tahir, S., Arshad, M. and Zahir, Z.A. 2004. Relative efficiency of rhizobacteria for auxin biosynthesis in rhizosphere and non-rhizosphere soils. *Aus. J.Soil Res*. 42:921-926.

9. Lee S., Flores, E.M., contreras , Z,M., Gracia , F,L., Escamilla, J,E., and Kennedy, C. 2004. IAA biosynthesis is deficient in Gluconacetobacter diazotrophicus strains with mutations in cytochrome c biogenesis gene .*Journal of Bacteriology*. 186(16): 5384- 5391.

10. Mahmoud, A.L.E. and Abd-Alla, M.H. (2001). Siderophore production by some microorganisms and their effect on Bradyrhizobium-Mung Bean symbiosis. *International Journal of Agricuture and Biology*, 3(2):157-162.

11.Neilands, J.B. (1981). Microbial iron compounds. *Annual review of biochemistry*, 50(1):715-731.

12. Pattern, C.L., Glick, B.R. (2002). Role of Pseudomanas putida indo lactic acid in development of the host plant root system. *App. Eniron. Microbeal.* 68, 3795-3801.

13. Probanza A, Lucas JA, Acero N, Gutierrez-Manero FJ. (1996). The influence of native rhizobacteria on european alder (Alnus glutinosa [L.] Gaertn.) growth. I. Characterization of growth promoting and growth inhibiting bacterial strains. Plant Soil. 182: 59–66.

14. Patten, C. L., and B.R. Glick. (1996). Bacterial biosynthesis of indole-3-acetic acid. *Canadian journal of microbiology,*42: 207-220.

15. Sneath PHA, (1986). Bacillus. In Bergey's Manual of Systematic Bacteriology, edited by. Mair NS, Sharpe ME, Holt JG, Baltimore, USA, Williams and Wilkins. 2:1105-1139.

16. Schwyn, B. and Neilands, J.B. (1987). Universal chemical assay for the detection and determination of siderophores. *Analytical biochemistry*, 160(1):47-56.

17. Sinha B. K. and Basu P. S. (1981). Indole-3-Acetic Acid and its Metabolism in Roo Nodules of *Pongamia pinnata* (L.) PIERRE, *Biochemie und Physiologie der Pflanzen.* 176, 218-227.

www.literaryendeavour.org ISSN 0976-299X

LITERARY ENDEAVOUR

International Refereed / Peer-Reviewed Journal of
English Language, Literature and Criticism

VOL. XII NO. 3 JULY 2021

Chief Editor
Dr. Ramesh Chougule

16

AUSTRALIAN ABORIGINE'S CRAVING FOR LIBERATION FROM THE WHITES' SO CALLED LEGITIMATE PROTECTION BOARD: AN ANALYTICA STUDY

Anna Shalini Garapati, *Ph.D. Research Scholar, Department of English, KLEF Deemed to be University, Vaddeswaram -Andhra Pradesh*
Dr. Sarakanam Srinivas, *Associate Professor. Department of English, KLEF Deemed to be University, Vaddeswaram -Andhra Pradesh*

Abstract:

From the very beginning, far-reaching incompatibilities were the main factors which led the Europeans and Aborigines being unable to come to terms with each other. The contrast was enormous in that one was 'civilised' and 'sophisticated' and the other considered 'uncivilised' and 'primitive'. Therefore, it was difficult for Europeans and the Aborigines to understand each other's complex societies, habits, intelligence and social values. To the Aborigines, an intrinsic part of their life was deep emotional attachment to the land, which had mythical and social values of considerable significance. The entire continent had mythical signs and values related to their tribal system and status. They were completely dependent on land for their dreams and aspirations. Through it, they had acquired their inspirations for art, music, dancing, and other forms of cultural standing and lived in comparative harmony with their environment. Their lives were not at all simple. They were with harsh climate, inhospitable land, droughts, and fires; they had a lot to contend with. Despite all the adversities, they lived in relative peace and harmony until the arrival of the Europeans.

Key words: *Assimilation policies, genocide, protection boards, terra-nullies etc.*

Ever since their introduction, Europeans failed to understand the Aboriginal values of environment appreciation, respect for the past, and privileges affecting them. These attributes had assured their future and their survival for over 60,000 years. From the moment Aborigines realised that Europeans had come not just to visit them but to settle permanently, the Aborigines regarded the intrusion into their lives with disdain. Many took up their primeval armaments and struggled for their survival. Due to the fact that they were unable to organise themselves into a fighting force and were against sophisticated British firing power, they were crushed. Later, most Aboriginal attacks became mere skirmishes on guerrilla basis; they seldom succeeded in pinning the enemy.

For ages land was the utmost component in the lives of Aboriginal Australians. They were intimately familiar with all aspects of it, as their dependence was directly related to it. Their everyday living demanded that they should have adequate knowledge of land. They were in harmony with all living creatures around them. Through mythical beliefs and dreaming their natural world was included in their social world. Ceremonial sites were of particular significance, unlike other areas for hunting and gathering. Not only the ceremonial sites but also the whole concept of land was sacred to them. Their mythical beliefs came very close to creation of land, and since myth was closely related to their socio-religious terms, land became the sacred issue in an Aboriginal culture. In British terms, land was a God-given gift to them. It was highlighted by special significance and related to their sacred beliefs with spiritual importance. Land was an inalienable and incontrovertible right of possession. Spiritual linkage to

land by birth thrust a particular tribe to a sector of land, which facilitated food, ceremonial sites, and everything else for everyday living. Even today, landowning groups can be easily identified all over Australia. Land holding was a spiritual phenomenon, only truly held by mythical beings. Their human representations were granted alien on land to hold not for themselves and their future off springs but for the dead as well. There was definite ownership linkage through birth, myth, and death. Land title was held by signifying ritual emblems possessed by a particular tribe who had relevant claim. The title was not transferable. It was inalienable heritage of the particular tribe.

Hot climate necessitate daily hunting, as no food could be stored for any length of time. They all shared in fishing, hunting, and gathering available plants and seeds. In those circumstances, they had very little time to do anything else. Every activity related to the commune rather than the individual. Their system of living and any form of government were quite informal. There was no chief or king or leader as such. If the clan was not sanctioned by an elder on matters of misdemeanour or disputes, they were left to float along very much like the unstable nature and variations of the environment. People were not static. Ecology played a part, where they were bound together in the scale of nature in complex relationships. There was no competition, little violence, and they lived in comparative peace. They developed a classless society, where struggle for anything else other than food would be no longer an issue. They buffeted round in a constantly transforming environment which sometimes brought about for the betterment.

Against this attitude to life, they were persuaded by the white society to be 'civilised', whenever they were conquered or whenever they came into contact with white missionaries or station owners. Naturally, it was a giant leap for them to adapt. Those who did not want to be 'civilised' were possibly shot or cleared away from the white environment by using deceptive strategies. Since the white men placed no value on the black women's consent, women were taken as they pleased. The Aboriginal girls were viewed as sexual commodity to be used by pastoral workforce of both whites and black stockman as they deemed fit. They ended up with all the vices and diseases of the white society. The Aborigines, then as now, could not overcome the huge obstacles which confronted them. This was largely due to the fact that the white society had mistakenly assumed that the Aborigines had no culture and badly needed civilising. Later, they systematically had begun to assimilate them and their children into the white culture, which the Aborigines consistently tried to reject. Others, such as the outback station owners and missionaries, merely regarded them as part of the environment which was there for them to exploit.

It is, therefore, no wonder that the Aborigines felt the undesirable, which up to this day they have constantly resisted. As the ages rolled on, the new age groups have not ready to lose their lawful inherited lands, most of which have been irretrievably lost to white Australians. Despite the High Court decision in 1992 in Mabo Case, this atlast re-established, inter alia, that home-grown individuals were the native residents of Australia, and, therefore, the ownership of land rested with them, successive governments have no guts and ethical staying power to severely put into practice of the High Court's verdict. Pemulwuy waged a radical war against the British invasion between 1788 and 1802. Due to his fight to the invaders, he championed himself as one of the most revered and recorded about chronological facts in Australian aboriginal narration. He was considered as a brave warrior. Pemulwuy, a Bidjigal man from the Botany Bay area, experienced the witnessed the harm done to Aboriginal society by the invaders. And he was not tempted to befriend them as Arabanoo and Bennelong has done. He took initiation for several battles on the settlement from Botany Bay to the Parramatta area and later to Toongabbee. During this time, he left a notorious criminal gamekeeper namely John McIntyre. And he was then sought after for slay. He was gunshot and hospitalised in a fight during 1797 at Parramatta. Yet he runs away with the help of his hamlet. Wanted dead or alive, Pemulwuy was at last assassinated in1802 and his head was sent to England. His son was Tedbury was captivated into custody in 1805. About one hundred years after Philip, the misconception that Aborigines never legally 'occupied' Australia was put to rest by the Mabo decision by the High Court.

Previously, judges were bound to follow the legal precedent that Australia was *terra nullius* (unoccupied) at the time of the settlement, and therefore, all Aboriginal land belonged to the Crown. Mabo Case recognised the principle of enduring native right.

Apart from the burning issues of land rights and reconciliation, improvements in their health and welfare remain much to bed desired. These pressing issues are dark blights on the whole Australian nation and source of constant criticisms by progressive nations of the world and those who postulate human rights and do nothing about them. Politicians of all shades bungle on regardlessly and because of certain attitude racism has bred through ignorance and xenophobia. The dim light on the horizon for the indigenous people is likely to remain dim for a very long time.

These Aboriginal people are communally addressed as the 'Stolen Generations' because quite a few generations were affected. Even today, several Aboriginal people are still search for their routes to roots. The expression *Stolen Generations* is used for Aboriginal people compellingly taken away (stolen) from their families between the 1890s and 1970s. Of these people, none of them have the chance to see neither their parents nor siblings. Several decades we speak of 'generations' (plural) rather than 'generation'. This is the most flaming fret for members of the Stolen Generations. While taking the aboriginal children white community stole Aboriginal people's bright future. The social domains like culture, language, tradition, knowledge, dances and spirituality could only sustain if moved on to their children. By denying this kind of life white community destined to abolish Aboriginal civilization within a short time and got out of 'the Aboriginal problem'. By the early 20th century, underneath the absorption strategy white Australians thought Aboriginal people would wash out. Within three generations, they thought, Aboriginal genes would have been 'bred out' when Aboriginal people had children with white people.

It was an assumption for several years that the Aboriginal girls would rise up and get married nice white boys. There was an unrevealed plan behind them that they would mrge as pleasant fairer kids. If the children were girls, they would marry white boys again and ultimately the dark colour would wash out. It was the deceptive sketch of the whites including A.O. Nevellie. The entire deceptive idea of stripping the children in the name of fostering them was adopted as a policy. It was based on the women because the women were considered as breed machine. Adult Aboriginal people resisted efforts to be driven out of towns by simply coming back. But children taken away were much easier to control. “I grew up feeling alone, a black girl in a white world, and I resented them for trying to make me white but they couldn't wash away thousands of years of dreaming (Aunty Rhonda Collard, member of the Stolen Generations” (10).

Female children of Aboriginals who were taken away were not treated well. They were also ill fed and used them for station workers and domestic servants. With this kind of cut-price and time and again underpaid wages, they were made servants. The White society unable to put up the riches and road and rail network that helped them prospers without these people. The economy was forcefully taken away and used for their development. This is how the story of the Stolen Generations and the stolen wages become single story. The high-hand authorities created the impression that the aboriginal children were as their Aboriginal parents would neglect them. There are facts, however, that kids were malnourished or famished because Aboriginal people were not paid the full wages they were to be paid.

The Aborigines were strained to live on the Government reserves or mission stations. Yet they chiefly lived in filth and dearth. Though, they received the basic necessities like medicine, shelter, a least of foodstuff that in most places was insufficient to continue a healthy life, and the customary blankets. In a few places some coaching and basic training in practical skills was also provided. There was a very high child mortality rate within the reserves. It is noticeable fact, whether the mission or reserve was church or government run; the original people who were placed there were strictly controlled and strictly punished if they did not abide by the set of laws set by the whites. Aborigines were put into suffering like mute and ignorant animals and chained slaves in thieir own Land. They had been disconnected of their previous way

of life and were not essential to the comfort and security of Aboriginal people in 1900. The land is not mere rocks or minerals or soil, but a holistic environment that sustains and is sustained by culture and people. For aboriginal Australians, the land is the centre of all religious mysticism and this relationship and the spirit of 'country' is inner to the issues that are important to aboriginal people today. Aboriginal Australians were gatherers and semi-nomadic, with each clan having its own territory from which they 'made their living'. These dwelling places, customary lands 'traditional lands' were interconnected by geographic borders such as lakes, rivers, and mountains. They are undeclared and cared for their varied environments, and attuned to them. "*We cultivated our land, but in a way different from the white man. We endeavoured to live with the land; they seemed to live off it. I was taught to preserve, never to destroy" (98).* Aborigine Tom Daystar aboriginal social contact of the land is simultaneous to their exceptional tracking skills based on their gather life and hunter. This includes the ability to trail down birds, animals, to make out and find edible vegetation, to find sources of water and fish.

At the same time, Aboriginal literature also adopts strategies of deliberate silence over certain issues, almost as a means of holding power in hand. It is interesting to look at various arguments about Aboriginal literature as the outcome of Aboriginal suffering. Critics express the view that Aboriginal Literature is a protest literature. And majority of the people express the view that Aboriginal literature is the psychological outcome of social oppression. Hence, we say that an indigenous legendary dialogue emerges from the Aboriginal pain as the new times gone by (in the short or the longer term) of settled folks expressing themselves in the language of the colonizer. However, the Aboriginal writers do adopt strategies of shaping this history by selective disclosure. Yet, although most Native fictional conversation deals with the colonial quandary, it is not confined to the colonizer or colonized discourse alone. This research pinpoints how Aboriginal literature works as an foreword to the history people and at hand tight spot, and an eye opener to non-Aboriginal people. Refusing to fit automatically into any Western intellectual discourse, Aboriginal literature emerges as a decolorized or decolonizing literature in its spirit, content, purpose and functions. This literature functions not only as literature, but also as a historical, social, political and economic discourse, and it also bends the English language inevitably.

It is pertinent to observe that Australian Aboriginal literature and Aboriginal movement had emerged influenced by the similar political, social and cultural conditions. The referendum of 1967 on the cultural, ethnical prejudice causes in Australian constitution and the establishment of Aboriginal Tent Embassy on the lawns of National parliament in 1972 illustrated the arrival of new era in Aboriginal affairs. The autonomy and the taking sides pressure of Aboriginals increased throughout the entire country and led to the granting of franchise to Aboriginals in 1961 and 'freedom rides' organized by Charles Perkins in 1965. These social and political movements consolidated around the values such as sovereignty, self-determination and community control in the areas of social action. This has brought in the issues of land rights, cultural heritage, health, education and housing for more concentration and equal availability.

These important socio-political changes altered the Aboriginal culture and prepared them to invite the literary experiments of Aboriginal literature. This has further consolidated the basic association between the socio-political environment and indigenous imaginative characters in English. Adam Shoemaker in *Black Words White Page: Aboriginal Literature-1929-1988* (2000) analyses the relationship that existed between social consciousness and literary consciousness: "It is complex relationship. It is not one in which the literature demonstrably operates as a direct reaction to socio-political events (although this is occasionally the case); nor is it a relationship in which literature observably influences Aboriginal behaviour or political action" (10). Shoemaker is of the view that Aboriginal literature has to be understood as a close proximate reflection of social events. The naturalism conveyed in Aboriginal novels and the inspiration espoused by Aboriginal plays stem from the personal experiences of Aboriginal writers. Most of the Aboriginal characters are modelled upon individuals to a

great extent on the familiarity of Aboriginal writers. In short, it must be examined and evaluated that Aboriginal literature cannot be studied in isolation but always in terms of social environment, the historical events and in the midst of responsible circumstances. However, the approach to Aboriginal literature is explicitly historical, sociological and cultural and it refuses to be deterministic under all the situations. These perspectives demonstrate that Aboriginal literature is a phenomenon worthy of serious cultural and critical considerations.

Aboriginal literature is primarily concerned with Aboriginal themes. But, there are also several White society writers who took up themes of Aboriginals. Some of the Australian writers deriving inspiration from Aboriginality depicted Aboriginal themes. This has brought in the question of Aboriginal identity to be defined on the lines of exclusive Aboriginality. The Aboriginal consciousness has defined that Aboriginal literature strictly should comprise of the writings by Aboriginals only. Though, this perspective limits the subject of Aboriginality as the property of Aboriginal writers, it has exposed the politics of representation. Representation of someone on behalf of community, race or class is viewed as act of domination. It is also viewed as an act of independence and self-proclamation. Every race, community, class, caste etc., is expected to carry the representation on its own irrespective of the disunity involved. The sagacity of idealism, progressivism, and humanism is found to be in the efforts involved in making the subjugated groups learn the act of representation. Ernie Blackmore in *Speaking Out Black* (2008) probes the issue of who is speaking out whom in relation to Urban/Indigenous voice reflected in Australian theatre argues the voice that speaks for the large number of Aboriginals should necessarily be an Aboriginal voice. Though literature is the product of cross-cultural communication, Aboriginal literature is particular about the concerns of few Europeans who established genuine criticism against their own dominant society. It is also very particular about the parallel and contrastive approaches adopted by Aboriginal and non-Aboriginal writers in dealing with controversial Aboriginal subjects. So, in the gradual evolution of Aboriginal literature, Aboriginal subjectivity has been shaped and moved from passive representation to deterministic uncompromising portrayal of ultra-post-colonial Aboriginality.

The Aborigines Protection Board was established to manage reserves and the welfare of the estimated 9000 Aboriginal people living in New South Wales in the 1880s. It was part of the Department of Police and was chaired by the Commissioner of Police. The Board had the power to: move Aboriginal people out of towns; set up managers, local committees and local guardians (police) for the reserves; control reserves; prevent liquor being sold to Aboriginals; and to stop whites from associating with Aboriginals or entering the reserves. The Board was renamed the Aborigines Welfare Board in 1940 by the Aborigines Protection (Amendment) Act 1940, which stipulated that Aboriginal people should be assimilated into mainstream white society. The existence of Aboriginal communities, many of whom were calling for "land in our own country", was a challenge to authorities. The Protection Board, initially charged with overseeing the gazettal of Aboriginal reserves, quickly took over control from the missionaries and installed its own managers. 2015 marks 100 years since amendments to the NSW Aborigines Protection Act gave the board far-reaching powers with consequences that are felt to this day.

The 1915 amendments gave the board complete power to remove Aboriginal children from their families. They also enabled the acceleration of the revocation of Aboriginal reserves and the casting off of Aboriginal families from largely independent and successful farms around the state. For many Aboriginal people of those times, this was a board not of protection, but persecution. The board utterly controlled the lives and affairs of Aboriginal people in NSW from 1883 until 1969.

References:

1. S. Slemon. "*Magic Realism as Post-Colonial Discourse*", Canadian Literature, No.116 (Spring 1988).
2. Shoemaker, Adam. *Black Words, White Page*. Queensland: University of Queensland Press, 1989

Print.
3. ----------."*White on Black/Black on Black*". The Oxford Literary History of Australia. Bruce Bennett, Jennifer Strauss, and Chris Wallace-Crabbe, ed. Melbourne: OUP, 1998. 20 March 2010.
4. Strickland, John. "*The Tired Australian*". LA Weekly (2002).11 Sept.2006.
5. Stokes, Geoffreyed. *The Politics of Identity in Australia.* Melbourne: Cambridge University Press, 1997Print.
6. Sontag, Susan. *On Photography*. New York: Farrar, Straus and Giroux, 1977Print.
7. Strelau, Marilyn. "*Whose Image*? *Whose Mirror*? (Aboriginal Writing)". Antipodes14.2 (2000).

WORLD JOURNAL OF PHARMACEUTICAL RESEARCH
SJIF Impact Factor 8.084
Volume 9, Issue 14, 1081-1088. Review Article ISSN 2277– 7105

CHARACTERIZATION OF CHITINASE PRODUCING BACILLUS SPECIES ISOLATED FROM CHILLI RHIZOSPHERES OF GUNTUR DISTRICT ANDHRA PRADESH

Phebe Sarah Koti Ratnam*

Department of Botany & Microbiology, Andhra Christian College, Guntur, Andhra Pradesh, India.

Article Received on
16 Sept. 2020,
Revised on 06 Oct. 2020,
Accepted on 27 Oct. 2020
DOI: 10.20959/wjpr202014-18597

***Corresponding Author**
Phebe Sarah Koti Ratnam
Department of Botany & Microbiology, Andhra Christian College, Guntur, Andhra Pradesh, India.

ABSTRACT

Chitin is the second most abundant organic and renewable source in nature, after cellulose. Chitinases are chitin-degrading enzymes have great importance in enzyme market. A total of 10 bacterial isolates belonging to *Bacillus* species isolated from chilli rhizosphere, Guntur district of Andhra Pradesh, India. All the isolates were tested for chitinase production on colloidal chitin medium. Among them four isolates i.e. Bacillus sp. PB-3(2.22 IU/ mg), Bacillus sp. PB-5(2.75 IU/ mg), Bacillus sp. PB-6(2.22 IU/ mg), and Bacillus sp. PB-8(3.46 IU/ mg) showed chitinase production. Optimization studies like incubation period, pH, carbon and nitrogen sources were determined by these four isolates. Chitinase production was maximum on 6 days of incubation (3.46 IU/ mg) period and the optimum pH was found to be 7.0. Carbon and nitrogen sources greatly influenced the chitinase production. Among them 1% glucose and 0.5% glycine was the best for chitinase activity.

KEYWORDS: Bacillus, Chitinase, Carbon and nitrogen sources

1. INTRODUCTION

Screening of diversified microorganisms from different habitats and their optimum utilization in industrial sector is the need of the hour. The increasing energy demands has drawn worldwide attention on the utilization of renewable resources particularly agricultural and forest residues, the major components of which are cellulose, starch, lignin, xylan and pectin. These materials have attracted considerable attention as alternative feed stock and energy source. Since they are available abundantly several microbes are capable of using these

substances as carbon and energy sources by producing a vast array of enzymes in different environmental niches. (Antranikian *et.al*., 1992).

Industrial biotechnology, using microorganisms and biological catalysts "enzymes" to produce goods and services has come of age. Search for new enzymes for use in commercial applications with desirable biochemical and physico chemical characteristics and a low production costs have been the focus of much research (Neetha *et .al,* 2011).

Chitinases (EC 3.2.1.14) can catalyze the hydrolysis of chitin to its monomer *N*-acetyl-D-glucosamine. Chitinase is an inducible enzyme secreted by many microorganisms in cultures containing chitin or its oligomers as sole carbon source. Chitinolytic microorganisms are considered to be more effective antagonists of fungal pathogens because of the direct action of chitinase alone (Yu *et al*., 2008) or in combination with other antifungal compounds produced by the antagonist (De Boer *et al*., 1998). Chitinase is known to process diverse characteristics worthy of detailed enzymatic studies related to their biological role and structural elucidation (Thamthiankul, Suan-Ngay et al. 2001; Liu, Kao *et al*., 2003). In Andhra Pradesh Guntur is famous for chilli production. Majority of the soils contain chilli rhizosphere. However the present study reveals that the chitinase production by bacillus species isolated from chilli rhizosphere. Optimization studies also reveal the chitinase activity on these isolates.

2. MATERIALS AND METHODS

2.1 Isolation

One gram representative soil sample was suspended in 10 ml of sterile distilled water and shaken thoroughly for 10 minutes. Microorganisms were isolated from collected samples by the serial dilution plate technique using Nutrient Agar Medium (NAM). Serial dilutions up to 10^{-5} of each sample were prepared by using sterilized water. Sample dilutions were plated (in triplicates) on NAM and incubated at 35^{o} C for 24 to 48 h. Pure Colonies were picked and maintained on NAM slants at 4^{o} C and further assessed for enzyme production in liquid medium.

2.2 Screening of chitinolytic microorganisms

Chitinase activity can be qualitatively assayed by determining the clearance zone developed around the colonies growing on the colloidal chitin agar medium (Cody, 1989; Wirth and Wolf, 1990). The potency of the isolates for chitinase production is determined on the basis

of ratio of zone of clearance (CZ) to colony size (CS) (Cody, 1989). This procedure requires longer incubation time for about 2 to 7 days and is relatively less sensitive because of the poor visualization of the CZ. Screening the chitinolytic microorganisms by incorporating calcofluor white M2R (0.001% w/v) in chitin agar has been developed (Vadiya *et al*., 2003).

2.3 Detection and quantification of chitinases activity

The activity of chitinases can be qualitatively assayed by using chitin agar plate either with or without fluorescent dye. Activity staining method can also be used for qualitative assay. Activity staining can be done by incorporating ethylene glycol chitin in the gel (Trudel and Asselin, 1989). However, this method has limitations since the gel can not be further used for protein staining and there is problem of mobility of chitinase in the gel because of the presence of polysaccharide in the gel. These problems have been over come by running protein sample in the gel without incorporating chitin followed by diffusion on chitin agar plate containing fluorescent dye (Gohel *et al*., 2005). Colloidal chitin with Remazol Brilliant Blue R was also used as a substrate for colorimetric assay of chitinase (Gómez Ramírez *et al*., 2004).

2.4 Optimization studies on chitinase production

In the present study a thematic attempt was made to investigate the effect of various parameters including incubation period, pH, temperature, carbon (Sucrose, Glucose, Maltose, Galactose and colloidal chitin) and nitrogen sources (sodium nitrate, ammonium sulphate, peptone, Yeast extract and glycine) on chitin broth medium. A classical approach using substrate fermentation medium under standard conditions mention earlier optimization studies like sub merged fermentation.

3. RESULTS AND DISCUSSION

3.1 Incubation period

A total of 10 isolates were obtained from chilli rhizosphere in the vicinity of Guntur, Andhra Pradesh. The preliminary characterization like cultural and biochemical characteristics of rhizobia was done by Bergey's manual of systemic bacteriology. All the isolates belong to Bacillus species according to their preliminary and biochemical studies. All the isolates were designated as Bacillus sp. PB-1 to Bacillus sp. PB-10 and tested for chitinase activity (Table-1). Among them four isolates i.e. Bacillus sp. PB-3(2.22 IU/ mg), Bacillus sp. PB-5(2.75 IU/ mg), Bacillus sp. PB-6(2.32 IU/ mg), and Bacillus sp. PB-8(3.46 IU/ mg) showed chitinase

production. Optimization studies like incubation period, pH, carbon and nitrogen sources were determined by these four isolates.

Table 1: Chitinase production (IU/mg) by Bacillus species.

Isolates	Chitinase production (IU/mg)
Bacillus sp. PB-1	-
Bacillus sp. PB-2	-
Bacillus sp. PB-3	**2.22**
Bacillus sp. PB-4	-
Bacillus sp. PB-5	**2.75**
Bacillus sp. PB-6	**2.32**
Bacillus sp. PB-7	-
Bacillus sp. PB-8	**3.46**
Bacillus sp. PB-9	-
Bacillus sp. PB-10	-

*Each data is an average of three replicates

3.2 Screening for chitinase production

Further the four strains were screened for chitinase production by different incubation periods like 2, 3, 4, 5, 6 and 7 days. After 2 days of incubation period the clear zone (CZ) was formed around the bacterial colony. Total colony size and clear zone was measured for 7 days of incubation period (Table-2). Maximum colony size was observed in 6 days of incubation period.

Table 2: Screening for chitinase production by Bacillus species.

S.No.	Bacillus Isolates	Clear zone around the colony (mm) at different incubation periods (days)					
		2	**3**	**4**	**5**	**6**	**7**
1	*Bacillus* sp. PB-3	-	2	4	6	8	8
2	*Bacillus* sp. PB-5	-	2	4	6	8	8
3	*Bacillus* sp. PB-6	2	4	6	8	10	10
4	*Bacillus* sp. PB-8	2	4	6	8	10	10

*Each data is an average of three replicates

3.3 Effect of incubation period on amylase production

Different incubation (2,3,4,5,6 and 7 days) periods were studied for the chitinase production on chitin broth medium. Maximum chitinase production was observed by 6 days of incubation period (Table-3). Maximum enzyme production could be obtained only after a certain incubation time which allows the culture to grow at a study state (Pandey *et al.*, 2000). Enzyme production of each strain is based on the specific growth rate of the strain.

Growth rate and enzyme synthesis of the culture are the two main characteristics which are mainly influenced by incubation time (Ellaiah *et al*., 2002).

Table 3: Effect of incubation period on Chitinase production by Bacillus species.

Incubation periods	*Bacillus* sp. PB-3	*Bacillus* sp. PB-5	*Bacillus* sp. PB-6	*Bacillus* sp. PB-8
2	0.22	0.75	0.88	0.66
3	0.25	1.05	1.11	0.98
4	0.45	1.45	1.67	1.45
5	0.78	2.33	2.11	1.98
6	2.22	2.75	2.32	3.46

3.4 Effect of pH

Different pH levels were maintained for the chitinase production by all the four species. All the isolates showed maximum chitinase production on neutral pH. Acidic phase to a neutral phase enzyme activity increased up to a pH of 4.0 and upon further increase in pH, enzymatic activity decreased (Table-4). Different organisms have different pH optima and any modification in their pH optima could result in a decrease in their enzyme activity (Adinarayana et al, 2005).

Table 4: Effect of pH on Chitinase production by Bacillus species.

Ph	*Bacillus* sp. PB-3	*Bacillus* sp. PB-5	*Bacillus* sp. PB-6	*Bacillus* sp. PB-8
pH-4	0.11	0.23	0.34	0.23
pH-5	0.88	0.97	0.88	1.23
pH-6	1.26	1.55	1.65	2.45
pH-7	2.22	2.75	2.32	3.46
pH-8	1.76	1.23	1.67	1.89

3.5 Influence of carbon sources

Several carbon substrates like Sucrose, Glucose, Maltose, Galactose and colloidal chitin were tested to evaluate the enzyme production. Among them glucose contain the medium produced maximum chitinase production (Table-5). Various reports supported to this type of results like, Glucose and starch when supplemented as additional carbon substrate to the medium has resulted in enhanced enzyme production. Among the tested substrate sucrose and glucose resulted in enhanced enzyme production (Prakasham 2007).

Table 5: Effect of different Carbon sources on Chitinase production by Bacillus species.

Additional Carbon sources	*Bacillus* sp. PB-3	*Bacillus* sp. PB-5	*Bacillus* sp. PB-6	*Bacillus* sp. PB-8
Control	0.23	0.34	0.45	0.67
Sucrose	1.78	1.11	1.31	1.79
Maltose	2.01	1.23	1.26	1.98
Galactose	1.05	1.76	1.89	2.44
Glucose	2.22	2.75	2.32	3.46
Colloidal chitin	1.11	1.99	1.76	1.77

3.6 Influence of nitrogen sources

Various nitrogen sources (sodium nitrate, ammonium sulphate, peptone, Yeast extract and glycine were induced the chitinase production among them glycine influenced the maximum (3.46 IU/mg) chitinase production (Table-6).

Table 6: Effect of nitrogen sources on Chitinase production by Bacillus species.

Nitrogen sources	*Bacillus* sp. PB-3	*Bacillus* sp. PB-5	*Bacillus* sp. PB-6	*Bacillus* sp. PB-8
Control	0.11	0.19	0.23	0.88
NaNo3	1.09	1.67	1.88	1.29
(NH4)SO4	1.16	1.90	1.75	2.89
Yeast extract	1.89	2.22	1.99	2.33
Glycine	2.22	2.75	2.32	3.46
Peptone	1.88	2.42	1.72	2.56

5. CONCLUSION

In the present study four bacillus species produced chitinase production on colloidal chitin medium. Among them *Bacillus* sp. PB-8 showed maximum chitinase production on the basis of optimization studies. Six days of incubation period and neutral pH was suitable for maximum chitinase for this strain. Maximum chitinase production was observed by using Glucose and glycine as carbon and nitrogen sources.

6. ACKNOWLEDGEMENT

Author would like to thank the department of Botany and Andhra Christian College, Guntur for providing necessary facilities to complete this research work.

7. REFERENCES

1. Antranikian G., 1992. Microbial degradation of starch. In: Winkelmann G, Ed. *Microbial degradation of natural products*. VCH, Weinheim, 27-51.
2. Adinarayana K., Kugen P., Suren S. 2005, Amylase production in solid state fermentation by the thermophilic fungus *Thermomyces lanugionosu. Journal of Biosciences and Bioengineering,* 100(2): 168-171.
3. Cody, R.M. Distribution of chitinase and chitobiase in Bacillus. *Curren Microbiology,* 1989; 19(4): 201-205.
4. De Boer, W., Gunnewiek, P.J.A.K., Lafeber, P., Jans, J.D., Spit, B.E., Woldendorp, J.W., 1998. Anti-fungal properties of chitinolytic dune soil bacteria. *Soil Biology Biochemistry,* 30: 193–203.
5. Ellaiah P., Adinarayana K., Bhavani Y., Padmaja P. and Srinivasulu B. 2002, Optimization of process parameters for glucoamylase production under solid-state fermentation by a newly isolated *Aspergillus sp. Process Biochemistry,* 38(4): 615-620.
6. Gohel, Anil Singh, Vimal M, Ashwini P, Chhatpar HS. 2006. Bio-prospecting and antifungal potential of chitinolytic microorganisms. *African Journal of Biotechnology,* 5(2): 54-72.
7. Liu, B. L., Kao, P. M., Tzeng, Y. M. and Feng, K. C. 2003. "Production of chitinase from *Verticillium lecanii* F091 using submerged fermentation." *Enzyme Microb. Technol,* 33: 410-415.
8. Neeta, R.S., Anupama, S., Anjuvan, S. and Giridhar, S., 2011. Production of polygalacturonase and pectin methyl esterase from agrowaste by using various isolation of Aspergillus niger. *Insight Microbiology*, 1(1): 1-7.
9. Pandey A., Nigam P., Soccol C. R., Soccol V. T. Singh D. and Mohan R. 2000. Review: Advances in microbial amylases. *Biotechnology and Applied Microbiology,* 31: 135-152.
10. Prakasham R., Subba Rao, Ch. and Sarma, P. N. 2005. Green gram husk-an inexpensive substrate for alkaline protease production by *Bacillus sp*.in solid state fermentation. *Bioresource Technology*, 97: 1449-1454.
11. Thamthiankul, S., Suan-Ngay, S., Tantimavanich, S. and Panbangred, W. 2001. "Chitinase from *Bacillus thuringiensis* subsp. *pakistani*." Appl. Microbiol. Biotechnol, 56: 395-401.
12. Yu, T., Wang, L., Yin, Y., Wang, Y., Zheng, X., 2008. Effect of chitin on the antagonistic activity of Cryptococcus laurentii against Penicillium expansum in pear fruit. International Journal of Food Microbiology, 122: 44–48.

13. Vaidya, R.J.; Shah, I.M.; Vyas, P.R.; Chhatpar, H.S. 2003. Production of chitinase and its optimization from a novel isolate Alcaligenes xylosoxydans: potential in antifungal biocontrol. World J. Microbiol. Biotechnol, 17: 691-696.

SOCIETY FOR SCIENCE AND NATURE
SCIENCE FOR LIFE

SOCIETY FOR SCIENCE AND NATURE
SCIENCE FOR LIFE

Bioscience Biotechnology Research Communications
An Open Access International Journal
P-ISSN: 0974-6455 E-ISSN: 2321-4007

Bioscience Biotechnology Research Communications
An Open Access International Journal

Indole 3-Acetic Acid Production by *Aspergillus* Species Isolated from Chilli *Rhizospheres*

Darsi Phebe Sarah Koti Ratnam*

Department of Botany and Microbiology, Andhra Christian College, Guntur, Andhra Pradesh, India

Corresponding author email: phebesarah63@gmail.com

DOI: http://dx.doi.org/10.21786/bbrc/13.4/80
Article Publishing History
Received: 24/10/2020
Accepted After Revision: 12/12/2020

ABSTRACT:

In the present study soil samples were collected from different chilli rhizospheres in the vicinity of Guntur, Andhra Pradesh, India and the filed trails were conducted in the year of 2018-2019. A total of 57 microbial strains were isolated from chilli rhizosphere. All the strains were isolated from potato dextrose agar media by using 10-4 serial dilutions. Fine and clear colonies were picked and transformed into a culture tubes for further studies. For the preliminary screening there are 10 isolates were considered as fungal strains based on spore morphology. The spores are round and irregular in shape with green to light brown in colour. Preliminary identification of these fungal isolates was based on morphological and cultural characters on potato dextrose agar medium. All ten strains showed the maximum indole acetic acid production on Czepakdox agar medium.

Various optimization studies like incubation period, pH, temperature and carbon and nitrogen sources were studied by affecting the indole acetic acid productions i.e., 10 days incubation period, pH 7.0 and 30°C. Carbon and nitrogen sources are also affected the indole acetic acid production in this optimization. A carbon and nitrogen source in the optimal medium plays a major role for the production indole acetic acid. Among them, the strain *Aspergillus* PB-7 in presence of Glucose and peptone showed the maximum IAA production of 110µg/ml and 75µg/ml. Successful inoculation of agricultural crops with biocontrol plant growth promoters includes the delivery of sufficient inoculum to the target, economical production of large quantities of microorganisms. Rhizospheric microbes especially plant growth promoting microorganism were promising to be developed as multifunctional biofertilizer.

KEYWORDS:

Plant growth promoters (PGP), Indole acetic acid (IAA), Potato Dextrose Agar (PDA).

INTRODUCTION

Chilli can be grown in a wide range of Black, Brown, Red and Clay soils, but black soils which retain moisture for long periods are suitable for rain fed crop whereas well drained soils, deltaic soils and sandy loams are good under irrigated condition.

Whereas Sandy and loamy soils poorly supported to chilli production when compare to black soils. Various climatic conditions like humid and hot weather supports to the chilli plants. Sometimes environmental conditions are also adversely affected the chilli growth and fruit production. India is the largest producer and consumer of chilli among other major producers in the world. India contributes about 47 per cent to the total world production, and assumes first position in terms of international trade, exporting 38 per cent of its total production. Chilli production in India is moving northwards on increasing demand from diversified sectors and changing consumption patterns.

Dry chilli production rose by nearly 52 per by nearly 52 per cent from 9.7 lakh tones in 1997-98 to about 18 lakh tonnes. More than 80% of the bacteria isolated from the rhizosphere can produce (IAA) Indole Acetic Acid (Khalid et al., 2004) in the presence of precursor, tryptophan either through root exudates or from the proteins released by the dead bacteria cells (Patten and Glick, 1996). Indole-3-acetic acid (IAA), a plant growth hormone compound, is a natural auxin produced by plants, bacteria, fungi and a diverse group of organisms. It is a metabolite derived from tryptophan by many tryptophan dependant and tryptophan independent pathways in plants as well as bacteria and fungi. These growth improvers act as biocontrol agents. (Pattern and Glick, 2002; Wesam et al., 2017).

Various soil microorganisms including bacteria, fungi (Finnie and Van Staden, 1985) and algae (Stein et al., 1990; Rifat Hayat et al., 2010) are capable of producing physiologically active growth hormones like auxins and gibberellins which may exert prominent effects on plant growth and development. Many PGPR (Plant growth promoting) microorganisms associated in chilli rhizosphere. Chilli is one of the important agriculture produce Andhra Pradesh also. Chillies from Andhra Pradesh are well known for their pungency and good red colour. Several districts like Guntur, Krishna, Prakasam, Nellore, Chittor and Anantapuram are the main chilli growing districts in Andhra Pradesh. The present study was mainly focussed on indole acetic acid production and optimization studies by fungal strains isolated from chilli rhizosphere. These strains were used as bio inoculants in application to the farmer's fields and it is useful for sustainable agriculture (Wesam et al., 2017).

MATERIAL AND METHODS

Isolation of fungi done using the rhizosphere soil samples from the chilli fields of 10 different areas of Guntur, district of Andhra Pradesh, India were collected for the study. Fungal strains were isolated on Potato Dextrose Agar (PDA) medium by soil dilution plate technique (Rapilly, 1968) using 10^{-3} to 10^{-5} dilutions. The plates were incubated at 28 ± 2°C for 5 days. Fungal colonies appeared in the plates were noted and sub cultured. After purified by single spore isolation method and they were maintained on potato dextrose agar (PDA) slants. Identification of Fungal solates was based on culture characters as well as microscopic parameters (conidiophores branching, phialides shape and position, spore size and shape) (Nagamani et al., 2006). The pure cultures were stored in the refrigerator at 4°C for further studies.

Screening of isolates for IAA production was determined based on the method described by Patten and Glick (2002) with slight modifications. One milli liter of supernatant was mixed with 2 ml of Salkowski reagent (1ml of 0.5M $FeCl_3$ in 50mL

of 35% $HClO_4$) and incubated for 1hr. Development of pink colour indicated the production of IAA. The quantification of IAA was read at 540 nm in a UV- Vis spectrophotometer. A standard curve was plotted for quantification of IAA solution and uninoculated medium with a reagent as a control. The amount of IAA in the culture was expressed as µg/ml (Gordon and Weber, 1951).

The optimization studies for IAA production to determine the IAA production, different incubation periods (7, 8, 9, 10, 11 and 12 days), pH levels (4, 5, 6,7, 8 and 9) and temperature (4,20, 25, 30, 35 and 40ºC) were studied. Various carbon (1%) and nitrogen (0.1%) sources were studied by using the above method.

For the statistical analysis, all measurements were carried out in triplicate. Statistical analyses were performed using one-way analysis of variance (ANOVA), and the significance of the difference between means was determined by Duncan's multiple range tests. Differences at < 0.05 were considered statistically significant.

RESULTS AND DISCUSSION

A total of 57 strains were isolated from chilli fields in the vicinity of Guntur district, Andhra Pradesh, India. All the strains were tested for IAA production; among them 10 strains were positive results on Potato dextrose agar medium (Figure-1). The present study mainly reveals the IAA production of the selected 10 fungal strains. Maximum IAA production was observed on *Aspergillus* sp. PB 7 strain which showed 110 µg/ml of IAA, followed by *Aspergillus* sp. PB 5 strain (63 µg/ml). Minimum IAA production was recorded in *Aspergillus* sp. PB 4 with 27 µg/ml. IAA productions by ten fungal strains between the range of 27-110 µg/ml. *Aspergillus flavus* Promoted the Growth of Soybean and Sunflower Seedlings which was reported by Humayun et al., (2019).

Figure 1: IAA production (µg/ml) by *Aspergillus species*

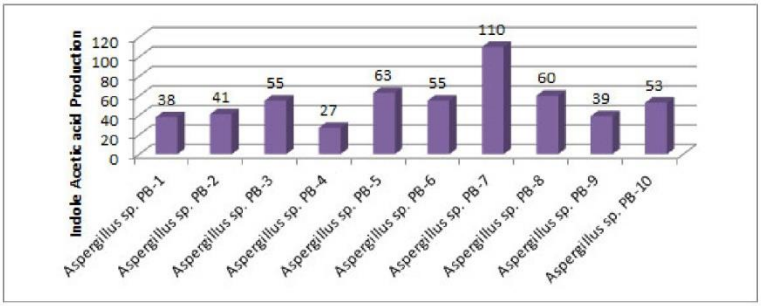

*The overall model is significant with $p<0.05$

Optimization studies for IAA production (µg/ml) by *Aspergillus* species PB 7: For the optimization studies we selected PB 7 *Aspergillus* strain which showed maximum IAA production and was tested with the effect of incubation period, pH and temperatures, carbon and nitrogen sources.

Effect of incubation period on IAA production by *Aspergillus* species PB 7: The IAA production was started between 7 to 12 days of incubation periods (Figure-2). The maximum IAA production was observed on 10^{th} day of incubation (110 µg/ml). Similarly Unyayar et *al.*, (2000) and Hansan (2002) reported that the maxumum

amount of IAA was synthesized during the stationnary phase of growth. May be these reason was that during stationnary phase the bacterium might be able to get maximum tryptophan from dead bacterial mass, which could result in more IAA production. Reduction of IAA production at the later might be due to release of IAA degrading enzymes by the bacteria (Hunter, 1989).

Figure 2: Effect of incubation period on IAA production (µg/ml) by *Aspergillus species* PB 7

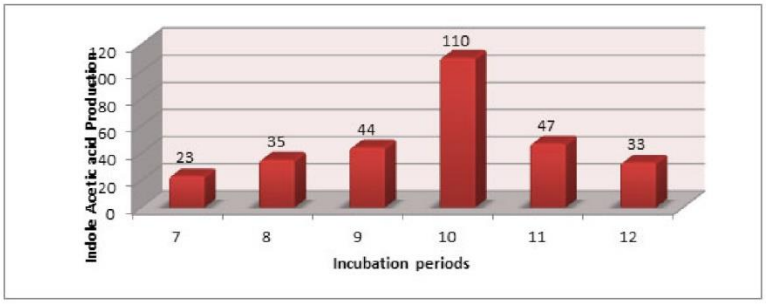

*The overall model is significant with $p<0.05$

Effect of pH on IAA production (µg/ml) by *Aspergillus* species PB-7: The pH of the medium showed a significant influence on the production of IAA by fungal strains. The maximum IAA production (110 µg/ml**)** was observed at pH 7 (Figure-3). For many authors, the optimum pH for IAA production is between 6 to 9. However, the below and above pH 8 the production of IAA was less, because *Streptomyces* sp population level is more in alkaline soil than the acidic soil (Shirokikh et al., 2007; Mohite, 2013; Bharucha et al., 2013; Dasri et al., 2014).

Figure 3: Effect of pH on IAA production (µg/ml) by *Aspergillus* species PB-7

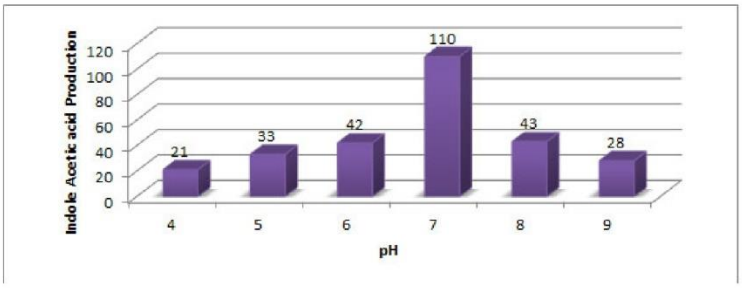

*The overall model is significant with $p<0.05$

Effect of different temperature on IAA production (µg/ml) by *Aspergillus* species PB-7: The effect of different temperature on IAA production by fungal strains showed that, the maximum IAA production was obtained at 30°C (65 µg/ml) followed by 35°C (44 µg/ml) and 40°C (29 µg/ml) respectively (Figure-4).

Figure 4: Effect of temperature on IAA production (µg/ml) by *Aspergillus* species PB-7

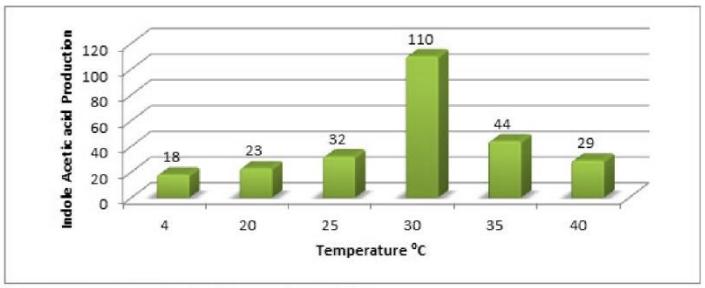

*The overall model is significant with $p<0.05$

Effect of different carbon source on IAA production (µg/ml) by *Aspergillus* species PB-7: Different carbon sources (mannitol, Starch, glucose, sucrose, fructose, lactose and Arabinose) were studied for their effect on IAA production by *Aspergillus* species PB-7 (Figure-5). Glucose in the medium gave maximum IAA production (110 µg/ml) followed by arabinose (51µg/ml) and lactose (48 µg/ml).

Figure 5: Effect of carbon sources on IAA production (µg/ml) by *Aspergillus* species PB-7

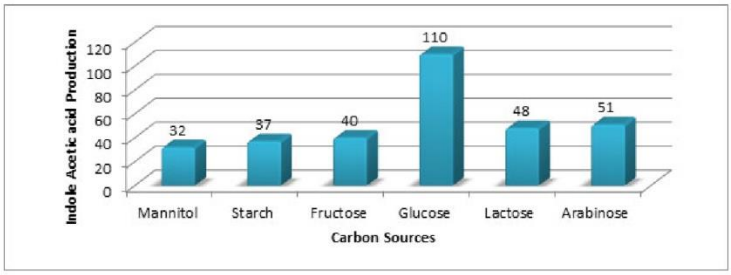

Effect of different nitrogen sources on IAA production (µg/ml) by *Aspergillus* species PB-7: Various nitrogenous compounds (Ammonium sulphate, potassium chloride, Yeast extract, peptone and beef extract). These nitrogen source have a significant effect on IAA production (Figure-6). Among all the nitrogen sources used, peptone was found to be the best nitrogen source for IAA production. Organic and inorganic nitrogen sources can be utilized by *Pseudomonas* sp. prefers yeast extract (Balaji, 2012), *Pantoea agglomerans* PVM prefer beef (Apine and Jadhav, 2011), and Ammonium sulphate was found to be for IAA production of *Acetobacter diazotrophicus* L1, the most suitable nitrogen source (Nita et al., 2011).

Figure 6: Effect of nitrogen sources on IAA production (µg/ml) by *Aspergillus* species PB-7

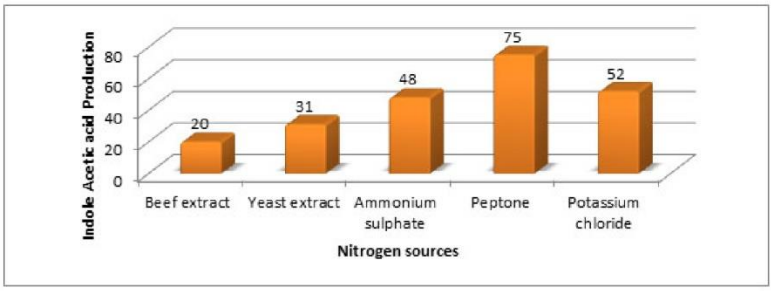

*The overall model is significant with $p<0.05$

CONCLUSION

From the results, it is clear that *Aspergillus species* PB 7 isolated form chilli rhizospheres preferred glucose and peptone as carbon and nitrogen sources respectively. The optimum conditions for this culture are incubation 12 days, pH 7.0 and 30°C temperature. There were several plant growth promoting rhizobacterial (PGPR) inoculants that seems to promote plant growth through different mechanism such as plant growth hormone production, nutrient acquisition and plant disease suppression. Thus the optimized microbial inoculants may be useful for the production of multifunctional biofertilizers.

ACKNOWLEDGEMENTS

Author would like to thank the Department of Botany and Andhra Christian College, Guntur for providing necessary facilities to complete this research work.

REFERENCES

Apine, O. A. and Jadhav, J. P. (2011). Optimization of medium for indole-3-acetic acid production using *Pantoea agglomerans* strain PVM. Journal of Applied Microbiology, 110(5), 1235-44.

Balaji, N., S. S. Lavanya, S. Muthamizhselvi and K. Tamilarasan (2012). Optimization of fermentation condition for indole acetic acid production by *Pseudomonas* species. International Journal of Advanced Biotechnology and Research, 3, 797-803.

Bharucha U., Patel K., and Trivedi U. B. (2013). Optimization of Indole Acetic Acid Production by *Pseudomonas putida* UB1 and its Effect as Plant Growth-Promoting Rhizobacteria on Mustard (*Brassica nigra*). Agric Res.

Dasri, K., Kaewharn, J., Kanso, S. and Sangchanjiradet, S., (2014). Optimization of indole-3-acetic acid (IAA) production by rhizobacteria isolated from epiphytic orchids. Asia-Pacific Journal of Science and Technology, 19: 268-275.

Finnie, J. F. and Van Staden, J. (1985). Effect of seed weed concentrate and applied hormones on *in vitro* cultured tomato roots. J Plant Physiol. 120: 215- 222.

Gordon, S.A. and Weber, R.P. (1951). Colorimetric estimation of indole acetic acid. Plant physiology, 26(1):192-195.

Hamayun, M., Hussain, A., Afzal Khan, S., Iqbal, A. and Lee, I.J., (2019). *Aspergillus flavus* promoted the growth of soybean and sunflower seedlings at elevated temperature. BioMed research international, 2019:1-13.

Hansan H.A.H. (2002). Gibberellin and auxin production by plant root fungi and their biosynthesis under salinity-calcium interaction. Rostlinna Vyroba, 48 : 101-106.

Hunter, W.J. (1989). Indole-3-acetic acid production by bacteroids from soybean root nodules. Physiol. Plant. 76 : 31-36.

Khalid A., Tahir, S., Arshad, M. and Zahir, Z.A. (2004). Relative efficiency of rhizobacteria for auxin biosynthesis in rhizosphere and non-rhizosphere soils. Aus. J. Soil Res. 42:921-926.

Mohite B. (2013). Isolation and characterization of indole acetic acid (IAA) producing bacteria from rhizospheric soil and its effect on plant growth. Journal of soil science and plant nutrition, 13(3): 638-649.

Nagamani A, Kunwar IK, and Manoharachary C. (2006). Handbook of soil fungi, IK Int Pvt Ltd. New Delhi: pp.425.

Nita B. Patil, Milind Gajbhiye, Sangita S. Ahiwale, Aparna B. Gunjal and Balasaheb P. Kapadnis. (2011). Optimization of Indole 3-acetic acid (IAA) production by *Acetobacter diazotrophicus* L1 isolated from Sugarcane. International Journal of Environmental Sciences, 2(1), 307-314.

Patten C. L. and Glick B. R. (2002). Regulation of indole acetic acid production in *Pseudomonas putida* GR12-2 by tryptophan and the stationary-phase sigma factor RpoS. Canadian journal of microbiology, 48(7):635-642.

Patten, C. L., and B.R. Glick. (1996). Bacterial biosynthesis of indole-3-acetic acid. Canadian journal of microbiology 42: 207-220.

Rapilly F. (1968). Les Techniques de mycologie en pathologie végétale. Ann. Epiphyt. 101p. Bruxelles.

Rifat Hayat, Safdar Ali, Ummay Amara, Rabia Khalid, and Iftikhar Ahmed. (2010). Soil beneficial bacteria and their role in plant growth promotion: a review. Ann Microbiol. 60: 579- 598.

Shirokikh, I. G., Zenova, G. M., Merzaeva, O.V., Lapygina, E.V., Batalova, G.A. and Lysak, L. V. (2007). Actinomycetes in the prokaryotic complex of the rhizosphere of oats in a soddy podzolic soil. Eurasian Soil Sci. 40: 158-162.

Stein, A., Fortin, J. A. and Vallee, G. (1990). Enhanced rooting of *Picea mariana* cuttings by ecto mycorrhizal fungi. Can J Bot. 68: 492-498.

Unyayar, S., Unal, E. and Unyayar, A., (2000). Production of auxin and abscisic acid by Phanerochaete chrysosporiumme446 immobilized on polyurethane foam. Turkish Journal of Biology, 24(4):769-774.

Wesam I. A. Saber, Khalid M. Ghoneem, Younes M. Rashad and Abdulaziz A. Al-Askar. (2017). *Trichoderma Harzianum* WKY1 : an indole acetic acid producer for growth improvement and anthracnose disease control in sorghum. Biocontrol Science and Technology, 27 (5), 654–676.

Online Contact

First Name

Last Name

Email Address

Subject

Your Message

Submit Form

Stay Connected

editor@bbrc.in

Mailing Address: Post Box 01 GPO Bhopal MP India Pin Code: 462001

Visitor Counter

0 2 6 0 7 2 0

Visit Today :
Visit Yesterday :
This Month :

Effect Of Loratadine Tablets on the Symptomatic Control Of Seasonal Allergic Rhinitis in Adults Challenged with Ragweed Pollen in the Environmental Exposure Unit in Compassion with Azelastine Nasal Spray with Loratadine Tablets, Cetirizine Tablets, and Placebo: A Post Hoc Analysis of Total Symptom Score

Dr. T. Sujatha
Professor of Chemistry
Sri Sarathi Institute of Engineering & Technology
NUZIVIDU
Krishna Dt. A.P

Dr.V.Ezra Vijay Sekhar
Head of Dept. of Botany
Andhra Christian College
GUNTUR.

Abstract

Loratadine is a second-generation, non-sedating antihistamine used for the relief of allergic rhinitis symptoms. Previous studies reported that when loratadine was encapsulated, the onset of action for symptom relief was 180 min. However, unmodified loratadine tablets were not evaluated at that time. Using data from a previously published Environmental Exposure Unit (EEU) study comparing azelastine nasal spray with loratadine tablets, cetirizine tablets, and placebo, this post hoc analysis determines the onset of action of loratadine tablets, by analyzing the total symptom score for the relief of nasal and ocular seasonal allergic rhinitis (SAR) symptoms.

Keywords: Allergic rhinitis, Environmental Exposure, Loratadine, Commencement of action, Ragweed pollen, Seasonal allergies, Outdoor allergy.

Introduction

A Phase IV, randomized, single-center, double-blind, placebo-controlled, double-dummy, four-way crossover study was conducted in the EEU. Seventy participants were randomized sequentially into one of the four treatments during ragweed pollen exposure. Nasal and ocular symptom scores were self-reported by the participants and recorded. The original study analysis was carried out by evaluating the nasal symptom scores only. For this post hoc analysis, both nasal and ocular data from the loratadine and placebo treatment arms were analyzed. The primary endpoint for this analysis was the Commencement of action of loratadine as measured

by the change in total symptom score (TSS) from baseline in comparison to placebo. The onset of ocular symptom relief using the total ocular symptom score (TOSS) was also reported.

Method of study Design and Treatment:

The study was conducted in the EEU and was comprised of a screening visit, a priming period, and four dosing / exposure periods with a 13-day washout between periods (Fig.I). After eligibility was determined, qualifying participants were randomized to a treatment sequence comprised of one dose of each of the four study medications, azelastine, nasal spray, loratadine tablet, cetirizine tablet, and placebo. All study treatments were administered as a combination of an oral tablet (active or placebo) and nasal spray (active or placebo) to maintain study blinding.

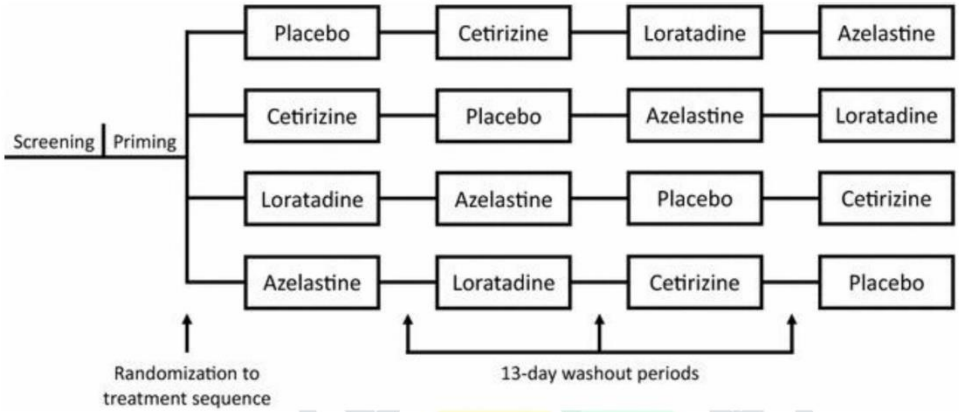

Fig: I Study Diagram

Each dosing period consisted of an 8-h ragweed pollen challenge in the EEU (mean pollen levels of 3500 ± 500 grains/m^3). The level of pollen used is consistent with other EEU studies used to determine the onset of allergy products and provides consistent symptomatic responses in a predictable time frame at a relevant pollen exposure level. Participants were administered their assigned treatment 2 h into the challenge. Nasal and ocular symptom severity was recorded by each participant at designated time points during the challenge. Symptom severity was rated on a scale of 0-3 (0= none, 1= mild, 2= moderate, 3= severe.) (Table: I). Appropriate combinations of symptoms comprised the total nasal symptom score **(TNSS).** total ocular symptom score **(TOSS).** and total symptom score **(TSS) are** an omnibus score comprised of all nasal and ocular symptoms are given in Fig:2

Table: I

Rating scale for symptoms of seasonal allergic rhinitis

Score	Grade	Guideline
0	None	No sign/symptom is evident
1	Mild	Sign/symptom clearly present, but minimal awareness; easily tolerated
2	Moderate	Definite awareness of sign/symptom that is bothersome, but tolerable
3	Severe	Sign/symptom are hard to tolerate, causes interference in session activity

Table: II

Total Nasal and **Total Ocular** symptoms of seasonal allergic rhinitis

Symptom	TNSS	TOSS	TSS
Runny Nose	X		X
Sneezing	X		X
Nasal Itching	X		X
Itchy/red/gritty eye		X	X
Watery eyes		X	X

TNSS total nasal symptom score, TOSS total ocular symptom score, TSS total symptom score

Total scores were the sum of each individual symptom score (rated between 0 and 3); TNSS (0–9), TOSS (0–6), TSS (0–15)

Results

Participant demographics

A total of 70 participants were randomized into the study. Four participants did not complete all four dosing periods and were excluded from the PP population. Briefly, the mean age (SD) was 35 (9.9) years and the majority of participants were Caucasian (97%) (Table 3). Nasal and ocular composite symptom scores were measured at baseline and summarized in Table 4.

Table: III

Summary of participant demographics

Characteristics	Overall (n = 66)
Mean age in years (SD)	35.0 (9.9)
Female (%)	39 (59)
Race (%)	
Caucasian	64 (97)
Black	0 (0)
Asian	2 (3)
American Indian/Alaska Native	0 (0)
Native	0 (0)

Hawaiian/Other Pacific Islander	
Other	0 (0)

Table: IV
Baseline symptom scores

Baseline symptom scores (SD)[a]	**Loratadine (n = 66)**	**Placebo (n = 66)**
TNSS	6.9 (1.7)	6.5 (1.8)
TOSS	4.0 (1.5)	3.7 (1.7)
TSS	10.9 (2.6)	10.2 (3.0)

Baseline symptom scores were collected immediately prior to dosing (i.e. 2 h after the start of allergen challenge on study day)

Safety

In this study, loratadine was well tolerated. Sixty-eight and 69 participants received one dose of loratadine and placebo respectively. Serious adverse events or deaths were not reported during the dosing periods. A total of 12 and 5 adverse events (AEs) were reported in the loratadine (4 mild and 8 moderate) and placebo (2 mild and 3 moderate) groups respectively. Only one report of mild urticaria was considered possibly related to the study medication (loratadine) (Table5).

Table: V

	Loratadine (n = 68)	**Placebo (n = 69)**
Number of participants reporting ≥ 1 AEs (%)		7 (10)
Number of AEs reported	12	5
Serious (%)		
No	12 (100)	5 (100)
Yes	0 (0)	0 (0)
Severity of AE (%)		
Mild	4 (33)	2 (40)
Moderate	8 (67)	3 (60)
Severe	0 (0)	0 (0)
Possible relationship to study medication (%)		
Not possibly related	11 (92)	5 (100)
Possibly related	1 (8)	0 (0)

Conclusion

The current post hoc analysis demonstrated an onset of action of 75 min for unmodified loratadine tablets. The longer onset of action previously reported by Day et al. is most likely attributed to a delayed release of loratadine from an over-encapsulated tablet that was evaluated in the study. As bioequivalence cannot be assumed between loratadine dosage forms, and since the active is a BCS Class II drug, one must be mindful when interpreting onset data generated with dosage forms that have been altered from their origin.

Abbreviations Used

AR allergic rhinitis

BCS Biopharmaceutics Classification System

EEU Environmental Exposure Unit

SAR seasonal allergic rhinitis

TNSS total nasal symptom score

TOSS total ocular symptom score

TSS total symptom score

PP per protocol

References

1. References Keith PK, Desrosiers M, Laister T, Schellenberg RR, Waserman S. The burden of allergic rhinitis (AR) in Canada: perspectives of physicians and patients. Allergy Asthma Clin Immunol. 2012;8(1):7. doi: 10.1186/1710-1492-8-7.
2. Schwindt CD, Settipane R. Allergic rhinitis (AR) is now estimated to affect some 1.4 billion people globally and continues to be on the rise. Editorial. Am J Rhinol Allergy. 2012;26(Suppl 1):S1. doi: 10.2500/ajra.2012.26.3844.
3. Bousquet J, van Cauwenberge P, Khaltaev N. Allergic rhinitis and its impact on asthma. J Allergy Clin Immunol. 2001;108:S147eS334. doi: 10.1067/mai.2001.118891.
4. Horak F, Zieglmayer UP. Azelastine nasal spray for the treatment of allergic and nonallergic rhinitis. Expert Rev Clin Immunol. 2009;5(6):659–669. doi: 10.1586/eci.09.38.
5. van Cauwenberge P, Bachert C, Passalacqua G, Bousquet J, Canonica GW, Durham SR, et al. Consensus statement on the treatment of allergic rhinitis. European Academy of Allergology and Clinical Immunology. Allergy. 2000;55(2):116–134. doi: 10.1034/j.1398-9995.2000.00526.x.
6. Wilken JA, Kane RL, Ellis AK, Rafeiro E, Briscoe MP, Sullivan CL, et al. A comparison of the effect of diphenhydramine and desloratadine on vigilance and cognitive function during treatment of ragweed-induced allergic rhinitis. Ann Allergy Asthma Immunol. 2003;91(4):375–385. doi: 10.1016/S1081-1206(10)61685-7.
7. Simons FER. Advances in H1-antihistamines. N Engl J Med. 2004;351(21):2203–2217. doi: 10.1056/NEJMra033121.
8. Del Carpio J, Kabbash L, Turenne Y, Prevost M, Hebert J, Bedard PM, Nedilski M, Gutkowski A, Schulz J. Efficacy and safety of loratadine (10 mg once daily), terfenadine (60 mg twice daily), and placebo in the treatment of seasonal allergic rhinitis. J Allergy Clin Immunol. 1989;84(5 Pt 1):741–746. doi: 10.1016/0091-6749(89)90303-5.
9. Van Cauwenberge P, Juniper EF. Comparison of the efficacy, safety and quality of life provided by fexofenadine hydrochloride 120 mg, loratadine 10 mg and placebo administered once daily for the treatment of seasonal allergic rhinitis. Clin Exp Allergy. 2000;30(6):891–899. doi: 10.1046/j.1365-2222.2000.00914.x.
10. Ellis AK, Zhu Y, Steacy LM, Walker T, Day JH. A four-way, double-blind, randomized, placebo controlled study to determine the efficacy and speed of azelastine nasal spray, versus loratadine, and cetirizine in adult subjects with allergen-induced seasonal allergic rhinitis. Allergy Asthma Clin Immunol. 2013;9(1):16. doi: 10.1186/1710-1492-9-16.

European Journal of Biotechnology and Bioscience
ISSN: 2321-9122; Impact Factor: RJIF 5.44
Received: 15-01-2020; Accepted: 16-02-2020; Published: 19-02-2020
www.biosciencejournals.com
Volume 8; Issue 1; 2020; Page No. 30-36

Isolation and characterization of *Streptomyces s*pp showing antagonistic activity against fungal pathogens effecting soybean crop

Quasim Turiki[1], Merakanapalli Kishore Babu[2], Kunchala Rajyalakashmi[3], VE Vijaya Sekhar[4], Syed Shabana[5], A Krishna Satya[6*]

[1-6] Department of Biotechnology, Acharya Nagarjuna University, Nagarjuna Nagar, Guntur, Andhra Pradesh, India

Abstract
A total 93 cultures of *Actinomycetes* were screened for their antagonistic activity against major fungal pathogens of soybean crop. Viz., *Colletotrichum lindemuthianum*, *Fusarium oxysporum,* and *Rhizoctonia solani*. Dual culture assay was performed**.** Glucose Casaminoacid yeast extract agar (GCY) plates were prepared. A 5mm fungal discs were placed on the one edge (1cm from the corner) with *Actinomycetes* streaked on the other edge of the plate (1cm from the corner) followed by incubation at 28 ± 2°C for four days. Control plate growth has covered the whole plate. The inhibition of fungal mycelium was measured as the distance of inhibition in cm. All the plates were maintained in triplicates and mean values were taken. Three isolates namely NAVS13, KNSS3, CHSS3 inhibited *C. lindemuthianum, F. oxysporum,* and *R. solani*. The isolates were further evaluated for Cellulase, Lipase, Protease, HCN, phosphate solubilization, production of growth hormone IAA, production of Siderophore, Chitinase, β-1, 3-Glucanase, and physiological properties. The isolates were subjected to molecular characterization and identified as *Streptomyces rochei, Streptomyces cavourensis* and *Streptomyces alfalfa.*

Keywords: soybean, actinomycetes, fungal pathogens, PGP traits, antagonistic activity

Introduction
Soybean (*Glycine max* (L.) is originated from East Asia. It is cultivated as one of the important pulse crops in India with a production of 15.68Metric tons in an area of 3.89 lakh hectares. However, the production can be still enhanced by limiting the problems due to diseases caused to Soybean especially from *Colletotrichum lindemuthianum, Fusarium oxysporum,* and *Rhizoctonia solani*. The fungal diseases cause more than 50 % loss to Soybean cultivation leading to huge economic losses (Agrio 2000) [1]. In order to combat the diseases, the farmers are highly dependent on various harmful chemicals which are not recommended when the environment and human health is concerned.

The environment-friendly options include the use of plant growth promoter's produced by microbes and vermicompost (Rupela *et al.,* 2005) [9]. It is evident from the past research that certain bacterial species such as *Pseudomonas* spp., *Bacillus* spp., *Trichoderma* spp, and *Streptomyces* spp., acted as bio-control agents against the pathogenic fungi. All these strains were isolated from the fields of cultivation and from the vermicompost (Gopalakrishnan *et al.,* 2011a) [2]. The soil contains a wide range of bacteria that are useful to the plants by enhancing the production of plant growth promoting substances, acts as antagonists against pathogenic fungi (Alekhya *et al.,* 2017) [2]. Vermicomposting is the process of biological degradation and conversion of agricultural and household wastes to use manure to plants. Vermicomposting improves the recycling of waste with environmentally safe and pollution free approach. It has the capacity to inhibit the growth of plant pathogens, to mobilize the nutrients, etc. (Postma *et al.,* 2003; Gopala krishnan and Rupela 2011a, c.) [18, 9] Hence, in the present study *Actinomycetes* sps were collected from both soil and vermicompost to check the presence of useful plant growth promoting substances that will enhance the disease resistance capacity of plants and nutrient uptake capability.

Materials & Methods
The soil samples were collected from Soybean (Glycine max (L.) Merr.) cultivated fields in both Kharif and Rabi seasons. The samples were collected up to 30cm depth of the rhizosphere soil and stored in sterile plastic bags, kept at room temperature. Samples were collected from different villages of Guntur district, Andhra Pradesh, India and are given codes as NAVS, KNSS, CHSS

Isolation of *Actinomycetes*
Ten grams of rhizosphere soil and vermicompost samples were added separately in to 90ml saline solution (0.85% of NaCl). The flasks were placed on orbital shaker with 100rpm for 1 hour at room temperature. At the end of the shaking, the samples were serially diluted up to10^{-4} to 10^{-6} respectively. Taken 0.1 ml of suspension spread on the *Actinomycetes* Isolation Agar (AIA) plate using spread plate technique. The plates were incubated at 28 ± 2°C for four days. The colonies were observed for morphology and physical properties, Grams staining (Sreevidya *et al.,* 2016) [23]. The pure cultures were subcultured as three replicates and maintained on Starch Casein Agar slants at 4°C for further studies.

In-Vitro Antifungal Activity by Dual Culture Assay (DCA)
A total 93 cultures of *Actinomycetes* were screened for their antagonistic activity against major fungal pathogens of Soybean crop. Viz., *Colletotrichum lindemuthianum*, *Fusarium oxysporum,* and *Rhizoctonia* solani acquired from MTCC (Microbial Type Culture Collection and Gene Bank, Chandigarh, India). Dual culture assay was performed as per the protocol of Anjaiah *et al.,* 1998 [4]**.** Glucose

Casaminoacid yeast extract agar (GCY) plates were prepared. A 5mm fungal discs were placed on the one edge (1cm from the corner) with *Actinomycetes* streaked on the other edge of the plate (1cm from the corner) followed by incubation at 28 ± 2°C for four days. Control plate growth has covered the whole plate. The inhibition of fungal mycelium was measured as the distance of inhibition in cm. All the plates were maintained in triplicates and mean values were taken.

Plant growth promoting and enzymatic activity

Cellulase production

Production of cellulase was estimated as per the protocol of Hendricks *et al.,* 1995 [12]. Cellulose Congo red agar plates were prepared and 6mm wells were made with borer. *Actinomycetes* (20 to 50µL) cultures were added and incubated at 28 ± 2°C for five days. Formation of the halo zone around the *Actinomycetes* colonies indicates the production of cellulase. Production was recorded on a 0-5 scale as follows: 0 = no halo zone; 1 = halo zone of 1–10 mm; 2 = halo zone of 11–20 mm; 3 = halo zone of 21–30 mm; 4 = halo zone of 31–40 mm; and 5 = 41–50 mm.

Lipase production

Production of lipase was estimated as per the protocol of Bhattacharya *et al.,* 2009 [6]; Gopalakrishnan *et al.,* 2011 a [2]. Tween 80 agar media was prepared and 6mm wells were made with borer. *Actinomycetes* (20 to 50µL) cultures were added and incubated at 28 ± 2°C for five days. Formation of halo zone around the cultures was identified as positive for Lipase production. Observations were record as 0-5 scale as follows: 0 = no halo zone; 1 = halo zone of the 1–10 mm; 2 = halo zone of 11–20 mm; 3 = halo zone of 21–30 mm; 4 = halo zone of 31–40 mm; and 5 = 41–50 mm.

Protease production

Production of protease was measured as per the protocol of Bhattacharya *et al.,* 2009 [6]: Gopalakrishan *et al.,* 2011 a. Casein agar media were prepared and 6mm wells were made with borer. *Actinomycetes* (20 to 50µL) cultures were added and incubated at 28 ± 2°C for five days. At the end of the incubation, the plates were observed for the halo zone around the colonies. Production was recorded on a 0-5 scale as follows: 0 = no halo zone; 1 = halo zone of 1–10 mm; 2 = halo zone of 11–20 mm; 3 = halo zone of 21–30 mm; 4 = halo zone of 31–40 mm; and 5 = 41–50 mm.

β- 1, 3-glucanase assay

The protocol for the β-glucanase assay was carried out according to the protocol of Singh *et al.,* 1999. The *Actinomycetes* were inoculated into Tryptic soy broth supplemented with 2% colloidal chitin. The three-day-old cultures were centrifuged at 10,000×g for 12mins and supernatant were collected. To 1mL of the supernatant, 0.1mL of Laminarin (2%wt /Vol) was added and incubated at 40°C for 1hour. Further, the reaction was stopped by adding 3mL of Di Nitro salicylic acid (DNS) reagent and kept them on boiling water bath for 10minutes. The color change from yellow to red indicated the presence of glucose produced by the activity of β-glucanase. Concentration of Enzyme activity was measured by taking absorbance at 530 nm.

Chitinase assay

Production of chitinase was estimated as per the protocol of Gopalakrishnan *et al.,* 2011 [2]; Hsu and Lockwood 1975. Minimal media containing chitin was prepared and 6mm well was made with the borer. *Actinomycetes* culture (20-30µL) was inoculated and incubated at 28 ± 2°C for five days. The chitinase produced by *Actinomycetes* breaks down the chitin present in the medium and this was measured and recorded as scale 0 to 5 where 0= No change; 1 = halo zone of 1–5 mm; 2 = halo zone of 6–10 mm; 3 = halo zone of 11–15 mm; 4 = halo zone of 16–20 mm; and 5 = 21–25 mm.

Indole acetic acid (IAA) production

Actinomycetes isolates were inoculated on Starch casein broth amended with L-tryptophan and incubated at 28±2 ºC with 180 rpm for five days. The culture was centrifuged at 10000×g for 15minutes, the supernatant was collected. 2mL of salkowsky's reagent was added into 1mL of supernatant and incubated for 30 min in a dark place. The color change to pink color after incubation indicates the presences of IAA. The amount of IAA produced by the culture was estimated by measuring absorbance at 530 nm. A standard curve was plotted to quantify the IAA (µg ml^{-1}) Patten and Glick1996; Gopalakrishnan *et al.,* 2011a [2].

Hydrocyanic acid (HCN) production

Presence of HCN was estimated qualitatively by the method of Lorck 1948. For this purpose, Bennet's agar with glycine (4.4 g l^{-1}) was prepared, poured into plates and *Actinomycetes* was streaked. Sterile Whatman filter paper no.1 (8 cm diameter) was soaked in 1% Picric acid and sprayed with 1mL of 10% Sodium carbonate and stuck underneath the Petri dish lids. The plates were sealed with Parafilm and incubated at 28±2 ºC for five days. The appearance of reddish brown color on the filter paper indicates the positive for HCN production. The intensity of color was measured and noted as scale 0 to 3 which indicates 0 = no color change; 1= positive (or) light reddish brown; 2 = medium reddish brown and 3 = dark reddish brown.

Siderophore production

The production of Siderophore was carried out by using the protocol of Macgnan *et al.,*2008; Schwyn and Neilands 1987 [21]. Kings'B broth was prepared and inoculated with *Actinomycetes* and incubated at 150 rpm in room temperature for four to five days. After incubation, the culture was centrifuged at 5000×g for12minutes and supernatant was collected. To 1mL of the supernatant, an equal amount of Chrome Azurole Sulphate (CAS) solution was added and incubated in the dark for 30minutes. The color change from blue to pink indicated the presence of siderophore. The amount of siderophore produced by the culture was estimated by measuring absorbance at 630 nm. The Siderophore production was estimated using the formula

$$\% \, of \; Siderophore \; units = A_r - A_s / A_r \times 100$$

$A_r =$ *Reference of OD value (un inoculated media + CAS solution)*

Where, $A_s = reference \; standard \; value (culture \; supernate \; + CAS \; solution)$

Phosphate solubilization

Phosphate solubilization was estimated as per the protocol of Gyaneshwar *et al.,* 1998 [11]; Alok Ranjan *et al.,* 2013. Rock phosphate buffer media was prepared and 6 mm wells were made with borer. *Actinomycetes* (20 to 50µL) cultures were added and incubated at 28 ± 2°C for five to seven days. At the end of the incubation, the plates were observed for the halo zone around the colonies, production was recorded on a 0-5 scale as follows: 0 = no halo zone; 1 = halo zone of 1–10 mm; 2 = halo zone of 11–20 mm; 3 = halo zone of 21–30 mm; 4 = halo zone of 31–40 mm; and 5 = 41–50 mm.

Molecular identification of selected *Actinomycetes*

The pure cultures of *Actinomycetes* were grown in starch casein broth medium and genomic DNA was isolated according to the protocol of Bazzicalupo and Fani 1995 [5]. The isolated DNA was tested qualitatively and quantitatively and then sent to Barcode biosciences, Bangalore for 16s rRNA sequencing. The sequence obtained from Biosciences was compared with similar sequences of Gen bank by using the BLAST program Altschul *et al.,*1990 [3]. The obtained results were aligned using the Clustal W software Thomposon *et al.,*1997. The phylogenetic tree was constructed by the neighbor-joining method using Mega X software. (Saitou and Nei 1987; Tamura *et al.,* 2007) [20, 24].

Experimental Method

1. DNA was isolated from the culture provided by the scientist. Its quality was evaluated on 1.0 %agarose gel, a single band of high-molecular weight DNA has been observed.
2. Fragment of 16S rRNA gene was amplified by 16SrRNA-F and 16SrRNA-R primers. A single discretePCR amplicon band of 1300 bp was observed when resolved on agarose gel.
3. The PCR amplicon was purified to remove contaminants.
4. Forward and reverse DNA sequencing reaction of PCR amplicon was carried out with 16SrRNA-Fand 16SrRNA-R primers using BDT v3.1 Cycle sequencing kit on ABI 3730xl Genetic Analyzer.
5. Consensus sequence of 16S rRNA gene was generated from forward and reverse sequence data using aligner software.
6. The 16S rRNA gene sequence was used to carry out BLAST with the 'nr' database of NCBI GenBank database. Based on maximum identity score first ten sequences were selected and aligned using multiple alignment software program Clustal W. Distance matrix was generated using RDP database and the phylogenetic tree was constructed using MEGA 6.

Results

Selection of *Actinomycetes* with antagonistic activity against fungal pathogens

A total of 93 isolates were isolated from different soil samples in the rhizosphere of Soybean. Among these 93 isolates, only three isolates were significantly inhibiting fungal pathogens. In dual culture assay, the three isolates significantly inhibited the *Fusarium oxysporum* (FOC), in the range of 1.7- 2.7cm, exhibited the antagonistic activity against *Colletotrichum lindemuthianum* in the range 0.9-1.8cm, inhibited *Rhizoctonia solani* in the range of 1.2-2.5cm when compared to control.

Plant growth promoting and enzymatic activity

In *in-vitro* studies, selected isolates showed effect on plant growth promoting attributes such as cellulase production (except DVS-11), lipase and protease production in all isolates, β-1,3-glucanase production up to 25.9-32.3, chitinase production, IAA production range is between them 18.2 to 81 µg/ml. HCN, siderophore, phosphate solubilization is found in all the isolates.

Molecular Identification

16S rDNA sequences of three promising antagonistic *Actinomycetes* were analyzed. When running the sequences in NCBI BLAST all the three isolates showed similarity to *Streptomyces* sp., with 98% similarity. Then compared with the sequences in NCBI and EzTaxon using BLAST program, aligned sequences with Clustal W software and constructed the phylogenetic tree (Dendrogram) by the neighbor-joining method. Sample which was labelled as NAVS-13 was found to be *Streptomyces rochei*, sample which was labeled as KNSS-3 was found to be *Streptomyces cavourensis*, sample which was labeled as CHSS-3 was found to be *Streptomyces alfalfae* showed high similarity with Top based on nucleotide homology and phylogenetic analysis.

Table 1: Antagonisticactivityagainst three fungal pathogens

Isolates	*Colletotrichum lindemuthianum*	*Fusarium oxysporum*	*Rhizoctonia Solani*
NAVS-13	1.6	1.9	1.5
KNSS-3	1.9	1.6	1.6
CHSS-3	1.8	1.7	1.7
Control	0	0	0
Mean	1.32	1.3	1.20
SE (Standard Error)	0.51	0.50	0.46
SD (Standard Deviation)	0.89	0.87	0.80
CV (coefficient of variation)	0.79	0.76	0.64

In vitro selected actinomycetes are showing antagonistic activity against major fungal pathogens in soybean crop. Values are the mean of 3 experiments (n = 3), each with 3 replicates per treatment. Means were subjected to factorial ANOVAs separate means.

Table 2: Enzymatic assay

Isolates	Cellulase (mm)	Lipase (mm)	Protease (mm)	HCN	IAA µg ml-1	Siderophore units	Phosphate (mm)	Chitinase (mm)	β- 1,3 glucanase units@
NAVS-13	18 mm	16 mm	18 mm	2	18.3	52.6	16 mm	17 mm	28.9
KNSS-3	16 mm	12 mm	19 mm	0	64.3	39.8	20 mm	16 mm	38.6

CHSS-3	14 mm	16 mm	18 mm	1	29.6	42.9	18 mm	18 mm	42.8
Control	0	0	0	0	0	0	0	0	0
Mean	12	11	13.75	0.75	28.05	33.82	13.5	12.75	27.57
SE (Standard Error)	4.71	4.37	5.299	1.85	15.62	13.39	5.28	4.93	11.13
SD (Standard Deviation)	66.67	57.33	84.25	2.75	27.06	23.19	83.66	72.91	371.82
CV (coefficient of variation)	68.04	68.84	66.75	127.65	96.51	68.59	67.76	66.97	69.93

In vitro PGP traits of selected *Actinomycete* isolates were observed. HCN, hydrocyanic acid; IAA, indole acetic acid; siderophore, cellulase, lipase and protease production as: 0-no halozone; 1-halozone of<1mm; 2- halozone of 1–3mm; 3-halozone of 4–6mm and 4-halozone of 7mm and above; (ii) HCN production as: 0-no colour change; 1-light reddish brown; 2-medium reddish brown and 3-dark reddish brown; (iv) -1,3-glucanase (U)– one unit is an amount of enzyme that liberated 1 mol of glucose hour^{-1} at defined conditions. Value son secondary (right) axis indicates IAA production. Values are the mean of 3 experiments (n=3), each with 3 replicates per treatment. Means were subjected to factorial ANOVAs separate means.

Table 3: salinity concentration (Nacl%)

Isolates N	0%	2%	4%	6% N	8%	10%	12%
NAVS-13	2	3	2	2	3	2	1
KNSS-3	3	2	2	3	2	1	1
CHSS-3	2	2	1	3	3	1	2
Control	0	0	0	0	0	0	0
Mean	1.75	1.75	1.25	2.00	2.00	1.00	1.00
SE (Standard Error)	0.72	0.72	0.55	0.81	0.81	0.47	0.47
SD (Standard Deviation)	1.58	1.58	0.83	2.00	2.00	0.66	0.66
CV (coefficient of variation)	71.9	71.9	66.33	70.71	70.71	81.65	81.65

The selected *Actinomycetes* were tested in different salts concentrations. Values are the mean of 3experiments (n=3), each with 3 replicates per treatment. Means were subjected to factorial ANOVAs separate means.

Table 4: Effect of Temperature and pH

Isolates	20oC	30oC	40oC	50oC	pH-5	pH-7	pH-9	pH-11	pH-13
NAVS-13	2	2	2	00	00	2	2	2	00
KNSS-3	3	3	3	00	00	3	3	3	00
CHSS-3	3	2	1	00	00	3	2	2	00
Control	00	00	00	00	00	00	00	00	00
Mean	2.0	2	1.5	00	00	2	1.75	1.75	00
SE (Standard Error)	0.81	0.72	0.74	00	00	0.816	0.72	0.72	00
SD (Standard Deviation)	2.0	2	1.67	00	00	2	1.58	1.58	00
CV (coefficient of variation)	70.71	71.90	86.07	00	00	70.71	71.9	71.9	00

The selected *Actinomycetes* are tested at different temperature and pH conditions. Values are the mean of 3 experiments (n=3), each with 3 replicates per treatment. Means were subjected to factorial ANOVAs separate means.

Table 5: Effect of carbon sources

Isolates	Glucose	Sucrose	Fructose	Starch
NAVS-13	2	2	2	00
KNSS-3	3	3	3	00
CHSS-3	3	2	1	00
Control	00	00	00	00
Mean	2.0	2	1.5	00
SE (Standard Error)	0.81	0.72	0.74	00
SD Standard Deviation)	2.0	2	1.67	00
CV (coefficient of variation)	70.71	71.90	86.07	00

The selected actinomycetes Effect of carbon sources. Values are the mean of 3 experiments (n = 3), each with 3 replicates per treatment. Means were subjected to factorial ANOVAs separate means Antagonistic activity against three fungal pathogens

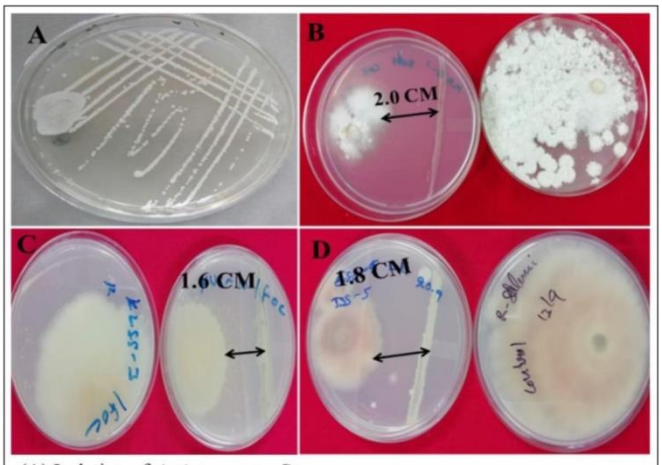

(A) Isolation of *Actinomycetes Sps*.
(B) Antagonistic activity against *Colletotrichum lindemuthianum*
(C) Antagonistic activity against *Fusarium oxysporum*.
*(D)*Antagonistic activity against *Rhizoctonia solani*

Fig 1

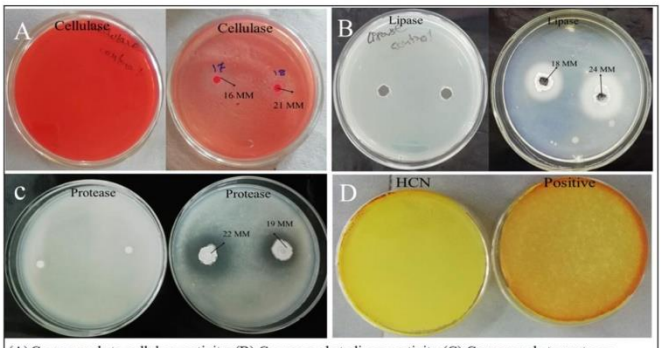

(A) Corresponds to cellulase activity. (B) Corresponds to lipase activity (C) Corresponds to protease activity. (D) Corresponds to HCN production. The cellulase, lipase and protease zone of inhibition is measured in mm. For HCN production the colour formation is measured 0= no colour change, 1= positive or slight colour change, 2= medium colour change, 3= good or excellent colour change.

Fig 2

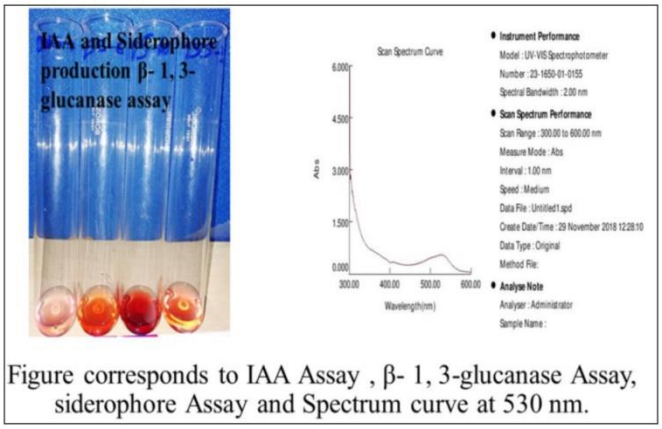

Figure corresponds to IAA Assay , β- 1, 3-glucanase Assay, siderophore Assay and Spectrum curve at 530 nm.

Fig 3

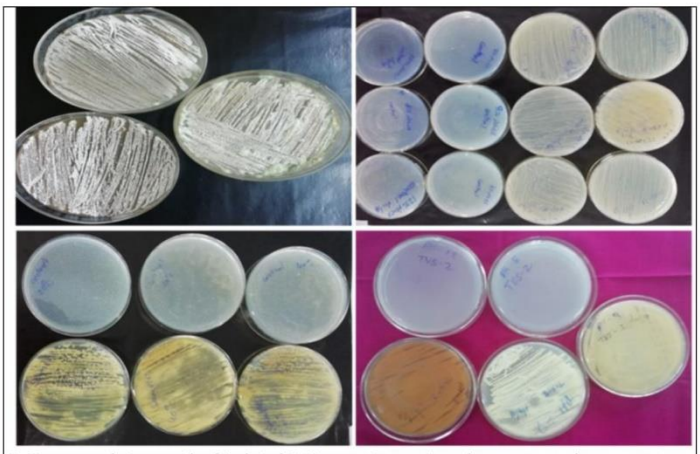

A. Corresponds to growth of isolated *Actinomycetes* sps in carbon sources, glucose, sucrose and starch
B. Corresponds to growth of isolated *Actinomycetes* sps at 2%, 4%, 6%, 8%, 10% and 12% of NaCl concentrations.
C. Corresponds to growth of isolated *Actinomycetes* sps at 30^{0}C, 40^{0}C and 50^{0}C temperature.
D. Corresponds to growth of isolated *Actinomycetes* sps at pH-5,7,9,11,13

Fig 4

Conclusion

Out of the 93 *Actinomycetes* isolates obtained from different soil samples collected in the fields of Soybean, and vermicompost only 29 isolates were found to have antagonistic activity. When the 29 *Actinomycetes* isolates were further evaluated for antagonistic activity against three fungal pathogens namely *C.lindemuthianum, F.oxysporum and R.solani* using dual culture assay method, three isolates namely NAVS13, KNSS3, CHSS3 inhibited *C.lindemuthianum, F.oxysporum,* and *R.solani*. From these results it can be concluded that NAVS13, KNSS3 and CHSS3 have good antagonistic activity and inhibit the three major fungal pathogens. The isolates were further evaluated for Cellulase, Lipase, Protease, HCN, phosphate solubilization, production of growth hormone IAA (Correa *et al.,* 2005), production of Siderophore, Chitinase, β-1, 3-Glucanase and physiological properties. The isolates were identified by molecular characterization as *Streptomyces rochei, Streptomyces cavourensis*and *Streptomyces alfalfa.*

Reference

1. Agrios GN. Significance of plant diseases. Plant Pathology. Academic Press, London, 2000, 25-37.
2. Alekhya G, Gopalakrishnan S. Biological control and plant growth-promotion traits of Streptomyces species under greenhouse and field conditions in chickpea. Agricultural Research. 2017; 6(4):410-420.
3. Altschul SF, Gish W, Miller W, Myers EW, Lipman DJ. Basic local alignment search tool. Journal of molecular biology. 1990; 215(3):403-410.
4. Anjaiah V, Koedam N, Nowak-Thompson B, Loper JE, Höfte M, Tambong JT, *et al*. Involvement of phenazines and anthranilate in the antagonism of Pseudomonas aeruginosa PNA1 and Tn 5 derivatives toward Fusarium spp. and Pythium spp. Molecular Plant-Microbe Interactions. 1998; 11(9):847-854.
5. Bazzicalupo M, Fani R. The use of RAPD for generating specific DNA probes for microorganisms. In. Clap JP (ed.) Methods in molecular biology, species diagnostic protocols: PCR and other nucleic acid methods, 1995.
6. Bhattacharya A, Chanda S, Barik S. Lipase and protease producing microbes from the environment of sugar beet field. Indian Journal of Agricultural Biochemistry. 2009; 22(1):26-30.
7. Donate-Correa J, León-Barrios M, Pérez-Galdona R. Screening for plant growth-promoting rhizobacteria in Chamaecytisusproliferus (tagasaste), a forage tree-shrub legume endemic to the Canary Islands. Plant and Soil. 2005; 266(1-2):261-272.
8. Gopalakrishnan S, Kiran BK, Humayun P, Vidya MS, Deepthi K, Jacob S, *et al*. Biocontrol of charcoal-rot of sorghum by actinomycetes isolated from herbal vermicompost. African Journal of Biotechnology. 2011; 10(79):18142-18152.
9. Gopalakrishnan S, Pande S, Sharma M, Humayun P, Kiran BK, Sandeep D, Rupela O, *et al*. Evaluation of actinomycete isolates obtained from herbal vermicompost for the biological control of Fusarium wilt of chickpea. Crop Protection. 2011; 30(8):1070-1078.
10. Gopalakrishnan S, Srinivas V, Alekhya G, Prakash B, Kudapa H, Rathore A, Varshney RK. The extent of grain yield and plant growth enhancement by plant growth-promoting broad-spectrum Streptomyces sp. in chickpea. Springer Plus. 2015; 4(1):31.
11. Gyaneshwar P, Kumar GN, Parekh LJ. Effect of buffering on the phosphate-solubilizing ability of microorganisms. World Journal of Microbiology and Biotechnology. 1998; 14(5):669-673.
12. Hendricks CW, Doyle JD, Hugley B. A new solid medium for enumerating cellulose-utilizing bacteria in

soil. Appl. Environ. Microbiol. 1995; 61(5):2016-2019.
13. Hsu SC, Lockwood JL. Powdered chitin agar as a selective medium for enumeration of actinomycetes in water and soil. Appl. Environ. Microbiol. 1975; 29(3):422-426.
14. Lorck H. Production of hydrocyanic acid by bacteria. Physiologia Plantarum. 1948; 1(2):142-146.
15. Macagnan D, Romeiro RDS, Pomella AW, deSouza JT. Production of lytic enzymes and siderophores, and inhibition of germination of basidiospores of Moniliophthora (ex Crinipellis) perniciosa by phylloplane actinomycetes. Biological Control. 2008; 47(3):309-314.
16. Pal KK, Tilak KVBR, Saxena AK, Dey R, Singh CS. Suppression of maize root diseases caused by Macrophominaphaseolina, Fusarium moniliforme and Fusarium graminearum by plant growth promoting rhizobacteria. Microbiological research. 2001; 156(3):209-223.
17. Patten CL, Glick BR. Bacterial biosynthesis of indole-3-acetic acid. Canadian journal of microbiology. 1996; 42(3):207-220.
18. Postma J, Montanari M, van den Boogert PH. Microbial enrichment to enhance the disease suppressive activity of compost. European journal of soil biology. 2003; 39(3):157-163.
19. Rupela OP, Gupta AP, Kapoor KK. Is high yield possible with biological approaches. Management of organic wastes for crop production. CCS Haryana Agricultural University, Hisar, Haryana, 2005, 193-203.
20. Saitou N, Nei M. The neighbor-joining method: a new method for reconstructing phylogenetic trees. Molecular biology and evolution. 1987; 4(4):406-425.
21. Schwyn B, Neilands JB. Universal chemical assay for the detection and determination of siderophores. Analytical biochemistry. 1987; 160(1):47-56.
22. Singh PP, Shin YC, Park CS, Chung YR. Biological control of Fusarium wilt of cucumber by chitinolytic bacteria. Phytopathology. 1999; 89(1):92-99.
23. Sreevidya M, Gopalakrishnan S, Kudapa H, Varshney RK. Exploring plant growth-promotion actinomycetes from vermicompost and rhizosphere soil for yield enhancement in chickpea. brazilian journal of microbiology. 2016; 47(1):85-95.
24. Tamura K, Dudley J, Nei M, Kumar S. MEGA4: molecular evolutionary genetics analysis (MEGA) software version 4.0. Molecular biology and evolution. 2007; 24(8):1596-1599.
25. Thompson JD, Gibson TJ, Plewniak F, Jeanmougin F, Higgins DG. The CLUSTAL_X windows interface: flexible strategies for multiple sequence alignment aided by quality analysis tools. Nucleic acids research. 1997; 25(24):4876-4882.

ejbps, 2019, Volume 6, Issue 9, 203-208. **Research Article** **SJIF Impact Factor 4.918**

EUROPEAN JOURNAL OF BIOMEDICAL AND PHARMACEUTICAL SCIENCES

http://www.ejbps.com

ISSN 2349-8870
Volume: 6
Issue: 9
203-208
Year: 2019

COMPARISON OF THE NON-SPECIFIC IMMUNE RESPONSE IN THE HEAD KIDNEY OF EDIBLE CARP AGAINST BACTERIAL INFECTION

Satyalatha B.D.J.* and Viveka Vardhani V.

*Dept. of Zoology, Government College for Women (A), Guntur (A.P.), India.
Dept. of Zoology and Aquaculture Acharya Nagarjuna University Nagarjunanagar - 522 510, A.P., India.

***Corresponding Author: Satyalatha B.D.J.**
Dept. of Zoology, Government College for Women (A), Guntur (A.P.), India.

Article Received on 25/06/2019 **Article Revised on 15/07/2019** **Article Accepted on 05/08/2019**

ABSTRACT

Introduction: Occurrence of diseases in edible carps is due to several factors like decreased resistance, poor water quality and bad managerial methods. The most significant factor effecting the health of fish is the incidence of bacterial pathologies in various organs, mainly the primary lymphoid organ, head kidney. *Aeromonas liquefaciens* (Bacterium) may behave as opportunistic pathogen by assailing already compromised or streseed paths. **Objectives:** With the above background, the present investigations were planned to assay protein and DNA profile and histological alterations in head kidney of *Labeo rohita*. **Material and Methods:** Four groups of experimental fish were infected with single doses (group A, 10^{-2} CFW/fish; group B, 10^{-4} CFU/fish; group C, 10^{-5} CFU/fish; group D, 10^{-6} CFU/fish) and two experimental group of fish were infected with multiple doses (4 days interval) (group E, 10^{-2}+10^{-2} CFU/fish; group F, 10^{-3} + 10^{+3} CFU/fish) of *A. liquefaciens* along with uninfected controls (groups, 66 fish). Six fish from a, b, c, d, e, f groups A, B, C, D and E, F and controls were necropsied on each day of eleven observations. Protein and DNA and histology were studied using standard methods. **Results and conclusion:** Protein and DNA level in head kidney of experimental fish (groups A, B, C and D) showed a significant increase and decrease in when compared with controls from hour 1 to 216 of infection. Protein level in head kidney showed a significant rise in experimental groups A and B when compared with controls; and in between the experimental groups A and B. Protein level in head kidney showed a significant rise in experimental groups E and F when compared with controls; and in between the experimental groups E and F. The DNA level in head kidney showed a significant decrease in experimental groups E and F when compared with controls and in between the experimental groups E and F. The statistical analysis showed a significant difference in the level of head kidney protein and DNA when comparison was made between singly infected groups B (10^{-4} CFU/fish) and D (10^{-6} CFU/fish) and repeatedly infected groups E (10^{-2} + 10^{-2} CFU/fish) and F (10^{-3} + 10^{-3} CFU/fish).The DNA level in head kidney showed a significant decrease in experimental groups A and B when compared with controls and in between the experimental groups A and B. The statistical analysis showed a significant difference in the level of head kidney protein and DNA when comparison was made between singly infected groups B (10^{-4} CFU/fish) and D (10^{-6} CFU/fish) and repeatedly infected groups E (10^{-2} + 10^{-2} CFU/fish) and F (10^{-3} + 10^{-3} CFU/fish).Infected carps showed lesions and necrosis in head kidney during experimentation. Present investigations indicate a high non-specific immune response in experimentally infected fish compared to controls.

KEYWORDS: Immune response, protein, DNA head kidney, histology, edible carp.

INTRODUCTION

Indian major carps are the most farmed fish in the country and its production is hampered by infectious microbial pathogens. *Aeromonas* species are causing infections in fish found in surface waters, estuarine water, fresh water, food products, sewage, diseased or health fish and in humans.[1-3] *A. liquefacines* as a food-borne pathogen, may cause zoonatic diseases and pathologic reaction in host tissues.[4-5] *Aeromonas* sps. cause degenerative histopathological changes in kidney, liver, gills, stomach and spleen of fish.[6] The carp immune system has several immune mechanisms responsible to defend against pathogenic bacteria through non-specific and specific (humoural or cell mediated) immune response. Disease resistance in fish is offered by natural (non-specific) and specific immune parameters.[7-9] Fish exposed to bacterial pathogens showed abnormal changes in biochemical profile, immune parameters and organ histology.[10-12] Head kidney, the primary lymphoid organ in fish produce and mature stem cells. The head kidney is characterized by the presence of lymphoid follicles and vessels. Morphological/pathological changes in the lymphoid organ associated with immune response. Lymphocytes

are the key effector cells of adaptive immunity and activated due to the exposure of self and non-self antigens. Overall, there is a paucity of data on the function of head kidney and lymphocytes in the present experimental model, *Labeo rohita.*

AIMS AND OBJECTIVES

With the above background, the present findings have planned to:

1. Estimate the protein and DNA content in head kidney of fish exposed to single and multiple doses of infection and uninfected controls.
2. Study the histopathological reactions in head kidney of infected and control fish.

MATERIALS AND METHODS

Fresh water fish, *L. rohita* were procured from a local fish farm, Nandivelugu (Guntur District), A.P., India. Fish were acclimatized in laboratory, fed with pellet feed and divided into 6 experimental (infected) (A, B, C, D, E, F; 66 fish in each group) and 6 control a,b,c,d,e, f groups.

The bacterial infection provided from Chandigarh (MTCC No. 2654) and pure culture of bacteria prepared by streak plate method. Four groups (A, B, C, D) of fish received infection (intramuscularly below the region of dorsal fin) as a single dose @ 10^{-2} CFU/fish (Group A), 10^{-4} CFU/fish (Group B), 10^{-5} CFU/fish (Group C) and 10^{-6} CFU/fish (Group D); 2 groups received infection via similar route as a repeated dose at 4 days interval @ 10^{-2} + 10^{-2} CFU/fish (Group E) and 10^{-3} + 10^{-3} CFU/fish (Group F) . 6 fish from the experimental (A, B, C, D) and control (a, b, c, d) groups were necroposied at hour 1, 3, 6, 12, 18, 24, 36, 48, 72, 96 and 216 of experimental period. 6 fish from experimental groups E, F and Control groups e, f were also mecropsied on the same designated hours (after infection). Protein and DNA were estimated from head kidney following[13] and Diphenyl amine method. For the histopathological studies, tissue specimens of head kidney were excised, embedded in paraffin and sectioned at 5 µ and tissue sections were stained with H and E method.

RESULTS AND DISCUSSION

Protein Activity In Head Kidney (Table 1)

Fish of group A (treated @10^{-2} CFU/fish) showe a decrease of protein from hour 1 to 216 when compared to controls (below normal level) There was a gradual decrease from hour 1 (62.41 mg/ml) 18 (57.58 mg/ml) and a slight increase (below normal level) from hour 18-216. In fish of group B, protein level decreased to below normal level on hour1(60.34 mg/ml) 3(61.72 mg/ml) and 6 (62.41 mg/ml) in comparison with controls (63.80 mg/ml). In group C protein level is slightly higher than control on hour 1 and a slight decrease from hour 1 to 216 (below normal levels). Higher level of protein was found on hour 1, 3, 6, 12 and 18; with highest increase on hour 6 (66.71 mg/ml). Decreased level of protein was found from 1 to 216 in groups E and F (below normal values) during the period of experimentation when compared with controls. There was a marked decrease of protein and DNA content the head kidney of both the experimental groups (A and B) from hour 1 to 216 of refection (except the slight increase of DNA on hour 1 and 6 in group B)

Dna Activity In Head Kidney (Table 1)

In case of groups A, B and C, there was decrease in DNA content from hour 1 to 216 of infection period in comparison with controls; all these values are found as below normals. In group D (10^{-6} CFU/fish), there was a marked increase of DNA from hour 1 to 72 and a decrease from hour 96 and 216 when compared with controls. In case of group E which received infection (10^{-2} CFU/fish $+10^{-2}$), the level of DNA was lower than controls on hour 1, 3 and 6,12,18,24,36,48,72,96 and 216; it was below normal throughout the infection period. Fish of group F showed a higher level of DNA on hour 1 of infection (12.22 mg/ml) from hour 1 to 6 (15.55 mg/ml), there is a gradual increase and all these increased values are higher than that of control values 11.11 mg/ml), a peak increase on hour 18 of reflection. The DNA level decreased to normal level from the hour 18 onwards till the day 9 of experimental period, the gradual decrease of DNA was (lower than that of control value.

In group A, there was a decrease in DNA content from hour 1 to 216, and these values are found to be lower than that of values of uninfected with C group (except the normal level on hour 48). Higher level of DNA was found in group B on hour 1 of infection, there is a decrease in DNA content (10.06 mg/ml)(below normal values). Group C showed a higher amount of DNA on hour 1(13.33 mg/ml) and from hour 1 to 12 of experimental period, there was a gradual decline of DNA. There was a significant decrease of protein in groups A and C when compared with controls (Table-1). Differences in the level of protein were statistically non-significant in the groups C and D when compared with controls and in between groups A and B, A and C and B and C; groups A, B and C showed significant difference when compared with group D. In comparision with controls. There was a significant increase of DNA in group D and significant decrease in groups A and B. There was no significant difference when compared in between groups C and controls, and A and C. There was a significant difference in group B when compared with groups C, D and A.

Table 1: Content of protein (mg/ml) and DNA (mg/ml) in the head kidney of experimental fish (group A, B, C, D, E and F) treated with 10^7 CFU/fish, 10^5 CFU/fish, 10^3 CFU/fish, 10^1 CFU/fish, 10^2 CFU/fish + 10^7 CFU/fish and 10^3 CFU/fish + 10^3 *Aeromonas liquifaciens* at different periods of infection and control (group G). Values are expressed in mean derived from five observations.

Hours of Necropsy	Experimental groups												Control Group	
	Group-A		Group-B		Group-C		Group-D		Group-E		Group-F		Group-G	
	Protein	DNA	Protein	DNA	Protein	DNA	Protein	DNA	Protein	DNA	Protein	DNA	Protein	DNA
1	62.41	10.0	60.34	13.33	64.13	13.33	65.86	18.88	58.96	10.0	52.75	12.22	63.79	11.11
3	61.72	9.0	61.72	10.06	61.72	10.0	65.17	16.66	58.27	7.77	50.68	13.33	63.79	11.12
6	58.27	7.77	62.41	8.88	61.72	11.11	66.79	15.55	55.51	7.77	48.62	15.55	63.77	11.11
12	57.93	8.88	63.10	7.77	60.34	8.88	65.51	14.44	54.82	6.66	47.93	11.11	63.77	11.09
18	57.58	10.0	63.79	7.78	60.96	14.44	64.13	12.22	52.06	5.55	45.17	10.0	63.78	11.11
24	60.34	6.66	62.41	7.77	61.37	10.0	63.79	16.66	51.37	4.44	56.89	8.88	63.78	11.12
36	61.03	8.88	61.72	7.76	61.06	10.0	62.75	16.66	51.03	1.11	57.58	7.77	63.78	11.13
48	61.72	11.11	62.06	7.77	61.72	7.77	62.06	15.55	51.37	5.55	57.93	6.66	63.78	11.09
72	62.41	10.0	62.41	6.66	60.72	5.55	63.79	14.44	56.89	4.44	55.86	5.55	63.79	11.11
96	60.34	6.66	62.06	5.55	60.68	4.44	62.41	10.06	58.62	5.55	57.58	5.54	63.78	11.10
216	59.65	4.44	63.10	2.22	60.34	4.44	63.79	9.99	58.62	4.44	58.27	5.55	63.77	11.11

Table 2: 't' values obtained for different groups of fish infected with 10^{-2} (group A), 10^{-4} (group B), 10^{-5} (group C) and 10^{-6} (group D) CFU/fish

	Experimental (A, B, C and D) and Control (a, b, c and d) groups							
	A	a	B	b	C	c	D	d
Head Kidney Protein Mean	60.30	63.76	62.28	63.78	61.34	63.78	64.19	63.78
	A a		B b		C c		D d	
t value	t=6.55* (P<0.05)		t=2.29@ (P>0.05)		t=7.65* (P<0.05)		t=0.88@ (P>0.05)	
	A B		A C		A D			
	t=2.29@ (P>0.05)		t=1.67@ (P>0.05)		t=5.56* (P<0.05)			
	B C		B D		C D			
	t=2.24@ (P>0.05)		t=3.60* (P<0.05)		t=5.13* (P<0.05)			
Head Kidney DNA Mean	8.49	11.1	7.78	11.01	9.08	11.01	14.64	11.1
	A a		B b		C c		D d	
t value	t=4.45* (P<0.05)		t=4.04* (P<0.05)		t=2.01@ (P>0.05)		t=4.15* (P<0.05)	
	A B		A C		A D			
	t=2.32* (P<0.05)		t=0.51@ (P>0.05)		t=5.94* (P<0.05)			
	B C		B D		C D			
	t=2.41* (P<0.05)		t=5.79* (P<0.05)		t=4.22* (P<0.05)			

P value at 5% level of significance is 2.306 *Statistically significant values @Statistically non-significant values

Table 2: 't' values obtained for different groups of fish infected with $10^{-2} + 10^{-2}$ (group E), and $10^{-3} + 10^{-3}$ (group F) CFU/fish.

Experimental (E and F) and Control (e and f) groups				
	E	e	F	f
Head Kidney Protein Mean	55.22	63.78	53.56	63.78
	E e	F f	E F	
t value	t=8.68* (P<0.05)	t=7.13* (P<0.05)	t=4.19* (P<0.05)	
Head Kidney DNA Mean	5.75	11.1	9.39	11.1
	E e	F f	E F	
t value	t=7.64* (P<0.05)	t=2.75* (P<0.05)	t=3.05* (P<0.05)	

t values obtained for groups B (10^{-4} CFU/fish) and E and for groups D (10^{-6} CFU/fish) and F				
	B	E	D	F
Head Kidney Protein Mean	62.28	55.22	63.91	53.56
	B E	D F		
t value	t=6.91* (P<0.05)	t=7.07* (P<0.05)		
Head Kidney DNA Mean	7.78	5.75	14.64	9.39
	B E	D F		
t value	t=2.33* (P<0.05)	t=3.98* (P<0.05)		

P value at 5% level of significance is 2.306
*Statistically significant values @Statistically non-significant values

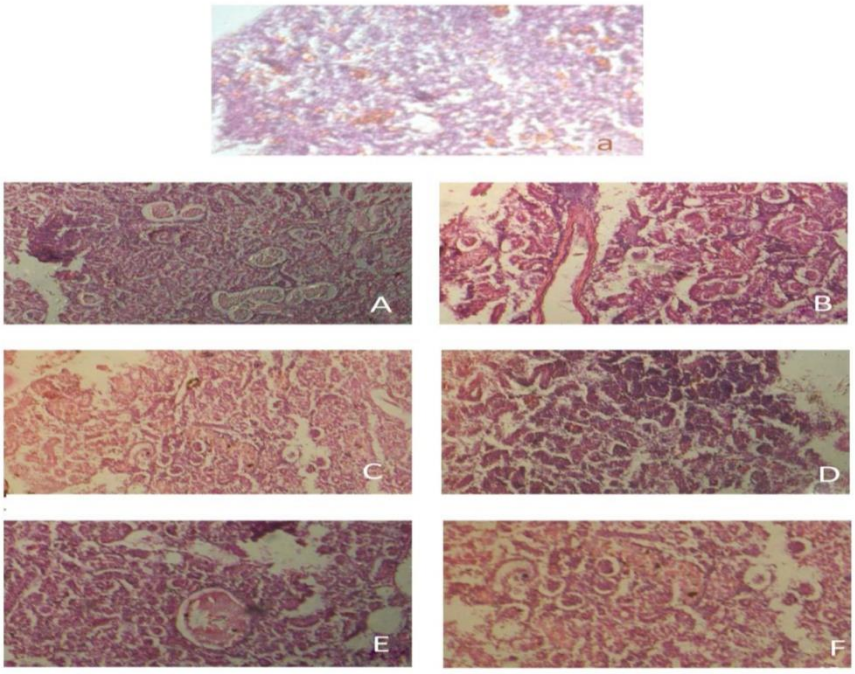

Figure showing head kidney from control (a) and infected (A,B,C,D,E andF) fish

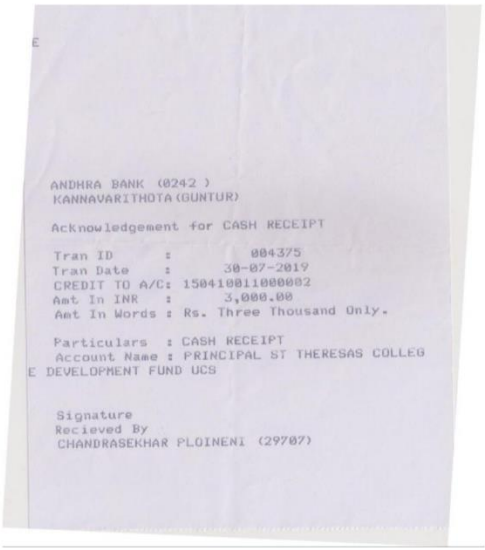

ANDHRA BANK (0242)
KANNAVARITHOTA (GUNTUR)

Acknowledgement for CASH RECEIPT

Tran ID : 004375
Tran Date : 30-07-2019
CREDIT TO A/C: 150410011000002
Amt In INR : 3,000.00
Amt In Words : Rs. Three Thousand Only.

Particulars : CASH RECEIPT
Account Name : PRINCIPAL ST THERESAS COLLEG
E DEVELOPMENT FUND UCS

Signature
Recieved By
CHANDRASEKHAR PLOINENI (29707)

HISTOPATHOLOGY

The multiple sections of normal head kidney showed normal parenchyma and interstitial tissue without any proliferation. The renal corpuscle is composed of glomerulas and its capsule showed intact texture. In group A and B, at day 9 post infection, the head kidney showed congestion of blood capillaries and glomerular tufts with heavy necrotic tissue. The hematopoietic tissue in the kidney was disrupted and the glomeruli were enlarged. Heavy infiltration of lymphocytes and macrophages were observed. Accumulation of pus and severe inflammation of sinusoids and serous membrane were observed(Fig.1 A). The multiple sections of the head kidney study in group B revealed heavy necrotic tissue. The hematopoietic tissue in the in the kidney was disrupted by the heavy infestation of bacteria. Glomeruli were enlarged and showed cell proliferation. Accumulation of pus and severe inflammation of sinusoids and serous membrane were observed. The glomeruli showed nodular out growths due to serious bacterial infestation (Fig.1B). In group C, head kidney showed severe necrosis, congestion of the renal capillaries and several accumulation of granular eosinophilic cells. Accumulation of pus, severe inflammation of sinusoids and serous membrane were observed. Hematopoietic tissue was severely disrupted. Glomeruli were enlarged (Fig.1 C). The multiple sections of the study revealed heavy necrosis and severe blood clots, heavy inflammation and enlargement of glomeruli in fish of group D. Accumulation of pus ans severe inflammation of sinusoids and serous membrane were observed. Severe infiltration of lymphocytes and neutrophils was observed (Fig.1D). Pathogenic bacterium (via intramuscular route) caused infiltration of lymphocytes, atrophy and necrosis throughout the infection period (from hour 1 to 216). In group E which received 10^{-2} + 10^{-2} CFU/fish, there was heavy destruction and damage of entire tissue due to bacterial invasion. Inflammatory reaction was evident by moderate increase of macrophages, lymphocytes and eosinophils and highly congested blood vessels. Glomeruli sparseley congested (Fig 1E). Heavy necrotic tissue and severe blood clots were seen in fish which received double dose of infection (10^{-3}+10^{-3} CFU/fish). Serous membranes of renal corpusles showed vacular degeneration and proliferative inflammation. The hematopoietic tissue was disrupted by the heavy infestation of bacteria. Glomeruli were enlarged with heavy cellular proliferation (Fig. 1 F). Renal capillaries showed congestion, proliferation and hyperplasia. Accumulation of pus and severe inflammation of sinusoids and serous membrane were observed. The glomeruli showed modular out growths due to severe bacterial infestation.

The virulent infectious *A. liquefaciens* might have caused abnormality in the level of protein and DNA in head kidney at different hours of experimental period in the present study.[13,14] also suggested that the infectious pathogenic bacteria may produce ill effects thereby disturbing the physiological mechanism of fish.[15,17] also reported that fish exposed to toxicants show impaired protein metabolism. The reduced level of protein at some hours of infection in the infected fish confirm that of[17] who reported that the lowered level of protein was due to reduction in the synthesis of proteins.

Fish suffering due to aeromoniasis (groups A,B,C and D) showed atrophy and necrosis in renal haemopiotic tissues as explored by[18] in Eel *(Anguilla japonica)* infected by aeromonads species. 19 also explained that head kidney is one of the target organ influenced by *A. hydrophila* and both acute and severe infection cause damage to the head kidney. The changes like necrotic lesion and aggregation of melanin containing macrophages in the head kidney of infected fish (during the entire experimental period) indicate the pathogenic effect of microbial organism in the head kidney; this is an indication of stressful condition of infected fish. These results compare well with that of[19] who also reported necrotic lesions and aggregation of melanin filled macrophages in kidney and spleen of fingerlings of *L.rohita* infected with *A. hydrophilla*.

These results confirm the observations of 14 who also observed biochemical alterations in liver and muscle tissue in fish, *Clarius batracus* during insecticide treatment. The alteration of tissue protein level in head kidney might be due to the synthesis of stress proteins as reported by.[20] Various authors[21,22 and 23] reported synthesis of stress proteins due to heavy metal treatment. In the present study, pathogenic aeromonads was pound as effective inducer of stress protein in altering the tissue protein fractions of experimental fish (exposed to various doses of *A. liquefactions*). The histopathological changes in head kidney explain the involvement of stress in aeromoniasis, the change like necrotic lesions and

aggregations of melanin containing macrophages were observed in the present study. The pathological changes brought out in fish by pathogenic bacteria strongly indicate that these lymphoid organs could provide sensitive indicator of stressful conditions in the aquatic environment. Fingerlings of *L.rohita* infected with *A. hydrophila* also indicated necrotic lesions and aggregation of melanine filled macrophages in kidney and spleen.[20]

REFERENCES

1. Dar GH, Dar SA, Kamili AN, Chishti MZ, Ahmad F. Detection and characterization of potentially pathogenic Aeromonas sobria isolated from sh Hypophthalmichthys molitrix (Cypriniformes: Cyprinidae). Microbial Pathogenesis, 2016; 91: 136-140.
2. Dias M.K.R. , Sampaio L.S., Proietti-Junior A.A., Yoshioka E.T.O., Rodrigues D.P., A.F.R. Rodriguez, R.A. Ribeiro, F.S. Faria, R.O.A. Ozório, M. Tavares-Dias Lethal dose and clinical signs of *Aeromonas hydrophila* in Arapaima gigas (Arapaimidae), the giant fish from Amazon Vet. Microbiol., 2016; 188: 12-15.
3. J.A. Plumb, L.A. Hanson. John Wiley & Sons; 2011. Health Maintenance and Principal Microbial Diseases of Cultured Fishes.
4. D. Stratev, S. Stoev, I. Vashin, H. Daskalov Some varieties of pathological changes in eximentalper infection of carps (*Cyprinus carpio*) with *Aeromonas hydrophila* J. Aquacult. Eng. Fish. Res., 2015; 1: 191-202.
5. H.T. Dong, C. Techatanakitarnan, P. Jindakittikul, A. Thaiprayoon, S. Taengphu, W. Charoensapsri, P. Khunrae, T. Rattanarojpong, S. Senapin *Aeromonas jandaei* and *Aeromonas veronii* caused disease and mortality in Nile tilapia, Oreochromis niloticus (L.).J. Fish Dis., 2017.
6. Sahoo, P. K., Das Mahapatra, K., Saha, J. N., Barat, A., Sahoo, M., Mohanty, B. R. Family association between immune parameters and resistance to Aeromonas hydrophila infection in the Indian major carp, Labeo rohita. Fish Shellfish Immunol, 2008; 25: 163-169.
7. Reyes, B. M., Salinas, I., Cuesta, A., Meseguer, J., Tovar, R. D., Ascencio, V. F. Oral delivery of live yeast Debaryomyces hansenii modulates the main innate immune parameters and the expression of immune-relevant genes in the gilthead seabream (Sparus aurataL.). Fish. Shellfish. Immunol, 2008; 25: 433-438.
8. Rodríguez, I., Novoa, B., Figueras, A. Immune response of zebrafish (Danio rerio) against a newly isolated bacterial pathogen Aeromonas hydrophila. Fish. Shellfish. Immunol, 2008; 25: 239-249.
9. Raida, M. K. and Buchmann, K. Development of adaptive immunity in rainbow trout, Oncorhynchus mykiss (Walbaum) surviving an infection with Yersinia ruckeri. Fish. Shellfish. Immunol, 2008; 25: 533-541.
10. Raida, M. K. and Buchmann, K. Innate immune response in rainbow trout(Oncorhynchus mykiss) against primary and secondary infections with Yersinia ruckeriO1. Dev. Comp. Immunol, 2009; 33: 35-45.
11. Mohanty, B. R. and Sahoo, P. K. Immune responses and expression profiles of some immune-related genes in Indian major carp, Labeo rohita To Edwardsiella tarda infection. Fish. Shellfish. Immunol, 2010; 28: 613-621.
12. Das, B.K. and Mukherjee, S.C. Toxicity of cypermethrin in *Labeo rohita* fingerlings: biochemical, enzymatic and haematological consequences. Comp. Biochem. Physiol. Toxicol. Pharmacol, 2003; 134(1): 109-121.
13. Lowry, O.H., Rosebrough, N.J., Farr, A.L. and Randall, R.J. Protein measurement with the folin phenol reagent. J. Biol. Chem., 1951; **193**: 265-275.
14. Begum, G. Carbofuran insecticide induced biochemical alterations in liver and muscle tissues of the fish *Clarias batrachus* (Linn.) and recovery response. Aquatic Toxicol., 2004; 66(1): 83-92.
15. Miyamoto, J. Degradation metabolism and toxicity of synthetic pyrethroid. Environ. Health Perspect, 1976; 14: 15-28.
16. Murty, A.S. and Devi, A.P. The Effect of Endosulfan and its Isomers on Tissue Protein, Glycogen and Lipids in the fish *Channa punctata*. Pesti. Biochem. Physiol, 1982; 17: 280-286.
17. Das, S. and Bhattacharya, T. Impact of Water Pollution on Fish Physiology – A Study. J. Aquaculture, 2006; 14: 1-16.
18. Chein, C.H. and Chein, E.J. Histopathological study of *Aeromonas hydrophila* in eel (*Anguilla japonica*), COA. Fish. Ser., 1994; 46: 13-24.
19. Mohanty, B.R., Mishra, J., Das, S., Jena, J.K. and Sahoo, P.K. An Outbreak of aeromoniasis in an organised composite carp culture farm in India: Experimental Pathogenicity and Antibiogram study. J. Aquaculture, 2008; 16: 27-37.
20. Welch, W.J. How cells respond to stress. Sci. Am., 1993; 268: 56-64.
21. Boone, A.N., and Vijayan, M.M. Constitutive heat shock protein 70 (HSC 70) expression in rainbow trout hepataytes: effect of heat shock and heavy metal exposure. Comp. Biochem. Physiol. Toxicol. Pharmacol., 2002; 132(2): 223-233.
22. Tabche, M.L., Gomes, O.L., Galar, M.M. and Lopez, L.E. Stress proteins produced by contaminated sediments with nickel in a pond with rainbow trout *Oncorhynchus mykiss* (Pisces: Salmonide). Rev. Biol. Trop., 2002; 50(3-4): 1159-1168.
23. Ali, K.S., Dorgai, L., Gazdag, A., Abraham, M. and Hermesz, E. Identification and induction of hsp 70 ene by heat shock and cadmium exposure in carp. Acta. Biol. Hung, 2003; 54(3-4): 323-334.

Journal of Non-Crystalline Solids 520 (2019) 119428

Contents lists available at ScienceDirect

Journal of Non-Crystalline Solids

journal homepage: www.elsevier.com/locate/jnoncrysol

Effect of Cr_2O_3 on the structural, optical and dielectric studies of LiF-SrO-B_2O_3 glasses

A. Ramesh Babu[a], S. Yusub[b,*], P.M. Vinaya Teja[c], P. Srinivasa Rao[d], V. Aruna[a], D. Krishna Rao[e]

[a] Department of Physics, Bapatla Engineering College, Bapatla 522102, AP, India
[b] Freshman Engineering Department, Lakireddy Bali Reddy College of Engineering (Autonomous), Mylavaram 521230, AP, India
[c] Department of Physics, A.C. College, Guntur 522001, AP, India
[d] Department of Physics, S.V.R.M. College, Nagaram 522268, AP, India
[e] Department of Physics, Acharya Nagarjuna university, Nagarjuna nagar, 522510, AP, India

ARTICLE INFO

Keywords:
FTIR
ESR
Optical band gap
Dielectric response
Ionic conductivity

ABSTRACT

The melt quench technique was involved in synthesizing the glass system LiF-SrO-B_2O_3 alloyed with Cr_2O_3 in the range of 0 to 0.25 mol%. The aperoidic nature of these glasses was affirmed by the X-ray diffraction (XRD). These glasses were analyzed by contemplating the dielectric characteristics (a.c. conductivity, σ_{ac}, dielectric constant, ε', and dielectric loss, tanδ etc.,), spectroscopic properties such as electron spin resonance (ESR) optical absorption and Fourier transform infrared (FTIR) analysis. The optical absorption spectra evinced two bands which are features of Cr^{3+} ions in the octahedral domain. Using absorption edges, Urbach energies and optical band gap of these samples were estimated. The hike in the Cr^{3+} ions in the glass C5 (0.05 mol% of Cr_2O_3) is confirmed by the proliferation in the ESR signal intensity and optical absorption peak. The maximum a.c. conductivity of glass C5 was due to the dominant presence of Cr^{3+} ions. FTIR bands revealed that at 0.05 mol% of Cr_2O_3, BO_4 units were converted into BO_3 units. It is perceived that the semiconducting nature of glass C5 was the highest among all the prepared glasses.

1. Introduction

B_2O_3 is an excellent glass former which can be incorporated in different types of glasses as a flux substance in order to achieve the materials with distinct remarkable chemical and physical characteristics useful for high technological and scientific applications [1,2]. Borate glasses are excellent vitreous components as they find prospective applications in the domain of modern science and technology. Boron forms BO_3 and BO_4 structural units by changing the coordination with oxygen [3–5]. Alkali and alkaline earth ions influence the chemistry of boron. When alkali fluorides are integrated with B_2O_3 then the glasses are expected to become more moisture resistant. The fluorine's of LiF burst the local symmetry of the glass. The Li^+ ions populate the interstitial positions of the glass and develop coordinate imperfections known as dangling bonds [6,7]. The lithium fluoroborate glasses are suitable for radiation dosimetry applications. These LiF-B_2O_3 glasses are assessed as the best materials as solar energy converters, laser host materials, phosphors and in a number of other electronic components [8,9]. Desirable changes can be done by incorporating the alkaline earth oxides in a borate glass system. The element "strontium" is a good modifier. The robustness of glasses can be enhanced substantially, by mixing them with SrO in suitable proportion. SrO is an excellent modifier and it penetrates the glass by disintegrating the random matrix [10,11]. The oxygens of such oxide fracture the internal regularity whereas the Sr^{2+} ions settle in the interstitial sites of the glass matrix. Sr^{2+} ions launch the bonding imperfections by cracking the borate bonds (B-O-B) which produces empty gaps and easy tracks for the other doped ions. Glasses combined with SrO expands the reticulation and rigidity of the network due to strong field strength values of Sr^{2+} ions. The glasses become more moisture resistant when SrO is added to them. Glasses containing SrO and their corresponding glass-ceramics can be used as gamma-ray shielding tools. The role of strontium is vital in the domain of bone restoration. It can enhance the metabolism of the bone [12–15].

The glasses amalgamated with transition metal ions have drawn much attention as they are widely used as magnetic materials, cathode materials in the batteries, memory and photo conducting devices [16–20]. Borate glasses are wonderful host materials for incorporation of chromium ions. Chromium is a transition metal ion which exhibits paramagnetic nature. When it deliquesces in the glasses then it makes

* Corresponding author.
E-mail address: syedyusuf1985@gmail.com (S. Yusub).

https://doi.org/10.1016/j.jnoncrysol.2019.05.004
Received 16 February 2019; Received in revised form 3 May 2019; Accepted 4 May 2019

Table 1
Physical characteristics of LiF-SrO-B_2O_3: Cr_2O_3 glasses.

Glass	Conc. Cr_2O_3 (mol%) x	Density ρ (g/cm^3) (± 0.0001)	Molar volume V_m (cm^3) (± 0.001)	Conc. of cromium ions N_i (x10^{21} ions/cm^3) (± 0.001)	Inter ionic distance of cromium ions R_i (Å) (± 0.001)	Polaron radius R_p (Å) (± 0.001)
C0	0	2.5400	23.589	–	–	–
C5	0.05	2.6456	22.668	1.328	9.097	3.665
C10	0.10	2.5429	23.603	2.552	7.318	2.949
C15	0.15	2.5483	23.563	3.833	6.390	2.575
C20	0.20	2.5617	23.460	5.135	5.796	2.336
C25	0.25	2.5628	23.467	6.417	5.381	2.168

them colored. These ions have a powerful hold on the spectroscopic properties and semiconducting nature of the samples. Chromium ions subsist in various valence positions in the samples. Among the different valence states of chromium ions, Cr^{3+} ions act like modifiers. These ions are in the form of CrO_6 structural frames in the glass whereas Cr^{5+} and Cr^{6+} ions infiltrate the glass system like network formers with CrO_4^{3-} and CrO_4^{2-} frames. The Cr^{3+} ion is a most stable ion. It is widely used as a luminescent material and luminescence sensitizer in different glasses [21]. The glasses integrated with chromium ions can be used as high pressure-calibrants, high-temperature sensors and solid-state lasers [22–24].

The objective of this article is to have a comprehensive understanding over the topology and valence states of chromium ions in LiF-SrO-B_2O_3 glass system, by a systematic study on dielectric properties coupled with spectroscopic investigations (optical absorption, ESR and IR spectra). These glasses are used as materials for optical components such as tunable solid state lasers, optical materials, optical filters, IR domes, memories, modulators, luminescence materials, phosphors, solar energy converters, fiber optic communication devices, radiation dosimetry, cathode materials in batteries and in a number of electronic gadgets. Glasses combined with mixed valence chromium ions are used as cathode materials in rechargeable batteries because of their high energy density and lofty capacitance [1–7].

In the present investigation, the concentration of Cr_2O_3 is varied with respect to B_2O_3, to analyze the action of chromium ions on the semiconducting nature of the glasses. A systematic study has been carried out on the dielectric properties of the glasses in a frequency scale 10^3–10^6 Hz and in the temperature scale 30-300 °C by estimating the values of dielectric breakdown strength in air, ε', tanδ and σ_{ac}. Different valence levels of chromium ions in the glasses were investigated by analyzing the Optical absorption, ESR spectra and FTIR.

2. Material and methods

The Glass system 30LiF-10SrO-(60-x) B_2O_3: xCr_2O_3 (varying x from 0 to 0.25 mol%) was selected for the present analysis. The samples are tagged as given below:

C0: 30LiF-10SrO-60 B_2O_3.
C5: 30LiF-10SrO-59.95 B_2O_3: 0.05 Cr_2O_3.
C10: 30LiF-10SrO-59.90 B_2O_3: 0.10 Cr_2O_3.
C15: 30LiF-10SrO-59.85 B_2O_3: 0.15 Cr_2O_3.
C20: 30LiF-10SrO-59.80 B_2O_3: 0.20 Cr_2O_3.
C25: 30LiF-10SrO-59.75 B_2O_3: 0.25 Cr_2O_3.

The basic chemicals viz., LiF, $SrCO_3$, H_3BO_3 and Cr_2O_3 were used in synthesizing the glasses. The materials were of Analar (AR) grade standard. These basic materials were weighed in an electrical balance to a reliability of 0.0001 g. The chemicals were assorted minutely in an agate mortar. This mixture was heated in a porcelain crucible at around 980 °C for 15 min so that deliquesce was free from the bubbles. The flux was then shifted on a brass slab placed at an ambient temperature. This flux was eventually annealed at 350 °C for 3 h. The XRD spectra of these samples were obtained by operating the XRD model, SO-DEBYE FLUX 202. Densities of these samples were determined to the correctness of ± 0.0001. O-xylene was used as a buoyant liquid. Employing the KBr pellet technique, FTIR spectra of the specimen were noted in a wave number scale 400–1600 cm^{-1} with JASCO FTIR 6200 Spectrometer. The glasses were cut, ground, polished and the thickness was reduced to 1 mm for recording optical absorption spectra. These spectra of the samples were obtained in the wavelength gauge 200–1000 nm. A UV-VIS-NIR double beam spectrophotometer JASCO-670 V with a resolution of 0.1 nm was used for the purpose. For recording the ESR spectra of the glasses, 100 mg moisture less powder of the samples were filled in a quartz tube. The spectra were procured using ESR spectrometer JEOL-FE-IX. This device functions at a frequency of 9.4 GHz. The field modulation frequency of the instrument was 100 kHz and the magnetic field was varied from 0 to 500 G with a micro power of 10 mW. For dielectric studies, the samples were painted with a thin layer of silver to work like electrodes. LF-impedance analyzer was employed for studying the dielectric properties. Hewlett-Packard model 4192A was used in measuring the dielectric parameters like ε' and tan δ. These values were recorded in a frequency guage of 10^3–10^6 Hz and the temperature was varied from 30 to 300 °C. The exactness in measuring the tanδ and ε' values was ~0.001 and ~0.01. A breakdown tester was used for estimating the dielectric breakdown strength of the samples. ITL BDV-7 model working at a voltage of 230 V ± 10%, at a frequency of 50 Hz was operated for the purpose.

3. Results

3.1. Characterization and physical parameters

The evaluated physical parameters of the glasses were listed in Table 1. The initial sample C0 was colorless. The color of the samples was changed gradually from light green to dark green (for the glasses from C5-C25). Fig. 1 displays the XRD pattern of C0, C10 and C25

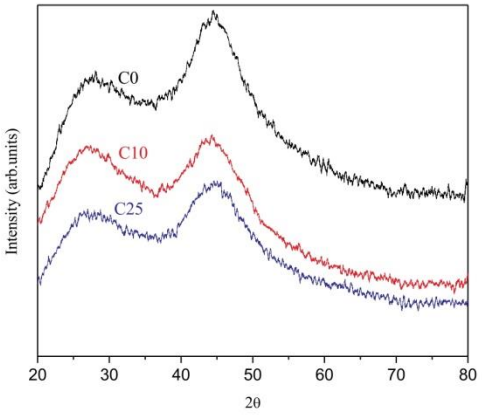

Fig. 1. XRD spectra of the 30LiF-10SrO-(60-x)B_2O_3: xCr_2O_3 system for x = 0, 0.1, 0.25 mol%.

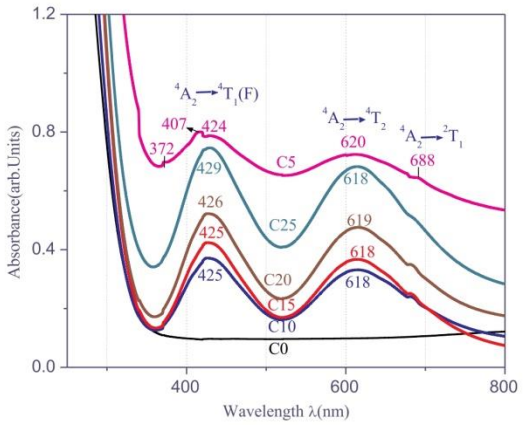

Fig. 2. Optical absorption spectra of LiF-SrO-B_2O_3 glass system alloyed with Cr_2O_3.

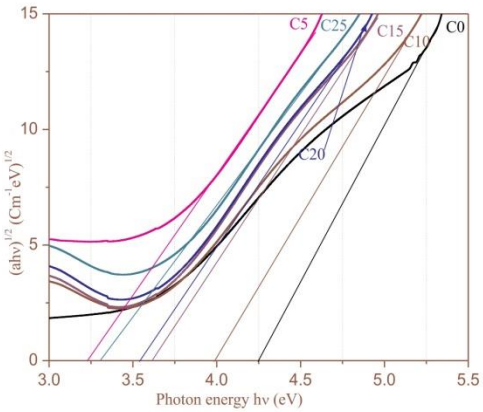

Fig. 3. Tauc plots of LiF-SrO-B_2O_3: Cr_2O_3 glasses.

glasses. Sharp Bragg peaks are absent in the XRD patterns of the glasses, confirming the amorphous character of the specimen. The parameters like density (ρ), molar volume (V_m), inter ionic distance of Chromium ions (R_i), polaran radius (R_p) are helpful to elucidate the magnitude of structural entities and transport properties as a variable of modifier oxide. The density of glass C0 is noticed to be 2.540 g/cm^3 and is escalated to 2.562 g/cm^3 (C25) with a gradual increase of Cr_2O_3. Interestingly the density (2.645 g/cm^3) of C5 glass sample is higher than that of 0.1 mol% of Cr_2O_3 doped C10 glass sample.

3.2. Optical absorption

Fig. 2 exhibits the optical absorption spectra of as prepared samples in the wavelength scale ranging from 250 to 800 nm. Glass C0 (Cr_2O_3 free) has not shown any absorption peak, but with 0.05 mol% doping of Cr_2O_3 two broad absorption bands centered at 424, 620 nm are observed along with two feeble bands around 372 and 688 nm. In addition a kink around 407 nm at shoulder of 424 nm peak also observed with further addition of Cr_2O_3 the baseline of absorption is decreased with red shift of 424 nm peak and blue shift of 620 nm, moreover the intensity of feeble band around 688 nm is increased at the expense of 372 nm as one goes through higher concentration.

The cutoff wavelength of the samples is determined from the optical absorption spectra and noted in Table 2. The cutoff wavelength of C0 detected at 210 nm red-shifted to 264.5 nm with a hike in the magnitude of Cr_2O_3. By extending the linear segment of the curves sketched between $(\alpha h\upsilon)^{1/2}$ versus photon energy ($h\upsilon$), to X-axis where $(\alpha h\upsilon)^{1/2} = 0$, the optical band gaps (E_g) of the glasses are estimated. These curves are demonstrated in Fig. 3. The magnitudes of E_g are recorded in Table 2. The optical band gap of C0 is perceived to be the highest 4.25 eV for the glass C0 and is systematically decreased to 3.299 eV with a raise in the content of dopant from 0.1 to 0.25 mol%. The least value of E_g, 3.217 eV is observed for the glass C5.

The Urbach law connects $\alpha(\upsilon)$ and Urbach energy (ΔE) as given below [21].

$$\ln \alpha(\upsilon) = (h\upsilon/\Delta E) + \text{constant} \quad (1)$$

The width of the tail of localized states in the band gap (ΔE) are estimated by drawing the curves between ln (α) (α = absorption coefficient) and hυ (photon energy) as shown in Fig. 4. These curves are called Urbach curves. The reciprocal of the slopes in the linear part of the parts give the ΔE values of the glasses. The ΔE values of the glasses are recorded in Table 2. The least and the highest values of ΔE are 0.08 eV and 0.117 eV for the glasses C0 and C5 respectively. Inset of Fig. 4 exhibits the modification of E_g and ΔE as a function of Cr_2O_3.

3.3. Electron spin magnetic resonance

The basic glass C0 does not contribute any ESR signal. This result indicates that the glass C0 has no paramagnetic ions. Because of adding the chromium ions to the basic glass, it exhibits the resonance signal in the spectrum of the sample. This resonance signal is due to Cr^{3+} ions infiltrating the glass system as paramagnetic agents. Fig. 6 manifests the ESR spectra of LiF-SrO-B_2O_3 samples alloyed with disparate mol% of Cr_2O_3. A profound absorption signal centered at g = 1.976 is noticed in the spectra of all the glasses. Two absorption lines are observed at g = 4.26 and 5.21 with a raise in the quantity of dopant. No change in the value of g is noticed with a hike in the content of Cr_2O_3 but an upswing in the strength of the signal is noticed with a hike in the content of Cr_2O_3 for the glasses from C10 to C25. The intensity of the signal is maximum for C5 glass. A resonance signal at g = 2.43 on the immediate lower magnetic field side of g = 1.976 is also observed.

Table 2
Dossier of optical absorption spectra of LiF-SrO-B_2O_3: Cr_2O_3 glasses.

Sample	λ_c (nm) (± 0.1)	$^4A_2 \rightarrow {}^4T_1(F)$ band positions of Cr^{3+} ions (nm) (± 0.1)	$^4A_2 \rightarrow {}^4T_2$ band positions of Cr^{3+} ions (nm) (± 0.1)	E_g (eV) (± 0.001)	ΔE (eV) (± 0.001)
C0	210.0	–	–	4.250	0.0801
C5	264.5	417	620	3.217	0.1171
C10	232.5	425	618	3.976	0.0858
C15	245.0	425	618	3.604	0.0935
C20	247.0	426	619	3.537	0.0966
C25	250.5	429	618	3.299	0.1024

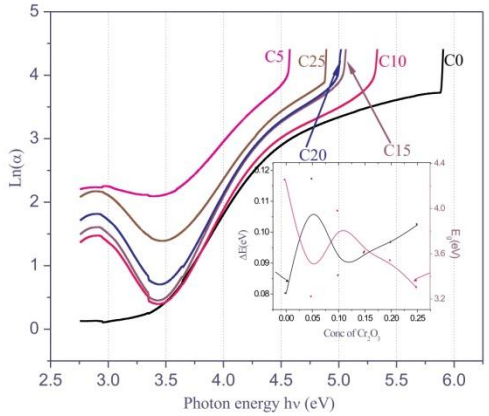

Fig. 4. Plots of ln (α) versus photon energy (hν) of LiF-SrO-B_2O_3 network integrated with Cr_2O_3. Inset displays the variation of optical band gap (E_g) and Urbach energy (ΔE) as a function of dopant concentration.

3.4. FTIR

Fig. 5 exhibits the FTIR spectra of the glasses. The assignments of the corresponding bands are listed in Table 3. Three important standard and wide bands are noticed in the spectra of glasses. These bands are anticipated to be formed due to the borate groups. A band at about 1383 cm^{-1} is expected to be created as a result of BO_3 units; the bands at around 1018 and 900 cm^{-1} are envisaged due to BO_4 groups. A band at 690 cm^{-1} is noticed on account of B-O-B bending vibrations. These three wide bands are formed as a result of entanglement of the discrete bands with one another. In the spectrum of pure glass C0, a weak band is noticed at 754 cm^{-1}. A fresh feeble band is found at 532 cm^{-1} when Cr_2O_3 is added to the basic glass. Intensity of this signal is detected to rise with a hike in the magnitude of Cr_2O_3. The bands at 1018 and 900 cm^{-1} are combined together to produce a fresh band at 980 cm^{-1} when the pure specimen C0 is alloyed with Cr_2O_3 initially. When the quantity of dopant is enhanced, the intensity of the signal at around 980, 690 cm^{-1} is spotted to diminish, whereas the intensity of the signal at 1383 cm^{-1} is found to rise.

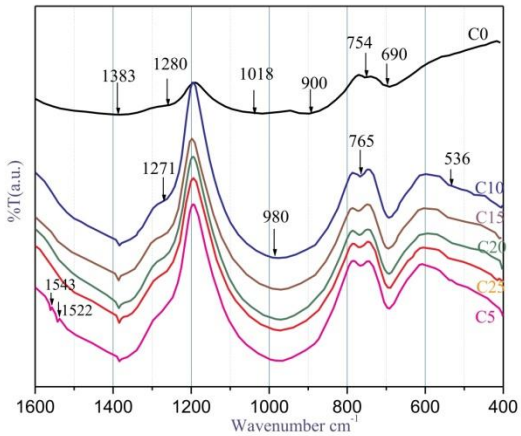

Fig. 5. FTIR spectra of LiF-SrO-B_2O_3: Cr_2O_3 glasses.

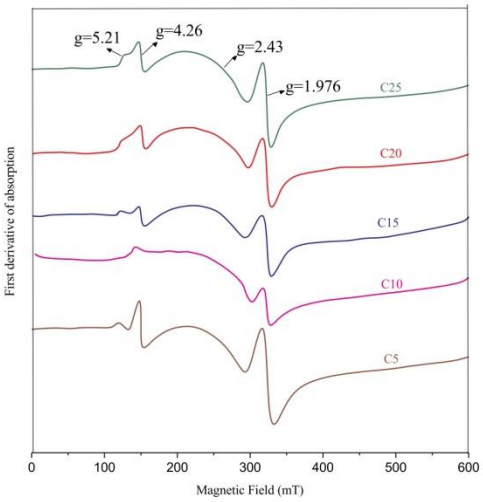

Fig. 6. ESR spectra of LiF-SrO-B_2O_3 glasses combined with Cr_2O_3.

3.5. Dielectric properties

The measured values of dielectric constant ε' and dielectric loss tanδ at an ambient temperature for the glass C0 (30LiF-10SrO-60B_2O_3) at 500 KHz are 4.19 and 0.008 specifically. The magnitudes of these variables are observed to rise with a fall in frequency for all the glasses. The value of ε' is noticed to escalate at room temperature with a hike in the content of Cr_2O_3 from 0.1 to 0.25 mol% (glass C10-C25) at any frequency. It is observed that ε' is maximum for the glass C5 (0.05 mol% of Cr_2O_3). Same tendency is perceived for tanδ at ambient temperature at any frequency. The values of tanδ also varied in a similar way with dopant concentration as that of ε'. The modification in the magnitudes of ε' and tanδ with the content of Cr_2O_3 at a frequency of 500 Hz is disclosed in Fig. 7. The response of ε' as a function of temperature for distinct magnitudes of Cr_2O_3 at 1 kHz is manifested in Fig. 8. Inset exhibits the response of ε' as a function of temperature for the glass C20 (0.2 mol% of Cr_2O_3). The value of ε' showed a significant growth at higher temperatures, predominantly at lower frequencies. The ε' and tanδ values are escalated with a proliferation in the impurity content from 0.1 to 0.25 mol% of Cr_2O_3 (C10-C25). These values are found to be maximum for the glass C5. Fig. 9 manifests the variation of tanδ for different contents of Cr_2O_3 computed at 10 kHz. This figure reveals the fact that the values of tanδ decreases with a hike in the frequency. Inset of Fig. 9 indicates the alteration of tanδ as a function of temperature for the specimen C5. The plots of pure and doped samples evidenced different maxima. With raising frequency the distinct maxima relocated towards higher temperature. When the temperature is increased the frequency maximum moves towards higher frequency. This phenomenon indicates the dielectric relaxation nature of tanδ of all the samples. The inspections on the fluctuation of tanδ against temperature for various concentrations of Cr_2O_3 demonstrate a continuous hike in broadness and $(tan\delta)_{max}$ of the relaxation curves with raise in the concentration from 0.1 to 0.25 mol% of Cr_2O_3 (glass C10-C25). Especially glass C5 has maximum value with a transfer of relaxation zone towards lower temperature. The analysis on the relaxation of effects of LiF-SrO-B_2O_3: Cr_2O_3 glass is listed in Table 4 along with activation energy for dipoles and breakdown strength. The activation energy (AE) W_d, for the dipoles is estimated employing the relation [21].

$$f = f_0 \exp.(-W_d/KT) \quad (2)$$

Table 3
Allotment of absorption bands in the FTIR spectra of LiF-SrO-B_2O_3: Cr_2O_3 Glasses.

C0	C5	C10	C15	C20	C25	Assignment
—	1522					Stretching vibrations of B—O^- in BO_2O^- units from different borate groups
	1543	—	—	—	—	
1383	1384	1384	1384	1384	1384	B-O $_{sym}$ stretching in BO_3 units from different kinds of borate groups
1280	1271	1265	1269	1267	1267	B-O $_{sym}$ stretching in BO_3 units from pyro and ortho borate family
1018						Stretching vibrations of B—O bonds in BO_4 units from tri, tetra, penta borate species
900	975	980	970	979	973	Stretching vibrations of B—O bonds in BO_3 units
754	765	765	768	765	763	O_4B-O-BO_3 bending vibrations
690	691	692	691	689	689	B-O-B bending vibrations
–	536	532	538	538	534	O-B-O bending vibrations

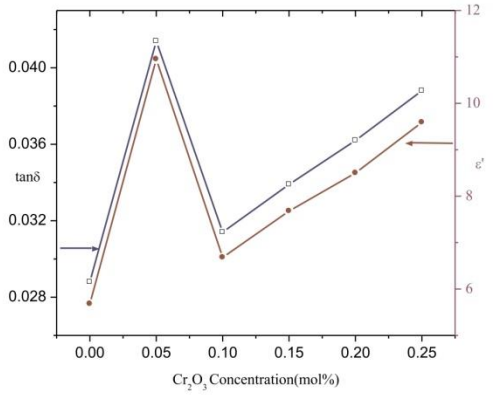

Fig. 7. Response of ε' and tan δ as a function of dopant concentration at 1 kHz for the LiF-SrO-B_2O_3 glasses.

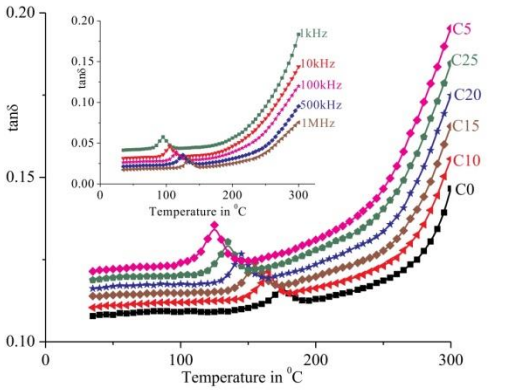

Fig. 9. Variation of tan δ with temperature at 10 kHz for different contents of Cr_2O_3 in LiF-SrO-B_2O_3 glasses. Inset displays the modification of tanδ with temperature at different frequencies of the glass C_5.

It is found that W_d is maximum for glass C0 and least for the glass C5. Table 4 contains the data related to dielectric loss.

The a.c. conductivity σ_{ac} of all the glasses at different temperatures is estimated using the relation [21]:

$$\sigma_{ac} = \omega\, \varepsilon' \varepsilon_0 \tan\delta \quad (3)$$

(Where ε_0 is the vacuum dielectric constant)

The curves of σ_{ac} versus 1/T at different frequencies for the sample C25 is shown in Fig. 10. From these curves, the activation energy for conduction (AEC) in the high temperature scale from the linear part of curves are estimated for all samples. These parameters are recorded in Table 5. The AEC value is the least for the glass C5 and noticed to escalate with further hike in the content of dopant. The response of σ_{ac} with 1/T for all the glasses alloyed with different contents of Cr_2O_3 at 10 kHz is presented in Fig. 11. This figure clearly indicates that σ_{ac} escalates with a hike in the content of Cr_2O_3 from 0.1 to 0.25 mol% (glass C10-C25). The value of σ_{ac} is the highest for glass C5. The linearity between activation energy and conductivity is displayed in the inset of Fig. 11.

The dielectric breakdown strength (DBS) is the highest 9.43 kV/cm for the glass C0 and noticed to diminish with a hike in the content of Cr_2O_3 from 0.1 to 0.25 mol% of Cr_2O_3 (glass C10-C25). The DBS is the minimum for glass C5. These parameters are mentioned in Table 4.

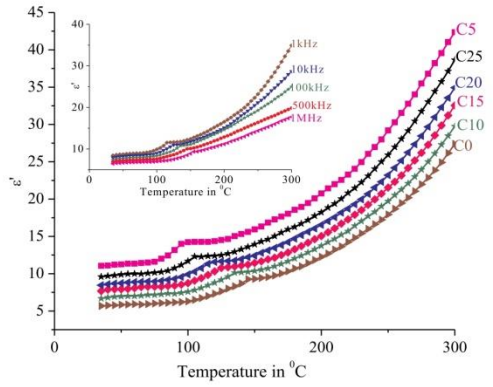

Fig. 8. Modification of ε' with temperature at 1 kHz for disparate concentrations of Cr_2O_3 in LiF-SrO-B_2O_3 glasses. Inset (a) exhibits the alteration of ε' with temperature for various frequencies of glass C20.

Table 4
Epitome of the report on dielectric loss of LiF-SrO-B_2O_3 glasses at 1 kHz.

Glass	$(Tan\delta)_{max}$ x (10^{-2})	Temp. region of relaxation (± 1) °C	AE for dipoles (± 0.001) eV	Breakdown strength (± 0.01) kV/cm
C0	0.361	146–164	3.722	9.43
C5	0.577	81–115	2.912	8.97
C10	0.394	119–140	3.552	9.36
C15	0.438	110–135	3.386	9.29
C20	0.483	99–128	3.224	9.18
C25	0.515	90–121	3.066	9.07

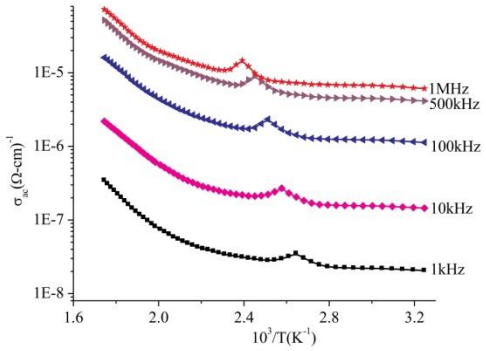

Fig. 10. Response of σ_{ac} with 1/T for the specimen C25 at different frequencies.

4. Discussion

4.1. Physical parameters

The densities of the glasses play a vital role in probing the structural changes. Density is a function of the magnitude of interstitial gaps, structural compactness/softening, crosslink density, change in geometrical configuration and coordination number of the glass [25]. The density of the glass is tremendously influenced by the atomic weight and ionic size of the impurities [25]. An increase in the density of glasses as a function of Cr_2O_3 is envisaged due to a substitution of lighter cation B^{3+} by massive one Cr^{3+} ions. The maximum density and minimum molar volume are due to its compact nature of glass C5 when compared to that of the glass C10. The reason for the increase in density of the glass C5 is as follows: When Cr_2O_3 is incorporated in the basic LiF-SrO-B_2O_3 glass with an initial doping of 0.05 mol%, and then the chromium ions settle in the interstices of borate glass system by generating the Sr-O-Cr and B-O-Cr linkages, in succession with transformation of BO_4 groups to BO_3 structural groups. The radii of B^{3+} ions (0.25 Å) in BO_4 structural units are greater than the radii of B^{3+} ions (0.15 Å) in BO_3 structural units [26]. The values of polaron radius (R_p) are small which indicate that the polarons are highly localized.

4.2. Optical absorption

No bands are perceived in the optical absorption spectra of pure glass C0. With an initial doping of 0.05 mol% of Cr_2O_3 in the basic glass C0, five absorption bands are noticed at 372 nm, 407 nm, 429 nm, 620 nm and 688 nm in the spectra. These bands are designated to the transitions $^4A_{2g} \rightarrow {}^2A_{1g}$, $^4A_2 \rightarrow {}^4T_1(F)$, $^4A_2 \rightarrow {}^4T_1(F)$ (peak 1), $^4A_2 \rightarrow {}^4T_2(F)$ (peak 2) and $^4A_2 \rightarrow {}^2E_g(G)$ respectively. Two prime bands perceived at 429 and 620 nm are due to the presence of Cr^{3+} ions in the glass in octahedral symmetry [27–30]. The intensity of these bands is recognized to raise with a change in the content of Cr_2O_3 from 0.1 to 0.25 mol% (C10-C25) but with the maximum intensity, with an increased baseline for the glass C5 (0.05 mol%). A feeble band is noticed at 372 nm due to Cr^{6+} ions. These Cr^{6+} ions infiltrate the glass as network formers in CrO_4^{2-} frames whereas Cr^{3+} ions invade the system as network modifiers [31]. When the quantity of Cr_2O_3 is enhanced above 0.05 mol% then the band at 372 nm expected to be merged with an intense band at 429 nm (peak 1). This situation is aroused because of the progressive change of Cr^{6+} ions into Cr^{3+} ions in the glasses. A tiny crimp witnessed at 688 nm owes to the spin and parity forbidden transitions. The intensity of this band escalates slowly and it merges with a dominant band at 620 nm when the dopant concentration in the glass is 0.25 mol% (glass C25).

Table 5
Synopsis of the data on a.c. conductivity of LiF-SrO-B_2O_3: Cr_2O_3 glasses at 1 kHz.

Glass	σ_{ac} at 70 °C (10^{-8}) $(\Omega\text{-cm})^{-1}$	$N(E_F)$ $(10^{20}\ eV^{-1}/cm^3)$			Activation energy for conduction (eV)
		Austin	Butcher	Pollak	
C0	0.951	2.088	0.871	2.123	1.153
C5	2.752	3.552	1.482	3.612	0.741
C10	1.249	2.393	0.999	2.433	1.038
C15	1.574	2.687	1.121	2.731	0.944
C20	1.848	2.911	1.215	2.960	0.865
C25	2.220	3.191	1.331	3.244	0.799

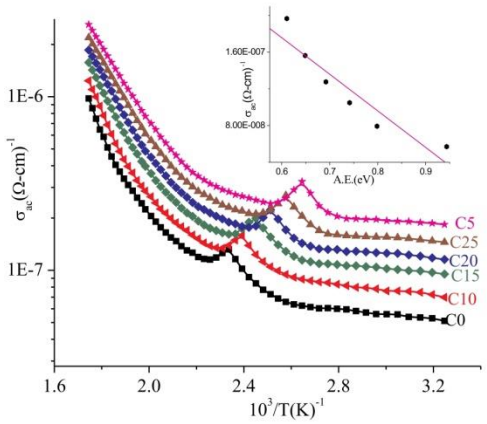

Fig. 11. Modification of σ_{ac} with 1/T at 10 kHz for different concentrations of Cr_2O_3 in LiF-SrO-B_2O_3 glasses. Inset gives the variation of σ_{ac} with activation energy at 70 °C of LiF-SrO-B_2O_3 glasses at 10 kHz.

The hike in intensity of absorption bands at $^4T_1$ and $^4T_2$ in the spectra of samples C10 to C25 is due to the gain in content of Cr^{3+} ions at the cost of Cr^{6+} ions. This growth in magnitude of Cr^{3+} ions in the specimen causes an augment in the assembly of non-bridging oxygens (NBO) [28]. The existence of these donor centres leads to the decrease in the E_g of the samples. Due to this reason, the absorption edge of the glasses shifted towards the longer wavelength side. Especially, in the glass C5 the bridging oxygens create bonds with Cr^{3+} ions resulting in the collapse of the glass system. This leads to a reduction in energy band gap of the glass [29].

The maximum Urbach energy for the glass C5 (0.1171 eV) specify the broad spread of the tails among the samples. The escalating ΔE values with a hike in the content of Cr_2O_3 in the glasses from C10 to C25 is envisaged owing to the creation of imperfections like dangling bonds and fluctuations in bond angle distortions [32,33]. The other component which enhances the edge widening is a static disorder which raises the density of localized states $N(E_F)$ of these defects [26].

4.3. Electron spin magnetic resonance

Two resonance signals are detected in ESR spectra of the specimens at g = 4.26 and g = 1.976. As per Laundry, the lower field spectral line at g = 4.26 is ascribed to the isolated Cr^{3+} ions and that of the high field spectral line is associated with the exchange coupled Cr^{3+} ion pairs [34]. The intensity of these resonance signal increases in the glasses C10 to C25 but with a maximum intensity for the glass C5. The maximum intensity of the signal at g = 4.26 indicates the maximum content of isolated Cr^{3+} ions engrossing the distorted octahedral position in all the samples. The signal observed at g = 1.976 is expected due to the exchange coupled Cr^{3+}–Cr^{3+} pairs [35]. The line width and

intensity of these signals are noticed to rise with a hike in the content of dopant. This result confirms the hike in the magnitude of Cr^{3+} ions which behave like glass modifiers and increases the agglomeration of NBOs in the specimen. These NBOs acts as donor centers and minimize the E_g of the glasses. A resonance signal at g = 2.43 is noticed owing to the large gap between two Kramer's doublets. A shoulder at g = 5.21 is also noticed in the spectra of all the glasses.

4.4. FTIR

FTIR spectra disclose the structural modifications of the glasses. When LiF is added to borate glass, it converts the BO_3 groups into BO_4 units. These BO_4 groups are more stable, and they form a long link of tetrahedral groups. When SrO is incorporated in the glass, the BO_4 groups are transformed into BO_3 groups by generating SrO polyhedron when it is circumjacent by BO_4 units. This pattern acts like an imperfection in the specimen [7,8,10]. When LiF-SrO-B_2O_3 glass is alloyed with Cr_2O_3, it will crush or deform the interlinked BO_4 units and increases disorder of the system. When the content of Cr_2O_3 is increased the intensity of the vibration bands BO_3 and the oscillations of B-O-B units also increase [21]. The progressive hike in the content of Cr_2O_3 from 0.1 to 0.25 mol% (C10-C25) raises the intensity of the vibration band at around 1383 cm^{-1} at the cost of vibration band at 980 cm^{-1}. This result is anticipated owing to the transformation of BO_4 groups into BO_3 groups. Interestingly a maximum intensity of the BO_3 band is noticed when the glass is doped with 0.05 mol% of Cr_2O_3 (glass C5). It is observed that the vibration band at 766 cm^{-1} corresponding to the O_4B-O-BO_3 structural units to vanish gradually and the decay in the intensity and blue shift of the B-O-B bending oscillations at 690 cm^{-1}. These changes are due to the production of a new type of linkages such as B-O-Cr by cracking B-O-B links and a plunge in the content of B_2O_3 in the glasses. An extra band at around 536 cm^{-1} is perceived due to the O-B-O bending units [21].

When Cr_2O_3 is mixed to the LiF-SrO-B_2O_3 glass network, it resulted in a cross-linking of asymmetrical BO_3 units. This hike in the intensity of such a vibration band at lower content of Cr_2O_3 (for the glass C5) indicates the increase of CrO_6 octahedral groups [21]. This leads to the hike in the Urbach energy, decay in the optical band gap and a hike in the ESR signal intensity in the glass C5.

4.5. Dielectric properties

The dielectric constant of a sample depends on the space charge, dipolar, ionic and electronic polarizations. Space charge polarization is a key factor in constructing the dielectric constant of a material [35]. It's a function of quality and perfectness of the material. A maximum hike in the magnitudes of σ_{ac}, tanδ and ε' is detected due to the addition of Cr_2O_3 with a concentration of 0.05 mol% to the initial glass LiF-SrO-B_2O_3. At a particular frequency, these values are noticed to increase with a raise in temperature of the specimen. This result is expected due to gain in the quantity of Cr^{3+} ions at the cost of Cr^{6+} ions with a hike in the content of Cr_2O_3 in the glasses from C10 to C25 but with a maximum raise of these Cr^{3+} ions in the sample C5. These Cr^{3+} ions along with Sr^{2+} ions act like modifiers and generate the imperfections by cracking Sr-O-Cr, B-O-Cr, B-O-Sr and B-O-B bonds [8]. These deficiencies produce easy tracks for the relocation of charge carriers. These factors construct a space charge polarization and enhance the dielectric variables [8]. The magnitudes of AEC and DBS are the least for the glass C5.

The dielectric relaxation effects are attributed to the strontium (Sr^{2+}) ions. These Sr^{2+} ions in combination with cationic vacancies establish the dipoles and demonstrate the relaxation effects [8]. The value of $\tan\delta_{max}$ is the highest for the glass C5 whereas these values increase gradually for the glasses from C10 to C25. This increase in the $\tan\delta_{max}$ values discloses the raise in the liberty for dipoles to rotate and align in the direction of the field. The transfer of relaxation region towards lower temperatures and decline in activation energy for dipoles for the glass C5 indicates reduction in the strength of glass.

The defect model given by Ingram is used to illustrate the conduction process in the maximum temperature zone [21]. When a curve is plotted between logσ(ω) versus AEC a linearity is detected. This linearity indicates the augmentation of conductivity suggesting the escalation in the ability of charge carriers to move in the high-temperature zone. The Sr^{2+} ions are massive and immobile so the lighter and mobile Li^+ ions are accountable for the conductivity in the glasses at this temperature region [8]. The increase in the conductivity of the glasses is noticed when the content of Cr_2O_3 is escalated from 0.1 to 0.25 mol %, but the conductivity is observed to be the highest at a concentration of 0.05 mol% for the glass C5. It is expected owing to improved modifying action of Cr^{3+} ions in the sample C5.

There are different strategies of conduction in the glassy substances namely conduction in localized states near the Fermi level, conduction in localized states near the band edge, band conduction and conduction in extended states. Conduction in the localized states at the Fermi level arises when σ_{ac} is independent of temperature and changes proportionately with frequency up to a temperature of 343 K. This fact could be described by quantum mechanical tunneling model (QMT) [21]. The conduction in these samples in the low-temperature zone (343 K) may be ascribed to occur by this process. The density of defect energy states near Fermi level $N(E_F)$, is estimated by the relation (4) [21,25].

$$\sigma(\omega) = \eta e^2 KT[N(E_F)]^2 \alpha^{-5} \omega [\ln(\upsilon_{ph}/\omega)]^4, \quad (4)$$

where $\eta = \pi/3$ (Austin and Mott) [25] = 3.66 $\pi^2/6$ (Butcher and Hyden) [25] = $\pi^4/96$ (Pollak) [25]. The symbols in this equation have normal meanings. The estimated values of $N(E_F)$ are listed in Table 5. The highest value of $N(E_F)$ indicates a maximum disorder in the glass C5. The breakdown strength of a glass is a function of rate of growth of ε'tanδ with temperature. It is observed to be maximum for a glass C5. The heat energy emancipated at the time of breakdown by giving a voltage across the glass increases ε'tanδ value. The DBS is inversely proportional to ε'tanδ [25]. The magnitude of ε'tanδ is maximum for the glass C5 so the DBS is the least for the specimen C5. This result supports a weak internal structure of the sample C5.

5. Conclusions

Glasses are fabricated with the composition 30LiF-10SrO-(60-x) B_2O_3: xCr_2O_3 (x taking the values from 0 to 0.25 mol%) by the melt quench and heat treatment process. The XRD spectra manifested the amorphous character of the samples. The intensity of optical absorption bands at 429 and 630 nm is increased gradually due to the hike of Cr^{3+} ions in the glasses from C10 to C25. These ions occupy the octahedral sites in the samples. The intensities of these bands are perceived to be the highest for the glass C5 with a maximum baseline. The optical band gap of the samples decreases from C10 to C25 with a hike in the quantity of Cr_2O_3. The value of E_g is the least for the glass C5. The Urbach energy values are observed to increase in the glasses from C10 to C25, with the highest value for the glass C5. These results are expected due to a raise in the density of localized states and the gain in the concentration of Cr^{3+} ions. ESR spectral studies of the glasses showed the existence of Cr^{3+} ions in the octahedral sites. The content of such ions is maximum for the glass C5. FTIR analysis exhibited the conventional bands due to the borate groups. The dielectric studies authenticate the best semiconducting nature of the glass C5.

References

[1] M.A. Hassan, F. Ahmad, Z.M. Abd El-Fattah, Novel identification of ultraviolet/visible Cr^{6+}/Cr^{3+} optical transitions in borate glasses, J. Alloys Compd. 750 (2018) 320–327, https://doi.org/10.1016/j.jallcom.2018.03.351.
[2] F. Ahmad, Study the effect of alkali/alkaline earth addition on the environment of borochromate glasses by means of spectroscopic analysis, J. Alloys Compd. 586 (2014) 605–610, https://doi.org/10.1016/j.jallcom.2013.10.105.

[3] N. Saad, M. Haouari, A. Bulou, A. Hadi Kassiba, H. Ben Ouada, Structural and optical properties of Cr^{3+} embedded in a P_2O_5-B_2O_3-ZnO-BaF_2-AlF_3 fluorobor-ophosphate glasses, Mat. Chem. Phys. 212 (2018) 461–470, https://doi.org/10.1016/j.matchemphys.2018.03.074.

[4] M.A. Hassan, Effect of halides addition on the ligand field of chromium in alkali borage glasses, J. Alloys Compds. 574 (2013) 391–397, https://doi.org/10.1016/j.jallcom.2013.05.177.

[5] Hongli Wen, Peter A. Tanner, Bing-Ming Cheng, Optical properties of $3d^N$ transition metal ion-doped lead borate glasses, Mater. Res. Bull. 83 (2016) 400–407, https://doi.org/10.1016/j.materresbull.2016.06.032.

[6] A.M. Abdelghany, H.A. ElBatal, R.M. Ramadan, The effect of Li_2O and LiF on structural properties of cobalt doped borate glasses, J. King Saud Uni-Sci. 29 (2017) 510–516, https://doi.org/10.1016/j.jksus.2016.09.003.

[7] Katha Narasimha Rao, M. Sharada, M. Anand Pandarinath, J. Shanker, D. Suresh Babu, FTIR and raman studies of LiF doped MgO-Bi_2O_3-B_2O_3 glass system, Mat. Today Proc. vol. 3, (2016) 3779–3783, https://doi.org/10.1016/j.matpr.2016.11.027.

[8] A. Ramesh Babu, Ch. RajyaSree, P.M. Vinaya Teja, S. Yusub, D. Krishna Rao, Influence of manganese ions on spectroscopic and dielectric properties of LiF-SrO-B_2O_3 glasses, J. Non-Cryst. Solids 358 (2012) 1391–1398, https://doi.org/10.1016/j.jnoncrysol.2012.03.012.

[9] C. Parthasaradhi Reddy, V. Naresh, K.T. Ramakrishna Reddy, Li_2O-LiF-ZnF_2-B_2O_3-P_2O_5: MnO glasses-thermal structural, optical and luminescence characteristics, Opt. Mat. 51 (2016) 154–161, https://doi.org/10.1016/j.optmat.2015.11.035.

[10] A.M. Abdelghany, M.A. Ouis, M.A. Azooz, H.A. ElBatal, G.T. El-Bassyouni, Role of SrO on the bioactivity behavior of some ternary borate glasses and their glass ceramic derivatives, Spe. Chim. Acta Part A: Mol. Bio. Spec. 152 (2016) 126–133, https://doi.org/10.1016/j.saa.2015.07.072.

[11] Hirokazu Masai, Go Okada, Toshiaki Ina, Noriaki Kawaguchi, Takayuki Yanagida, Temperature-dependent luminescence of Ce-doped SrO-B_2O_3 glasses, J. Lum. 207 (2019) 316–320, https://doi.org/10.1016/j.jlumin.2018.11.014.

[12] M.A. Marzouk, F.H. ElBatal, W.H. Eisa, N.A. Ghoneim, Comparative spectral and shielding studies of binary borate glasses with the heavy metal oxides SrO, CdO, BaO, PbO, or Bi_2O_3 before and after gamma irradiation, J. Non-Cryst. Solids 387 (2014) 155–160, https://doi.org/10.1016/j.jnoncrysol.2014.01.002.

[13] Mohamad Raheem Ahmed, B. Ashok, Shaik Kareem Ahmmad, Abdul Hameed, Md. Shareefuddin, Infrared and Raman spectroscopic studies of Mn^{2+} ions doped in strontium alumino borate glasses: describes the role of Al_2O_3, Spe. Chim. Acta Part A: Mol. Bio. Spec. 210 (2019) 308–314, https://doi.org/10.1016/j.saa.2018.11.053.

[14] Navdeep Kaur, Gurbinder Kaur, Devender Kumar, K. Singh, Mechanical and thermal properties of SrO/BaO modified Y_2O_3-Al_2O_3-B_2O_3-SiO_2 glasses and their compatibility with solid oxide fuel cell components, J. Phy. Chem. Solids 118 (2018) 248–254, https://doi.org/10.1016/j.jpcs.2018.03.021.

[15] A.M. Abdelghany, H.A. ElBatal, Effect of TiO_2 doping and gamma ray irradiation on the properties of SrO-B_2O_3 glasses, J. Non-Cryst. Solids 379 (2013) 214–219, https://doi.org/10.1016/j.jnoncrysol.2013.08.020.

[16] B. Aktas, S. Yalcin, K. Dogru, Z. Uzunoglu, D. Yilmaz, Structural and radiation shielding properties of chromium oxide borosilicate glasses, Rad. Phy. Che. 156 (2019) 144–149, https://doi.org/10.1016/j.radphyschem.2018.11.012.

[17] G. Rama Sundari, V. Pushpa Manjari, T. Raghavendra Rao, D.V. Satish, Ch. Rama Krishna, Ch. Venkata Reddy, R.V.S.S.N. Ravikumar, Characterization of Cr^{3+} doped mixed alkali ions effect in zinc borate glasses–physical and spectroscopic investigations, Opt. Mat. 36 (2014) 1329–1335, https://doi.org/10.1016/j.optmat.2014.03.023.

[18] G. Ramadevudu Samdani, M. Narasimha Chary, Md. Shareefuddin, Physical and spectroscopic studies of Cr^{3+} doped mixed alkaline earth oxide borate glasses, Mat. Chem. Phy. 186 (2017) 382–389, https://doi.org/10.1016/j.matchemphys.2016.11.009.

[19] E. Ebrahimi, M. Rezvani, Optical and structural investigation on sodium borosilicate glasses doped with Cr_2O_3, Spe. Chim. Acta A: Mol. Bio. Spec. 190 (2018) 534–538, https://doi.org/10.1016/j.saa.2017.09.031.

[20] H.A. ElBatal, A.M. Abdelghany, N.A. Ghoneim, F.H. ElBatal, Effect of 3d-transition metal doping on the shielding behavior of barium borate glasses: a spectroscopic study, Spe. Chim. Acta A: Mol. Bio. Spec. 133 (2014) 534–541, https://doi.org/10.1016/j.saa.2014.06.044.

[21] S. Yusub, D. Krishna Rao, The role of chromium ions on dielectric and spectroscopic properties of Li_2O-PbO-B_2O_3-P_2O_5 glasses, J. Non-Cryst. Solids 398 (399) (2014) 1–9, https://doi.org/10.1016/j.jnoncrysol.2014.04.022.

[22] Hanzhen Zhu, Qilong Liao, Fu Wang, Yunya Dai, Mingwei Lu, The effects of chromium oxide on the structure and properties of iron borophosphate glasses, J. Non-Cryst. Solids 437 (2016) 48–52, https://doi.org/10.1016/j.jnoncrysol.2016.01.013.

[23] I. Kashif, A. Ratep, Safaa K. El-Mahy, Structural and optical properties of lithium tetraborate glasses containing chromium and neodymium oxide, Mat. Res. Bull. 89 (2017) 273–279, https://doi.org/10.1016/j.materresbull.2017.02.006.

[24] P. SrinivasaRao, P. RameshBabu, R. Vijay, T. Narendrudu, N. Veeraiah, D. KrishnaRao, Spectroscopic and dielectric response of zinc bismuth phosphate glasses as a function of chromium content, Mater. Res. Bull. 57 (2014) 58–66, https://doi.org/10.1016/j.materresbull.2014.05.030.

[25] S. Yusub, Ch. Rajyasree, A. Ramesh Babu, P.M. Vinaya Teja, D. Krishna Rao, Influence of alkaline earth oxides (R = Ca, Sr and Ba) on spectroscopic and dielectric studies of iron doped RO–Na_2O–B_2O_3 glasses, J. Non-Cryst. Solids 364 (2013) 62–68, https://doi.org/10.1016/j.jnoncrysol.2012.12.045.

[26] S. Yusub, P. Srinivasa Rao, D. Krishna Rao, Ionic conductivity, dielectric and optical properties of lithium lead borophosphate glasses combined with manganese ions, J.Alloys Compd. 663 (2016) 708–717, https://doi.org/10.1016/j.jallcom.2015.12.147.

[27] R. Lachheb, A. Herrmann, K. Damak, C. Rüssel, R. Maâlej, Optical absorption and photo luminescence properties of chromium in different host glasses, J. Lumi. 186 (2017) 152–157, https://doi.org/10.1016/j.jlumin.2017.02.030.

[28] Changwei Lin, Jianlei Liu, Lei Han, Hua Gui, Jun Song, Cui Li, Taoyong Liu, Anxian Lu, Study on the structure, thermal and optical properties in Cr_2O_3- incorporated, MgO-Al_2O_3-SiO_2-B_2O_3 glass, J. Non-Cryst. Solids 500 (2018) 235–242, https://doi.org/10.1016/j.jnoncrysol.2018.08.004.

[29] N. Kiran, C.R. Kesavulu, A. Suresh Kumar, J.L. Rao, Spectral studies on Cr^{3+} ions doped in sodium-lead borophosphate glasses, Phys. B Cond. Mat. 406 (2011) 1897–1901, https://doi.org/10.1016/j.physb.2011.02.051.

[30] F.A. Moustafa, A.M. Fayad, F.M. Ezz-Eldin, I. El-Kashif, Effect of gamma radiation on ultraviolet, visible and infrared studies of NiO, Cr_2O_3 and Fe_2O_3-doped alkali borate glasses, J. Non-Cryst. Solids 376 (2013) 18–25, https://doi.org/10.1016/j.jnoncrysol.2013.04.052.

[31] C.R. Kesavulu, R.P.S. Chakradhar, R.S. Muralidhara, J.L. Rao, R.V. Anavekar, EPR, optical absorption and photoluminescence properties of Cr^{3+} ions in lithium borophosphate glasses, J. Alloys Compds. 496 (2010) 75–80, https://doi.org/10.1016/j.jallcom.2010.02.119.

[32] M.V. Sambasiva Rao, Ch. Rajyasree, T. Narendrudu, S. Suresh, A. Suneel Kumar, N. Veeraiah, D. Krishna Rao, Physical and spectroscopic properties of multi-component Na_2O-PbO-Bi_2O_3-SiO_2 glass ceramics with Cr_2O_3 as nucleating agent, Opt. Mat. 47 (2015) 315–322, https://doi.org/10.1016/j.optmat.2015.05.048.

[33] J. Santhan Kumar, J. Lakshmi Kumari, M. Subba Rao, Sandhya Cole, EPR, optical and physical properties of chromium ions in CdO-SrO-B_2O_3-SiO_2 (CdSBSi) glasses, Opt. Mat. 35 (2013) 1320–1326, https://doi.org/10.1016/j.optmat.2013.01.012.

[34] B.V. Padlyak, W. Ryba-Romanowski, R. Lisiecki, V.T. Adamiv, Ya.V. Burak, I.M. Teslyuk, Synthesis, EPR and optical spectroscopy of the Cr-doped tetraborate glasses, Opt. Mat. 34 (2012) 2112–2119, https://doi.org/10.1016/j.optmat.2012.06.014.

[35] R. Vijay, P. Ramesh Babu, V. Ravi Kumar, M. Piasecki, D. Krishna Rao, N. Veeraiah, Dielectric dispersion and ac conduction phenomena of Li_2O-Sb_2O_3-PbO-GeO_2: Cr_2O_3 glass system, Mat. Sci. Semi. Proc. 35 (2015) 96–108, https://doi.org/10.1016/j.mssp.2015.02.082.

మద్రాసు క్రైస్తవ కళాశాల

(స్వయం ప్రతిపత్తి)

తెలుగుశాఖ (స్థాపితం - 1887)

తాంబరం, చెన్నై - 600 059, తమిళనాడు.

Madras Christian College

Department of Telugu

భావిన ప్రత్యేక సంచిక

Journal of Telugu Literary, Culture & Language Studies

Vol. 16 - Issue. 01 - Spl. Edition - September 2019 - ISSN No. : 2456-4702

జాతీయ సదస్సు - 2019

తెలుగులో గిరిజన సంస్కృతి - సాహిత్యం

సదస్సు సంచాలకులు :

డా॥ శ్రీపురం యష్ణ శేఖర్

శాఖాధ్యక్షులు, తెలుగు విభాగం,

మద్రాసు క్రైస్తవ కళాశాల, తాంబరం, చెన్నై - 600 059.

మద్రాసు క్రైస్తవ కళాశాల

ద్వయంత్రైమాసిక పత్రిక

తెలుగుశాఖ (స్థాపితం - 1887)

తాంబరం, చెన్నై - 600 059, తమిళనాడు.

Madras Christian College

Department of Telugu

భావవీణ ప్రత్యేక సంచిక

Journal of Telugu Literary, Culture & Language Studies

Vol. 16 - Issue. 01 - Spl. Edition - September 2019 - ISSN No. : 2456-4702

జాతీయ సదస్సు - 2019

తెలుగులో గిరిజన సంస్కృతి - సాహిత్యం

సదస్సు సంచాలకులు :

డా॥ శ్రీపురం యజ్ఞ శేఖర్

శాఖాధ్యక్షులు, తెలుగు విభాగం,

మద్రాసు క్రైస్తవ కళాశాల, తాంబరం, చెన్నై - 600 059.

[redacted]

భావవీణ ప్రత్యేక సంచిక – సెప్టెంబర్ 2019
ISSN No. : 2456-4702 - RNI No. APTEL/2003/12253
BHAVAVEENA SPECIAL EDITION
UGC Approved Journal No. 42501

గిరిజనుల ఆర్థిక పరిస్థితులు – జీవన విధానం

– కనపాల జోసఫ్, శాఖాధిపతి, తెలుగు విభాగం, ఆంధ్ర క్రైస్తవ కళాశాల, గుంటూరు

అభివృద్ధి సాధారణంగా మార్పు యొక్క ఒక అంశంగా భావించబడుతుంది. ఇది విస్తృతంగా ప్రభుత్వ చర్య ద్వారా ప్రణాళిక చేయబడింది మరియు నిర్వహించబడుతుంది. ఈ విధంగా, అభివృద్ధి, భావన(ఎ) మార్పు యొక్క ఒక అంశం; (బి) ఒక ప్రణాళిక లేదు ఫ్రిడిక్షన్; (సి) ఆ ప్రణాళిక సాధించినందుకు ప్రభుత్వ ప్రమేయం లేదా goal హించిన లక్ష్యం. "అభివృద్ధి" అనే పదాన్ని అనుమతించే ప్రక్రియ కోసం కూడా ఉపయోగిస్తారు. వారి స్వంత ఆకాంక్షలను తీర్చడానికి ప్రజలను ప్రోత్సహిస్తుంది. అందువల్ల ఇది తప్పనిసరిగా సంబంధం కలిగి వుంటుంది.

"అభివృద్ధి"అనే పదం మానవ కార్యకలాపాల యొక్క అన్ని అంశాలను కలిగి ఉంటుంది. ఇంకా విస్తృత సందర్భంలో, దేశాలు అభివృద్ధి చెందినవి లేదా అభివృద్ధి చెందుతున్నవిగా నిర్వహించబడ్డాయి. కానీ దాని ఎలా సమర్థించవచ్చు ఒకటి అభివృద్ధి చెందాల్సిన వారి కంటే అభివృద్ధి చెందింది. ఈ ప్రశ్నలు ఉన్నాయి ఈ రోజుల్లో కొన్ని గోళాలలో అభివృద్ధి చెందని వాటిని కనుగొన్నప్పుడు లేదా చాలా సున్నితంగా మారుతుంది. మరొకటి ప్రతిచోటా, ఉదాహరణకు, ఒక సమాజం లేదా దేశం మరింత అభివృద్ధి చెందవచ్చు. ఆర్థికముందు; ఏదేమైనా, ఇది సామాజిక ముందు అభివృద్ధి చెందకపోవచ్చు. కాబట్టి, ఒకరు చేయలేరు. కొన్ని అంశాలలో మాత్రమే అభివృద్ధిని నిర్వచించండి; బదులుగా, దీనిని బహుమితీయంగా చూడాలి. యాభైలలో మరియు అరవైల ప్రారంభంలో ఉన్న అభివృద్ధి యొక్క ఇరుకైనా భావన తీవ్రంగా ప్రశ్నించబడింది మరియు ఆర్థికేతర అంశాలను కూడా చేర్చడానికి విస్తరించింది.

భారతదేశంలో విధాన రూపకర్తలు, నిర్వాహకులు మరియు సామాజిక శాస్త్రవేత్తలు మరియు చర్చను అడ్డుకున్నారు. వారి సామాజిక - ఆర్థిక పరివర్తన యొక్క అర్థం, పాత్ర మరియు దిశపై కొనసాగుతుంది. అంతకు ముందు మానవ శాస్త్రవేత్తలు మరియు ఇతర సామాజిక శాస్త్రవేత్తలు జరిపిన అధ్యయనాలు వివిధ గిరిజన వర్గాలలో నిరంతరం వివిధ సమస్యలకు ఎత్తి చూపడం, గిరిజన అభివృద్ధి మరియు మంచి ఫలితాలను తీసుకురావడానికి సూచనలు ఇచ్చింది. కమిటీల నివేదికలు మరియు గిరిజన అభివృద్ధిపై అధ్యయనాలు, ప్రయత్నాలు తరువాత జరిగాయి వివిధ రకాల నిబంధనలను అందిచడం ద్వారా గిరిజన పరిస్థితిని మెరుగుపరచడానికి మరియు పథకాలు అయినప్పటికి, దురదృష్టవశాత్తు గిరిజనులు తగినంతగా పొందలేకపోయారు ప్రణాళిక బద్ధమైన అభివృద్ధి యొక్క ఈ ప్రక్రియ నుండి ప్రయోజనం. గిరిజన అభివృద్ధి అనేది నిజం దేశంలో సమస్యను మూసపోత దృగ్విషయంగా వరిగణించలేము. ఇది మారుతుంది ఒక ప్రాంతం నుండి మరొక ప్రాంతానికి.

ఆంధ్రప్రదేశ్ రాష్ట్రంలో మరియు మొత్తం దేశంలో గిరిజన జనాభా ఉంది. తీవ్రమైన ఆర్థిక మినహాయింపును ఎదుర్కొంటున్న అత్యంత అణగారిన మరియు హాని కలిగించే సంఘం. కొన్ని రాజ్యంగ భద్రతలు అందించినప్పటికీ, ఆర్థికంగా లేదు. ఈ సమాజాలలో సామాజిక మరియు రాజకీయ చైతన్యం. షెడ్యూల్ కులాలకు విరుద్ధం మరియు ఇతర వెనుకబడిన కులాల కారణంగా కొంత స్థాయిలో పురోగతి సాధించారు. ప్రభుత్వ రక్షణ వివక్ష విధానాస్త్రాలు,షెడ్యూల్డ్ తెగలు అలాగే ఉన్నాయి.

ఆంధ్ర ప్రదేశ్‌లోని గిరిజన సమూహాలు :

అధికారికంగా షెడ్యూల్డ్ తెగలుగా నియమించబడిన 35 వర్గాలకు ఆంధ్ర ప్రదేశ్ ఉంది. (ఎస్టీలకు)2001 జనాభా లెక్కల ప్రకారం వారి సంఖ్య 50,24,104.35

స్టీలలో, ఇటీవల రెండు కమ్యూనిటీలు, అవి నక్కల/ సర్వికరన్, ధులియా / పైకో / పుటియా (జిల్లాల్లో ిశాఖపట్నం మరియు విజయనగరం) రాష్ట్రంలో ూచించబడ్డాయి. పన్నెండు తెగలు, అవిబోడో గడాబా, గుటోబ్ గడాబా, బోండో పోరాజా, ఖొండ్ పోరాజా, పరంగి పెర్జా, చెంచు డొంగారియా ఖొండ్స్, కుట్టియా ఖండ్స్, కోలం, కొండారెడ్డిస్ కొండా సవారస్ మరియు తోటిని ఆదిమ గిరిజన సమూహాలు (పిటిజి)గా గుర్తించారు.

రాష్ట్రంలో అధికారికంగా గుర్తించబడిన షెడ్యూల్డ్ తెగ సమూహాల జాబితా

1. బగాటా (విశాఖపట్నం జిల్లాలోని ఏజెన్సీ ప్రాంతాలు)
2. భిల్ (శ్రీకాకుళం మరియు విజయనగరం జిలాల్లాల ఏజెన్సీ ప్రాంతాలు - ఉత్తర తీరం ప్రాంతం)
3. చెంచు (కర్నూలు, ప్రకాశం మరియు ఏజెన్సీ ప్రాంతాలు, గుంటూరు జిల్లాలు - నల్లమల అడువులు.
4. గదాబాస్, బోడో గడాబా, కల్లాయి, గడాబా, పరంగి గడాబా, కథెరా గడాబా, కపు గదాబ్ (విశాఖపట్నం జిల్లా ఏజెన్సీ ప్రాంతాలు - ఉత్తర తీరం ప్రాంతం)
5. గౌడు (పశ్చిమగోదావరి జిల్లాలు)
6. హిల్ రెడ్డిస్ (తూర్పు మరియు పశ్చిమగోదావరి జిల్లాలు)
7. జాతవస్ (శ్రీకాకుళం మరియు విజయనగరం జిల్లా ఏజెన్సీస్ ప్రాంతాలు - ఉత్తరం తీరం ప్రాంతం)
8. కమ్మారా (తూర్పు మరియు పశ్చిమ గోదావరి జిల్లాలు)
9. కొండా ధోరస్, కుబి (తూర్పు మరియు పశ్చిమ గోదావరి జిల్లాలు)
10. కొండా కపుస్(తూర్పు మరియు పశ్చిమ గోదావరి జిల్లాలు)
11. కొండా రెడ్డిస్ (తూర్పు మరియు పశ్చిమ గోదావరి జిల్లాలు)
12. కొండ్స్, కోడి, కొడు, దేశయ కొండ్స్, డోంగ్రియా కొండ్స్, కుట్టియా కొండ్స్, టికిరియా కొండ్స్, యెనిటీ కొండ్స్, కువింగా (నార్త్ కోస్టల్ ఏరియా యొక్క ఎజన్సీ ట్రాక్ట్)
13. కొటియా, బెంతో ఒరియా, బార్టికా, దులియా, హోల్లా, సాన్రోనా, సిధోపెకో (ఏజెన్సీ ట్రాక్ట్లు)
14. కోయ, డోలీ కోయా, గుత్తా కోయ, కమ్మారా కోయ, ముసర కోయ, ఒడ్డి కోయ, పత్తిడికోయ, రాజా, రాషా కోయ, లింగాధారి కోయ (సాధారణ), కొట్టు కోయ, టైన్కోయా, రాజ్ కోయ (తూర్పు మరియు పశ్చిమ గోదావరి జిల్లాలు)
15. కులియా (ఉత్తర తీర ప్రాంత ఏజెన్సీ ప్రాంతాలు)
16. మన్నాధోరా (ఖమ్మం)
17. ముఖధోరా, నూకా ధోరా (తూర్పు మరియు పశ్చిమ గోదావరి జిల్లాలు)
18. నాయకులు (ఏజెన్సీ ట్రాక్ట్స్ నార్త్ కోస్టల్ ఏరియాలో)
19. పోర్జా, పరంగి పెర్జా (విశాఖపట్నం జిల్లా మరియు ఉత్తర తీరంలోని ఏజెన్సీ ప్రాంతాలు ప్రాంతం)
20. రోనా, రెనా (నార్త్ కోస్టల్ ఏరియా యొక్క ఏజెన్సీ ప్రాంతాలు)
21. సవారస్, కాపు సవారస్, మాలియా సవారస్, ఖుట్టో నవారన్ (శ్రీకాకుళంలోని ఏజెన్సీ ప్రాంతాలు మరియు విజయనగరం జిల్లాలు - ఉత్తర తీర ప్రాంతం)
22. సుగాలిస్, లంబాదాస్, బంజారా (అదిలాబాద్, వరంగల్, నిజామాబాద్, ఖమ్మం)
23. వాల్మీకి (విశాఖపట్నం, శ్రీకాకుళం, విజయనాగ్రామ్, షెడ్యూల్డ్ ప్రాంతాలలో తూర్పు మరియు పశ్చిమ గోదావరి జిల్లాలు)

24. నక్కల కుర్వికరన్ (శ్రీకాకుళం మరియు విజయనగరం జిల్లాల ఏజెన్సీ ప్రాంతాలు - ఉత్తర తీర ప్రాంతం)
25. ధులియా, సైకో, నుటియా (విశాఖపట్నం మరియు విజయనగరం జిల్లాల్లో)

గిరిజనుల జీవనంలో పోడు సాగు :

కొండప్రాంతాలలో నివసిస్తున్న భారతదేశ గిరిజన వర్గాలు పొరుగు ప్రాంతాల కొండలపై అటవీ పాచెస్ కత్తిరించి కాల్చడం ద్వారా సాగు పద్ధతిని అనుసరిస్తాయి. 'పోడు', 'దహి' మరియు 'పమ్' వంటి వివిధ స్థానిక పదాలలో ఇది తెలుసు. ఆంగ్ల పత్రాలలో దీనిని స్వీదన్ లేదా స్లాష్ మరియు బర్న్ లేదా షిఫ్టింగ్ సాగు అంటారు. ఇది గిరిజన ఆర్థిక వ్యవస్థ యొక్క ఆసక్తికరమైన అంశం. ఈ పద్ధతి రెండు లేదా కనీసం మూడు వార్షిక పంటలను అనుమతిస్తుంది. మరియు రెండవ నింపడానికి అనుమతించటానికి చెట్టు మళ్ళీ తగినంతగా పెరిగే వరకు ఆ భూమిని వదిలివేస్తాయి. మట్టి మరియు విత్తనం లేకుండా భూమి కొట్టుకుపోయే వరకు ఈ ప్రక్రియ కొనసాగుతుంది. అటవీ వృద్ధి సాధ్యంకాదు. ఇది చివరకు వదిలేయబడుతుంది మరియు ముళ్ళు, లత మరియు ముతక గడ్డిని మాత్రమే ఉత్పత్తి చేసే ఏ ప్రయోజనం కోసం పనికిరాని కొండచిలువ ఉంది. తూర్పు కనుమల లోని కొండ గిరిజన రైతులు 'పోడు' సాగును ఆచరించే సంప్రదాయాన్ని కలిగిఉన్నారు.

పోడు భూములలో సాధారణంగా వండించే పంట రాగి, రెడ్‌గ్రామ్, ఛాంపు, ఖరాసా, జుడెంగా, కంగు, భోసాలా, హార్స్‌గ్రామ్, కాస్టర్, నుమా మరియు కొర్ర. ఎకరాల పోడు భూమిలో ప్రతి పంట సగటు దిగుబడి 15-20కిలోలు, , 8-10కిలోల కాయధాన్యాలు. మొత్తం యైల్డ్ 20-25 కిలోలు, మైదానాల్లోని లోతట్టు దేశంలో ఎకరానికి సగటు ఈల్డ్ 40-50కిలోలు. వాణిజ్య పంట సాధారణంగా కొండలపై పెరగవు కాబట్టి కొండపై పంట విలువ సమాన విస్తీర్ణంలో సాదావశంలో పండిన దానిలో సగం ఉంటుంది.

పోడు సాగు చాలా కాలంగా సానుకూల చెదురుగా గణించబడుతున్నప్పటికీ, దానిని పరిమితం చేయడాని లేదా నిర్మూలించడానికి ప్రణాళికాబద్ధమైన ప్రయత్న చేయలేదు. వ్యవసాయం, అడవులు మరియు వర్షపాత యొక్క దృక్కోణాలకు పోడు సాగు హానికరం అ పాక్షికంగా Wxcluded ప్రాంతాల కోసం కమీటీ వ్య యించిన అభిప్రాయం. రాబోయే కాలంలో దీనిని హర్తగా తొలగించడానికి తీవ్రమైన ప్రయత్నాలు చేయాలి. ఈ ప్రయోజనం కోసం ప్రభుత్వం ఒక సీనియర్ సబ్-డివ్యూ కలెక్టర్ పర్యవేక్షణలో సంయుక్తంగా పనిచేస్తారు. ఈ అధికారులు పోడు సాగును పూర్తిగా ఎంపిక చేసిన ఒక చిన్న ప్రాంతంతో ప్రారంభించడానికి ఒక కార్యక్రమాన్ని రూపొందించాలి. వారు ఒక పోడును ప్రత్యేకంగా మరియు పాక్షికంగా జీవించే ప్రజల జనాభా గణనను తీసుకోవాలి మరియు పోడు సాగు కింద సుమారు ఎకరాలు. ఈ ప్రజలకు మొదటి ఐదేళ్ళకు అంచనా లేకుండా ఉచితంగా ఇవ్వవలసిన సాగు భూముల సగటును వారు సిఫార్సు చేయాలి. ఈ సాగు భూములను మైదాన ప్రాంతాలలో లేదా కొండల అడుగున ప్రారంభించాలి. సహకార సంఘాల ఏజెన్సీ ద్వారా లేదా గిరిజనులకు ఎద్దులు మరియు వ్యవసాయ పనిముట్లను అందించడానికి ఎస్టేట్ ద్వారా బకాయిలు వసూలు చేయడానికి అనువైన ఏ ఇతర ఏజెన్సీ ద్వారా వారికి రాయితీలు లేదా రుణాలు పొందటానికి చర్యలు తీసుకోవాలి. కొండ శిఖరాలపై అటవీ భూములను పరిరక్షించడానికి చట్టాలను ఉల్లం ఘించిన నేరస్థులకు అపరాధ శిక్షను అందించడానికి అవ సరమైన శాసన చట్టాలను ఆమోదించాలి.

❁❁❁

Govt of India Approved | UGC Sponsored

Proceedings of the International Conference on Impact of Languages, Literature and Education on Intellectual Property Rights 2020

Feb 28-29, 2020

Organized by

SIR C R REDDY COLLEGE ELURU

Aided, Autonomous, CPE and Thrice Accredited with A Grade by NAAC
College with Potential for Excellence | An ISO 9001:2015 Certified Institution

in collaboration with

IMRF Institute of Higher Education & Research

www.imrfedu.org | Vijayawada, India

PROCEEDINGS OF THE INTERNATIONAL CONFERENCE ON IMPACT OF LANGUAGES, LITERATURES & EDUCATION ON INTELLECTUAL PROPERTY RIGHTS – 2020

Feb 28-29, 2020

ISBN 978-81-944859-5-7

Govt of India Approved Conference
(Govt of India Approved: MHA Vide : F.No 42180123/CC-1590 ; MEA : F.No. AA/162/01/2020-306)
UGC Sponsored – Autonomy Grant

Organized by

SIR C R REDDY COLLEGE
(Aided& Autonomous), Eluru, A.P
Affiliated to Adikavi Nannaya University, Rajamahendravaram
[Thrice Accredited with A Grade by NAAC]
College with Potential for Excellence
An ISO 9001:2015 Certified Institution

In collaboration with

IMRF INSTITUTE OF HIGHER EDUCATION & RESEARCH, INDIA
www.imrfedu.org

CONTENTS

| ISBN 978-81-944859-5-7

యాత్రికులు - ఆంధ్రుల ప్రస్థానం

కనపాల. జోసఫ్

ప్రాంతీయ, జాతీయ అంతర్జాతీయ భాషా సాహిత్యాలపై ఇటీవల కాలంలో సదస్సులు నిర్వహించటం మంచి పరిణామం. దీనివల్ల ఆయాదేశాల సంస్కృతి సాంప్రదాయాలు తదితర విషయాలను ఏక కాలంలో తెలుసుకోవడానికి అవకాశం కలుగుతుంది. అసలు ఏదేశానికైనా భాషా సంస్కృతుల్లో ఆ దేశ మనుగడకు మూల స్థంభాలు. అందువల్ల యిలాంటి అంతర్జాతీయ సదస్సుల్లో ఎన్నుకునే అంశాలకు ఎల్లలు అనేవి ఉండవు. కనుక నా పత్ర సమర్పణకు సంబంధించిన వ్యాసం కూడా ఆ కోవలోకి వస్తుందని భావిస్తూ.. అంతర్జాతీయ దేశాలైన చైనా, టిబెట్ దేశాలలో తెలుగు వారితో వుండే సంబంధాలను ఈ వ్యాసంలో ప్రస్తావించాను.

***

కనపాల. జోసఫ్
ఆంధ్రోపన్యాసకులు
ఆంధ్ర క్రైస్తవ కళాశాల
గుంటూరు.

ISBN 978-81-944859-5-7

SIR C R REDDY COLLEGE

(AIDED & AUTONOMOUS)

ELURU - 534 007, W.G. DIST. A.P. INDIA

కందుకూరి వీరేశలింగం శతవర్ధంతి సందర్భంగా

అంతర్జాతీయ సదస్సు International Conference

సాహిత్యం - సంస్కరణ దృక్పథం

साहित्यक्य संस्कवणदृक्पथ: साहित्य-सुधावादी दृष्टिकोण

14th & 15th December 2018

Sponsored by UGC (Autonomous Grants)

in Association with
Department of Language & Culture, Govt. of A.P.

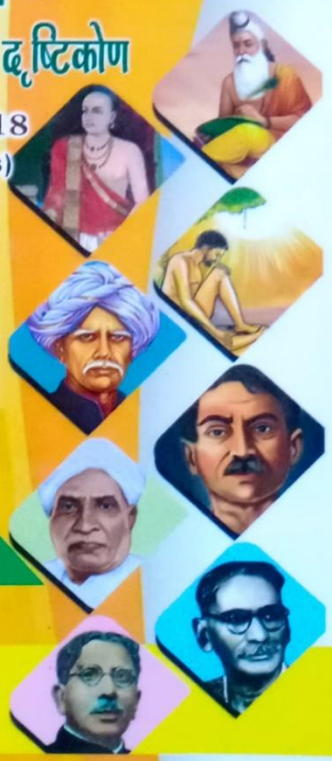

భావవీణ ప్రత్యేక సంచిక

International Journal of Telugu, Literary, Culture & Language Study

Special Edition. Vol - III. Dec - 2018

ISSN No. 2456-4702 (UGC approved Journal No. 42500)

Organised by Telugu & Oriental Languages
(Sanskrit & Hindi)

Affiliated to Adikavi Nannaya University, Rajamahendravaram

(THRICE ACCREDITED AT 'A' LEVEL BY NAAC, BENGALURU ; COLLEGE WITH POTENTIAL FOR EXCELLENCE)

AN ISO - 9001:2015 CERTIFIED INSTITUTION

భావవీణ ప్రత్యేక సంచిక
ISSN : 2456 - 4702

BHAVA VEENA SPECIAL EDITION
UGC Approved Journal No: 42506

SIR C R REDDY COLLEGE

(AIDED & AUTONOMOUS)

ELURU-534 007, W.G.DIST. A.P., INDIA

Affiliated to Adikavi Nannaya University, Rajamahendravaram

(Thrice accredited at 'A' level by NAAC, Bengaluru. College with potential for Excellence)

AN ISO-9001:2015 CERTIFIED INSTITUTION

In Association with **LANGUAGE AND CULTURAL DEPARTMENT, GOVT OF A.P.**

Two Day International Conference on

LITERATURE - REFORMED PERSPECTIVE

అంతర్జాతీయ సదస్సు

సాహిత్యం - సంస్కరణాదృక్పథం

साहित्य-सुधारवादी दृष्टिकोण

साहित्यस्य संस्करणादृक्पथः

14th & 15th DECEMBER 2018

Sponsored by
UGC, NEW DELHI
(Under Autonomy Grant)

ज्ञान - विज्ञान विमुक्तये

Organised by

DEPARTMENTS OF TELUGU & ORIENTAL LANGUAGES (SANSKRIT & HINDI)

SIR C. R. REDDY COLLEGE, ELURU

విషయ సూచిక

ISSN : 2456 - 4702

BHAVA VEENA SPECIAL ADDITION
UGC Approved Journal No. 42500

శ్రీ గోస్వామి తులసీదాసు జీవనరేఖలు

కసపాల.జోసఫ్
ఆంధ్రోపన్యాసకులు
ఆంధ్రక్రైస్తవ కళాశాల, గుంటూరు

ప్రసిద్ధ పుణ్యక్షేత్రమైన ప్రయాగ సమీపమున 'బాందా'జిల్లాలో 'రాజాపురము' అను గ్రామము గలదు. అచట ఆత్మారామ్ దూబే - అను సుప్రసిద్ధమైన సరయూపారీణబ్రాహ్మణుడు ఉండెను. శ్రీమతి హులసీదేవి ఆయనధర్మపత్ని. క్రీ.శ. 1497, విక్రమశకం 1554వ సంవత్సరమున శ్రావణ శుద్ధ సప్తమినాడు అభుక్తమూలా నక్షత్రమున ఆ పుణ్యదంపతులకు జన్మించిన ముద్దుల బిడ్డడే మన గోస్వామి తులసీదాసు. అతడు మాతృగర్భమున 12(పండ్రెండు)మాసములు మసలెను. శిశువైన తులసీదాసు పుట్టగనే రోదనము కావింపలేదు. అతని ముఖము నుండి 'రామ్' అను శబ్దము (రామనామము) వినిపించెను. ఆయన నోటిలో ముప్పది రెండు (32) దంతములుండెను. చూచుటకు అతడు ఐదు(5) సంవత్సరముల ఈడుగల బాలకునివలె ఒప్పుచుండెను. ఇట్టి అద్భుతలక్షణములు గల బాలకుని జూచి, ఆయన తండ్రి అమంగళములను శంకించి భీతిల్లెను. కుమారుని విషయమై ఆత్మారాముడు పెక్కు విధములగు ఊహాగానములను చేయసాగెను. తల్లియైన 'హులసి' మిక్కిలి చింతించెను. అశుభములను శంకించి, ఆమె ఆ పసికందును దశమినాటి రాత్రి దాసీచేతిలలో ఉంచి, ఆ దాసి యొక్క అత్తగారింటికి పంపెను. మరునాడే ఆ పవిత్ర మాతృమూర్తి ఈ లోకమును వీడెను. 'చునియాఁ' అను పేరుగల ఆదాసి ఆ శిశువును మిక్కిలి ప్రేమానురాగములతో పెంచెను. తులసీదాసునకు దాదాపు ఐదున్నర సంవత్సరములప్రాయమున చునియాఁ గూడ దివంగతురాలయ్యెను. ఇప్పుడతడు అనాథబాలుడై ఇంటింటికిని తిరుగసాగెను. జగజ్జననియైన పార్వతీదేవికి ఈ అమాయకబాలునిపై కృపగలిగెను. ఆమె బ్రహ్మణస్త్రీ వేషమున ప్రతిదినము ఆ బాలునికడకు వచ్చి, స్వహస్తములతో అన్నము తినిపించుచుండెడది.

రామశైలనివాసియైన శ్రీ అనంతానందజీ ప్రియశిష్యుడు శ్రీ నరహరి ఆనంద. అతడు పరమేశ్వర ప్రేరణచే ఈ బాలకుని వెదకుచు వచ్చెను. ఈ బాలునకు 'రామ్‌బోలా' అను పేరు పెట్టి, అతడు వానిని తనతో అయోధ్యకు తీసికొనివెళ్ళెను. విక్రమ శకము1561(క్రీ॥శ॥1504)వ సంవత్సరమున మాఘ శుద్ధ పంచమీ శుక్రవారము నాడు అతడు ఆ బాలునకు ఉపనయన సంస్కారములను జరిపెను. ఎవ్వరి ప్రేరణ లేకయే ఏకసంతగ్రాహియైన 'రామ్‌బోలా'గురూపదేశమైన వెంటనే గాయత్రీమంత్రమును ఉచ్చరించెను. దానిని జూచి అందఱును చకితులైరి. పిమ్మట నరహరి స్వామి రామ్‌బోలాకు వైష్ణవ సంప్రదాయమును అనుసరించి, పంచసంస్కారములను జరిపించి, రామమంత్ర దీక్షను ఒసంగెను. అయోధ్యయందే అతనిచే విద్యాధ్యయనము చేయించెను. బాలకుడైన రామ్‌బోలా మిక్కిలి బుద్ధిమంతుడు, చురుకైనవాడు. అతడు ఏకసంతగ్రాహి. 'గురుముఖతః' ఒకసారి విన్నంతనే ఆ విషయము అతనికి కంఠస్థమగుచుండెను. ఆ గురుశిష్యులిద్దరును అచట కొంతకాలము గడిపి, అనంతరము 'వరాహక్షేత్రము'నకు చేరిరి. అక్కడ శ్రీ నరహరిస్వామి తులసీదాసునకు రామచరితము వినిపించెను. కొలదిదినముల పిమ్మట వారు కాశీనగరమును చేరిరి. కాశీలో శేషసనాతనస్వామివారికడ తులసీదాసు పదునైదు(15) సంవత్సరముల కాలము అధ్యయనము చేసి, వేదములను, వేదాంగములను జిహ్వాగ్రమున నిలుపుకొనెను. ఇచ్చట ఆయనకు సాంసారిక వాసనలు జాగృతములయ్యెను. గురువాజ్ఞను దీసికొని, తిరిగి తన జన్మ స్థానమునకు చేరెను. అచట తన వారెవ్వరును మిగిలి యుండకపోవుటను అతడు గ్రహించెను. తన మాతాపిత్రాదులకు విధ్యుక్తములైన శ్రాద్ధకర్మలనాచరించెను. అచటనే యుండి జనులకు శ్రీరామచరితమును వినిపించసాగెను.

విక్రమ శకము 1583(క్రీ॥శ॥1526)వ సంవత్సరమున జ్యేష్ఠశుద్ధ త్రయోదశీ గురువారము నాడు భారద్వాజగోత్రజయైన 'రత్నావళి'యను సుందరి(కన్య)తో ఆయనకు వివాహమయ్యెను. ఆ క్రొత్త దంపతులు సుఖసంతోషములతో తమజీవితమును కొనసాగించుచుండిరి. ఒకసారి రత్నావళి తన సోదరునితో గూడి, పుట్టింటికి వెళ్లెను. కొంతసేపైన తరువాత తులసీదాసు భార్యమీది ప్రేమతో తన ఇంటినుండి బయలుదేఱి, తన భార్యపుట్టింటికి చేరెను. అతనిని జూచి, భార్య రత్నావళి తన భర్తను చులకన చేయుచూ ఇట్లనెను. "రక్తమాంసములతో గూడిన ఈ నా తనువు పైగల ఆసక్తిలో సగమైనను మీకు భగవంతునిపై ఉన్నచో మీరు తరించియుండెడివారు". ఆమె మాటలుల తులసీదాసు మనస్సులో బాగుగా నాటుకొనెను. దానితో ఆయనలో అంతర్మథనము జరిగెను. ఆయనకు కనువిప్పు కలిగెను. వెంటనే ఆయన మనస్సు భగవంతునిమీదికి మఱలెను. మఱుక్షణముననే అతడు అచటి నుండి తన ఇంటికి చేరెను. పిదప ప్రయాగ వెళ్ళెను. అచ్చట తులసీదాసు గృహస్థవేషమును పరిత్యజించి, సాధువేషమును స్వీకరించెను. పిమ్మట తీర్థయాత్రలను గావించుచు అతడు కాశీ చేరెను. ఈ సమయముననే ఆయనకు మానససరోవరమును 'కాకభుశుండి' దర్శనమాయెను.

కాశీలో తులసీదాసు రామకథాప్రవచనమును చేయసాగెను. ప్రతినిత్యము తులసీదాసు తన సంధ్యావందనము ముగి
పిమ్మట ఆ తీర్థమును ఒక చెట్టు మొదట చల్లుచుండెడివాడు. ఆ చెట్టు పైనున్న ఒక బ్రహ్మరాక్షసుడు ఆ తీర్థప్రభావము
శాపవిముక్తుడై, మానవరూపమున తులసీదాసు సమ్ముకమున నిలిచెను. అతడు "నీ తీర్థప్రభావమును నాకు శాపవిముక్తి కలిగిం
నీకు నేను ఏ విధముగా సహాయపడగలవో తెలుపుము". అని తులసీదాసును అడిగెను. అప్పుడు తులసీదాసు "నాకు శ్రీరాము
దర్శనము కలుగు ఉపాయమును తెలుపుడు" - అది ఆయనను ప్రార్థించెను. అప్పుడు అతడు "అట్టి శక్తి నాకు లేదు. నీ
హనుమంతుని ఆశ్రయించినచో నీ కోరిక నెఱవేఱును" అని పలికెను. "అది సరే! హనుమంతుని దర్శనము కలుగుట ఎట్ల
అని తులసీదాసు ప్రశ్నించెను. దానికి సమాధానముగా అతడు -

"యత్ర యత్ర రఘునాథకీర్తనం, తత్ర తత్ర కృతమస్తకాంజలిమ్ ।
బాష్పవారిపరిపూర్ణలోచనం, మారుతిం నమత రాక్షసాంతకమ్॥"

అను శ్లోకమును పఠించెను -అనగా శ్రీ రఘురాముని కథాప్రవచనము (కీర్తనము)జరుగుచోట ఆంజనేయుడు తప్ప
ఉండితీరును.

తులసీదాసు ప్రవచనమును వినుటకు నిత్యము ఒక వృద్ధబ్రాహ్మణుడు వచ్చుచుండెడివాడు. అతడు శ్రీ రామకథ శ్రవణ
చేయుచు ఆర్ద్ర హృదయముతో ప్రేమవిహ్వలుడగుచుండెను. అతడు ఎవరో కాదు, మారువేషమున వచ్చిన ఆంజనేయస్వామియే
తులసీదాసు ఆయనకు ప్రణమిల్లి "స్వామీ! మీరు ఎవరు? అందరికంటెను ముందుగా వచ్చి, చివరకు వెళ్ళుచున్నారు" అ
అడిగెను. అప్పుడు ఆంజనేయుడు ఆయనకు తన రూపమును జూపెను. అంతట తులసీదాసు మిక్కిలి హర్షితుడై "స్వామి! నా
శ్రీరామునిదర్శనము కలిగింపుము" అని ప్రార్థించెను. ఆంజనేయుడు ఇట్లు నుడివెను. "నీవు చిత్రకూటమునకు వెళ్ళుము
అచ్చను నీకు శ్రీరఘునాథుని దర్శనము కాగలదు". ఈ మాటలను విని, తులసీదాసు శ్రీరామదర్శనమునకు త్వరపడుచున్నవాడై
చిత్రకూటమునకు చేరెను. అక్కడ రామఘట్టమునందు ఒక పీఠమును ఏర్పఱుచుకొనెను. ఒకనాడు అతడు కామదగిరి
ప్రదక్షిణమొనర్చుటకు బయలుదేఱెను. మార్గమున ఆయనకు శ్రీరాముని దర్శనమాయెను. మిక్కిలి అందమైన ఇద్దరు రాజకుమారు
ధనుర్బాణములను ధరించి, గుఱ్ఱములపై వెళ్ళుచుండిరి. తులసీదాసు వారిని జూచి ముగ్ధుడాయెను. కాని వారిని అత
గుర్తింపలేదు. పిమ్మట ఆంజనేయుడు ఆయనకడకు వచ్చి, వాస్తవమును ఎఱింగించెను. అప్పుడతడు మిక్కిలి పశ్చాత్తాపపడసాగె
హనుమంతుడతనిని అనునయించి, మఱల మరునాటి ప్రాతఃకాలమున శ్రీరామ దర్శనమగునని తెలిపెను.

వి॥శ॥ 1607వ సంవత్సరమున మౌనిఅమావాస్య, (పుష్యబహుళ అమావాస్యయూ బుధవారమునాడు శ్రీరామచం
ప్రభువు మఱల అతనిముందు ప్రత్యక్షమాయెను. బాలరూపుడుగా ఉన్న శ్రీరాముడు తులసీదాసుతో "బాబా! మాకు చందనమ
ఇమ్ము" అని అడిగెను. ఈ సారి పొరపాటు జరుగకుండ ఆంజనేయుడు చిలుక రూపము ధరించి ఈ దోహాను పలికెను.

చిత్రకూట కే ఘాట్‌పర్ భఇ సంతన కీభీర్। తులసిదాస చందన్ ఘిసేఁ తిలక్ దేత రఘువీర్॥

అనగా చిత్రకూటమునందలి రామఘట్టమున సజ్జన సమూహములు గలవు. తులసీదాసు చందనము దీసెను. రఘువీరుడ
తిలకమును దిద్దెను.

నీవు తీయు చందనమును దిద్దువాడు సాక్షాత్తు శ్రీరామచంద్రభగవానుడే. తులసీదాసు అద్భుతమైన రాముని తేజస్సునకు
అబ్బురపడి, తన శరీరస్పును కోల్పోయెను. భగవానుడు తనచేతితో చందనమును దీసికొని తనకును, తులసీదాసునకు
ముఖములయందు తిలకమును దిద్దెను. అనంతరము అతడు అంతర్ధానమాయెను.

వి॥శ॥1628 సంవత్సరమున ఆంజనేయుని అనుమతితో తులసీదాసు అయోధ్యకై బయలుదేఱెను. ఆ సమయమున
ప్రయాగయందు మాఘమేలా జరుగుచుండెను. అతడు అచ్చట కొన్ని దినములు గడిపెను. అట్లు పర్వదినము పిమ్మట ఒక
వటవృక్షచ్ఛాయయందు ఆయనకు మహర్షులైన భరద్వాజ, యాజ్ఞవల్క్యుల దర్శనమయ్యెను. వరాహక్షేత్రమునందు గురువుద్వారా
తాను వినిన కథయే అచట చెప్పబడుచుండెను. అచటినుండి అతడు కాశీనగరమునకు చేరి, ప్రహ్లాదఘట్టమున ఒక బ్రాహ్మణు
యింటి యందు నివసించసాగెను. అచ్చట అతనిలో కవితాశక్తి జాగృతమయ్యెను. సంస్కృత భాషలో శ్లోకరచన చేయసాగెను
కాని పగటివేళ వ్రాసిన శ్లోకములన్నియును రాత్రియందు లుప్తములగుచుండెను. ఈ సంఘటనము ప్రతిదినము కొనసాగుచువచ్చెను
ఎనిమిదవ దినమున తులసీదాసునకు ఒక కల వచ్చెను. ఆ కలలో "నీవు నీ (వ్యవహార) భాషయందు కావ్యరచ చేయుము" అ

అతనిని పరమేశ్వరుడు ఆదేశించెను. తులసీదాసు మేల్కొని కూర్చుండెను. ఆ సమయమున శివపార్వతులు అతనికి ప్రత్యక్షమైరి. తులసీదాసు ఆ ఆది దంపతులకు ప్రణమిల్లెను. పరమేశ్వరుడు పలికెను. "నీవు అయోధ్యకు వెళ్ళి వ్యవహార(అవధి) భాషలో కావ్యరచనచేయుము. నా ఆశీర్వాద(ప్రభావమున నీకవిత సామవేదముతో సమానముగా ఫలములను గూర్చును. సామవేదమువలె దీనిని ప్రజలందఱును గానము చేయుదురు." ఇట్లు ఆశీర్వదించి, గౌరీశంకరులు అంతర్ధానమైరి. వారి ఆజ్ఞలను శిరసావహించి, తులసీదాసు కాశీనుండి అయోధ్యకు చేరెను.

త్రేతాయుగమున శ్రీరామదినోత్సవము జరుపబడునట్లే 1631వ సంవత్సరమున అయోధ్యలో శ్రీరామనవమి ఉత్సవములు జరుపబడుచుండెను. ఆనాడు ప్రాతఃకాలమున శ్రీ తులసీదాసు 'శ్రీరామచరితమానస' రచనను ప్రారంభించెను. రెండు సంవత్సరముల ఏడు మాసములు ఇఱువది అఱుదినములలో ఆ గ్రంథరచన పూర్తియయ్యెను. 1633వ సంవత్సరమున మార్గశిర శుక్లపక్షమున శ్రీ సీతారాముల వివాహమహోత్సవమునాడు ఏడుకాండములును సంపూర్ణమాయెను.

ఆ పిదప తులసీదాసు భగవదాజ్ఞను అనుసరించి, కాశీ చేరెను. అచట అన్నపూర్ణావిశ్వేశ్వరులకు 'శ్రీరామచరిత మానసమును' విన్పించెను. ఆ రాత్రి ఆ గ్రంథము విశ్వనాథుని మందిరమున ఉంచబడెను. ప్రాతఃకాలమున పుస్తకమును తెఱచిచూడగా అందు 'సత్యం, శివం, సుందరమ్' అను మధురపద(త్రయము వ్రాయబడి యుండెను. క్రింద శంకరభగానుని సంతకముగూడ ఉండెను. అచ్చట నున్న జనులు 'సత్యం, శివం, సుందరమ్' అను పదములను గూడ వినిరి.

ఈ విషయములను వినిన అక్కడి పండితుల మనస్సులలో ఈర్ష్య జనించెను. వారు అందరును ఒకటై తులసీదాసును నిందింపసాగిరి. ఆ(గ్రంథమును గూడ నష్టపరుచుటకు ప్రయత్నించిరి. దానిని దొంగలించి తీసికొని వచ్చుటకై ఇద్దఱు దొంగలను పంపిరి. వారు వెళ్ళి చూడగా తులసీదాసు కుటీరసమీపమున ఇద్దఱు వీరులు ధనుర్బాణములను ధరించి, కాపలాకాయుచుండిరి. వారు శ్యామగౌరవర్ణశోభితులై యుండిరి. వారి దర్శనముతో చోరులబుద్ధి మాఱిపోయెను. వెంటనే చోరవృత్తికి స్వస్తిపలికి, శ్రీరామభజనను చేయసాగిరి. తనకొరకై భగవంతుడు కష్టపడినట్లు తెలిసికొని, కుటీరమునందలి వస్తువులనన్నింటిని అతడు దానమొనర్చి, గ్రంథమును మాత్రము తన మిత్రుడైన 'తోడర్‌మల్' కడనుంచెను. ఆ పిమ్మట అతడు మఱి యొక ప్రతిని వ్రాసెను. దీనిని ఆధారముగా చేసికొనియే ఇతర(ప్రతులు సిద్ధపఱచబడినవి. ఈ గ్రంథము క్రమ(క్రమముగా ప్రసిద్ధి వహించెను.

ఇచ్చట పండితులకు ఏమియు తోచక ఆ పుస్తకమును పరిశీలింపవలసిందిగా శ్రీ మధుసూదన సరస్వతిగారిని ప్రార్థించిరి. శ్రీ మధుసూదనసరస్వతిగారు ఆ గ్రంథమును సావధానముగా సమ(గ్రముగా పరిశీలించి, మిక్కిలి ప్రసన్నులై తమ సమ్మతిని ఇట్లు తెల్పిరి.

ఆనందకాననేహ్యస్మిన్ జంగమస్తులసీతరుః । కవితాపంజరీ భాతి రామ(భ్రమరభూషితా॥

"కాశి"యను ఆనంద వనమున 'తులసీదాసు' అనెడి సంచరించుతులసియొక్క కలదు. దాని కవితారూపమంజరి మిక్కిలి సుందరమైనది. దానిపై శ్రీరాముడనెడి తుమ్మెద సర్వదా పరి(భ్రమించు చుండును.

దీనితో పండితులకు సంతుష్టి కలుగకపోగా, వారి ఈర్ష్య ఇంకను అధికమైనది. ఈ గ్రంథ ప్రామాణిక పరీక్షకు వారు మఱియొక ఉపాయమును ఆలోచించిరి. వారు విశ్వేశ్వరుని ఎదుట ఒక పీఠము పై వేదశాస్త్ర పురాణ(గ్రంథములను, వాటి అన్నింటికిని అడుగుభాగమున తులసీరామాయణ(గ్రంథమును ఉంచిరి. పిమ్మట మందిరము మూయబడెను. ప్రాతఃకాలమున మందిరద్వారములు తెఱచిచూడగా అట్టడుగున ఉంచబడిన శ్రీరామచరితమానసము వేదపురాణాది(గ్రంథములపై భాగమున వారికి గనబడెను. పండితులందరును సిగ్గుతో తలవంచుకొనిరి. వారు శ్రీ తులసీదాసగోస్వామి వారికి క్షమాపణ చెప్పుకొని భక్తితో ఆయన పాదోదకమును సేవించిరి.

ఇపుడు తులసీదాసు 'అసీఘట్టము'న ఉండసాగెను. ఒకనాటి రాత్రి కలిపురుషుడు ఆయనయొద్దకు వచ్చి, ఆయనను బాధింపసాగెను. గోస్వామీజీ ఆంజనేయుని ధ్యానించెను. 'మారుతి' వినయపదములను వ్రాయుమని ఆయనను అజ్ఞాపించెను. తులసీదాసు 'వినయ పత్రిక'ను రచించి భగవంతుని పాదముల కడ సమర్పించెను. శ్రీరాముడు దానిపై తనహస్తాక్షరములను ఉంచెను. ఆయనకు అభయ(ప్రధానము చేసెను. అంతట తులసీదాసునకు కలిపురుషుని భయము తొలగిపోయెను. 1680 సంవత్సరమున ఆషాఢ బహుళ తదియ శనివారము నాడు అసీనఘట్టస్థన రామనామమును స్మరించుచు తులసీదాసు తన తనువును వీడి, పరమపదమును జేరెను.

www.vimalvimarsh.com

ISSN : 2348 - 5884

विमल-विमर्श

वार्षिक शोध–पत्रिका

A Multi-disciplinary Refereed Research Journal

Vol. 1 (Special Edition) Year : 6, 2018

INTERNATIONAL CONFERENCE

Executive Editor

Dr. P.K. Jayalakshmi

Editor

Vinay Kumar Shukla *'Vidrohi'*

St. Joseph's College for Women (A)

Reaccredited by NAAC with A Grade

Visakhapatnam - 530 004 (A.P.), Ph. : 0891-2558346

e-mail : sjcwvizag@gmail.com, web : www.stjosephsvizag.com

31. ఇనాక్ నాటకాలు - స్త్రీ వాదం

కనపాల. జోసఫ్
అంధ్రోపన్యాసకులు
ఆంధ్రక్రైస్తవ కళాశాల, గుంటూరు. ఆం.ప్ర.
చరవాణి : 9849025505

1939 జూలై -1 తారీఖున జన్మించిన ఆచార్య కొలకలూరి ఇనాక్ గారు బహుగ్రంధకర్త, బహుముఖ ప్రజ్ఞాశాలి. సమకాలిక సాహితీ జగత్తులో సుప్రసిద్ధ విమర్శకుడు. కవి. రచయిత. కధకుడు. నాటకకర్త. కవిత్వం, నాటకం, నవల, కథ, వ్యాసం, విమర్శ, పద్యంలాంటి అన్ని ప్రక్రియల్లో చేయి తిరిగిన వ్యక్తులు తెలుగు సాహిత్యంలో అరుదుగా కనిపిస్తారు. అలాంటి వారిలో ఆచార్య కొలకలూరి ఇనాక్ గారు ఒకరు.

'కావ్వేషు నాటకం రమ్యమ్' అనీ 'నాటంకాంతం హి సాహిత్యమ్' అనీ సంస్కృత అలంకారికులు నాటక సాహిత్య విశిష్టతను చెప్పి ఉన్నారు. శ్రవ్య, దృశ్యకావ్యాలలో దృశ్యకావ్యాలలో దృశ్యకావ్యాలకే సాహితీ లోకంలో గౌరవాదరణలు మెండు. ఒక విషయాన్ని విని అర్థం చేసుకోవడంలో సౌలభ్యం ఉంది. దృశ్యకావ్యానికి మనసుకు హత్తుకుపోయే లక్షణం ఉంది. ప్రేక్షకుల హృదయాల్లో పదికాలాల పాటు సుస్థర స్థానాన్ని దృశ్యకావ్యాలు సంపాదించుకొంటాయి. నడుస్తున్న కాలంలో నాటక సాహిత్య రచయితల్లో చెప్పుకోదగిన కొద్ది మందిలో ఇనాక్ ఒకరు. ముఖ్యులు కూడా.

ఇనాక్ సాక్షి, ముని వాహనుడు లాంటి మత సంబంధ ఇతివృత్తాలున్న నాటకాలను, నాగార్జునుడు లాంటి చారిత్రక నాటకాన్ని, కీ, మనలాంటి మనిషి, జై హింద్ లాంటి సాంఘిక నాటకాలనూ రాశారు. 1950-70ల నడిమి కాలంలోని సినీ జీవిత నేపథ్యంలో రాసిన నాటకం 'కీ'. 1962లో జరిగిన చైనా దురాక్రమణ ఇతివృత్తంతో రాసిన 'జైహింద్' నాటకం దేశభక్తి ప్రబోధకంగా ఉంటుంది. 'మనలాంటి మనిషి' నాటకంలో దారి తప్పిన స్త్రీ అగచాట్లను రామాయణ కథాంసంతో అభేదం కల్పిస్తూ మానవ సంబంధాలు చిత్రించబడ్డాయి. స్త్రీని కేంద్ర బిందువుగా నిల్పి రాసిన నాటకం 'మనలాంటి మనిషి' స్త్రీ వాద దృష్టితో రాసిన నాటకంగా ఇది నిలుస్తుంది.

స్త్రీ పురుష సంబంధాలు ఈ నాటకంలో ప్రధానంగా చర్చింబడిన అంశం స్త్రీ పురుష సంబంధాలలో ద్వంద్వనీతి. వివాహేతర సంబంధాలని గ్లోరిఫై చేసిన సమాజమే విధిలేని పరిస్థితుల్లో అవసరార్థం తప్పుదారి పట్టిన స్త్రీలను మాత్రం వేధించి వెంట తరుముతుంది. ఈ అంశాన్నే ఇతి వృత్తంగా 'మనలాంటి మనిషి' నాటకం రచించబడింది. స్త్రీకి ప్రమాదవశాత్తు ఏర్పడిన అవాంఛనీయ పరిస్థితుల్ని అనుకూలంగా చేసుకొని సంఘం ఆమెను వేధించడాన్ని ఈ నాటకం చక్కగా చిత్రించింది. ప్రత్యక్షంగానూ ఎన్నోరకాలుగా దోపిడీకి గురవుతున్న స్త్రీని ప్రధాన పాత్రగా మలిచి, ఆమె సమస్యలకు పరిష్కారాన్ని కూడా రచయిత సూచించాడు. ఈ నాటకంలో రామ బ్రహ్మం, రామలింగం, రామకోటి రామ్మూర్తి, ఆంజనేయులు, చలమయ్య, రాజారావు అనే పురుష పాత్రలు, సీత అనే స్త్రీ పాత్ర ఉన్నాయి. రెండు తప్ప మిగిలిన అన్ని పేర్లూ రామాయణ ఇతిహాస సంబంధమైన పేర్లే. రాముడు కూడా మనలాంటి మనిషేనన్న తత్వాన్ని ఈ నాటకంలో రచయిత ఇమిడ్చాడు. రామాయణంలో రాముడు సీత కోసం శ్రమిస్తే, నాటకంలో రామ్మూర్తి కోసం సీత శ్రమిస్తుంది.

రామాయణంలో రాముని ఎడబాటు భరించలేని స్త్రీ ఉంటే; సీత ఎక్కడుంటే నేనూ అక్కడే అని రామ్మూర్తి ఈ నాటకంలో అంటాడు. ఇంకా ఎన్నో రామాయణాంశాలను నాటకంలో సర్మగర్భంగా దర్శనమిస్తాయి.

సంపన్న కుటుంబంలో పుట్టిన సీత రామబ్రహ్మంతో కలిసి కాలు బైట పెట్టడమేకాక కాలు జారింది. మోసపోయిన సీత వేశ్యా గృహంలో కొంతకాలం గడిపి కన్నవారిల్లు చేరిన సీతకు ఆదరణ దొరకలేదు. పైగా తనపై హత్యాప్రయత్నం జరగబోతుండగా తప్పించుకొని బైటపడుతుంది. మొదట రామలింగానికీ, తర్వాత రామ్మూర్తికీ భార్య అవుతుంది. మొదటి భర్త రామలింగం దగ్గర కష్టాల్ని, అవమానాల్ని భరిస్తుంది.. తనను మనసారా ప్రేమించి ఆదరించిన రామ్మూర్తి కోసం పడుపువృత్తి చేసి అతన్ని బ్రతికించుకొంటుంది. తర్వాతి రోజుల్లో రామ్మూర్తి గొప్ప పేరు ప్రఖ్యాతులు తెచ్చుకొనే విధంగా సీత సహకరిస్తుంది. రామ్మూర్తికి సీత నైతికమైన అండ. ఈ విషయాలన్నిటినీ తనకు జరిగిన సన్మాన కార్యక్రమంలో సభముందు చెప్పి ప్రస్తుత సామాజిక వ్యవస్థను సంఘసంస్కరణావశ్యకతను వివరించే ప్రయత్నం చేస్తాడు రామ్మూర్తి.

ఈ నాటకంలో పతిత అయిన సీతను రామ్మూర్తి స్వీకరించడం విలక్షణమైన, విసూత్నమైన, విప్లవాత్మకమైన అంశంగా పాఠకులు లేదా ప్రేక్షకులు గుర్తిస్తారు. సన్మాన గ్రహీత రామ్మూర్తి తనకు సాయపడిన వారికే ఈ సన్మానం చెందుతుందని, తన సన్మానాన్ని 'సీత'కు అంకింత చేయటం రెండవ అంశం. సన్నివేశ చిత్రణ బలంగా ఉన్న నాటకంలో నాటి సామాజిక ఇతివృత్తం ప్రధాన అంశం. మొదట సీత ప్రేమించిన రామబ్రహ్మం పలాయనం, తర్వాత ఒంటరిగా మిగిలిన సీతతో రామలింగంల సాహచర్యం వల్ల కలిగిన కష్టాల కన్నీళ్ళు, చివరగా సీతారామ్మూర్తుల అన్యోన్య దాంపత్యం, చలమయ్య రామారావు నీచ వృత్తాంతాలు నాటక సన్నివేశాలకు పతాక శీర్షికలు. 'లోకో భిన్న రుచిః' అన్నది ఆర్యోక్తి. భిన్నమైన అలవాట్లు, భినమైన వేషభాషలతో కలగలిపిన సంఘం విభిన్న మనస్తత్వాల కూడలి. ఈ నాటకంలో మనకు నిత్యం తారసపడే సంఘటనలే చోటు చేసుకొని ఉన్నాయి. రామబ్రహ్మాన్ని ప్రేమించి మోసపోయిన సీత ఒంటరిగా కనిపించడం, రామలింగం ప్రలోభానికి లోబడి అతనితో అవస్థలు పడటం, చివరికి రామ్మూర్తి నీడలో జీవితాన్ని సార్థకం చేసుకోవడం 'సీత' ఒడిదుడుకుల జీవితంలోని ఘట్టాలు. తెలిసీ తెలియని వయసులో తప్పు చేయటం విశ్లేషిస్తూ, మేడిపండు మనస్తత్వం లాంటి సమాజం స్త్రీ మనస్సులోని పవిత్రతను చూడదు. కాబట్టి విధిలేక పతితగా మారిన స్త్రీని పశువుకన్నా హీనంగా చూడకుండా, ఆమెలోని అంతరంగాల్ని గమనించి ఆమెలోని సహజమైన సంస్కారానికి విలువనివ్వాలి - అనే ఉద్దేశ్యాన్ని రచయిత ఈ నాటకం ద్వారా సమాజానికి తెలియజేశాడు.

బహు భార్యత్వం కల్గిన పురుషున్ని శృంగార పురుషుడిగా లోకం కీర్తిస్తుంది. అదే విధంగా బహు బహుబహర్భృత్వం వున్న స్త్రీలను సమాజం దూషిస్తుంది. పితృస్వామిక వ్యవస్థలో పురుషున్ని సమర్థించడం, స్త్రీని నిందించడం, అనాది కాలంగా ఆనవాయితీ అయిపోయింది. కానీ దారి తప్పిన స్త్రీల చర్యల్ని పక్కన పెట్టి వారిలోని మానవతా విలువల్ని, అంచనా వేయాలనేది స్త్రీవాదులు అభిమతం. అంతేగాక గతి తప్పిన నిస్సహాయ స్త్రీ పట్ల పురుషులు నెరపే సంబంధాలకు పురుషుల కరివేపాకు మనస్తత్వాలకూ ఈ నాటకం అద్దమే.

'స్త్రీ' సమాజంలో అన్ని విధాలుగా సమానత్వం సాధించడానికి వివిధ కారణాలు ఆటంకాలు అయినట్లే 'కులం' కూడా ఒక ఆటంకం అని నిరూపించి, ఆ కుల అసమానత్వాన్ని చెరిపి కులరహిత సమాజ నిర్మాణం జరిగి సమసమాజ నిర్మాణం రావాలని ఆకాంక్షించడం కనిపిస్తుంది.

DECOMPOSITION OF PRE A*- ALGEBRA WITH M_x

D. Kalyani
Lecturer in Mathematics, D. S. Government College for Women, Ongole - 523 001, A.P., India. Email: satyakalyani27@gmail.com
B. Rami Reddy
Head, Dept. of Mathematics, Hindu College, Guntur, A.P., India
J.Venkateswara Rao
Professor of Mathematics, Mekelle University, Mekelle, Ethiopia
Email: venkatjonnalagadda@yahoo.co.in
B. Vijaya Kumar
Lecturer in Mathematics, A.C. College, Guntur, A.P., India

Abstract: This paper is a study on the decomposition of Pre A*- algebra. In fact, it is proved that if A is a Pre A*- algebra and $x \in A$, then the set, $M_x = \{s \in A / s \leq x\}$ is a Pre A*- algebra under the induced operations $\wedge,\vee$ where the complementation is defined by $s^* = x \wedge s^{\sim}$, the relation $\leq$ (less than or equal to) defined on Pre A*- algebra A by $s \leq x$ if $s \wedge x = x \wedge s = s$. Based on the well known result, if B is a Boolean algebra and $a \in B$, the set $(a] = \{x \in B / x \leq a\}$ ($[a) = \{x \in B / a \leq x\}$) is a Boolean algebra under the induced operations $\wedge$, $\vee$ where the complementation is defined by $x^* = a \wedge x'$ ($x^* = a \vee x'$), and then B is isomorphic to $(a] \times [a)$, it is attested a similar decompositions for a Pre A*- algebra as well.

Keywords: Centre of Pre A*- Algebra, Decomposition of Pre A*- Algebra, Pre A*- Algebra, Pre A*- Isomorphism.

1. Introduction: Koteswara Rao (1994) firstly introduced the notion of A*- algebras and if-then-else structures based on Manes (1993) Adas and the Equational Theory of If-then-else. Later, Venkateswara Rao (2000) introduced the concept of Pre A*- algebras as a reduct of A*- algebra. Venkateswara Rao and Srinivasa Rao (2010) studied the well known Cayley's theorem on centre of Pre A*- algebras. Furthermore, Venkateswara Rao et.al., (2011) observed a decomposition of Pre A*- algebra.
In this manuscript, we will continue our study to establish some more results in this conception.

2. Preliminaries:
Definition: An algebra $(A, \wedge, \vee, (-)^{\sim})$ where A is a nonempty set with 1; $\wedge$, $\vee$ are binary operations and $(-)^{\sim}$ is an unary operation satisfying
(i) $x^{\sim\sim} = x$, for all $x \in A$
(ii) $x \wedge x = x$, for all $x \in A$
(iii) $x \wedge y = y \wedge x$, for all $x, y \in A$
(iv) $(x \wedge y)^{\sim} = x^{\sim} \vee y^{\sim}$, for all $x, y \in A$
(v) $x \wedge (y \wedge z) = (x \wedge y) \wedge z$, for all $x, y, z \in A$
(vi) $x \wedge (y \vee z) = (x \wedge y) \vee (x \wedge z)$, for all $x, y, z \in A$
(vii) $x \wedge y = x \wedge (x^{\sim} \vee y)$, for all $x, y \in A$, is called a Pre A*- algebra.

Example: 3 = {0, 1, 2} with operations $\wedge$, $\vee$, $(-)^{\sim}$ defined below is a Pre A*- algebra.

$\wedge$	0	1	2
0	0	0	2
1	0	1	2
2	2	2	2

$\vee$	0	1	2
0	0	1	2
1	1	1	2
2	2	2	2

x	$x^{\sim}$
0	1
1	0
2	2

Definition: Let A be a Pre A*- algebra. An element $x \in A$ is called central element of A if $x \vee x^{-} = 1$ and the set $\{x \in A / x \vee x^{-} = 1\}$ of all central elements of A is called the centre of A and it is denoted by B (A).

Definition: Let $(A_1, \vee, \wedge, (-)^{-})$ and $(A_2, \vee, \wedge, (-)^{-})$ be two Pre A*- algebras. A mapping $f : A_1 \to A_2$ is called a Pre A*- homomorphism if
(i) $f(a \wedge b) = f(a) \wedge f(b)$; (ii) $f(a \vee b) = f(a) \vee f(b)$; (iii) $f(a^{-}) = (f(a))^{-}$.
If the homomorphism $f : A_1 \to A_2$ is onto, then, f is called an epimorphism.
If the homomorphism $f : A_1 \to A_2$ is one-one, then, f is called a monomorphism.
If the homomorphism $f : A_1 \to A_2$ is one - one and onto, then, f is called an isomorphism, and A_1, A_2 are said to be isomorphic, denoted in symbols $A_1 \cong A_2$.

Definition: Let A be a Pre A*- algebra and $x \in A$, then $M_x = \{s \in A / s \leq x\}$ with the operation $\leq$ defined by $s \leq x$ if $s \wedge x = x \wedge s = s$.
Note: M_x is a Pre A*- algebra under the induced operations $\wedge, \vee$ where the complementation is defined by $s^* = x \wedge s^{\sim}$.

3. Decompositions of Pre A*- Algebra: If B is a Boolean algebra and $a \in B$, then we know that B is isomorphic to $(a] \times [a)$. In this paper we prove a similar decomposition for a Pre A*- algebra.

Lemma: Let A be a Pre A*- algebra with 1, $a \in B(A)$ and $x, y \in A$. Then we have, $a \wedge x = a \wedge y$, $a^{\sim} \wedge x = a^{\sim} \wedge y \Leftrightarrow x = y$.

Theorem: If A is a Pre A*- algebra with 1 and $a \in B(A)$, then A can be embedded into $M_a \times M_{a^{\sim}}$.
Note: In the above theorem, for a = 0, we have $M_a = \{0, 2\}$, $M_{a^{\sim}} = \{0, 1, 2\}$ and $M_a \times M_{a^{\sim}} = \{(0, 0), (0, 1), (0, 2), (2, 0), (2, 1), (2, 2)\}$. So we can't find x such that $\alpha(x) = (2, 0)$. Hence α is not an onto mapping. But we have the following theorem.

Theorem: If A is a Pre A*- algebra with 1 and $a \in B(A)$, $M_a = \{s \in B(A) / s \leq a\}$ and $M_{a^{\sim}} = \{t \in B(A) / t \leq a^{\sim}\}$, then $B(A) = M_a \times M_{a^{\sim}}$.

Theorem: Let A be a pre A*- algebra with 1 and A_1, A_2 be pre A*- algebras with $1_1, 1_2$ respectively such that $A \cong A_1 \times A_2$. Then there exists an element $a \in B(A)$ such that $A_1 \cong M_a$ and $A_2 \cong M_{a^{\sim}}$.
Proof: Let $\phi : A \to A_1 \times A_2$ be an isomorphism and $a = \phi^{-1}(1_1, 0_2)$ (where $1_1, 1_2$ denote the $\wedge$ – identities of A_1 and A_2 respectively).
Consider, $(1_1, 0_2) \in B(A_1) \times B(A_2) = B(A_1 \times A_2)$.
So, we have, $(1_1, 0_2) \in B(A_1 \times A_2)$.
This leads to, $a = \phi^{-1}(1_1, 0_2) \in B(A)$ (as $A \cong A_1 \times A_2$).
Hence by the above we can define $f : A_1 \to M_a$ by $f(x_1) = \phi^{-1}(x_1, 0_2)$ for all $x_1 \in A_1$.
Consider, $a \wedge \phi^{-1}(x_1, 0_2)$
$= \phi^{-1}(1_1, 0_2) \wedge \phi^{-1}(x_1, 0_2)$
$= \phi^{-1}(x_1, 0_2)$ (since ϕ^{-1} is a homomorphism)
So, $a \wedge \phi^{-1}(x_1, 0_2) = \phi^{-1}(x_1, 0_2)$.
This results, $\phi^{-1}(x_1, 0_2) \in M_a$ (by definition of M_a) $\Rightarrow f(x_1) \in M_a$.
Thus f is well defined.
One can evidently examine that f preserves $\wedge, \vee$ and that f is one-one.
Now we prove that f preserves the unary operations $(-)^{\sim}$.
Let $x_1 \in A_1$.
Consider, $f(x_1^{\sim}) = \phi^{-1}(x_1^{\sim}, 0_2)$
$= \phi^{-1}(1_1 \wedge x_1^{\sim}, 0_2 \wedge 1_2)$
$= \phi^{-1}(1_1, 0_2) \wedge \phi^{-1}(x_1^{\sim}, 1_2)$ (since, ϕ^{-1} is a homomorphism)
$= a \wedge (\phi^{-1}((x_1, 0_2))^{\sim}$
$= a \wedge f(x_1)^{\sim} = f(x_1)^*$.

Therefore, we have that $f(x_1^{\sim}) = (f(x_1))^*$.
Finally we prove that f is onto.
Let $x \in M_a$.
Then $\phi(x) = (x_1, x_2)$ for some $x_1 \in A_1$ and $x_2 \in A_2$.
Consider, $(x_1, x_2) = \phi(x)$
$= \phi(a \wedge x)$
$= \phi(a) \wedge \phi(x)$
$= (1_1, 0_2) \wedge (x_1, x_2)$
$= (x_1, 0_2)$.
Therefore, $(x_1, x_2) = (x_1, 0_2)$.
Thus, $x_2 = 0_2$ and $f(x_1) = \phi^{-1}(x_1, 0_2) = \phi^{-1}(x_1, x_2) = x$(by above).
Hence, f is onto.
Thus, $A_1 \cong M_a$.
Similarly, one can verify that, $A_2 \cong M_{a^{\sim}}$.
Hence, we conclude that,

$$A \cong A_1 \times A_2$$
$$\cong M_a \times M_{a^{\sim}}$$

Hence we must have, $A \cong M_a \times M_{a^{\sim}}$.
Note: We remark that for $a, b \in B(A)$ with $a \wedge b = 0$ (we can call such a pair (a, b) as distinct orthogonal), we derive a necessary and sufficient condition for M_a to be isomorphic to M_b.

Lemma: If A is a Pre A*- algebra with 1, $a \in B(A)$, $x \in M_a$ and $y \in M_{a\sim}$, then
(i) $a \wedge y = 0$ and $a^{\sim} \wedge x = 0$
(ii) $a \wedge (x \vee y) = x = a \wedge (y \vee x)$ and $a^{\sim} \wedge (x \vee y) = y = a^{\sim} \wedge (y \vee x)$.
Proof: Let $x \in M_a$ and $y \in M_{a\sim}$.
Then we have, $x \leq a$ and $y \leq a^{\sim}$.
This leads to, $x \wedge a = x$ and $y \wedge a^{\sim} = y$.
Consider, $a \wedge y$.
$a \wedge y = a \wedge (y \wedge a^{\sim})$ (since, $y = y \wedge a^{\sim}$)
$= (a \wedge a^{\sim}) \wedge y$
$= 0 \wedge y$
$= 0$.
Hence, $a \wedge y = 0$.
Also Consider $a^{\sim} \wedge x$
$a^{\sim} \wedge x = a^{\sim} \wedge x \wedge a$ (as $x \wedge a = x$)
$= (a^{\sim} \wedge a) \wedge x$
$= 0 \wedge x$
$= 0$.
So, $a^{\sim} \wedge x = 0$.
Hence by above, we must have, $a \wedge y = 0 = a^{\sim} \wedge x$.
Furthermore, consider, $a \wedge (x \vee y)$
$a \wedge (x \vee y) = (a \wedge x) \vee (a \wedge y)$
$= x \vee 0$
$= x$.
Hence, $a \wedge (x \vee y) = x$.
Further, $a \wedge (y \vee x) = (a \wedge y) \vee (a \wedge x)$
$= 0 \vee x$ (by above)
$= x$.
Hence, we have $a \wedge (y \vee x) = x$
Therefore, $a \wedge (y \vee x) = a \wedge (x \vee y)$ (By above).
In the same way, we can observe that $a^{\sim} \wedge (x \vee y) = a^{\sim} \wedge (y \vee x)$.

Lemma: Let A be a pre A*- algebra with 1. Then, for any a, $b \in B(A)$, $a \wedge b \in B(M_a)$.
Proof: Clearly we have, $a \wedge b \leq a$.

Hence $a \wedge b \in M_a$ (as $M_a = \{s \in B(A)/s \leq a\}$.
Consider, $(a \wedge b) \vee (a \wedge b)^*$
$= (a \wedge b) \vee (a \wedge (a \wedge b)^{\sim})$ (By definitions of *).
$= (a \wedge b) \vee (a \wedge (a^{\sim} \vee b^{\sim}))$
$= (a \wedge b) \vee ((a \wedge a^{\sim}) \vee (a \wedge b^{\sim}))$
$= (a \wedge b) \vee (o \vee (a \wedge b^{\sim}))$ (since, $a \wedge a^{\sim} = o$ as $a \in B(A)$)
$= (a \wedge b) \vee (a \wedge b^{\sim})$
$= a \wedge (b \vee b^{\sim})$
$= a \wedge 1$
$= a$.
Hence, $(a \wedge b) \vee (a \wedge b)^* = a$.
Therefore, $a \wedge b \in B(M_a)$ (as $(-)^*$ is an operation in M_a to satisfy the condition for an element in $B(M_a)$).

Theorem: Let A, A_1, A_2 be Pre A*- algebras with 1, 1_1, 1_2 respectively such that $A \cong A_1 \times A_2$. Let $a, b \in B(A)$ such that $a \wedge b = o$. Then M_a is isomorphic to M_b if and only if there exists an isomorphism $\alpha : A \to A$ such that $\alpha(a) = b$.
Proof: Let $a, b \in B(A)$ with $a \wedge b = o$.
Let us suppose that $\phi : M_a \to M_b$ be an isomorphism.
Consider $a^{\sim} \wedge b = (a^{\sim} \wedge b) \vee o$
$= (a^{\sim} \wedge b) \vee (a \wedge b)$ (as $a \wedge b = o$)
$= (a^{\sim} \vee a) \wedge b$
$= 1 \wedge b$ (as $a \in B(A)$, $a^{\sim} \vee a = 1$)
$= b$.
This implies, $a^{\sim} \wedge b = b$.
This results, $b \in M_{a^{\sim}}$ (By definition of $M_{a^{\sim}}$) and $b^* = a^{\sim} \wedge b^{\sim}$.
As $a^{\sim} \wedge b = b$, in the same way one can observe that $b^{\sim} \wedge a = a$ (Simply by inter-changing the roles of a and b). Then we have the following:
(i) $A \cong A_1 \times A_2$
$\cong M_a \times M_{a^{\sim}}$
$\cong M_a \times M_{a^{\sim} \wedge b} \times M_{(a^{\sim} \wedge b)^*}$ (follows by the sequence of decompositions and isomorphisms)
$\cong M_a \times M_b \times M_{a^{\sim} \wedge b^{\sim}}$ (since, as $a^{\sim} \wedge b = b$ and $(a^{\sim} \wedge b)^* = a^{\sim} \wedge b^{\sim}$)
The above holds under the isomorphism, $x \xrightarrow{\beta} (a \wedge x, b \wedge x, (a^{\sim} \wedge b^{\sim}) \wedge x)$.
Similarly,
(ii) $A \cong M_b \times M_{b^{\sim}}$
$\cong M_b \times M_{b^{\sim} \wedge a} \times M_{(b^{\sim} \wedge a)^*}$
$\cong M_b \times M_a \times M_{a^{\sim} \wedge b^{\sim}}$
The above holds under the isomorphism, $x \xrightarrow{\gamma} (b \wedge x, a \wedge x, (a^{\sim} \wedge b^{\sim}) \wedge x)$.
Similarly we have,
(iii) $M_a \times M_b \times M_{a^{\sim} \wedge b^{\sim}} \cong M_b \times M_a \times M_{a^{\sim} \wedge b^{\sim}}$ holds under the isomorphism, $(x, y, z) \xrightarrow{\delta} (\phi(x), \phi^{-1}(y), z)$.
Now define $\alpha : A \to A$ by $\alpha = \alpha^{-1} o \delta o \beta$, where, o denotes the composition of mappings.
Then α is an isomorphism of A onto A and
$\alpha(a) = (\gamma^{-1} \text{ o } \delta \text{ o } \beta)(a)$
$= \gamma^{-1}(\delta(a, 0, 0))$ (since $b \wedge a = 0 = a \wedge a^{\sim}$)
$= \gamma^{-1}(b, 0, 0)$ (since, $\phi(a) = b$, $\phi(0) = 0$)
$= b$ (since $\gamma(b) = (b, 0, 0)$).
Hence, α is an isomorphism of A such that $\alpha(a) = b$.
Conversely, suppose that, $\alpha: A \to A$ is an isomorphism such that $\alpha(a) = b$.
Let λ be the restriction of α to M_a.
Now, we prove that, λ is an isomorphism of M_a onto M_b.
For $x \in M_a$,
consider, $b \wedge \lambda(x) = b \wedge \alpha(x)$
$= \alpha(a) \wedge \alpha(x)$
$= \alpha(a \wedge x)$

$= \alpha(x)$
$= \lambda(x)$.

Hence we have, $b \wedge \lambda(x) = \lambda(x)$. This leads to $\lambda(x) \in M_b$.
Hence λ is well defined.
One can easily verify that, λ is a homomorphism and one-one.
We shall prove that λ is onto.
Let $x \in M_b$. Since α is onto, there exists $y \in A$ such that $\alpha(y) = x$.
Consider, $a \wedge y \in M_a$.
Then, $\lambda(a \wedge y) = \alpha(a \wedge y) = \alpha(a) \wedge \alpha(y)$
$= b \wedge x$
$= x$ (since, $x \leq b$).
Hence, we have $\lambda(a \wedge y) = x$.
Hence λ is an isomorphism of M_a onto M_b.

Concluding Remarks: This study made us to conclude the following:
If A is a Pre A*- algebra and $x \in A$, then the set $M_x = \{s \in A / s \leq x\}$ with the operation $\leq$ defined by $s \leq x$ if $s \wedge x = x \wedge s = s$ is a Pre A*- algebra under the induced operations $\wedge, \vee$ where the complementation is defined by $s^* = x \wedge s^{\sim}$.
If A is a Pre A*- algebra with 1, $a \in B(A)$ and $x, y \in A$, then we have obtained, $a \wedge x = a \wedge y$, $a^{\sim} \wedge x = a^{\sim} \wedge y$ if and only if $x = y$.
If A is a Pre A*- algebra with 1 and $a \in B(A)$, then A can be embedded into $M_a \times M_{a^{\sim}}$.
We note that in the above theorem, for $a = 0$, we have $M_a = \{0, 2\}$, $M_{a^{\sim}} = \{0, 1, 2\}$ and $M_a \times M_{a^{\sim}} = \{(0, 0), (0, 1), (0, 2), (2, 0), (2, 1), (2, 2)\}$. So we can't find x such that $\alpha(x) = (2, 0)$. Hence α is not an onto mapping.
If A is a Pre A*- algebra with 1 and $a \in B(A)$, $M_a = \{s \in B(A) / s \leq a\}$ and $M_{a^{\sim}} = \{t \in B(A) / t \leq a^{\sim}\}$, then $B(A) = M_a \times M_{a^{\sim}}$.
If A is a Pre A*- algebra with 1 and A_1, A_2 are Pre A*- algebras with 1_1, 1_2 respectively such that $A \cong A_1 \times A_2$, then there exists an element $a \in B(A)$ such that $A_1 \cong M_a$ and $A_2 \cong M_{a^{\sim}}$.
We remarked that for $a, b \in B(A)$ with $a \wedge b = 0$, we derive a necessary and sufficient condition for M_a to be isomorphic to M_b.
We obtained that if A is a Pre A*- algebra with 1, $a \in B(A)$, $x \in M_a$ and $y \in M_{a^{\sim}}$, then
(i) $a \wedge y = 0$ and $a^{\sim} \wedge x = 0$
(ii) $a \wedge (x \vee y) = x = a \wedge (y \vee x)$ and $a^{\sim} \wedge (x \vee y) = y = a^{\sim} \wedge (y \vee x)$.
Further, if A is a Pre A*- algebra with 1, then, for any a, $b \in B(A)$, $a \wedge b \in B(M_a)$.
It is observed that if A, A_1, A_2 be a Pre A*- algebras with 1, 1_1, 1_2 respectively such that $A \cong A_1 \times A_2$. and $a, b \in B(A)$ such that $a \wedge b = 0$, then M_a is isomorphic to M_b if and only if there exists an isomorphism $\alpha : A \to A$ such that $\alpha(a) = b$.

References:

1. Koteswara Rao.P(1994):, A*- algebras and if-then- else structures (Doctoral thesis), Acharya Nagarjuna University, A.P., India, 1994.
2. Manes E.G. (1993): Adas and the Equational Theory of If-then –else, Algebra Universalis, 30(1993), 373-394.
3. Venkateswara Rao.J(2000): On A*-algebras (Doctoral thesis), Acharya Nagarjuna University, A.P., India 2000.
4. Venkateswara Rao. J and Srinivasa Rao. K, (2010): Cayley's theorem on centre of Pre A*-algebras, International Journal of Computational and Applied Mathematics Vol 5, No.1 (2010), pp. 103–111.
5. Venkateswara Rao. J, Srinivasa Rao. K, Kalyani. D: Decomposition of Pre A*-Algebra, International Journal of Mathematical Sciences and Applications, Vol. 1 No. 1 (January, 2011).

***

Available online at www.joac.info

ISSN: 2278-1862

Journal of Applicable Chemistry

2018, 7 (5): 1137-1142

(International Peer Reviewed Journal)

Isolation and Identification of Bio Active Photochemical Compounds from *Ventilago denticulata* Stem using GC-MS

J. Rajendra Kumar[1*], P. Anitha Pranuti[1], M. Kusuma Kumari[1], M.Kanthi Kirani[1] and K. Bhagya Lakshmi[2]

1. Dept of Chemistry, Andhra Christian College, Guntur, INDIA
2. Dept of Chemistry, Govt. College for Women, Bapatla, INDIA

Email: rajendrakumarjeli@gmail.com

Accepted 20th August, 2018

ABSTRACT

The present study explore the primary phytochemical study using gas chromatography-mass spectroscopy (GC-MS) and in vitro antimicrobial study (against gram positive bacteria and gram negative bacteria) was performed on n-hexane(50%)+Benzene (25%)+25% ethanol stem extract of Ventilago denticulata. Preliminary phytochemical screening revealed that plant contains 17bio active compounds with different concentrations. Qualitative analysis of the plant parts the presence of various components of therapeutic importance including tannins, saponins, phenolic compounds, glycosides, flavonoids etc., The present study provides information about the availability of some bio active phytoconstituents, which can be useful to provide dietary elements and it may also help in developing new drug formulations. There was a need to evaluate the extracts of the plant in order to provide scientific proof for its application and to explore the possibility of treating various diseases and disorders. Literature review indicates that very less work has been done on this plant and there is a wide scope for investigation.

Graphical Abstract

Ventilago denticulata stem [Family: Rhamnaceae]

Keywords: Isolation, Bio active photochemicals, *Ventilago denticulata*, Stem extract GC-MS.

INTRODUCTION

Plant secondary metabolites have been referred to as phytochemical compounds that are naturally occurring and have potential disease inhibiting capabilities. Phytochemicals are excellent sources of many bioactive compounds, such as volatile oils, steroids, alkaloids and natural antioxidants, i.e., flavonoids and other phenolic compounds, with beneficial effects on human health [1]. Herbal medicine has been practiced worldwide and it is recognized by WHO as essential building blocks for primary health care. WHO has estimated that up to 80 % of people still rely on traditional remedies, which are 21,000 plants around the world, among them 2500 species are in India, out of these 150 species are commercially used [2]. Hence standardization of medicinal plants and natural products will provide useful information with regards to its correct identity and will help to differentiate from other closely related species as well as from other commercially available crude drugs.

The development of microbial resistance towards antibiotics has highlighted the importance of the search for new potential effective plants and plant constituents against pathogenic microorganisms [3]. Antimicrobial screening of plant extracts and the phytochemical represent a starting point for antimicrobial drug discovery [4]. *V. denticulata* (Rhang Dang) belonging to the family Rhamnaceae (Figure 1). It is considered as an important medicinal plant by the traditional people of tribal people in India. Various parts of the plants used for treatment of many diseases. The plant is rich in many pharmaceutical active ingredients. The stem bark contains Friedel in and several anthraquinones that can be applied to treat skin diseases and sprains. The root contains anthraquinones, ventinones A and B, used for a tonic dyspepsia, mild fever and debility. The leaves give lupeol, betasitosterol and its glucoside [5]. The ethanolic extract of plant also shoes anti-inflammation and anti-microbial activity [6]. V. *denticulata* leaves are often used as tea products. Frequently drunk, it can help to diuretic cure, reduce cholesterol and blood sugar, serve as a relaxant, strengthen health, arthritis, reduce blood pressure and diet. The present study reports on the phytochemical analysis and antimicrobial activities of various extracts from *Ventilago denticulata* stem using GC-MS analysis.

Available online at www.joac.info

ISSN: 2278-1862

Journal of Applicable Chemistry

2018, 7 (5): 1132-1136

(International Peer Reviewed Journal)

Pesticide Residues in Selected Vegetables Collected from Local Markets in Vijayawada City

M. Krishna Murthy [1]*, N. J. Solomon Babu[2], M. J. Kennedy[2], Y. Durga Prasad[3] and M. Kamala Karuna[3]

1. Acharya Nagarjuna University Research Center, SVRM College, Nagarjuna - 522268, INDIA
2. Department of Chemistry, Andhra Christian College, Guntur – 522001, INDIA
3. Department of Chemistry, Government Degree College for Women, Guntur – 522001, INDIA

Email: mannamkm@gmail.com

Accepted 15th August, 2018

ABSTRACT

Vegetable samples of green chilly, cabbage, tomato and brinjal collected from market in five regions of Vijayawada municipality in April 2017. Selected vegetables tested for the presence of pesticide residues like pyrethroids, organo chlorine compounds and organo phosphorous compounds using a gas chromatograph equipped with electron capture and Thermo sensitive detectors of the samples tested, chilly, cabbage, Tomato and brinjal were found to have pesticide residues in above the permissible residues. Among the organo chlorine compounds α-endosulfan, was detected in 2.34 % of the samples with residues. These were taken from green chili and cabbage samples. Parathyroid residues, such as deltamethrin detected in 10.24 % of the samples with residues in tomato and brinjal, organo phosphate compound residues such as chlorpyrifos and Malathion were found in 18 % of the samples with residues, which were taken from all vegetable of the positive samples. 10.2 % were found contain residues exceeding the prescribed maximum residue limit. The average pesticide residue content across all the vegetable samples was ranging from 0.04 to 1.024 ppm.

Graphical Abstract

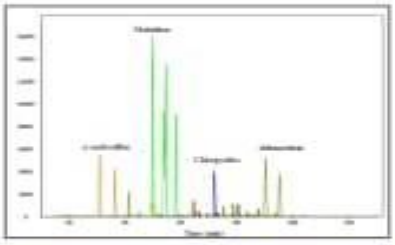

GC MS spectra of pesticide residues in the vegetable samples

Keywords: Pesticide Residues, Vegetable samples.

INTRODUCTION

Pesticides are chemical substances used to kill insects and animals that destroy crops. They are characterized by pronounced persistence against chemical/biological degradation, high environmental mobility, strong tendency for bioaccumulation in human and animal tissues, and significant impacts on human health and the environment, even at extremely low concentrations [1]. Pesticides such as insecticides, herbicides, fungicides and acaroids are an abundant and diverse group of chemical compounds. Pesticides are widely applied during cultivation and postharvest storage to improve the quantities and quality of crops and food [2]. India is one of the largest agricultural pesticide consumers worldwide and is the second largest manufacturer of pesticides in Asia. There is a sequential rise in the productionand consumption of pesticides in India during last three decades. The consumption pattern of pesticides differs from rest of the world, as in Indi. In Andhra Pradesh, vegetable cultivation has increased in recent years because of greater market demand, higher returns, and an increased awareness among farmers. This has led to large stretches of vegetable growing areas with intensive management practices. Such intensive cultivation, coupled with the availing humid tropical climate, has resulted in increased pest and disease incidence. As the vegetables are grown in 449.2 ha only, the per capita pesticide consumption in the vegetable growing areas of Andhra Pradesh (3,586g) far exceeds the national average of 450 g [3].

The intensive cultivation of vegetables has gained momentum in recent years with excessive pesticide usage due to increased market demand. As the presence of pesticide residues in food produce is a serious concern and no data are available on the levels of pesticide residues in vegetables, a study was conducted to ascertain the presence of pesticide residues in major vegetables used locally in Vijayawada town of Andhra Pradesh at different locations.

MATERIALS AND METHODS

3.3.1 Number of research papers published per teacher in the Journals notified on UGC CARE list during the last five years

Title of paper	Name of the author/s	Department of the teacher	Name of the Journal	Year of Publication	ISSN number	Link to the recognition in UGC enlistment of the Journal /Digital		
						Link to website of the Journal	Link to article / paper / abstract of the article	Is it listed in UGC CARE list
HASYACHANDRIKA "AADHUNIKA SAAHITYAMLO HAASYA PRAADAANYATA"	Dr . K . Joseph	Telugu	NATIONAL SEMINAR	2023	2394-5427			YES
HEAT TRANSFER IMPACTS ON CASSON FLUID FLOW	Dr.K.Moses	Mathematics	JOURNAL OF APPLIED SCIENCE AND COMPUTATIONS (JASC)	2022	0022-1945	https://j-asc.com/	https://drive.google.com/file/d/1nMww6f3xFBPxWnzTYMROmDkaBj2c5cnz/view	YES
ON FNS-COMPACTNESS IN FUZZY NEUTROSOPHIC SUPRA TOPOLOGICAL SPACES	Dr.K.Moses	Mathematics	JOURNAL OF PHYSICS : CONFERENCE SERIES	2022		https://iopscience.iop.org/journal/1742-6596	https://iopscience.iop.org/issue/1742-6596/2332/1	YES
THE INFLUENCE OF CU2+ IONS ON THE IONIC, ELECTRONIC CONDUCTIVITY AND OPTICAL CHARACTERISTICS OF LI2O-SRO-B2O3 SYSTEM	P.M.Vinaya Teja	Physics	JOURNAL OF NON-CRYSTALLINE SOLIDS	2022	0022-3093	www.elsevier.com/locate/jnoncrysol	https://www.sciencedirect.com/science/article/abs/pii/S0022309321005731	YES
KAASIPATNAM RAMARAO KATHALU - SAMAJIKA NEPADHYAM	Dr . K . Joseph	Telugu	INTERNATIONAL JOURNAL OF MULTIDISCIPLINARY EDUCATIONAL RESEARCH	2022	2277-7881	www.ijmer.in	http://s3-ap-southeast-1.amazonaws.com/ijmer/pdf/volume11/volume11-issue12(3)/volume11-issue12(3)-2022.pdf	YES
INDOLE -3 ACETIC ACID PRODUCTION BY ASPERGILLUS SPECIES ISOLATED FROM CHILLI RHIZOSPHERES	Dr.D.Phebe Sarah	Botony	INTERNATIONAL JOURNAL OF SCIENCE ACADEMIC RESEARCH	2021	2321-4007	https://bbrc.in/	http://www.scienceijsar.com	YES
CHARACTERIZATION OF L-ASPARGINASE AND LIPASE PRODUCING ASPERGILLUS SP. DPB-365 ISOLATED FROM CHILLI RHIZOSPHERES	Dr.D.Phebe Sarah	Botony	INTERNATIONAL JOURNAL OF SCIENCE ACADEMIC RESEARCH	2021	2582-6425	http://www.scienceijsar.com	Characterization of l-Asparginase and lipase producing Aspergillus sp. dpb-365 isolated from Chilli Rhizospheres | IJSAR (scienceijsar.com)	YES
OPTIMIZATION STUDIES ON PLANT GROWTH PROMOTING BACTERIAL ISOLATES FROM CHILLI RHIZOSPHERE	Dr.D.Phebe Sarah	Botony	INTERNATIONAL JOURNAL OF CREATIVE RESEARCH THOUGHTS (IJCRT)	2021	2320-2882	www.ijcrt.org	https://ijcrt.org/papers/IJCRT2008269.pdf	YES

AUSTRALIAN ABORIGINE'S CRAVING FOR LIBERATION FROM THE WHITES' SO CALLED LEGITIMATE PROTECTION BOARD: AN ANALYTICAL STUDY	G. Anna Shalini	English	LITERARY ENDEAVOUR	2021	0976-299X	www.literaryendeavour.org	https://www.literaryendeavour.org/files/8taotcrmqvcs4jdb8vik/2021-07%2016.%20AUSTRALIAN%20ABORIGINE'S%20CRAVING%20FOR%20LIBERATION%20FROM%20THE%20WHITE%20SO%20CALLED%20LEGITIMATE%20PROTECTION%20BOARD%20AN%20ANALYTICAL%20STUDY%20-%20Anna%20Shalini%20Garapati%20&%20Dr.%20Sarakanam%20Srinivas.pdf	YES
CHARACTERIZATION OF CHITINASE PRODUCING BACILLUS SPECIES ISOLATED FROM CHILLI RHIZOSPHERES OF GUNTUR DISTRICT ANDHRA PRADESH	Dr.D.Phebe Sarah	Botany	WORLD JOURNAL OF PHARMACEUTICAL RESEARCH	2020	2277-7105	www.wjpr.net	Abstract File (wjpr.net)	YES
INDOLE 3- ACETIC ACID PRODUCTION BY ASPERGILLUS SPECIES ISOLATED FROM CHILLI RHIZOSPHERES	Dr.D.Phebe Sarah	Botany	BIOSCIENCE BIOTECHNOLOGY RESEARCH COMMUNICATIONS	2020	2321-4007	https://bbrc.in/	https://bbrc.in/indole-3-acetic-acid-production-by-aspergillus-species-isolated-from-chilli-rhizospheres	YES
EFFECT OF LORATADINE TABLETS ON THE SYMPTOMATIC CONTROL OF SEASONAL ALLERGIC RHINITIS IN ADULTS CHALLENGED WITH RAGWEED POLLEN IN THE ENVIRONMENTAL EXPOSURE UNIT IN COMPASSION WITH AZELASTINE NASAL SPRAY WITH LORATADINE TABLETS, CETIRIZINE TABLETS, AND PLACEBO: A POST HOC ANALYSIS OF TOTAL SYMPTOM SCORE	Dr. V. Ezra Vijay Sekhar	Botany	JOURNAL OF EMERGING TECHNOLOGIES AND INNOVATIVE RESEARCH (JETIR)	2020	2349-5162	www.jetir.org/	https://www.jetir.org/papers/JETIR1907A69.pdf	YES
ISOLATION AND CHARACTERIZATION OF *STREPTOMYCES S* PP SHOWING ANTAGONISTIC ACTIVITY AGAINST FUNGAL PATHOGENS EFFECTING SOYBEAN CROP	Dr. V. Ezra Vijay Sekhar	Botany	EUROPEAN JOURNAL OF BIOTECHNOLOGY AND BIOSCIENCE	2020	2321-9122	www.biosciencejournals.com	8-2-20-812.pdf (biosciencejournals.com)	YES
COMPARISON OF THE NON-SPECIFIC IMMUNE RESPONSE IN THE HEAD KIDNEY OF EDIBLE CARP AGAINST BACTERIAL INFECTION	Dr.Satyalatha B.D.J	Zoology	EUROPEAN JOURNAL OF BIOMEDICAL AND PHARMACEUTICAL SCIENCES	2019	2349-8870	http://www.ejbps.com	https://www.ejbps.com/ejbps/abstract_id/6081	YES

GENDER DIVERSITIES , IDENTITY CONCERNS AND CHALLENGES IN THE CONTEXT OF SHASHI DESPANDE'S WRITINGS	G. Anna Shalini	English	INTERNATIONAL JOURNAL OF RESEARCH	2019	2236-6124	https://ijrpublisher.com/		YES
EFFECT OF Cr203 ON THE STRUCTURAL, OPTICAL AND DIELECTRIC STUDIES OF LIF-SrOB203 GLASSES	P.M.Vinaya Teja	Physics	Journal of Non-Crystalline Solids	2019	0022-3093	www.elsevier.com/locate/jnoncrysol	https://www.sciencedirect.com/science/article/abs/pii/S0022309319302753	YES
GIRIJANULA ARTHIKA PARISTHULU ' JIVANA VIDHANAM	Dr . K . Joseph	Telugu	BHAVAVEENA PRATYEKA SANCHIKA	2019	2456-4702	UGC Approved Journal -42500	JTLCLS KJ VOL 16 ,ISSUE 01,SEPTEMBER 2019	YES
YAATRIKULU' ANDHRULA PRASTHAVANA	Dr . K . Joseph	Telugu	IMRF INTERNATIONAL PUBLICATIONS	2019	ISBN 978-81-944859-5-7	www.imrfedu.org		YES
SRI GO SWAMI TULASI DASU JEEVANA REKHALU	Dr . K . Joseph	Telugu	SAHITHYAM - SAMSKARANA DRUKPADHAM	2018	2456-4702	https://telugujournalbhavaveena.blogspot.com/		YES
VIMAL - VIMARSH	Dr . K . Joseph	Telugu		2018	2348-5884	www.stjosephsvizag.com		
DECOMPOSITION OF PRE A*- ALGEBRA WITH Mx	Dr.B.Vijaya Kumar	Mathematics	INTERNATIONAL MULTIDESIPLINARY RESEARCH FOUNDATION (IMRF)	2018	2278-8697	https://www.imrfjournals.com/	https://drive.google.com/file/d/1wzaDgtOKn4fvhSKNKEBG4Ck-r3v_8qoW/view	YES
PESTICIDE RESIDUES IN SELECTED VEGETABLES COLLECTED FROM LOCAL MARKETS IN VIJAYAWADA CITY	Dr.N.J.Solomon Babu	Chemistry	JOURNAL OF APPLICABLE CHEMISTRY	2018	2278-1862	www.janc.info	http://www.joac.info/AbstractPaper/2018/4-Conference%20paper%204A.pdf	YES
PESTICIDE RESIDUES IN SELECTED VEGETABLES COLLECTED FROM LOCAL MARKETS IN VIJAYAWADA CITY	Y. Durga Prasad	Chemistry	JOURNAL OF APPLICABLE CHEMISTRY	2018	2278-1862	www.janc.info	http://www.joac.info/AbstractPaper/2018/4-Conference%20paper%204A.pdf	YES
PESTICIDE RESIDUES IN SELECTED VEGETABLES COLLECTED FROM LOCAL MARKETS IN VIJAYAWADA CITY	M. Kusuma Kumari	Chemistry	JOURNAL OF APPLICABLE CHEMISTRY	2018	2278-1862	www.janc.info	http://www.joac.info/AbstractPaper/2018/4-Conference%20paper%204A.pdf	YES
ISOLATION AND IDENTIFICATION OF BIO ACTIVE PHOTOCHEMICAL COMPOUNDS FROM VENTILAGO DENTICULATA STEM USING GC-MS	M. Kusuma Kumari	Chemistry	JOURNAL OF APPLICABLE CHEMISTRY	2018	2278-1862	www.janc.info	http://www.joac.info/ContentPaper/2018/5-Conference%20paper%205.pdf	YES
ISOLATION AND IDENTIFICATION OF BIO ACTIVE PHOTOCHEMICAL COMPOUNDS FROM VENTILAGO DENTICULATA STEM USING GC-MS	M. Kanthi Kirani	Chemistry	JOURNAL OF APPLICABLE CHEMISTRY	2018	2278-1862	www.janc.info	http://www.joac.info/ContentPaper/2018/5-Conference%20paper%205.pdf	YES